uranium in granites

Canada

1982

Uranophane crystals in red pegmatite, Faraday Mine, Hastings Co., Ontario. National Mineral Collection, specimen no. 62644.
(GSC 202899-E)

Cristaux d'uranophane dans une pegmatite rouge, Mine Faraday, comté de Hastings, Ontario. Collection nationale de minéraux, spécimen no. 62644.
(CGC 202899-E)

PAPER 81-23

URANIUM IN GRANITES

edited by
Y.T. MAURICE

1982

Proceedings of a workshop held in
Ottawa, Ontario, 25–26 November, 1980

Available in Canada through

authorized bookstore agents
and other bookstores

or by mail from

Canadian Government Publishing Centre
Supply and Services Canada
Hull, Québec, Canada K1A 0S9

and from

Geological Survey of Canada
601 Booth Street
Ottawa, Canada K1A 0E8

A deposit copy of this publication is also available
for reference in public libraries across Canada

Cat. No. M44-81/23E Canada: $12.00
ISSN 0-660-11141-1 Other countries: $14.40

Price subject to change without notice

Production Editing and Layout

M.J. Kiel

Text Preparation

Sharon Parnham
Shirley Kostiew
Susan Gagnon
Janet Gilliland
Janet Legere

FOREWORD

This volume consists of papers presented at the Uranium in Granites Workshop, which was held in Ottawa on 25-26 November, 1980. The purpose of this workshop was to provide the participants in the Canadian Uranium in Granites Study with an opportunity to discuss the results of their most recent research activities.

The Canadian Uranium in Granites Study had its origin in 1976 when the Nuclear Energy Agency, a division of the Organization for Economic Co-operation and Development located in Paris, and the International Atomic Energy Agency, a United Nations organization based in Vienna, established a joint working group to be concerned with research and development into methods of uranium exploration. This working group was charged with establishing a series of projects suitable for international collaborative research relevant to a variety of problems and situations encountered in uranium exploration. The projects range through geophysical and geochemical techniques to instrumentation development, and to mineralogical, petrological and broader geological topics.

The proposal for a project on uraniferous granites originated in France, following from the fact that most of the French uranium production has been derived from vein and pipe-like bodies within granites. Much detailed research has been undertaken in France on uraniferous granites, and the resulting ideas on the origin of granites and their associated mineralization are of theoretical and practical interest to explorationists in Canada. With this in mind, and in order to prepare a Canadian contribution to the NEA/IAEA project, a group of Canadian geologists from the GSC and several of the provincial geological surveys and some universities agreed to share their experience on granites. The workshop was designed to bring together a cross-section of their recent work.

Much interesting work is being done, but it is apparent that current research in any particular locality is generally confined to a few types of investigation. There are a few places where a variety of complementary geological, petrological, geochemical and geophysical data are being obtained but unfortunately these are all too rare. Yet most scientists will acknowledge that convincing answers to fundamental questions such as origin and economic questions such as mineralization potential, can only be obtained through broad-based investigations. So by indicating where there are partially investigated granites awaiting further work this publication will provide a valuable service, especially if researchers can be persuaded to fill in the gaps. It is my hope that the following papers will create greater awareness of the importance and interest of uranium in granites and generate ideas for new research.

Thanks are due to Dr. Y.T. Maurice for making all the preparations and arrangements necessary to hold this workshop, for subsequent liaison with the authors, and for editing the manuscripts.

A.G. Darnley,
Chairman, NEA/IAEA Joint Group on
Uranium Exploration R & D

AVANT-PROPOS

Ce volume est composé de communications présentées à l'Atelier sur l'uranium dans les granites, tenu à Ottawa les 25 et 26 novembre 1980. Le but de cet atelier était de fournir aux participants à l'Etude canadienne sur l'uranium dans les granites l'occasion de discuter des résultats de leurs plus récentes activités de recherche.

L'Etude canadienne sur l'uranium dans les granites débuta en 1976 lorsque l'Agence pour l'énergie nucléaire, une des divisions de l'Organisation de coopération et de développement économique située à Paris et l'Agence internationale de l'énergie atomique des Nations-Unies située à Vienne, ont établi un groupe de travail conjoint s'intéressant à la recherche et au développement de méthodes d'exploration de l'uranium. Ce groupe de travail fut chargé d'établir une série de projets de recherche pouvant s'accomplir en collaboration internationale et touchant une variété de problèmes et de situations rencontrés dans l'exploration de l'uranium. Les projets vont des techniques géophysiques et géochimiques au développement d'instruments et incluent des sujets aussi vastes que la minéralogie, la pétrologie et la géologie.

Ce projet sur les granites uranifères fut proposé initialement en France, car la majeure partie de l'uranium produit dans ce pays provient de veines et de gisements en forme de cheminées dans les granites. Beaucoup de recherches très détaillées ont été entreprises en France sur les granites uranifères, et les idées qui en résultent sur l'origine des granites et leur minéralisation associée sont d'un intérêt théorique et pratique pour les prospecteurs au Canada. Ayant cela à l'esprit et afin de préparer la contribution canadienne au projet de l'AEN/AIEA, un groupe de géologues canadiens travaillant pour les services géologiques du gouvernement fédéral et de plusieurs gouvernements provinciaux ainsi que de quelques universités ont accepté de mettre en commun leur expérience sur les granites. L'atelier a été conçu pour rassembler les grandes lignes de leurs travaux récents.

Un travail très intéressant est en voie d'être accompli mais il est clair que la recherche actuelle dans chaque localité particulière est généralement limitée à certains types d'investigations. Il y a quelques endroits où l'on a pu obtenir diverses données complémentaires géologiques, pétrologiques, géochimiques et géophysiques, mais malheureusement ces cas sont trop rares. Pourtant, la plupart des spécialistes reconnaitront que pour obtenir des réponses convaincantes aux questions fondamentales comme l'origine, et à des problèmes d'ordre économique tel le potentiel de minéralisation, on ne peut se fier qu'à des recherches très approfondies. Ainsi, en indiquant où se trouvent les granites partiellement étudiés, qui nécessiteraient de plus amples études, cette publication rendra un service valable surtout si des chercheurs peuvent être persuadés d'entreprendre des études complémentaires. J'espère que les communications qui suivent seront à l'origine d'une plus grande prise de conscience de l'importance et de l'intérêt de l'uranium dans les granites et susciteront des idées pour entreprendre de nouvelles recherches.

Nous devons remercier spécialement Y.T. Maurice qui s'est chargé de préparer l'atelier, et d'assurer la liaison postérieure avec les auteurs ainsi que de l'édition des manuscrits.

A.G. Darnley
Président du groupe conjoint AEN/AIEA
sur la recherche en exploration de l'uranium

INDEX MAP

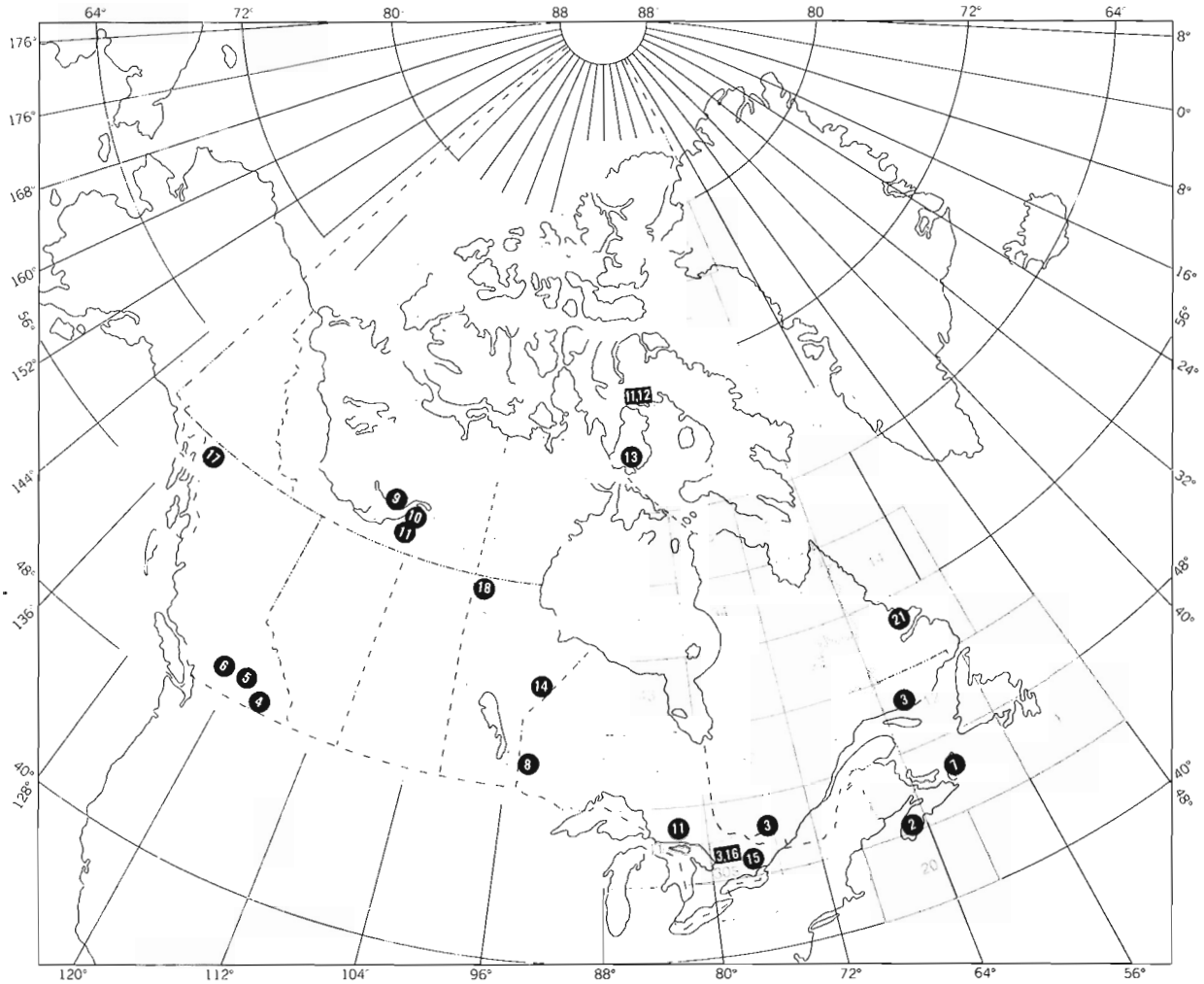
64°
72°
80°
88°
88°
80°
72°
64°
176°
176°
168°
160°
152°
144°
136°
128°
8°
0°
8°
16°
24°
32°
40°
48°
40°
48°
56°
56°
120°
112°
104°
96°
88°
80°
72°
64°
56°
11,12
13
17
9
10
11
18
21
6
5
4
14
3
8
1
11
3
2
3,16
15
20

CONTENTS

Numbers in brackets refer to report numbers, see Index Map for location.

INTRODUCTION

This publication is concerned with uranium in granites sensu lato and the title 'Uranium in Granites' is perhaps less precise than 'Uranium in Granitoids', 'Uranium in Granitic Rocks' or even 'Uranium in Plutonic Rocks' would have been. Indeed, several papers in this volume describe rock types for which the chemical and/or mineralogical compositions extend far beyond what modern petrology defines as 'granite'. Thus, monzonite, granodiorite, tonalite, etc. appear in the volume almost as frequently as granite. Some papers describe differentiated suites of rocks that range from diorites and gabbros to syenites and shonkinites. In many cases, especially in regional studies, the rock types have not been accurately defined and the authors call them 'granitic' rocks, a reference to their granite-like appearance, the presence of quartz, and a low colour index.

Uranium mineralization associated with 'granite' is described in a few papers; the majority, however, focus on the plutonic rocks themselves, examining the behaviour of uranium during magmatic processes and/or defining their characteristics either as source rocks or host rocks. The methods of investigation are also diverse. They range from classical petrographic and mineralogical studies to airborne radiometrics and gravity measurements. Above all, the volume contains a vast number of chemical analyses.

The papers are arranged more or less in the order in which they were presented at the workshop. They had been selected to cover as great a geographical distribution as possible within Canada (see index map). Thus, of the twenty-one papers (including three abstracts), five are on the Northwest Territories, four on British Columbia, three on Ontario, two each on Nova Scotia and Manitoba, one on Quebec and one on Newfoundland. All are preceded by an overview by A.G. Darnley.

The organization of the workshop and subsequent preparation of this volume required input from many people, far too many to individually acknowledge. However, there are some who do require special mention: A.G. Darnley, Director of Resource Geophysics and Geochemistry Division of the Geological Survey of Canada gave his whole-hearted support to the project. C.C. Durham was of invaluable help in making the physical arrangements for the workshop and B.W. Charbonneau provided much appreciated suggestions and assistance in the preparation of this volume.

Every paper was critically read by at least two reviewers whose efforts have led to much improvement in the quality of the papers. In alphabetical order they are: R.T. Bell, G.R. Bernius, D.R. Boyle, F.W. Chandler, B.W. Charbonneau, R.F. Emslie, K.L. Ford, S.S. Gandhi, R.G. Garrett, W.D. Goodfellow, I.R. Jonasson, P.G. Killeen, A.N. Lecheminant, J.B. Leech, A.R. Miller, K.A. Richardson, and S.M. Roscoe.

Finally, Mrs. Mary-Ann Blondin of the Resource Geochemistry Subdivision (GSC) was always at hand when typing was required.

Y.T. Maurice
Editor and Chairman of Uranium in Granites Workshop

INTRODUCTION

Cette publication est à propos d'uranium dans les granites au sens large et le titre 'l'Uranium dans les granites' est peut être moins précis que l'aurait été 'l'Uranium dans les granitoïdes', 'l'Uranium dans les roches granitiques' ou même 'l'Uranium dans les roches plutoniques'. De fait, les types de roches décrits dans plusieurs des textes de ce volume ont des compositions chimiques ou minéralogiques qui s'éloignent beaucoup de ce que la pétrologie moderne définit comme 'granite'. Ainsi, la monzonite, la granodiorite, la tonalite, etc. apparaissent dans le volume au moins aussi fréquemment que le granite. Certains textes décrivent des suites de roches différenciées qui vont des diorites et des gabbros aux syénites et shonkinites. Dans de nombreux cas, surtout dans les études régionales, les types de roches n'ont pas été définis très précisement et les auteurs les appellent 'granitiques', à cause de leur espect semblable au granite, de la présence de quartz et d'un faible indice colorimétrique.

Certains textes décrivent des minéralizations en uranium associées aux 'granites'. La majorité, toutefois, se concentre sur les roches plutoniques elles-mêmes en examinant le comportement de l'uranium durant les processus magmatiques et/ou en définissant leurs charactéristiques comme roches sources ou roches encaissantes. Les méthodes de recherche sont aussi très diversifiées. Elles s'étendent de la pétrographie et la minéralogie classiques aux levés radiométriques aéroportés et aux mesures gravimétriques. Le volume comporte surtout un grand nombre d'analyses chimiques.

Les textes sont disposés plus ou moins dans l'ordre dans lequel ils ont été présentés à l'atelier. Ils furent sélectionnés de façon à présenter le plus de diversité géographique possible à l'intérieur du Canada (voir la carte index). Ainsi, sur les vingt-et-un textes (incluant trois résumés), cinq discutent de cas dans les Territoires du Nord-Ouest, quatre en Colombie Britannique, trois en Ontario, deux en Nouvelle-Ecosse ainsi qu'au Manitoba, un au Quebec et un à Terre-Neuve. Tous sont précédés d'une synthèse par A.G. Darnley.

L'organisation de l'atelier et la préparation de ce volume ont nécessité l'apport de plusieurs individus, trop nombreux pour pourvoir les remercier individuellement. Il y en a, toutefois, qui doivent être mentionnés d'une facon spéciale: A.G. Darnley, directeur de la Division de la géophysique et géochimie appliquées de la Commission géologique du Canada a apporté son appui à ce projet. C.C. Durham a été d'une aide précieuse dans les préparatifs de l'atelier et B.W. Charbonneau a fourni des suggestions et une assistance fort appréciées dans la préparation de ce volume.

Chaque texte a subi la critique d'au moins deux reviseurs dont les efforts ont grandement amélioré la qualité des textes. Par ordre alphabétique ce sont: R.T. Bell, G.R. Bernius, D.R. Boyle, F.W. Chandler, B.W. Charbonneau, R.F. Emslie, K.L. Ford, S.S. Gandhi, R.G. Garrett, W.D. Goodfellow, I.R. Jonasson, P.G. Killeen, A.N. Lecheminant, J.B. Leech, A.R. Miller, K.A. Richardson, et S.M. Roscoe.

Finalement, Mme Mary-Ann Blondin de la sousdivision de la géochimie-ressources (CGC) était toujours disponible lorsque des travaux à la dactylo étaient requis.

Y.T. Maurice
Rédacteur en chef et président de l'atelier sur l'Uranium dans les granites

"....possession of large radium (uranium) resources will endow that country with power and authority which will dwarf that held by the owners of gold, land, or capital."

*Vernadskii (1910)**

* Vernadskii, V.I. O neobkhodimoski issledovaniya radioaktivnykh mineralov Rossiiskoi imperii (The Need for Prospecting for Radioactive Minerals in the Russian Empire). 1910. – Izbrannye Sochineniya, Vol. 1. 1954.

1.

'HOT' GRANITES: SOME GENERAL REMARKS

A.G. Darnley[1]
Geological Survey of Canada

Darnley, A.G., 'Hot' granites: some general remarks; in Uranium in Granites, ed. Y.T. Maurice; Geological Survey of Canada, Paper 81-23, p. 1-10, 1982.

Abstract

Radioactive decay generates thermal energy, the driving force for most of the earth's internal processes. The radioelements, principally potassium, uranium and thorium have been progressively transferred from the mantle to the continental crust through time. Granitic rocks provide the largest repository for these elements. A small proportion of granitic (and syenitic) rocks contain above normal radioelement concentrations. Under a favourable combination of structural and hydrological conditions the heat generating capacity of these 'hot' granites is significant with respect to low temperature mineralizing processes. Uraniferous granites constitute a special class and Hercynian examples suggest that certain gross compositional and alteration features are indicative of genetically associated uranium mineralization (e.g. a high U/Th ratio combined with uranium levels 2 to 5 times the clarke; muscovite-biotite; accessory uraninite; strong negative Bouguer gravity anomalies). The South Mountain batholith of SW Nova Scotia meets several of these criteria. In western Canada a linear negative gravity anomaly extending 1600 km from Edmonton to Baker Lake, is coincident with a zone of high uranium, mostly in granitoid rocks, which is in the exposed Shield NE of the Athabasca basin, and present in the prairie Precambrian basement to the SW. The gravity anomalies can be traced beneath the Athabasca basin with the inference that there is associated high uranium. This combined gravity-radioelement linear anomaly is termed the Athabasca axis. There is some evidence to suggest it developed through crustal tension. The rich mineralization of the Athabasca basin can be attributed to the favourable conjunction of heat sources, source material, hydrology, and structure, in turn attributable to the Athabasca axis which has deep crustal or mantle connections.

General questions are posed as to the distribution of 'hot' granites in time, their origins and tectonic associations, and their possible significance with respect to the stabilization of cratons.

Résumé

La désintégration radioactive produit de l'énergie thermique, la force motrice de la plupart des processus internes de la terre. Les radioéléments, principalement le potassium, l'uranium et le thorium ont été progressivement transférés du manteau à la croûte continentale avec le temps. Les roches granitiques représentent le plus grand lieu de concentration de ces éléments. Une petite proportion de roches granitiques (et syénitiques) contient des concentrations de radioéléments au-dessus de la normale. En présence d'une combinaison favorable de conditions structurales et hydrologiques, la capacité de production de chaleur de ces granites 'chauds' est significative si l'on considère les processus de minéralisation à basse température. Les granites uranifères constituent une catégorie spéciale et des exemples hercyniens suggèrent que certaines caractéristiques grossières de la composition et des altérations sont indicatives de minéralisation en uranium qui leur sont génétiquement associés (par exemple, un rapport élevé U/Th combiné avec des taux d'uranium de 2 à 5 fois le clarke; présence de muscovite et biotite; présence d'uraninite accessoire; de fortes anomalies de gravité Bouguer négatives associées). Le batholithe South Mountain du sud-ouest de la Nouvelle-Ecosse présente plusieurs de ces caractéristiques. Dans l'ouest du Canada, une anomalie de gravité linéaire et négative s'étendant sur 1600 km d'Edmonton au lac Baker, coïncide avec une zone riche en uranium, principalement dans des roches granitoïdes, qui sont dans le Bouclier exposées au NE du bassin de l'Athabasca et présentes au sud-ouest dans le socle précambrien des Prairies. On peut déceler les anomalies de gravité sous le bassin de l'Athabasca et supposer qu'une teneur élevée en uranium leur est associée. Cette anomalie linéaire combinée, gravité-radioéléments, est appelée l'axe de l'Athabasca. Certains faits tendent à suggérer qu'elle s'est développée sous l'effet d'une tension de la croûte. La riche minéralisation du bassin de l'Athabasca peut être attribuée à la conjonction favorable de sources de chaleur, de matériaux d'origine, de l'hydrologie et de la structure, attribuable à son tour à l'axe de l'Athabasca qui est relié en profondeur avec la croûte ou le manteau.

Des questions d'ordre général sont posées concernant la distribution des granites 'chauds' dans le temps, leur origine et leurs associations tectoniques, ainsi que leur rôle possible dans la stabilisation des kratons.

[1] 601 Booth Street, Ottawa, Ontario, K1A 0E8

Introduction

Radioactive decay generates thermal energy which has been the principal driving force for the earth's internal processes throughout most of geological time. The growth of the crust, orogenesis, metamorphism, igneous intrusion, vulcanism and plate tectonics, as well as minor processes such as ore formation, are linked directly or indirectly to this source of energy. Radioactive decay is an intrinsic property of the radioelements, potassium, uranium and thorium which, in the course of time, have been progressively transferred from the interior of the earth into the crust. (O'Nions, Evensen and Hamilton, 1979). Granitoids[1] in general are the principal repository for radioelements within the crust. However, those granitoids which contain more than the average concentrations of radioelements warrant special attention for a variety of reasons which extend beyond exploration for uranium. This short paper will touch upon some of these reasons.

Uraniferous granites can be considered a special category within a broader group of anomalously radioactive or 'hot' granitoids. Thus, the first practical consideration is to recognize a granitoid as being anomalous. Considering granitoids in general, variations in their radioelement content provide an almost instantaneous means of subdividing them into classes, which may or may not coincide with visible petrological differences. The most convenient instrument for everyday field use is a small scintillation counter which, if properly used, is capable of providing reproducible quantitative measurements. Unfortunately until recently a practical impediment to the use of scintillation counters for systematic radiometric mapping (as distinct from prospecting) has been the lack of any generally accepted measurement unit. A scintillation counter measures total radioactivity. Most commercially available field scintillation counters have had scales graduated in any one of a variety of units: counts per second, counts per minute, millivolts, micro-roentgens per hour, etc. In order to overcome this confusion, an International Atomic Energy Agency committee recommended in 1976 that the measurement of total radioactivity in geological situations should be standardized on the unit of radioelement concentration abbreviated Ur (International Atomic Energy Agency, 1976). The arguments for adopting this unit were reviewed and endorsed at a meeting convened by the Nuclear Energy Agency and the countries of the European Economic Community at a meeting in Paris, November 1980. Since 1976 facilities for calibrating field equipment have been established at Ottawa, Saskatoon and Calgary. Details are contained in Killeen and Conaway (1978). The definition of a Ur and examples of the range that may be encountered are contained in Table 1.1

A simple scintillation counter does not discriminate between the radioactive elements and this is a disadvantage. A properly calibrated instrument will nevertheless establish the level of total radioactivity as the first step in the classification process. It can be seen from Table 1.1 that average crustal granite has a total radioactivity of about 20 Ur. This table illustrates the response of a scintillation counter to high radioactivity caused by thorium rather than uranium. The level of total radioactivity that may accompany an economically significant granite is quite low. The Mortagne granite from the Vendée district in France, which is closely associated with uranium mineralization, is about one third more radioactive than average granite, but in the Hercynian environment this modest increase is not diagnostic. Additional criteria are necessary which are discussed in the section Uranium in Granites.

Table 1.1. Measurement of Total Radioactivity

The recommended unit is the unit of radioelement concentration, defined as follows:

"A geological source with 1 unit of radioelement concentration produces the same instrument response (e.g. count rate) as an identical source containing 1 part per million uranium in radioactive equilibrium"

- International Atomic Energy Agency Technical Report 174, 1976.

Note that the recommended abbreviation is now Ur, not ur.

Radioelement Ur equivalents

1 part per million of uranium in equilibrium (1 ppm eU)	≃ 1 Ur
1 part per million of thorium in equilibrium (1 ppm eTh)	≃ 0.5 Ur
1 per cent potassium (1% K)	≃ 2 Ur

Note that the conversion from Th and K concentrations to Ur units is approximate. Ideally it should be determined for each type of scintillation counter as it will vary with energy threshold and crystal size. A near linear relation between Th and K concentration and Ur units is obtained with a threshold setting of 0.4 MeV.

Rock Ur equivalents

Basalt 0.75% K + 0.5 ppm eU + 1.5 ppm eTh	≃ 3 Ur
*Average granite 4% K + 4 ppm eU + 16 ppm eTh	≃ 20 Ur
Mortagne granite, Vendée district, France 4% K + 9 ppm eU + 17 ppm eTh	≃ 26 Ur
Conway granite, N.H., U.S.A. 4% K + 15 ppm eU + 57 ppm eTh	≃ 52 Ur
Fort Smith granitoid belt, N.W.T. 5% K + 11 ppm eU + 80 ppm eTh	≃ 61 Ur

*Note that "average" values quoted by different authors cover a range between 2.5 and 4.2% K, 3 and 4.5 ppm U, 8.5 and 18 ppm Th.

Anomalously radioactive granitoids may be rich in thorium, in both uranium and thorium, or more rarely, in uranium alone. It is not uncommon in geological literature to see the anomalous radioactivity of some granites attributed to their high potassium content. Potassium contributes to the radioactivity of rocks as can be seen from Table 1.1, but a high potassium granite with, for example, 6% K, would have a total radioactivity of approximately 12 Ur if there were no uranium or thorium present. This is significantly less than the radioactivity of average granite (about 20 Ur). The anomalous radioactivity which is commonly associated with high potassium granitoids is caused by the fact that such examples also have a high uranium and/or thorium content, following the geochemical affinities between the three elements in a normal magmatic environment.

[1] The term 'granitoid' is used as a compositional term, to signify any high silica, high alkali crystalline rock of igneous or metamorphic origin. The term 'granite' is used in a somewhat narrower sense to include any high alkali, generally quartz-bearing, intrusive plutonic rock.

Radioactive Granitoids and Mineralization

The economic incentive to recognize anomalously radioactive granitoids follows from the observation that they tend to be more commonly associated with certain types of mineralization than are granitoids of average radioelement content. Uranium may be locally enriched in certain zones within a granitoid, or it may be concentrated in an adjacent geological trap. In either case the mineralization may be contemporaneous with or much younger than the intrusion of the granite. Other metals may be more strongly concentrated than uranium; for example, tin, tungsten, molybdenum, niobium and tantalum.

The association between mineralization and anomalously radioactive granitoids is more than a matter of geochemical affinities. Depending upon its radioelement content, an anomalous granitoid has a heat generating capacity which may be up to 4 times greater than average granite (see Table 1.2). Although the amount of heat produced is small, it is produced over a long period of time with a half-life controlled by the decay of the parent nuclides. This fact can maintain the temperature of an anomalous granite above its surroundings for hundreds of millions of years, up to 100 times the cooling period of an 'average' intrusion. The temperature at its centre will be related to the concentration of radioelements, the size and shape of the body, the rate of heat loss by fluid transfer and the time since intrusion. Heat loss by fluid transfer is dependent upon the permeability of the ganitoid and the availability of water. It should be emphasized that the temperatures achieved in this way will not be as high as will have occurred during the initial cooling of the intrusion, and only low temperature mineralization processes are likely to occur. Fehn, Cathles and Holland (1978) have provided a quantitative analysis of the many factors involved in their modelling study of the Conway granite of New Hampshire. In this model the maximum temperature difference between the centre of the granite and country rocks at the same depth several kilometres from the granite is about 150°C.

The structural setting of a radioactive granite is important in that the greater the amount of post intrusion fracturing and faulting the greater the opportunity for the rock to transfer its heat to groundwaters, and provide the opportunity for soluble elements to be mobilized and reprecipitated. However, excess continuous flow will cool the granite, so there are clearly optimum flow rates for these processes. The volume of granite that has been affected is also important as it may make all the difference between economic and noneconomic concentration. Given a large granitoid with a high radioelement content, an associated hydrothermal convection system may develop at any time there is a coincidence of suitable permeability and hydrological conditions during its prolonged cooling history. The ability of a hydrothermal system to produce mineral deposits depends upon the availability of the necessary elements and a connection to suitable physical and/or chemical traps over periods of time sufficient to form deposits. Intermittent opening and closing of fractures probably provides the optimum conditions. Thus wherever large radioactive granitoids are known to exist, their long term importance as crustal heat sources deserves consideration because they may have activated extensive low temperature hydrothermal events up to hundreds of millions of years after intrusion took place. As an example, the writer would now accept this as the most plausible explanation for the spread of uranium-lead ages (Darnley et al., 1965) observed in the mineralized vein systems accompanying the Hercynian batholith of southwest England, which meets all the criteria of a 'hot' granite.

Table 1.2. Radioelement Heat Generating Capacity (same examples as Table 1.1)

Basalt	3	cal/m^3/year
Average granite	19	"
Mortagne granite	30	"
Conway granite	63	"
Fort Smith granitoid	69	"

Note that the heat generating capacity is quoted somewhat unconventionally in calories per cubic metre per year. This provides a better appreciation of the amount of heat involved than the scientifically more conventional units. Approximate equivalents are as follows:

1 Heat generating unit (1 HGU) = 10^{-13} cal/cm^3/sec
≃ 0.417 μW/m^3
≃ 3.16 cal/m^3/year

Uranium in Granites

For the reasons given above, any anomalously radioactive granitoid and its geological environment merits careful examination. However, it is granites associated with uranium mineralization which are of particular concern to this review.

A definition for the term 'uraniferous granite' is appropriate at this stage. Since all granites, like most rocks, contain some uranium it is suggested that use of the prefix 'uraniferous' should only be applied to those granites which contain at least twice the clarke. Since the clarke is 4 ppm U, a uraniferous granite would therefore contain 8 ppm U or more. The presence of associated uranium mineralization should not by itself warrant describing the granite as uraniferous.

A number of features can be identified as indicators of granites with associated uranium mineralization. In France, potassic hydrous leucogranites characterized by muscovite and biotite most commonly contain such mineralization (Moreau, 1976). In addition, small amounts of cordierite, sillimanite and garnet are present as minor constituents in many of these leucogranites.

Granites in France and eastern Canada associated with vein-type uranium mineralization are usually uraniferous as defined above, but often not by a large margin. Many other uraniferous granites in these regions have no known associated uranium mineralization. Nevertheless there are other diagnostic features. In situ gamma ray spectrometer measurements made by the writer in 1978 on outcrops of some European Hercynian granites (see Table 1.3) suggest that a higher than average uranium to thorium ratio, caused by a two to four times above average uranium content, without any corresponding increase (and sometimes a lowering) of thorium content, is a common characteristic of those Hercynian granites which contain mineralized structures. The same feature is observed in the South Mountain granite in Nova Scotia (K.L. Ford, personal communication). Granites with this characteristic U/Th ratio include examples from France reported to contain small

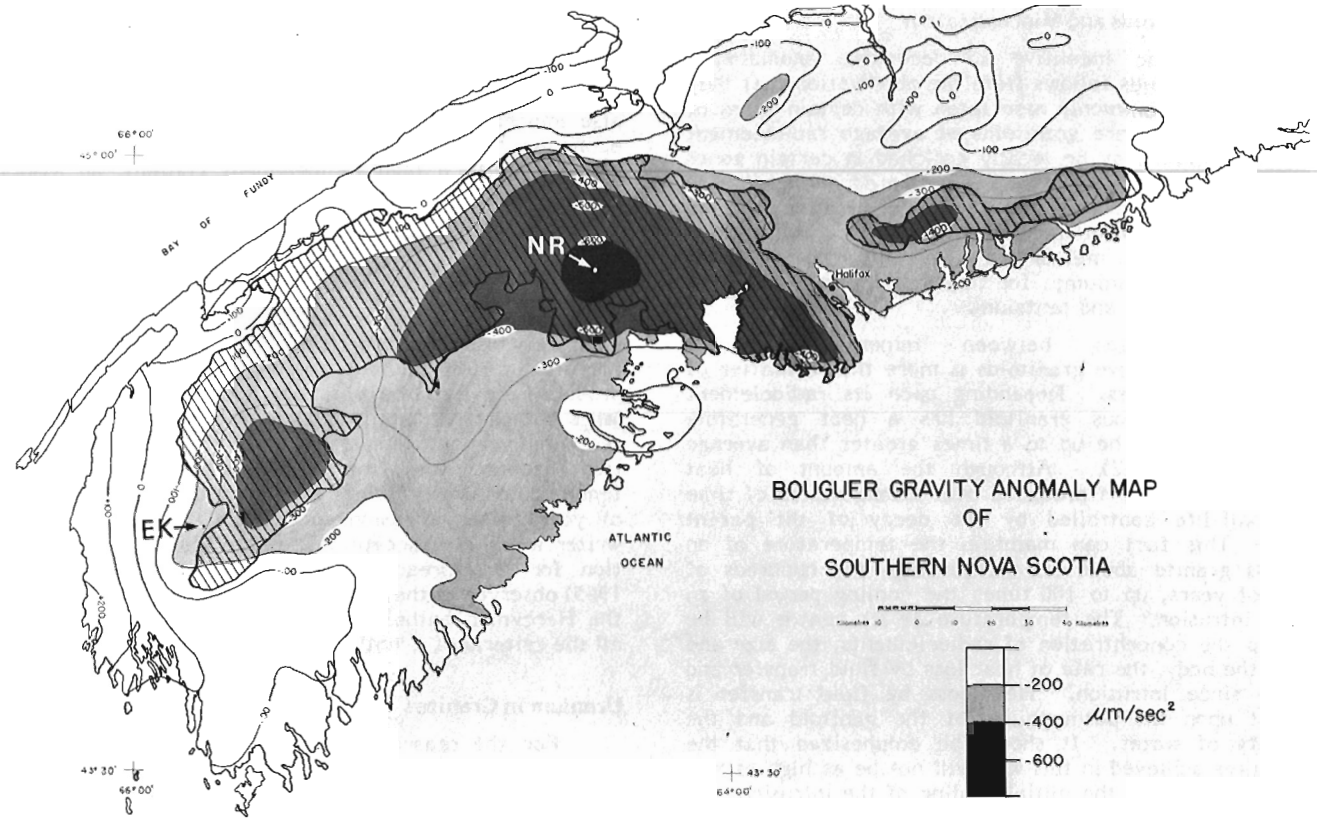

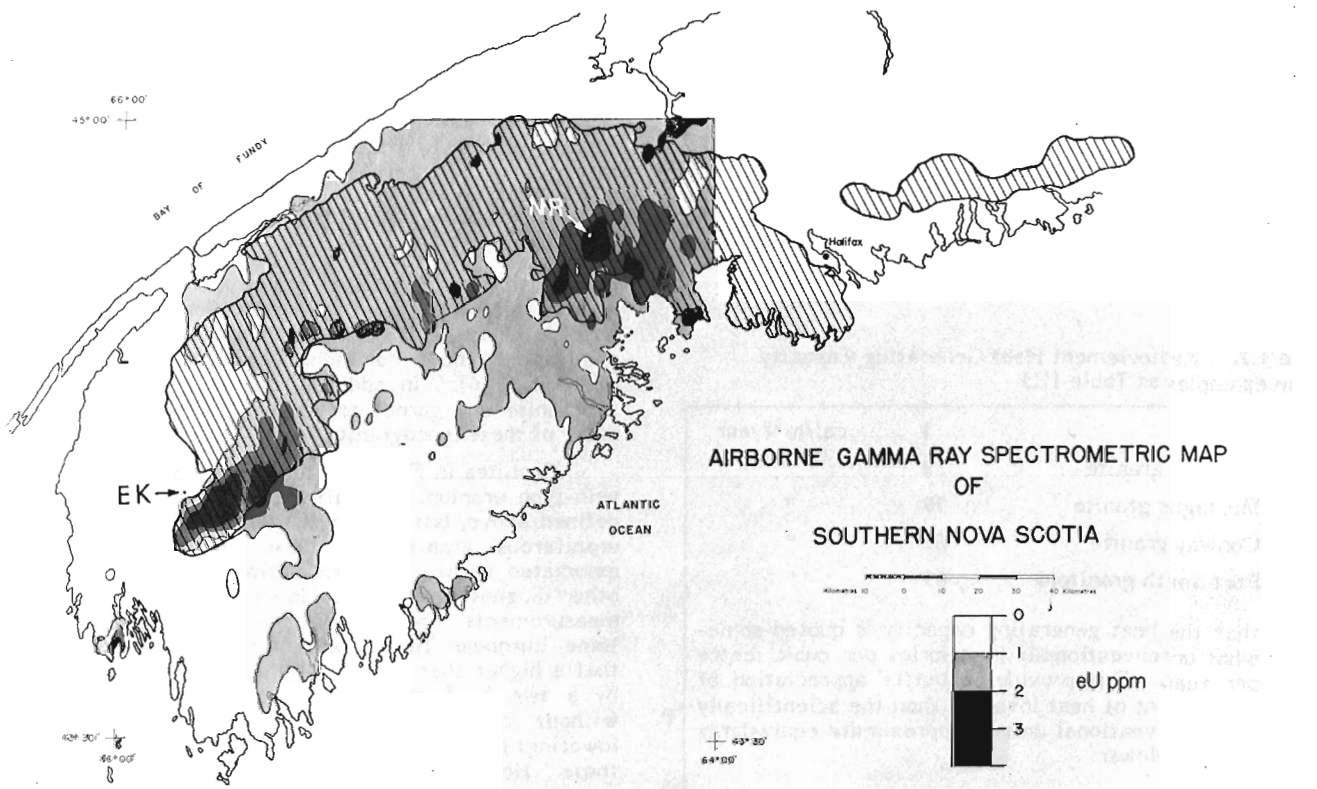

Figure 1.1. *SW Nova Scotia: outline of South Mountain Granite with gravity anomalies and surface uranium distribution superimposed. Area mapped as granite shown by oblique shading. Airborne gamma ray spectrometer data only shown for area south of latitude 45°N and west of longitude 64°W. NR = New Ross; EK = East Kempville; 10 μm/sec² = 1 mGal.*

amounts of accessory uraninite (Moreau, 1976). In areas which have not been glaciated this mineral is normally difficult or impossible to find in near-surface samples because of weathering and it is necessary to obtain fresh specimens from a depth of several metres in order to confirm its presence (Ball and Basham, 1979). Under these conditions, unweathered granite samples normally have a somewhat higher uranium content than samples at surface, but in general this does not reduce the utility of surface gamma ray spectrometer measurements. Some strongly radioactive Hercynian granites are characterized by high thorium, and are not known to be associated with uranium mineralization, even though their uranium concentrations may be higher than that of average granite. The U/Th ratio of these granites is lower than that of those genetically associated with known uranium mineralization (Table 1.3).

One field characteristic of mineralized compared with unmineralized granites noted by the author which may be observed hundreds or thousands of metres from detectable mineralization, is slight but pervasive alteration which renders the granite more breakable than normal fresh granite when struck with a hammer. As mineralized zones are approached the presence of clay minerals becomes obvious to the naked eye.

Apart from their geochemical and mineralogical characteristics, uraniferous granites may also have a distinctive geophysical expression. Strong negative Bouguer gravity anomalies have been identified as an important characteristic of known uraniferous granites in France (Moreau, 1976) and the British Isles (Brown et al., 1979). These intrusions exhibit negative Bouguer anomalies of the order of -40 mGal relative to their surroundings suggesting that the relatively low density material of which they are formed extends to greater depths than is usual for most acid intrusions of comparable surface area, which have closer to average composition, and lack the distinctive radioelement concentration. Reference should be made to the 1:1 million Carte Gravimétrique de la France (Bureau de Recherches Géologiques et Minières, 1974) and the 1:250 000 Bouguer Gravity Anomaly Map Series of the United Kingdom.

It should be noted that Plant et al. (1980) have also drawn attention to the tendency for strong long wavelength aeromagnetic anomalies to be associated with uraniferous granites in Scotland.

Canadian Examples

There are a number of Canadian examples where there is a correlation between uraniferous granites, gravity lows, and uranium mineralization. There are also associated magnetic features, but these are not discussed here. The South Mountain batholith in Nova Scotia shows these relationships very well. Figure 1.1 outlines the portion of Nova Scotia which includes this large batholith. It indicates the main features of the Bouguer gravity anomaly field, and the surface uranium concentration, as determined by airborne gamma ray spectrometry, over an area of more than 20 000 km^2, of which about 40 per cent is the South Mountain granite. The two minima in the Bouguer field, centred in the vicinity of New Ross and East Kemptville, closely coincide with the maxima in surface uranium concentration. Significant uranium mineralization is present in the New Ross area and polymetallic tin veins are present near East Kemptville. High heat flow has been recorded in the New Ross area (Hyndman et al., 1979) inferring that high radioelement concentrations measured on the surface of the granite extend to a depth of several kilometres.

Table 1.3. Radioelement content of Hercynian granites

Hercynian granites with genetically associated uranium mineralization

Surface concentration, in ppm	n	eU	eTh	eU/eTh
Mortagne, Vendée, France	16	9	17	0.53
Limousin, France	44	12	28	0.43
Bärhalde, Black Forest, Germany	7	19	14	1.4

Hercynian granites with no known associated mineralization

Surfaced concentration, in ppm	n	eU	eTh	eU/eTh
Gerardmer I, Vosges, France	38	3	32	0.09
Gerardmer II Vosges, France	27	8	28	0.29
Ballon de Servance (centre), Vosges France	13	10	50	0.20
Kaysersberg, Vosges France	11	5	42	0.12
Albtal, Black Forest, Germany	8	10	29	0.34

All measurements made on flat outcrops using a calibrated portable gamma-ray spectrometer (McPhar Spectra 44D) following standard procedures, as described in Gamma Ray Surveys in Uranium Exploration (International Atomic Energy Agency, 1979).

n = number of sites sampled

Whereas the South Mountain batholith is of Middle to Late Paleozoic age, there are also a number of examples of similarly anomalous granitoid bodies from the Precambrian. Figure 1.2 is a composite map of the uranium distribution over part of western Canada, overlain with an outline of the major negative Bouguer anomalies taken from the published gravity map of Canada (Earth Physics Branch, 1974).

Within the area covered, uranium is concentrated in two principal 'zones' (1) along the northwestern edge of the Shield from Great Bear Lake to the west end of Lake Athabasca (Darnley et al., 1977), and (2) in a broad band from Melville Peninsula N.W.T. to the vicinity of Edmonton, Alberta. Zone 1 shows no distinct association with gravity anomalies; its southern portion (the Fort Smith belt) coincides closely with a regional magnetic low (see Magnetic Anomaly Map of Canada, McGrath et al., 1977). In contrast the uranium highs along the northwestern side of zone 2 show a general coincidence with a line of gravity lows, defined by the -80 mGal contour on the Gravity Map of Canada (Earth Physics Branch, 1974). They are both aligned parallel to the dominant trend of the magnetic anomaly pattern of the region. The gravity lows form a distinct linear feature striking NE from the vicinity of Edmonton to Baker Lake. The feature branches from the east side of the Cordilleran gravity low and has been referred to by Burwash and Cumming (1976) as the Edmonton-Kasba Lake gravity low. The writer suggests that the name Athabasca axis is preferable because the feature is distinguished by a high uranium content as well as a relative mass deficiency, and it passes under the central portion of the Athabasca basin. It is important to note from Figure 1.2 that along this axis the coincidence between low density and high uranium content

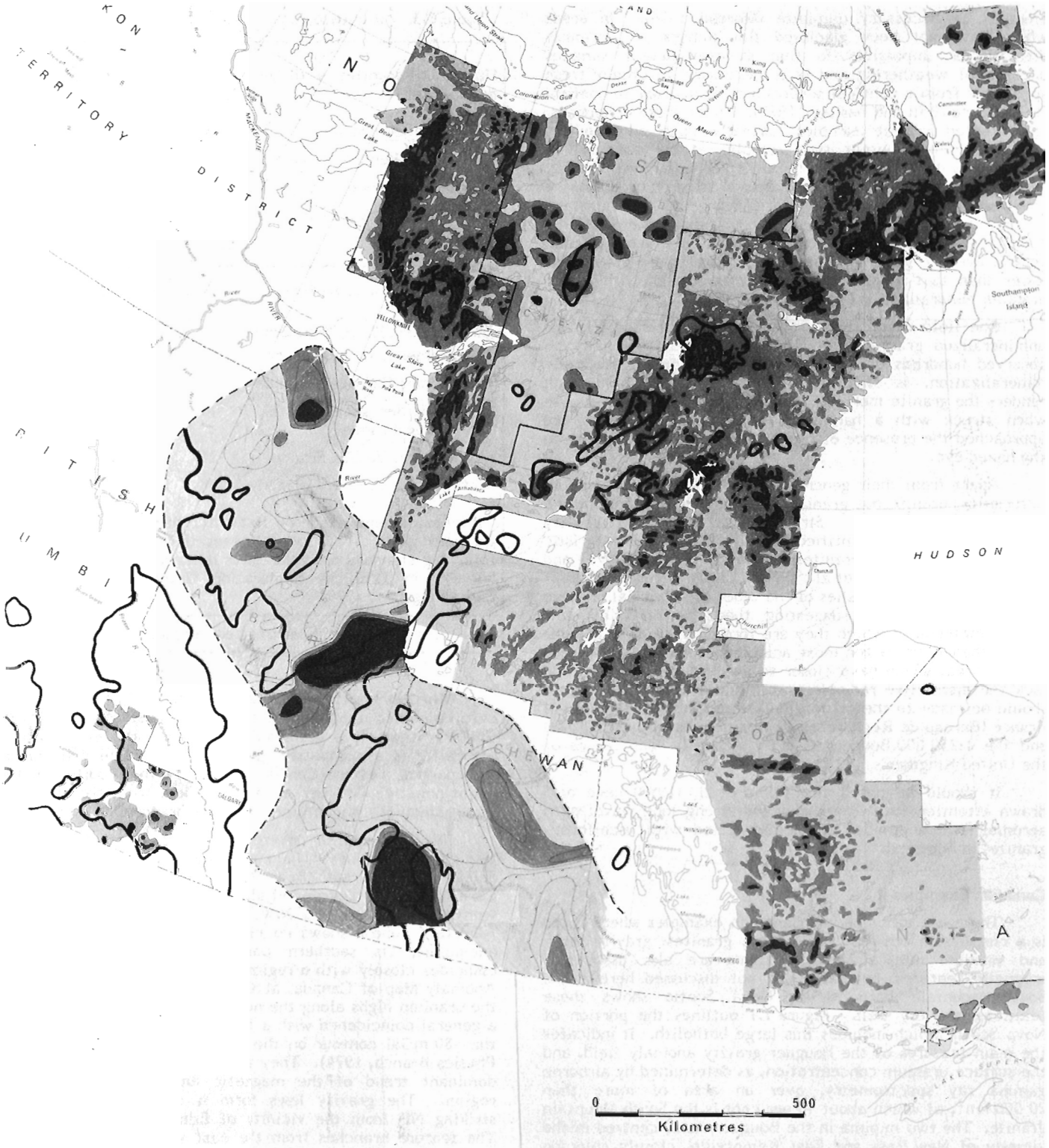

Figure 1.2. *West-central Canada: gravity anomalies superimposed on uranium distribution. Solid contour along the Athabasca axis represents -80 mGal: (taken from Earth Physics Branch, 1974). The uranium distribution is compiled from the following sources: for the exposed Shield, airborne gamma ray spectrometry maps (GSC Open Files); for the unexposed Shield under the prairies, Burwash and Cumming's (1976) uranium trend surface map based on the analysis of basement borehole cores; for SE British Columbia, uranium in stream sediment data (GSC Open Files). The different types of uranium measurements are not suitable for direct numerical comparison in their present form so this figure is only intended to show the qualitative distribution pattern. Each data set has its own scale. Darkest shading within each data set coincide with areas of highest concentration.*

exists both where the Shield is concealed beneath the prairies, and where it is exposed, for example between the Athabasca basin and Baker Lake.

Gibb and Halliday (1974) in an extended review of the gravity data in what they term the Central Belt (the portion of the Athabasca axis from 58°N to 64°N) comment that 'the coincidence of low gravity values and subdued magnetic pattern in this narrow belt probably reflects the occurrence of granitic rocks not only in those parts of the low where they have been mapped but along the entire length.'

Southwest of Baker Lake there are many examples of uraniferous acid and alkaline intrusions of Aphebian and Helikian age in the period 1.9-1.7 Ga, as well as uranium in volcanics, associated sediments and fault structures (Curtis and Miller, 1980). This region was dominated by tensional tectonics during this period, mostly normal to a northeasterly trend (A.N. LeCheminant, personal communication). Detailed radiometric ground surveys have not yet been undertaken in this region, but by analogy with other areas (e.g. Fort Smith belt, Charbonneau, 1980; see also Charbonneau et al., 1976) where airborne gamma ray spectrometry data have been verified at ground level, it is probable on the basis of measurements from the air that some of the exposed large granitic areas contain in the order of 10 to 15 ppm eU. In view of the observation that large gravity lows are associated with high uranium content, both north and south of the Athabasca basin, there is a clear inference that the sub-Athabasca gravity lows are caused by granitoid rocks with an above average uranium content. Walcott (1968) undertook an analysis of the available regional gravity data for the basin, which indicate two parallel gravity lows trending in a NE direction. Walcott's model, reproduced in Figure 1.3, which shows good agreement with the observed data, entails the presence of two blocks of below average crustal density and somewhat reduced thickness relative to adjoining crust. He concluded that the feature 'is due at least in part to granite'. It is interesting to note that the two gravity lows, which show good correlation with the magnetic anomaly pattern of the basin can be traced back to a Y-junction some 125 km SW of the basin margin. There is now a considerable amount of pertinent literature on the geology and tectonic history of this region, and it is not possible to review it in this short paper. Reference should be made to the Geological Map of Saskatchewan (MacDonald and Broughton, 1980) and Lewry and Sibbald (1979) to see the spatial relationship of various shear zones, tectonic domains and younger granites to the gravity anomalies. It may be noted that Ramaekers (1980) has suggested that the Athabasca basin itself was divided into a series of subparallel basins divided by NE-trending faults characterized by both tensional and transcurrent displacement, with movement taking place in several stages over several hundred million years. The width and amplitude of the sub-Athabasca basin gravity lows, and the distance between their centre lines is similar to that observed in a modern rift system such as east Africa, for example in the parallel Lake Tanganyika and Rukwa rifts in Tanzania (Bullard, 1936). Thus there is an inference concerning the Athabasca axis gravity and radiometric features that the intrusion of uraniferous granitoids was in some way related to crustal extension, either as a cause or an effect.

The foregoing circumstantial evidence points to a situation which appears to satisfy all the essential conditions of the Fehn et al. (1978) model for ore formation involving low

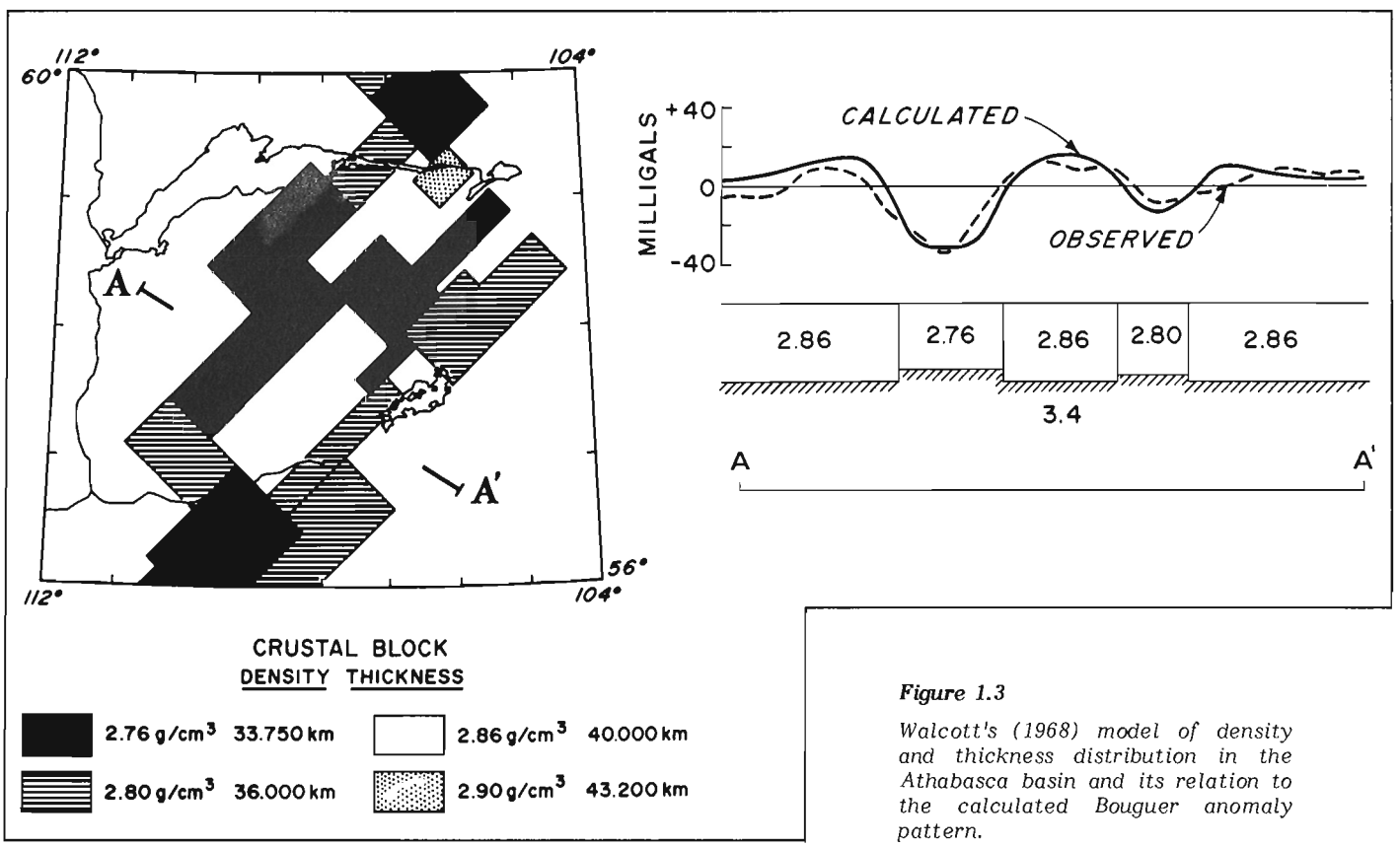

Figure 1.3

Walcott's (1968) model of density and thickness distribution in the Athabasca basin and its relation to the calculated Bouguer anomaly pattern.

temperature hydrothermal systems driven by the heat produced in anomalous radioactive plutons. A closed intracratonic basin with several 'hot' intrusions beneath, cut by prominent fracture systems which are periodically reactivated, would be ideal from the points of view of hydrology, high heat flow, source of materials, and recurrent enrichment. This last fact in particular is probably responsible for the high metal concentrations which are an unusual characteristic of several of the deposits, for example those at Cluff Lake, Key Lake, Midwest Lake, and Maclean Lake.

Figure 1.4 is a cartoon summarizing the situation. It should be noted that while this paper was in preparation, Clark and Burrill (1981) have published a paper reaching a similar conclusion.

Open Questions

The importance of the radioelements in providing the energy for earth processes has been pointed out at the beginning of this paper. Radioelements in the mantle provide most of the energy that moves and disrupts the crust. Loss of radioelements from the mantle reduces thermal input which in turn reduces convection activity. In the course of time radioelements have been progressively fractionated from the mantle because of their large ionic radius combined with their heat generating property, and became a constituent of the melts that have formed the crust. Extreme fractionation can take place in the mantle, producing rocks such as carbonatites which usually have high radioelement content. The possibility must be considered that some anomalously radioactive granites in the crust have evolved by continuous fractionation of melts derived from the mantle under special conditions. For discussion of this topic see Rogers et al. (1978) and Simpson et al. (1979). Therefore it is of interest to establish how 'hot' granites have been distributed in time and space. Is their formation restricted to or preferentially concentrated during particular intervals of time? It appears that many were intruded about the end of the Early Proterozoic in Canada and Australia, the end of Precambrian (Pan-African) in south-central Africa and Brazil and the end of the Paleozoic (Hercynian) in Europe. How common were they at other times? There is much scope for systematic geochronological work on 'hot' granites. To what extent are the most radioactive granites the youngest in any cycle of intrusion?

With respect to intrusion loci, are 'hot' granites more commonly associated with zones of crustal tension (e.g. Athabasca axis) and shearing (e.g. South Mountain in Nova Scotia, Brittany-Vendée in France), than with compressive orogenic belts? Is the common association with prominent gravity lows an indication of abnormally deep seated or mantle origin? Is the fact that some 'hot' granites lack prominent associated gravity lows (e.g. Fort Smith belt, Great Bear batholith) merely confirmation that some granites of this type may have no greater depth than average granites, or could it be that intrusion under compressive conditions has squeezed out their low density root zone? What other criteria are there to indicate whether 'hot' granites are of mid-crustal, deep crustal, or mantle origin? One French school of thought (e.g. Moreau, 1976) believes that radioactive granites are the product of crustal anatexis under Himalayan type continental collision conditions. This school considers that typical 'hot' granites possess characteristics which have come to be known as S-type (Chappell and White, 1974) such as high alumina, high silica, high $^{87}Sr/^{86}Sr$, low ferric iron due to their formation by anatexis of aluminous sediments. In contrast, Plant et al. (1980) consider that in the British Isles the distinctions between S and I type granites (the latter derived from melts of pre-existing rocks of igneous composition) are not clear cut and are of doubtful validity. Strong (1980) is of the same opinion with respect to Newfoundland. Plant et al. (1980) argue that many uraniferous granites possess some S-type characteristics as a result of near surface water-magma interaction and are probably modified I-type. They consider that these granites are from a mainly juvenile subcrustal source.

If 'hot' granites may be of mantle origin it is reasonable to question what particular circumstances might give rise to uraniferous granites which are relatively low in thorium. Is it a pre- or post-intrusion effect? Does it relate to the quantity, composition and oxidation state of magmatic or meteoric fluids, or does it reflect heterogeneities in the source material? A great variety of analytical studies will be needed to shed light on these and the other related questions.

There is one final point which can be made on the subject of whence 'hot' granites have been derived. Jordan (1979) has summarized evidence for the existence of up to 400 km deep chemically distinct, relatively cool root zones beneath stable cratons. It follows from this evidence that there is a deficiency of heat generating elements in these root zones, which stabilizes the continental crust against convective disruption. It seems reasonable to relate the intrusion of a large volume of 'hot' granites in the time preceding the onset of cratonic stability, to their expulsion from the underlying mantle. It can be speculated that prior to this final event the continental crust had been gradually thickening over time, and intervals between disruption by subcrustal heating and convection were gradually lengthening. Each successive event would require a greater build up of thermal energy before disruption occurred. Therefore it seems plausible that the last known major disruptive event would be accompanied by greatest

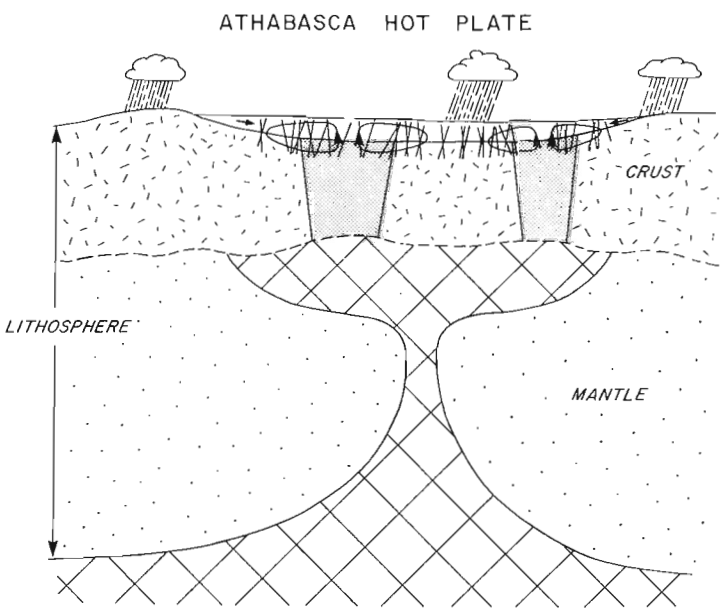

Figure 1.4. *Cartoon to illustrate working hypothesis: Athabasca basin, heated by 'hot' granites distributed along the Athabasca axis contains complex circulating hydrothermal systems each time fractures open. Cross hatching = asthenosphere; close stipple = cryptic rift zones occupied by granitic intursions with high radioelement content producing high heat flow.*

fractionation of source material and the greatest concentration of radioelements. Once this event took place, and the granitic intrusions along the Athabasca axis might be one example of such an event, it could be inferred that there were insufficient radioelements and therefore insufficient thermal energy remaining in the continental mantle root zone to cause further disruption of the Churchill craton.

The speculations in this short paper are presented with the intention of suggesting that a multi-disciplinary study of anomalously radioactive granitoids and the environments in which they occur may prove to be particularly rewarding in understanding the mechanisms which give rise to many geological phenomena. The search for uranium mineralization is only one small facet of the importance of 'hot' granites.

Acknowledgments

Material assistance in obtaining and/or preparing data used in this brief review has been provided by: H. de la Roche, formerly of CRPG, Nancy, France; R.A. Burwash, University of Alberta, Edmonton; J. Needham, formerly of McPhar Geophysics, Toronto, and K.A. Richardson, K.L. Ford, S. Elsmore, and N. Goodman, GSC, Ottawa. Many others have contributed indirectly through discussions and the author expresses his appreciation to all concerned.

This manuscript has benefitted considerably from critical reviews by A.N. LeCheminant, B.W. Charbonneau, and Y.T. Maurice.

References

Ball, T.K. and Basham, I.R.
1979: Radioactive accessory minerals in granites from south-west England; Ussher Society Proceedings, v. 4, p. 437-448.

Brown, G.C., Plant, J.A., and Lee, M.K.
1979: Geochemical and geophysical evidence on the geothermal potential of Caledonian granites in Britain; Nature, v. 280, p. 129-131.

Bullard, E.C.
1936: Gravity measurements in East Africa; Royal Society of London, Philosophical Transactions, Series A, v. 235, p. 445-531.

Bureau de Recherches Géologiques et Minières
1974: Carte gravimétrique de la France à 1/1,000,000; Bureau de Recherches Géologiques et Minières, Orléans, France.

Burwash, R.A. and Cumming, G.L.
1976: Uranium and thorium in the Precambrian basement of western Canada. I Abundance and distribution; Canadian Journal of Earth Sciences, v. 13, p. 284-293.

Chappell, B.W. and White, A.J.R.
1974: Two contrasting granite types; Pacific Geology, v. 8, p. 173-174.

Charbonneau, B.W.
1980: The Fort Smith radioactive belt, Northwest Territories; in Current Research, Part C, Geological Survey of Canada, Paper 80-1C, p. 45-57.

Charbonneau, B.W., Killeen, P.G., Carson, J.M., Cameron, G.W., and Richardson, K.A.
1976: Significance of radioelement concentration measurements made by airborne gamma-ray spectrometry over the Canadian Shield; in Exploration for Uranium Ore Deposits, International Atomic Energy Agency, STI/PUB/434, p. 35-53.

Clark, L.A. and Burrill, G.H.R.
1981: Unconformity-related uranium deposits, Athabasca area, Saskatchewan, and East Alligator River area, Northern Territory, Australia; Canadian Institute of Mining and Metallurgy Bulletin, v. 74, no. 831, p. 63-72.

Curtis, L. and Miller, A.R.
1980: Uranium geology in the Amer-Dubawnt-Yathkyed-Baker Lakes region, Keewatin District, N.W.T. Canada; in Uranium in the Pine Creek Geosyncline, International Atomic Energy Agency, STI/PUB/555, p. 595-616.

Darnley, A.G., English, T.M., Sprake, O., Preece, E.R., and Avery, D.
1965: Ages of uraninite and coffinite from southwest England; Mineralogical Magazine, v. 34, p. 159-176.

Darnley, A.G., Charbonneau, B.W., and Richardson, K.A.
1977: Distribution of uranium in rocks as a guide to the recognition of uraniferous regions; in Recognition and Evaluation of Uraniferous Areas, International Atomic Energy Agency, STI/PUB/450, p. 55-86.

Earth Physics Branch
1974: Bouguer anomaly map of Canada; Gravity Map Series 74-1, Earth Physics Branch, Ottawa.

Fehn, V., Cathles, L.M., and Holland, H.D.
1978: Hydrothermal convection and uranium deposits in abnormally radioactive plutons; Economic Geology, v. 73, no. 8, p. 1556-1566.

Gibb, R.A. and Halliday, D.M.
1974: Gravity measurements in southern district of Keewatin and southeastern district of Mackenzie, N.W.T. with maps 124-131 inclusive; Gravity Map Series, Earth Physics Branch, Ottawa, 36 p.

Geological Survey of Canada Open Files
(see note p. 10)

Hyndman, R.D., Jessop, A.M., Judge, A.S., and Rankin, D.S.
1979: Heat flow in the Maritime Provinces of Canada; Canadian Journal of Earth Sciences, v. 16, p. 1154-1165.

International Atomic Energy Agency
1976: Radiometric reporting methods and calibration in uranium exploration; International Atomic Energy Agency, Technical Report 174, STI/DOC/10/174, 57 p.

1979: Gamma-ray surveys in uranium exploration; International Atomic Energy Agency, Technical Report 186, STI/DOC/10/186, 89 p.

Jordan, T.M.
1979: The deep structure of the continents; Scientific American, v. 240, p. 92-107.

Killeen, P.G. and Conaway, J.G.
1978: New facilities for calibrating gamma-ray spectrometric logging and surface exploration equipment; Canadian Institute of Mining and Metallurgy Bulletin, v. 71, no. 793, p. 84-87.

Lewry, J.F. and Sibbald, T.C.
1979: A review of pre-Athabasca basement geology in northern Saskatchewan; in Uranium Exploration Techniques, Geological Society of Saskatchewan, Spec. Pub. 4, p. 19-40.

MacDonald, R. and Broughton, P.
1980: Geological map of Saskatchewan, provisional edition 1980; Saskatchewan Department of Mineral Resources, Regina.

McGrath, P.H., Hood, P.J., and Darnley, A.G.
1977: Magnetic anomaly map of Canada, 3rd edition; Geological Survey of Canada, Map 1255A.

Moreau, M.
1976: L'uranium et les granitoïdes: essai d'interprétation; in Geology, Mining and Extractive Processing of Uranium, ed. M.J. Jones; Institution of Mining and Metallurgy, London, p. 83-102.

O'Nions, R.K., Evensen, N.M., and Hamilton, R.J.
1979: Geochemical modeling of mantle differentiation and crustal growth; Journal of Geophysical Research, v. 84, p. 6091-6101.

Plant, J., Brown, G.C., Simpson, P.R., and Smith, R.T.
1980: Signatures of metalliferous granites in the Scottish Caledonides; Institution of Mining and Metallurgy Transactions, Section B, v. 89, p. B198-B210.

Ramaekers, P.
1980: Stratigraphy and tectonic history of the Athabasca Group (Helikian) of northern Saskatchewan; in Summary of Investigations 1980, Saskatchewan Geological Survey, p. 99-106.

Rogers, J.J.W., Ragland, P.C., Nishimori, R.K., Greenberg, J.K., and Hauck, S.A.
1978: Varieties of granitic uranium deposits and favorable exploration areas in the eastern United States; Economic Geology, v. 73, p. 1539-1555.

Simpson, P.R., Brown, G.C., Plant, J., and Ostle, D.
1979: Uranium mineralization and granite magmatism in the British Isles; Royal Society of London, Philosophical Transactions, Series A, v. 291, p. 385-412.

Strong, D.F.
1980: Granitoid rocks and associated mineral deposits of eastern Canada and western Europe; in The Continental Crust and its Mineral Deposits, Geological Association of Canada, Special Paper 20, p. 742-769.

Walcott, R.I.
1968: The gravity field of northern Saskatchewan and northern Alberta with maps; Dominion Observatory (now Earth Physics Branch), Ottawa, Gravity Map Series 16 to 20.

NOTE: Geological Survey of Canada Open Files

All Geological Survey of Canada Open Files relating to radiometric and geochemical data referred to in this paper are available for reference in Geological Survey of Canada libraries located at:

Geological Survey of Canada,
601 Booth St.,
Ottawa, Ontario
K1A 0E8;

Institute of Sedimentary and Petroleum Geology,
3303-33rd Street N.W.,
Calgary, Alberta
T2L 2A7;

Atlantic Geoscience Centre,
Bedford Institute of Oceanography,
Dartmouth, Nova Scotia
B2Y 4A2;

Cordilleran Geology Division,
100 West Pender Street,
Vancouver, British Columbia
V6B 1R8.

Radiometric data: the data used to compile the uranium map shown in Figures 1.1 and 1.2 consist of both flight line profiles and contour maps showing total count, potassium, uranium, and thorium corrected count rates, and U/Th, U/K, Th/K ratios at a scale of 1:250 000. The contour maps show the main trends of radioelement distribution, while profiles provide detailed information along the flight lines.

All material is available as white prints, from a commercial sales agent, and most of it is available as microfiche from the Publications Office, Geological Survey of Canada, 601 Booth St., Ottawa, Ontario, K1A 0E8. This office can supply lists relating Open File or Geophysical Series Map Numbers to specific areas.

Geochemical data: the data incorporated in Figure 1.2 are available in National Geochemical Reconnaissance 1:2 000 000 Coloured Compilation Map Series which may be purchased from Campbell Reproductions, 880 Wellington St., Ottawa, Ontario, K1R 6K7.

2.

GEOCHEMISTRY AND THE DISTRIBUTION OF URANIUM AND THORIUM IN THE GRANITOID ROCKS OF THE SOUTH MOUNTAIN BATHOLITH, NOVA SCOTIA: SOME GENETIC AND EXPLORATION IMPLICATIONS

A.K. Chatterjee[1] and G.K. Muecke[2]

Chatterjee, A.K. and Muecke, G.K., Geochemistry and the distribution of uranium and thorium in the granitoid rocks of the South Mountain Batholith, Nova Scotia: some genetic and exploration implications; in Uranium in Granites, ed. Y.T. Maurice; Geological Survey of Canada, Paper 81-23, p. 11-17, 1982.

Abstract

The peraluminous South Mountain Batholith (SMB) of Nova Scotia consists of a cogenetic granitoid suite ranging in composition from biotite granodiorites to highly leucocratic monzogranites. Economically significant U-Sn prospects and numerous occurrences show a close spatial and genetic association with the more highly differentiated phases of the SMB, and in particular with a paraintrusive suite developed in these bodies. In the cogenetic suite uranium concentrations increase progressively with differentiation, but thorium follows two distinct trends. Thorium concentrations and Th/U ratios decrease with differentiation in the New Ross complex, and the Lake George, East Dalhousie and West Dalhousie plutons. However, in the Davis Lake and Plymouth plutons thorium values increase concomitantly with uranium enrichment. Airborne gamma ray spectrometric maps have been used to distinguish areas of high total radioactivity (i.e. highly differentiated) and high thorium values within the batholith. Such areas correspond to bodies showing the thorium-enrichment trend and are concentrated near the margins of the batholith. Major U-Sn occurrences in the batholith appear to be preferentially associated with these bodies and airborne gamma ray spectrometric surveys provide information on the location of such bodies in less well known parts of the batholith. The strong enrichment of elements such as Li, Be, F, Rb, Cs, U, and Sn in members of the paraintrusive suite provides another possible lithogeochemical exploration tool.

Résumé

Le batholite peralumineux de South Mountain (BSM) de la Nouvelle-Ecosse est formé d'une série de granitoïdes co-génétiques dont la composition varie des granodiorites à biotite aux monzogranites fortement leucocrates. Des gisements d'U-Sn ayant un potentiel économique ainsi que de nombreux autres indices de métaux indiquent une association spatiale et génétique proche avec les phases les plus différenciées du BSM et en particulier avec une série para-intrusive qui s'est développée dans ces masses. Dans la série co-génétique, les concentrations d'uranium augmentent progressivement avec la différenciation, mais le thorium suit deux tendances distinctes. Les concentrations de thorium et les rapports Th/U diminuent avec la différenciation dans le complexe de New Ross, le pluton du Lac George, celui de Dalhousie Est et celui de Dalhousie Ouest. Cependant, dans les plutons de Davis Lake et de Plymouth, les valeurs du thorium augmentent parallèlement à l'enrichissement en uranium. Des cartes de spectrométrie aérienne des rayons gamma ont été utilisées pour distinguer les zones de radioactivité totale élevée (c'est-à-dire fortement différenciées) et les valeurs élevées en thorium dans le batholite. Ces régions correspondent aux masses montrant la tendance à l'enrichissement en thorium et sont concentrées près des marges du batholithe. Les indices importants d'U-Sn dans le batholithe semblent être associés de préférence à ces masses et les levés spectrométriques aériens des rayons gamma donnent des renseignements sur l'emplacement de tels masses dans les parties les moins bien connues du batholithe. Les forts enrichissements en éléments comme Li, Be, F, Rb, Cs, U et Sn dans les membres de la série para-intrusive fournissent un autre instrument d'exploration lithogéochimique possible.

Introduction

The South Mountain Batholith (SMB) is a posttectonic, peraluminous granodiorite-granite complex which outcrops over an area $>10^4$ km^2 of southwestern Nova Scotia (Fig. 2.1) and is one of the largest batholiths in the Appalachian geological province. During the past decade the SMB has been the site of increasingly intense mineral exploration which has culminated recently in the discovery of a major Sn (East Kemptville, Shell Minerals Ltd.) and a major U (Millet Brook, Aquitaine Mining Corp.) prospect, as well as numerous other showings of these metals (Fig. 2.1).

The SMB mainly intrudes deformed metawackes and metapelites of the Cambro-Ordovician Meguma Group, but along its northwestern margin it cuts metasediments and volcanics ranging in age from Ordovician to Lower Devonian (Emsian). Country rock deformation and metamorphism is attributed to the Acadian Orogeny, which in this region has been dated at 415-400 Ma (Reynolds and Muecke, 1978). Clastic sediments of Tournaisian age are found resting unconformably on eroded SMB. These stratigraphic controls necessitate that the intrusion, crystallization, uplift and erosion of the batholith be bracketed betwen Emsian and

[1] Nova Scotia Department of Mines and Energy, Halifax, N.S. B3J 2X1
[2] Department of Geology, Dalhousie University, Halifax, N.S. B3H 3J5

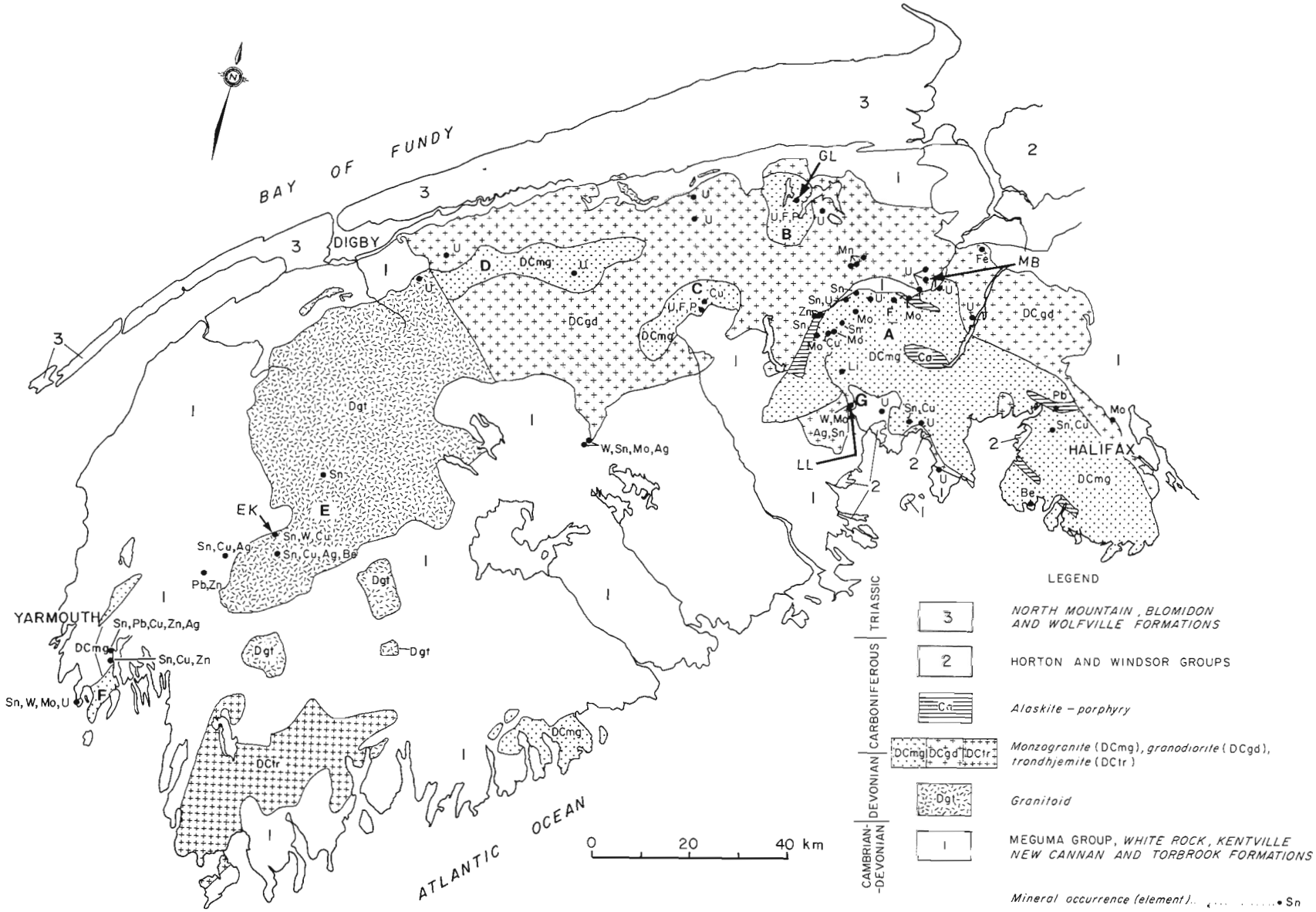

A = *New Ross complex*
B = *Lake George pluton*
C = *East Dalhousie pluton*
D = *West Dalhousie pluton*
E = *Davis Lake pluton*
F = *Plymouth pluton*
G = *Long Lake area*

Specific occurrences mentioned: Millet Brook (MB), Lewis Lake (LL), East Kemptville (EK), Gaspereau Lake (GL).

Figure 2.1. *Geological map of southern Nova Scotia showing the extent of the South Mountain Batholith and the distribution of major rock types. All known occurrences and prospects of U and Sn within, or closely associated to, the granitoid rocks are indicated.*

Tournaisian times. Recent Rb-Sr isochron ages of 372-361 Ma are assigned by Clarke and Halliday (1980) to the various episodes of intrusion in the batholith. K-Ar and $^{40}Ar/^{39}Ar$ studies by Reynolds et al. (1981) gave a mean age of 367 Ma for the batholith, in good agreement with the Rb-Sr ages. The intrusive episode therefore straddles the Devonian-Carboniferous boundary and the time span between complete solidification and surface exposure of parts of the SMB cannot have been more than a few million years. Such rapid unroofing of the batholith during (?) and following its emplacement has had a profound effect upon the localization of associated mineralization.

Petrology and Geochemistry

The main mass of the SMB consists of biotite granodiorites into which are intruded a number of smaller, discrete bodies of biotite-muscovite monzogranites (including porphyry), leucocratic monzogranites, dykes and irregular bodies of aplite and pegmatite (Fig. 2.1). Geochemically this suite varies in Thornton-Tuttle differentiation index from about 75-95 and contains 1-3 per cent normative corundum (McKenzie and Carke, 1975). The major and many trace elements of this suite show continuous variation trends from the early to late-stage rocks. From this, McKenzie and Clarke (1975) concluded that the SMB consists of a cogenetic suite whose chemical trends were controlled by fractional crystallization involving mainly plagioclase and biotite. Recent age determinations and Sr isotope studies strongly support such a cogenetic model. Although most large ion lithophile elements, especially Rb and Cs, show a predictable increase in abundance with increasing degree of differentiation some, such as the rare earth elements (REE), show a regular, but unexpected, decrease. Muecke and Clarke (1981) concluded from the REE and Sr isotope data that fractional crystallization alone cannot account for the trace element geochemistry of the late-stage rocks. They suggest that three processes, namely fractional crystallization, country rock assimilation, and fluid phase transfer, have all operated during the crystallization history of the SMB. The generation of a fluid phase, possibly enriched in fluorine, is thought to have played a major role in determining geochemical trends during the terminal phases of crystallization. The presence of such a fluid would also have had a profound influence on the behaviour of such economically important elements as Sn and U, since they can form stable fluoride complexes in aqueous solutions.

A paraintrusive suite, which consists of biotite leucogranites, argillized and sericitized granites, albitized granites and albitites, as well as various types of greisen, appears to be the product of the interaction of such a fluid phase with residual magma and/or the cogenetic crystalline rocks. The principal Sn-W, Sn-Be, Sn-W-U, W-Mo-U, and U-P-F mineralization in the SMB is usually spatially and genetically associated with the monzogranite and leucocratic monzogranite bodies, and in particular with paraintrusive rocks found within these complexes (Fig. 2.1).

Mineralization

The principal types of U and Sn mineralization so far recognized in the SMB are typified by the following:

i) In the New Ross area uraniferous shear zones occur in granodiorites at Millet Brook, in leuco-monzogranite at Lewis Lake, and at many other localities within the greisen zones. The shear zones show distinct evidence of cataclasis and generally trend northerly with varying dips. The uraniferous shear zones are usually characterized by strong alteration which includes hematization, muscovitization, albitization and in some cases silicification. The mineralized shear zones are characterized by autunite – torbernite – pitchblende associations and the gangue minerals may include calcite, quartz, hematite, pyrite, chalcopyrite, apatite, Li-micas, and albite.

ii) The uranium mineralization at Gaspereau Lake is restricted to an easterly dipping shear zone in leuco-monzogranite. The mineralization is characterized by autunite – meta-autunite – torbernite associated with hydroxyl – and fluor-apatites. Phosphatization, muscovitization and hematization of the wall rocks are typical alteration features. The style and geological setting of the mineralization at East Dalhousie is essentially similar to the Gaspereau Lake prospect. However, the shearing is more pronounced at East Dalhousie and uraniferous shear zones have a sheeted vein appearance. Also, albitization of the wall rocks is more intense and pitchblende is found in addition to uranium phosphate minerals.

iii) The Sn-W-Cu ± Mo mineralization at Davis Lake, Plymouth, and Long Lake is restricted to greisen zones and greisenized granites within discrete bodies (?) of leuco-monzogranite. The dominant polymetallic mineralization at these localities is found mostly as disseminations and as quartz-topaz-cassiterite-sulphide veins. The greisen zones and the veins range in width from hairline fractures to tens of metres. Diagnostic alteration associated with the mineralization includes fluoritization, muscovitization and albitization.

Sampling and Analytical Techniques

In the course of this project both surface and drill core samples were analyzed for major and trace constituents. Surface samples were carefully selected to include only the least weathered material and generally came from road cuts or trenches. No systematic differences could be detected between U or Th/U values obtained from outcrop samples and those from drill cores. An exception to this observation is one drill core from the New Ross area in which U is strongly depleted in the upper 100 m of core. We do not believe that this depletion is a surficial phenomenon but think that it stems from late-stage hydrothermal interaction.

U and Th were determined by instrumental neutron activation analysis (INAA) and delayed neutron activation analysis (DNAA). Other trace elements referred to in the text were determined by INAA (REE, Cs, Ta, Sc, Hf), atomic absorption spectrometry (Li) and X-ray fluorescence analysis (Rb, Ba, Sr, Ti, Zr, Sn).

Uranium-thorium distributions

In the cogenetic suite the mean U and Th abundances (3.9 ppm and 11.5 ppm, respectively) of the biotite granodiorites fall close to those postulated for average continental crust and the global average for granodioritic rocks (3 ppm, 10 ppm; Taylor, 1966). With increased degree of differentiation (using Thornton-Tuttle index) the mean U content rises to 6.1 ppm in the monzogranites and 8.3 ppm in the leuco-monzogranites for rocks from the New Ross, Lake George, East Dalhousie, and West Dalhousie plutons (Fig. 2.2). Thorium, on the other hand, decreases in abundance and mean Th/U ratios change from 3 in the granodiorites to 0.5 in the leuco-monzogranites (Fig. 2.3).

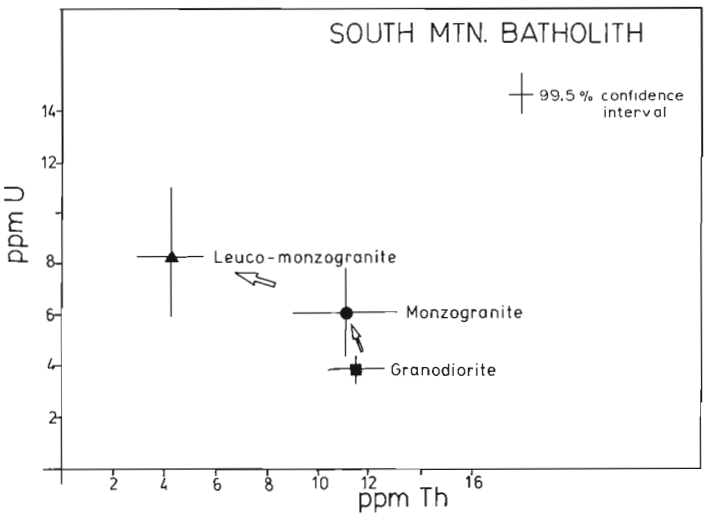

Figure 2.2

Th-U variation diagram showing means of major rock types of the cogenetic South Mountain Batholith suite and 99.5% confidence intervals on the means. Data for the monzogranites and leuco-monzogranites include the New Ross complex, Lake George pluton, East Dalhousie pluton, and West Dalhousie pluton.

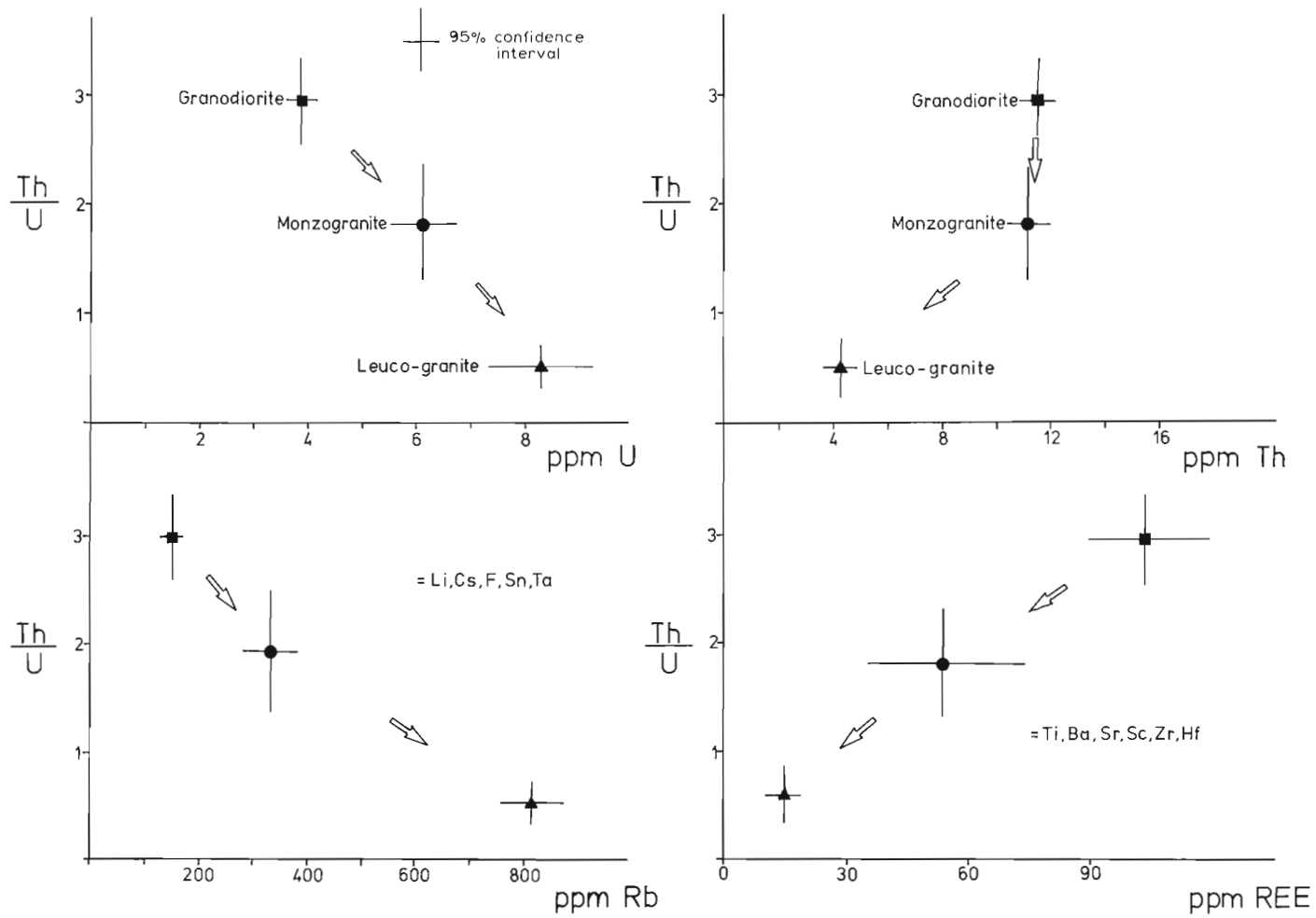

Figure 2.3. *Mean Th/U ratios of rock types constituting the cogenetic suite plotted against U and Th. Also shown are correlations with other trace elements. Note that REE, Ba, Sr, Ti, Sc, Zr, and Hf decrease with decreasing Th/U ratio (increased differentiation) in a manner similar to Th. Li, Rb, Cs, F, Sn, and Ta increase with decreasing Th/U, as does U. Data base same as Figure 2.2.*

Such a decrease in Th and Th/U (also of REE) is most unusual for a differentiated intrusive suite. The decrease in Th/U with differentiation is accompanied by strong progressive enrichments in F, Be, Li, Rb, Cs, Ta, Sn, and U, and depletions in Sr, Ba, REE, Sc, Zr and Hf (Fig. 2.3).

In the paraintrusive suite the elemental correlations described above often break down as particular elements may show extreme enrichments (e.g. U, Sn, Li) or depletions (e.g. REE, Th). For example, in some greisen zones REE values have been found to be depleted by a factor of up to 50 relative to host monzogranites, whereas Li enrichment commonly exceeds a factor of 10 (Charest, 1976). Thorium levels remain low during the alteration process.

The negative correlation between Th and U and the Th depletion with increasing differentiation (Fig. 2.2) which we have observed for most of the plutons is, however, not shared by all plutons in the SMB or those associated with it. Notable exceptions are the Davis Lake and Plymouth plutons which show a positive correlation between U and Th and elevated Th abundances in the most differentiated rocks and the paraintrusive suite (Fig. 2.4); both bodies are associated with substantial Sn-W mineralization.

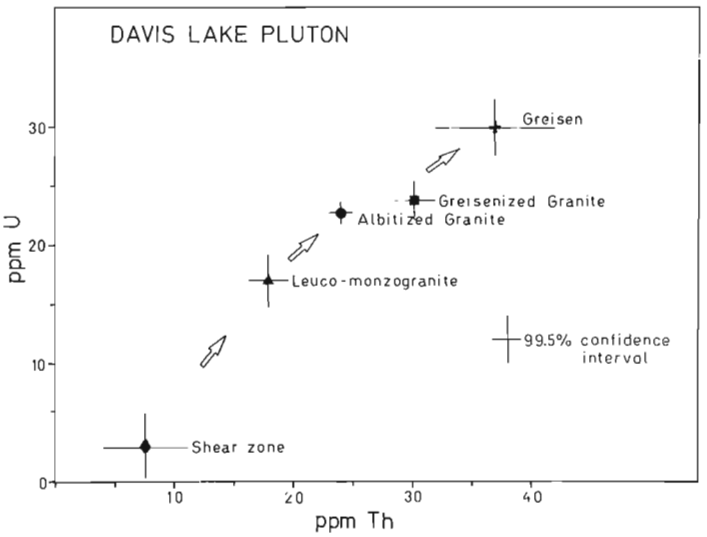

Figure 2.4. *Th-U variation diagram showing means of major rock types from the Davis Lake pluton. Note positive correlation between Th and U in contrast to trends observed in most plutons within the SMB (Fig. 2.2).*

Exploration Implications

From the above discussion it appears that two distinct geochemical trends can be discerned in the plutons which constitute the SMB: i) a Th-depletion (also REE depletion) trend in which increased igneous differentiation leads to low Th and low Th/U, both in the cogenetic and paraintrusive suites; and ii) a Th-enrichment trend in which highly differentiated rocks and paraintrusives are characterized by a concomitant increase in Th and U.

Airborne gamma ray spectrometric maps with 5 km line spacing flown in an E-W direction are available over the area of the SMB for total count (Ur), eK, eU and eTh (Geol. Surv. Can., 1977). We have analyzed these in an attempt to delimit the locations of bodies which display the above geochemical trends. In general, the areas of high total count (taken as >10 Ur; Fig. 2.5) conform to the major bodies of monzogranite and more highly differentiated rocks (e.g. New Ross complex, Davis Lake pluton). In some cases these more highly radioactive bodies show low Th counts (e.g. New Ross complex) in accord with the Th-depletion trend observed in ground sampling (Fig. 2.2, 2.5). The low Th content of Lake George and East Dalhousie monzogranites has apparently depressed the total count below our chosen threshold and contributed to the lack of strong total count anomalies over these bodies and confirms their affinity with the Th-depletion trend. In other cases, the high total count value is accompanied by a high Th count (>6 ppm eTh) and confirms the Th-enrichment trend observed in ground samples (e.g. Davis Lake). Superposition of the high total count (>10 Ur) and high Th (>6 ppm eTh) areas yields an interesting areal distribution (Fig. 2.5). High Th and high total count areas within the SMB show a well developed zonal distribution and lie near the margins of the batholith. Furthermore, a comparison of Figures 2.1 and 2.5 shows a close correlation between such areas and major mineral occurrences (i.e. Plymouth and Davis Lake plutons with Sn prospects; Millet Brook U prospect) which may be of exploration interest. This approach suggests that bodies in the SMB which show the Th-enrichment trend may be more favourable areas for Sn-U mineralization than those showing the Th-depletion trend. Using these criteria other areas in sparsely mapped portions of the SMB stand out as possible exploration targets, such as an oblong area south of West Dalhousie pluton along the southern margin of the batholith and an oval area west of Lake George pluton.

Other possible lithogeochemical indicators of Sn-U mineralization in the SMB are the strong enrichments of F, Be, Li, Rb, Cs, Ta, Sn and U encountered in the associated paraintrusive suite. From the available data it appears that the strongest Li enrichment is associated with those bodies showing predominant U mineralization (Fig. 2.6). Furthermore, a preliminary study of REE in fluorites from Sn-U mineralized and apparently barren areas (Muecke and Clarke, 1981) has shown that fluorites in the former have elevated REE concentrations and may prove to be guides to mineralization. Relative REE distributions in all the fluorites closely resemble those observed in the leucomonzogranites and reflect the close genetic link between the highly differentiated, late crystallized fractions of the batholith and the evolution of the fluid phase which gave rise to the observed mineralization in the SMB.

Vertical profiles of U distributions in the New Ross area show that near-surface samples (<100 m) can be markedly deficient in uranium, but other areas (e.g. Davis Lake) do not exhibit such a trend. We suggest that such distribution patterns are the result of the interaction of differentiated granitoid rocks with heated meteoric and/or internally generated fluids. These released and concentrated U through oxidation and complex formation.

Conclusions

The South Mountain Batholith consists of a series of plutons which were emplaced into Lower Paleozoic metasediments 372-361 Ma ago. Compositions range from early crystallized biotite granodiorites to late stage leuco-monzogranites, all of which are peraluminous and appear to be members of a cogenetic suite. Uranium always shows progressive enrichment with increased differentiation, but thorium follows two distinct trends. In the New Ross complex, Lake George, East Dalhousie and West Dalhousie

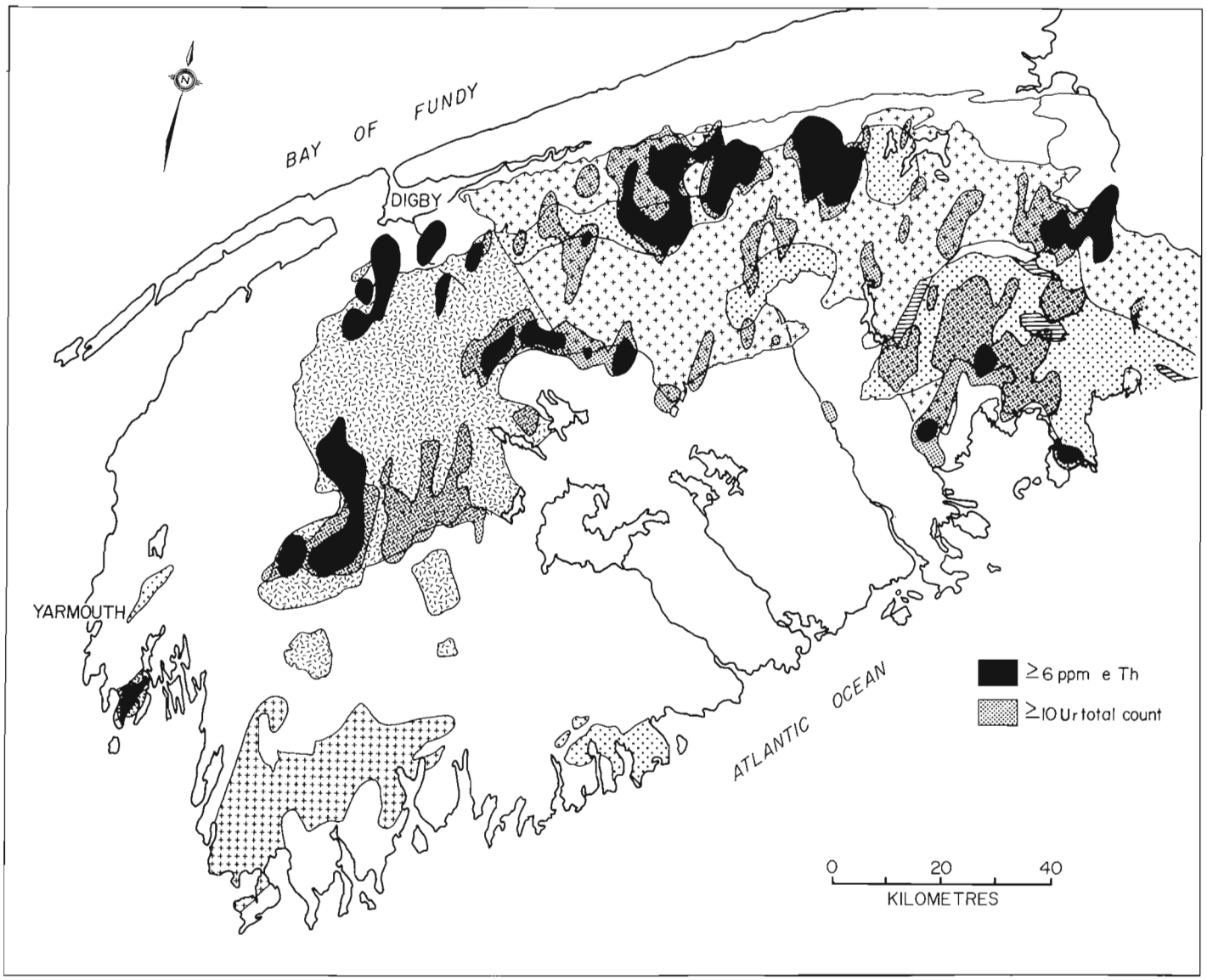

Figure 2.5 *(above). Map of southern Nova Scotia showing the correlation between areas of high total count (>10 Ur) and high thorium values (>6 ppm eTh), obtained from airborne gamma ray spectrometric maps (Geol. Surv. Can., 1977), and bedrock geology. Note the occurrence of high total count plus high thorium areas near the margins of the batholith. Lithologic symbols as in Figure 2.1.*

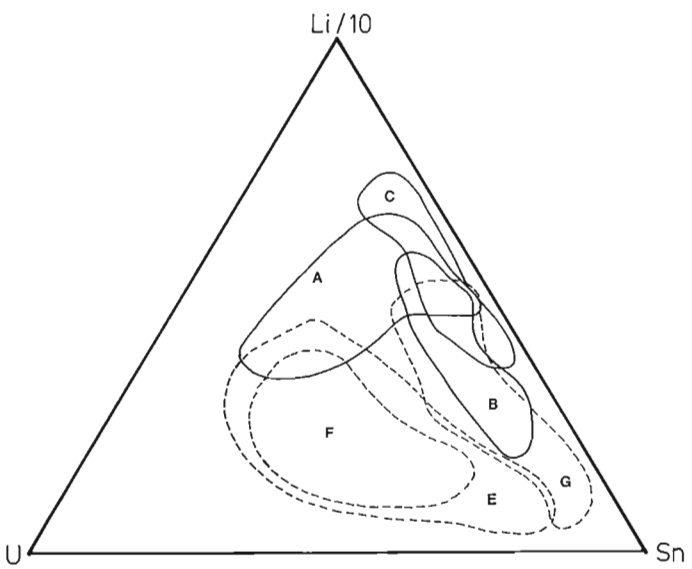

Figure 2.6. *Ternary variations diagram of Li-U-Sn for subdivisions of the South Mountain Batholith. The New Ross complex (A), Lake George pluton (B), and East Dalhousie pluton (C) are mainly associated with U mineralization and tend to show higher Li concentrations. The Davis Lake pluton (E), Plymouth pluton (F), and Long Lake area (G) are mainly associated with Sn mineralization and show lower Li concentrations.*

plutons, thorium decreases markedly with igneous differentiation, as does the Th/U ratio. On the other hand, in the Davis Lake and Plymouth plutons Th increases concomitantly with U. The paraintrusive rocks which are associated with the Th-depletion trend show the same trends as those observed in their cogenetic precursors; it has yet to be determined whether a similar relationship exists for the Th-enrichment trend. In the paraintrusive equivalents the elemental correlations observed in the cogenetic suite are, however, frequently obliterated by extreme enrichments or depletions of certain elements. Airborne gamma ray spectrometric maps can be used to identify areas in the SMB which exhibit the Th-enrichment or Th-depletion trends. Thorium-enriched areas show a strikingly consistent areal distribution and are located near the margins of the SMB. Major known occurrences of Sn and U appear to be spatially associated with the Th-enriched bodies and this correlation provides a criterion for favourable future exploration targets. The close association of the mineralization with the paraintrusive suite and characteristic strong elemental enrichments, particularly of Be, F, Li and Rb, provide further lithogeochemical guides to mineralization.

The localization of U mineralization along shear zones in the SMB suggests that the rapid unroofing of the batholith following its emplacement produced dilatancy and shear fractures which acted as channelways for mineralizing fluids which were produced as internally generated fluids or by the interaction of the differentiated granitoid rocks with hot meteoric water. Uranium concentrations of economic interest in the SMB are, therefore, the cumulative result of igneous differentiation processes and a hydrothermal system which acted on the cooling batholith during an episode of rapid uplift.

Acknowledgments

The authors gratefully acknowledge D.R.E.E. and N.S.E.R.C. grants in support of research, and the co-operation and assistance of Aquitaine Mining Corp. Canada Ltd., Esso Mineral Exploration and Lacana Mining Corporation.

References

Charest, M.H.
1976: Petrology, geochemistry and mineralization of the New Ross area, Lunenburg County, Nova Scotia; unpublished M.Sc. thesis, Dalhousie University, Halifax, N.S., 154 p.

Clarke, D.B. and Halliday, A.N.
1980: Strontium isotope geology of the South Mountain batholith, Nova Scotia; Geochimica et Cosmochimica Acta, v. 44, p. 1045-1058.

Geological Survey of Canada
1977: Airborne gamma-ray spectrometric maps, Annapolis-Shelburne, Nova Scotia; Open File 429.

McKenzie, C.B. and Clarke, D.B.
1975: Petrology of the South Mountain batholith, Nova Scotia; Canadian Journal of Earth Sciences, v. 12, p. 1209-1218.

Muecke, G.K. and Clarke, D.B.
1981: Geochemical evolution of the South Mountain batholith, Nova Scotia: rare-earth element evidence; Canadian Mineralogist, v. 19, p. 133-145.

Reynolds, P.H. and Muecke, G.K.
1978: Age studies on slates: applicability of the $^{40}Ar/^{39}Ar$ stepwise outgassing method; Earth and Planetary Science Letters, v. 40, p. 111-118.

Reynolds, P.H., Zentilli, M., and Muecke, G.K.
1981: K-Ar and $^{40}Ar/^{39}Ar$ geochronology of granitoid rocks from southern Nova Scotia: Its bearing on the geological evolution of the Meguma zone of the Appalachians; Canadian Journal of Earth Sciences, v. 18, p. 386-394.

Taylor, S.R.
1966: The application of trace element data to problems in petrology; Physics and Chemistry of the Earth, v. 6, p. 135-213.

3.

MINERALOGICAL AND PETROCHEMICAL PROPERTIES OF HETEROGENEOUS GRANITOID ROCKS FROM RADIOACTIVE OCCURRENCES IN THE GRENVILLE STRUCTURAL PROVINCE, ONTARIO AND QUEBEC

J. Rimsaite[1]
Geological Survey of Canada

Rimsaite, J., Mineralogical and petrochemical properties of heterogeneous granitoid rocks from radioactive occurrences in the Grenville Structural Province, Ontario and Quebec; in Uranium in Granites, ed. Y.T. Maurice; Geological Survey of Canada, Paper 81-23, p. 19-30, 1982.

Abstract

Granitoid rocks from radioactive occurrences in the Grenville Structural Province locally reach ore grade uranium concentrations of more than 0.05 per cent U. This paper discusses properties of ore grade specimens from the operating Madawaska uranium mine and several closed mines in the Bancroft area, Ontario, and compares them with those from radioactive occurrences in Mont-Laurier and Baie-Johan-Beetz areas, Quebec. One property common to all the granitoid rocks studied here is their heterogeneity, represented by the following features:

1. *erratic distribution of U, Th and rare-earth elements; discordant U, Th, Pb isotopic ages;*
2. *unusual hybrid petrographic characteristics of mineralized rocks;*
3. *heterogeneous minerals in hybrid mineralized zones; and*
4. *fracturing and associated diverse alterations.*

The heterogeneous nature of the host rocks, discordant isotopic Pb/U, Pb/Th and $^{207}Pb/^{206}Pb$ apparent ages and erratic variations of Pb/U and U/Th ratios in radioactiv minerals reflect a complex geological history which resulted in modifications of U-Th-Pb systems in the areas studied.

Résumé

Des roches granitoïdes radioactives localisées dans la province structurale de Grenville atteignent par endroits des concentrations de minerai d'uranium de plus de 0,05% d'U. Ce document a pour but de décrire les propriétés des spécimens de minerais provenant de la mine d'uranium de Madawaska an exploitation et de plusieurs mines fermées dans la région de Bancroft, en Ontario, et de les comparer avec ceux provenant de roches radioactives des régions de Mont-Laurier et de Baie-Johan-Beetz, au Québec. Une des propriétés communes à toutes les roches granitoïdes étudiées ici est leur hétérogénéité, représentée par les caractéristiques suivantes:

1. *une distribution erratique d'U, de Th et de terres rares; des âges isotopiques discordants d'U, de Th et de Pb;*
2. *des caractéristiques pétrographiques hybrides inhabituelles des roches minéralisées;*
3. *des minéraux hétérogènes dans les zones minéralisées hybrides; et*
4. *la formation de fissures accompagnées d'altérations variées.*

La nature hétérogène des roches hôtes, les âges apparents isotopiques discordants de Pb/U, Pb/Th et $^{207}Pb/^{206}Pb$ et les variations erratiques dans les rapports Pb/U et U/Th des minéraux radioactifs reflètent une histoire géologique complexe qui a amené des modifications dans les systèmes U-Th-Pb dans les régions étudiées.

Introduction

The Grenville Structural Province includes a great variety of polymetamorphic sedimentary and plutonic rocks. It occupies the southeastern portion of the Canadian Shield as a 300 km wide, 2000 km long belt from Georgian Bay northeast to the Atlantic Ocean (Fig. 3.1). Numerous radioactive occurrences, locally reaching ore grade uranium concentrations of more than 0.05 per cent U, are related to granitic and syenitic rocks which contain xenoliths of metasediments and metagabbro.

The purpose of this study is to establish favourable criteria for locating uranium ore zones in vast granitic terranes using mineralogical, petrochemical and isotopic characteristics of radioactive occurrences. Three areas selected for comparative field and laboratory studies are the Bancroft area, Ontario (45°N, 78°W), and Mont-Laurier (46°50'N, 75°20'W) and Baie-Johan-Beetz (50°16'N, 65°30'W) areas, Quebec (Fig. 3.1). References to previous studies and maps showing radioactive occurrences and sampling localities in these three areas are given in previous reports (Rimsaite, 1978, 1980a, 1981a). Only selected references to basic geological studies and mapping of the three areas are included here, namely, extensive studies of radioactive occurrences in the Bancroft area by Hewitt (1957) and Satterly (1957); mapping and petrology of Patibre Lake area, north of Mont-Laurier by Kish (1977) and of Baie-Johan-Beetz area by Cooper (1957).

[1]601 Booth Street, Ottawa, Ontario K1A 0E8

Table 3.1. Partial chemical analyses * of selected minerals and rocks from radioactive occurrences in the Grenville Structural Province

Specimen	Elements in ppm					Oxides weight per cent								
	U	Th	U/Th	Rb	Sr	SiO_2	Al_2O_3	MgO	FeO**	Fe_2O_3	CaO	Na_2O	K_2O	H_2O/F
Bancroft area, Ontario: mineralized zones between mafic xenoliths, granite, fluorite and marble														
1. Melanocratic ore***	3660	8600	0.42	60		33.0	4.0	3.0	6.0	3.0	19.0	1.0	1.0	50.0
2. Melanocratic ore***	2530	1830	1.43	90		49.9	10.1	4.5	7.6	4.1	13.3	3.0	2.1	0.20
3. Melanocratic ore***	6370	3610	1.67	90		46.0	8.0	4.0	5.1	3.0	17.0	3.0	1.0	0.67
4. Leucocratic ore	932	518	1.67	60		70.1	13.5	0.4	1.2	0.1	3.1	7.0	1.0	33.3
5. Leucocratic ore***	4210	940	5.00	220		58.6	12.5	2.9	3.6	1.7	6.9	4.0	4.3	2.50
6. High grade ore***	36100	10200	3.33			50.0	8.0	1.0	(4.5)		5.0	1.0	0.5	10.0
7. Muscovite	8			1630	33	46.5	32.4	1.5	1.0	3.4	0.0	0.6	10.0	50.0
8. Biotite from ore 6	900	70	12.5	8009	120	41.9	10.4	14.3	10.5	6.3	0.2	0.1	9.7	0.43
9. Phlogopite in CaF_2	< 1			478	17	43.5	11.6	27.9	0.3	0.8	1.5	0.3	9.5	0.36
10. Hornblende from ore	2					42.8	11.4	10.4	11.3	7.2	11.4	2.3	1.6	0.67
11. Biotite in migmatite	3			730	67	41.3	13.1	16.2	11.8	2.1	0.5	0.1	9.1	1.00
12. Hornblende with 11	2			40		45.1	8.9	12.5	9.9	5.7	11.3	1.4	1.4	1.25
Baie-Johan-Beetz area, Quebec: mineralized transition zones between paleosome and neosome rocks														
13. Metagabbro	4	8	0.50	15		41.7	9.8	5.9	12.8	6.9	12.0	1.5	1.0	33.3
14. Mica schist	10	3	3.33	129		47.6	12.3	8.9	9.1	4.2	6.8	3.1	1.9	50.0
15. Mica schist/syenite	4620	586	7.69	90		62.8	21.8	0.1	0.2	0.1	2.8	9.3	0.7	50.0
16. Syenite ore	3060	617	5.00	114		61.0	15.0	1.0	3.1	2.0	1.0	6.0	1.0	20.0
17. K-spar-rich neosome	50	41	1.25	1125		53.4	12.7	4.9	11.7	3.5	0.1	0.8	7.1	5.00
18. Pyrochlore-rich ore***	287	896	0.33	112		65.3	15.8	0.4	1.5	2.8	1.7	7.2	0.8	50.0
19. Silica-rich noesome	1020	303	3.33	120		77.4	12.6	0.2	0.8	0.5	1.0	4.5	2.2	10.0
20. Biotite in pegmatite				1525		37.3	17.6	7.9	16.6	4.4	0.1	0.5	8.4	3.70
21. Muscovite with 20				2125		44.3	33.6	1.0	1.2	4.2	0.0	0.7	10.1	20.0
Mont-Laurier area, Quebec: mineralized transition zones between biotite schist and pegmatite														
22. Metagabbro	0.3	3	0.10	4	60	47.6	4.4	13.1	7.9	1.6	17.1	0.5	0.5	10.0
23. Mafic xenolith	3	13	0.25	36	80	57.7	13.3	5.4	5.0	3.1	6.8	3.6	1.2	5.88
24. Biotite schist	2	15	0.13	112	290	68.3	15.7	1.2	2.1	1.2	3.1	4.6	2.7	9.09
25. Rusty biotite gneiss	6	19	0.33	105	160	63.6	15.1	2.3	0.0	6.0	2.9	3.8	2.0	12.5
26. Mica pegmatite	1120	278	5.00	162	210	71.2	15.0	0.4	1.2	0.2	1.8	3.9	4.6	10.0
27. Mica pegmatite	2580	608	5.00	255	50	66.0	11.2	1.9	4.6	4.0	1.8	1.7	4.0	7.69
28. Silica-rich granite	230	472	0.50	122	110	79.9	10.9	0.7	1.0	0.7	1.3	3.4	1.2	5.88
29. Zoisitic pegmatite	131	152	0.83	103	220	74.2	14.1	0.1	0.6	0.1	1.5	4.3	3.4	10.0
30. Oxidized syenite	533	2120	0.25	24	510	61.6	19.8	0.0	1.2	2.1	3.6	7.3	1.7	100.0
31. K-spar pegmatite	697	3180	0.22	280		74.3	12.3	0.6	0.5	1.0	0.7	1.5	6.8	7.14

* Uranium (ppm) determined by neutron activation analysis by Atomic Energy of Canada, Ltd.
Thorium (ppm) determined by X-ray fluorescene analysis by Bondar-Clegg & Co., Ltd.
Chemical analyses (wt %) by the Analytical Section, Central Laboratories and Technical Services Division, Geological Survey of Canada

** Brackets indicate total iron reported as FeO.

*** Ore specimens contain the following constituents: no. 1 abundant anhydrite; no. 2, 3 and 5 calcite and fluorite; no. 6 abundant allanite and titanite; no. 18 monazite and xenotime

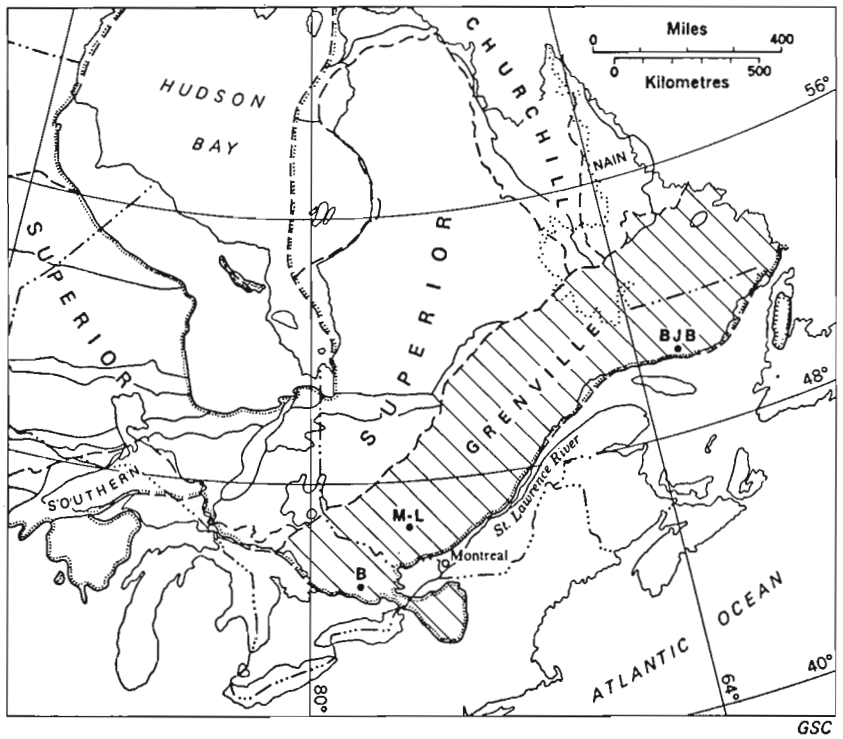

Figure 3.1

Geological sketch map showing subdivisions of the Canadian Shield and three locations of radioactive granitic rocks in the Grenville Structural Province selected for this study: B = Bancroft area, Ontario; M-L = Mont-Laurier area, Quebec; BJB = Baie-Johan-Beetz area, Quebec.

This paper summarizes preliminary results of isotopic, mineralogical, petrological and petrochemical studies (Tables 3.1., 3.2, 3.3) of selected ore grade and lower grade radioactive occurrences, and discusses the following features common to the three areas;

1. erratic distribution of U, Th and rare-earth elements (REE) and discordant U, Th and Pb/Pb isotopic ages;
2. unusual hybrid petrographic characteristics of mineralized rocks;
3. heterogeneous minerals in hybrid mineralized zones;
4. fracturing and associated diverse alterations.

Laboratory research included optical study of thin and polished thin sections under the petrographic microscope; study of distribution of radioactive minerals in autoradiographs of thin sections (Fig. 3.2a,b); determination of Pb, U and Th concentrations in whole rocks, in mineral concentrates and in individual mineral grains using neutron activation, X-ray fluorescence and energy dispersive spectrometer (EDS) methods; chemical analysis of minerals and rocks (Table 3.1); and scanning electron microscope (SEM), EDS and isotope studies of radioactive minerals (Fig. 3.3, 3.4, 3.5; Tables 3.2, 3.3). Figure 3.3 illustrates the advantage of backscattered electron images (BEI) over a photomicrograph taken under reflected light of poorly-reflecting minerals; in reflected light (Fig. 3.3a) uraninite, ilmenite, chlorite and REE-bearing mineral aggregates appear uniformly grey and can hardly be distinguished from one another, whereas in BEI (Fig. 3.3b), because of the difference in mass number of these minerals, uraninite appears white, REE-bearing portions of the rim are pale grey and chlorite in the rim and ilmenite appear dark grey. Thus BEI have been used to study replacements of uraninite by poorly-reflecting minerals.

Acknowledgments

These studies were supported by neutron activation analyses for U by Atomic Energy of Canada Limited; X-ray fluorescence determinations of Th by Bondar-Clegg and Company Ltd.; chemical and spectrographic analyses by the staff of the Analytical Chemistry Section; scanning electron microscope and energy dispersive spectrometer analyses by M. Bonardi, G.J. Pringle and D.A. Walker of the Mineralogy Section, Central Laboratories and Technical Services Division; preparation of drawings by S.B. Green of the Economic Geology Division and photographic plates by the staff of the Photography Section, Geological Survey of Canada; isotopic studies by G.L. Cumming and D. Krstic of the Department of Physics, University of Alberta (research contracts 0SU77-00353, 0SU78-00319 and 0SU79-00273, reports 1978, 1979 and 1980); and constructive criticism of the manuscript by R.T. Bell of the Geological Survey of Canada. The author gratefully acknowledges these contributions.

Erratic distribution of U, Th and REE and discordant U, Th and Pb isotopic ages

Radioactivity measurements in the field indicated erratic variations of U and Th within a distance of a few centimetres across some contacts between paleosome and neosome phases. About 50 samples representing major rock types and ore grade mineralization in the three areas were analyzed quantitatively for U, Th, major constituents and trace elements. Some of these analyses, including twenty-three elements and oxides determined on Baie-Johan-Beetz area have been discussed in some detailed in relation to chemical and mineralogical evolution of radioactive pegmatites (Rimsaite, 1981a, Table 17.2).

Table 3.2. Partial chemical analyses of selected radioactive and REE-bearing minerals and of their alteration products from granitic rocks in the Grenville Structural Province

Mineral	Element weight per cent*														
	U	Th	Pb (Zr)	Y (Ba)	Ce (Hf)	La,Pr Nd	Sm,Gd Er,Yb	Si	Ti	Al (Ta)	Fe	Mg (Nb)	Ca	P	Other
Fresh primary minerals															
1. Uraninite (BJB)**	61.0	5.4	8.0	3.2	-	-	-	0.2	1.6	-	0.8	-	-	-	-
2. Uranothorite (BJB)	11.0	37.4	-	2.8	2.2	2.4	1.8	5.8	0.4	0.6	0.8	-	0.2	1.2	-
2a. Uranothorite (M-L)	25.4	35.8	1.0	0.4	-	-	-	8.4	-	-	1.0	-	1.8	0.2	Cr,Mn
3. Pyrochlore (B)	21.0	0.4	-	0.8	0.8	0.4	0.8	1.2	0.2	(3.8)	1.2	(32)	1.8	-	Bi,Mn,W
3a. Pyrochlore (BJB)	14.8	2.8	-	10.2	-	-	-	0.8	15.2	0.6	4.4	(12)	1.4	-	-
4. Monazite (BJB)	-	3.8	-	-	23.2	21.2	4.2	0.6	-	-	-	-	-	11.4	-
4a. Xenotime (B)	-	-	-	35.4	-	-	15.	-	-	-	-	-	-	16.	-
5. Allanite (B)	0.1	1.0	0.2	0.1	9.	8.	0.3	15.	0.5	6.3	12.9	0.3	8.1	-	-
Secondary mineral aggregates replacing uraninite (U) and uranothorite (Th)															
6. Th, Si phase after U-1	43.0	12.2	5.8	1.6	1.2	-	-	2.4	-	0.2	3.6	-	1.4	0.2	-
7. REE phase after U (BJB)	23.2	5.0	4.0	7.2	8.6	7.0	-	3.6	1.0	0.4	6.6	-	1.4	0.4	-
8. Pb-rich phase after U	15.0	4.8	38.2	0.4	-	0.4	-	0.2	0.4	-	0.2	-	1.0	0.8	S
9. Brannerite-like (BJB)	34.0	0.8	-	3.6	1.8	0.6	1.8	1.6	23.0	-	2.2	(0.8)	1.6	-	-
10. Uranophane-like (B)	57.4	3.4	2.8	-	-	-	-	4.8	-	-	0.6	-	3.0	-	-
11. Kasolite-like (BJB)	39.0	-	15.0	(1.6)	-	-	-	3.8	0.2	1.8	6.6	0.4	0.2	-	Cr,K
12. Pb-rich after Th(M-L)	15.2	20.0	19.4	0.6	1.8	1.0	-	5.4	-	-	1.6	-	0.8	-	Mn,S
13. Fe-rich gummite (M-L)	12.8	11.6	0.8	-	-	-	-	2.0	-	1.4	35.6	-	-	0.4	Cr
14. REE-rich phase (BJB)	0.4	1.6	0.8	-	23.	21.4	-	2.8	-	1.6	-	-	2.2	-	K
Decomposition of metamict pyrochlore and separation of U, Nb, Ta and Y-rich phases (B), Figure 3.4d**															
15. U-rich phase	38.6	2.4	-	-	-	-	-	0.8	0.4	(4.6)	3.2	(19)	0.6	-	Bi,W
16. Nb-rich phase	1.8	-	-	-	-	0.2	1.2	-	0.8	(6.4)	12.	(48)	1.8	-	Mn
17. Ta-rich phase	14.2	0.4	-	3.0	-	-	-	1.4	0.4	(16.6)	0.4	(18)	2.0	-	-
18. U, Y, REE-bearing phase	11.8	1.2	0.4	5.0	0.4	0.4	7.5	-	1.2	0.2	2.4	-	3.4	-	-
Decomposition of metamict allanite and separation of U, Th, Fe and REE-rich phases (M-L), Figure 3.4e**															
19. Allanite altered	2.2	1.1	2.2	-	1.6	1.8	0.4	18.6	-	10.0	13.2	2.0	-	-	K
20. U-rich phase	10.0	8.6	5.2	0.6	2.8	3.4	-	4.4	1.0	0.8	20.8	-	0.8	-	-
21. U, Th-rich phase	12.0	29.6	1.4	2.8	2.0	2.4	1.2	5.8	0.4	0.6	3.0	-	0.2	0.6	-
22. Fe-rich phase	9.0	4.0	5.6	1.0	1.8	3.2	0.2	5.2	0.4	1.2	29.6	-	0.2	-	-
23. REE-rich phase	-	-	-	-	22.8	24.2	-	-	-	-	-	-	5.2	-	Sr
24. Allanite altered	3.2	3.6	1.8	0.2	4.	4.	0.4	10.2	0.2	4.4	6.6	0.8	0.8	-	K
Radioactive material in fractures and in rims surrounding mineral grains															
25. U-Pb phase (BJB)	32.4	-	25.8	-	-	-	-	6.2	0.6	1.4	5.4	-	0.4	-	Cr
26. U, Ti, Y phase (BJB)	13.6	3.4	1.6	7.6	-	-	-	3.0	27.6	0.8	4.2	(0.6)	1.2	1.5	S
27. U, REE-bearing phase	22.4	5.0	4.0	6.8	8.6	7.4	2.4	3.4	1.2	0.4	6.4	-	1.4	-	-
28. U, Th, Zr-bearing phase	17.6	10.8	(13.6)	2.2	(1.)	-	-	7.8	-	1.6	10.2	-	0.4	1.2	Cr

* Semiquantitative EDS analysis by G.J. Pringle of Central Laboratories and Technical Services Division, Geological Survey of Canada (Method described by Pringle and Thorpe, 1980)

** Specimens are from the following locations: (B) = Bancroft area, Ontario; (M-L) = Mont Laurier area, Quebec, (BJB) = Baie-Johan-Beetz area, Quebec

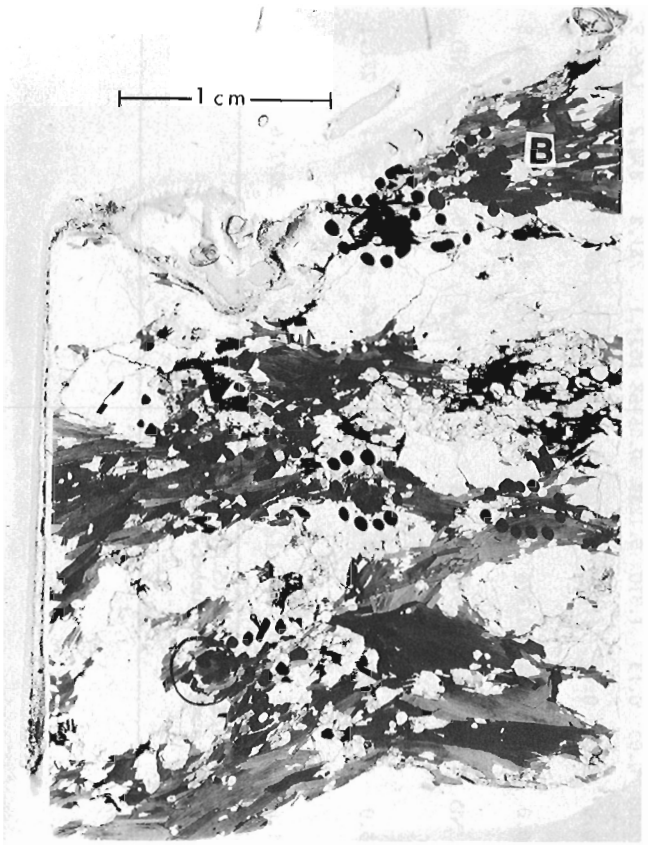

Figure 3.2a

Polished thin section of radioactive biotite-rich (B) pegmatite with black circles marking areas selected for scanning electron microscope (SEM) and energy dispersive spectrometer (EDS) analyses (GSC 203572-P).

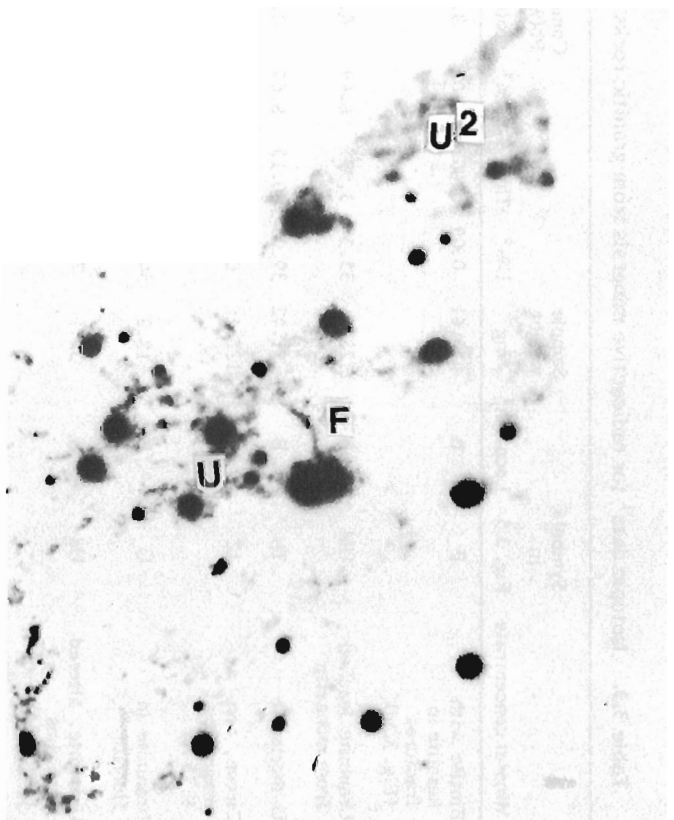

Figure 3.2b

Autoradiograph of the same polished thin section showing distribution of strongly radioactive primary uraninite and uranothorite (U), fractures filled with radioactive crusts (F) and cloudy grey areas of secondary radioactive minerals coating biotite flakes (U^2).

Table 3.3. Isotopic data[1] for radioactive minerals from granitic rocks in the Grenville Structural Province

Mineral concentrate	Symbol in Fig. 3.5	Location[2]	Sample weight mg	U%[3]	Th%[3]	Pb%[3]	Common Pb(% of total)	U/Th	Pb/Th	Pb/U	Apparent isotopic ages (Ma) $^{207}Pb/^{235}U$	$^{206}Pb/^{238}U$	$^{208}Pb/^{232}Th$	$^{207}Pb/^{206}Pb$	$^{206}Pb/^{238}U$	$^{207}Pb/^{235}U$	$^{208}Pb/^{232}Th$
Biotite with kasolite in fractures (Fig. 3.3d)	B	B	453.61	0.09	0.007	0.02	3.	12.99	0.07	0.22	2.249	0.2154	1.5025	1088.	1257.3	1196.4	18541.
Uraninite leached from monazite	UM	BJB	28.1	35.5	3.99	6.49	0.39	9.09	0.07	0.18	1.922	0.1931	0.04109	991.7	1338.0	1088.8	813.9
U-thorianite	Th	B	21.42	39.09	40.15	8.65	0.04	0.98	0.07	0.15	1.907	0.1841	0.05547	1072.	1089.2	1083.6	1091.3
Zircon, non-magnetic at 1.75 A	1Z	B	127.1	6.57	0.74	1.17	0.21	9.09	0.06	0.17	1.838	0.1822	0.09964	1019.	1078.8	1059.2	1919.8
Uraninite in fluorite	U	B	18.2	54.6	15.5	9.71	0.25	3.33	0.06	0.16	0.818	0.1773	0.05390	1051.7	1051.7	1051.9	1061.1
Uraninite, altered with rims (Fig. 3.3c)	Ua	B	37.1	7.4	4.4	1.19	0.46	1.67	0.06	0.13	1.540	0.1545	0.03266	994.5	926.	946.5	649.6
Monazite residue after HNO_3 leaching	M	BJB	250.7	0.61	0.427	0.361	0.26	1.43	0.45	0.20	1.495	0.1500	0.06500	995.0	900.9	928.5	1272.8
Allanite (Fig. 3.4e)	6A	B	394.1	1.27	0.65	0.19	1.52	2.00	0.05	0.13	1.310	0.1289	0.06468	1033.1	781.8	850.2	1266.9
Feldspar with uraniferous crusts	F	BJB	579.74	0.01	0.001	0.01	88.6	10.0	0.04	0.11	1.099	0.1105	0.1306	990.0	675.7	753.0	2480.0
Zircon with pyrite impurities	Z	M-L	37.6	0.31	0.007	0.025	3.52	50.0	0.25	0.08	0.776	0.0834	0.0854	852.0	516.6	583.2	1655.8
Titanite with uraniferous crusts (Fig. 3.3b)	T	B	421.7	0.03	ND	0.017	59.43	ND	ND	0.25	0.530	0.0538	ND	970.6	338.0	421.1	ND
Pyrochlore in muscovite (Fig. 3.4d)	8B	B	225.4	11.3	0.479	0.19	0.36	25.0	0.05	0.02	0.126	0.0179	0.0135	230.6	114.6	120.1	271.1
Feldspar with uraniferous crusts	FB	B	578.18	0.01	0.006	0.033	2.95	1.67	0.91	2.50	19.72	1.787	2.0718	1197.	6608.1	3077.6	22683.

[1] Isotopic data from Cumming, reports 1978, 1979, 1980, research contracts 0SU77-00353, 0SU78-00319 and 0SU79-00273.
[2] Location: B = Bancroft area, Ontario; BJB = Baie-Johan-Beetz area, Quebec; M-L = Mont-Laurier area, Quebec.
[3] Abbreviated from six decimal figures.
ND= not determined.

Thirty-one partial chemical analyses of selected rocks and rock forming minerals from the three areas are compared in Table 3.1 and show the following relationship between the lithology, U and Th concentrations and U/Th ratios: metagabbro and mafic xenoliths contain more thorium than uranium, the ratio U/Th being between 0.1 and 0.5; mica schists and gneisses contain somewhat more uranium than mafic rocks and variable proportions of thorium. In the mica schists analyzed here, the U/Th ratio varies between 0.13 and 3.3. The analyzed micas, muscovite, biotite and phlogopite contain only a few ppm uranium. However, Rb-F-rich biotite from the high grade uranium ore in the Madawaka Mine, Bancroft area, contains 900 ppm U and 70 ppm Th, mainly in uraniferous crusts that coat its basal fractures. The high U/Th ratio in this biotite (12.5) results from the presence of uranyl-bearing Th-poor, Pb-U-rich kasolite-like aggregates in its fractures (mica analyses 7, 8, 9, and 11 in Table 3.1). In ore grade samples U/Th ratios vary from 0.22 to 7.7 (Table 3.1, analyses 31 and 15), depending on type and degree of alteration of ore and accessory minerals.

Table 3.2 presents partial chemical analyses of the major types of fresh radioactive minerals and of their alteration products, thus indicating changes in concentrations of U, Th, Pb and other elements during alteration and pseudomorphous replacements by secondary compounds. The U/Th ratio was observed to vary by a factor of >20 from 0.09 to 2.0 in a single uraninite grain. This is because the uranium in the heterogeneous grain was replaced by a Th-Si phase (Fig. 3.3f). The high Th content creates problems in extracting uranium, therefore data on the variable U/Th ratio and on replacements of uraninite by Th-bearing compounds may be of a great importance in planning mining and recovery procedures. In metamict pyrochlore and allanite which contain U-rich, Th-rich, REE-rich and barren spots and bands, U/Th ratios vary also more than ten times, from 0.23 to 2.5 (Table 3.2, Fig. 3.4d,e).

In concentrates of radioactive ore and accessory minerals prepared for isotope research, U/Th ratios vary between 1 and 50, depending on mineral species.

Because radioactive minerals may provide direct information on the age of uranium deposits and on periods of alteration and mobilization of radioactive and radiogenic elements, the radioactive ore and accessory minerals were dated using their U/Pb, Th/Pb and $^{207}Pb/^{206}Pb$ isotope ratios. Proportions of radiogenic and common lead, other isotopic data and discordant isotopic ages in Table 3.3 and Figure 3.5 yield useful information on the stability and alterations of U, Th, Pb systems in various minerals that can be summarized as follows:

1. Two discordia lines intersect the concordia curve at approximately 980 Ma and 1090 Ma at the upper intersections and at 80 Ma and 120 Ma at the lower intersections respectively. The other Pb/U isotope ratios fall between these two discordia lines reflecting the age of crystallization and relative stabilities of U, Pb (Th) systems in the radioactive ore and accessory minerals in the three areas studied.
2. Only fresh uraninite from fluorite and thorianite yield nearly concordant isotopic ages and points on the concordia curve.
3. Most of the radioactive accessory minerals, namely allanite, pyrochlore, titanite and zircon yield points below the concordia curve thus implying preferential losses of radiogenic lead.
4. Titanite with uraniferous coating and crusts in fractures also yield discordant isotopic ages as a result of isotopic composition of mobilized uranium and radiogenic lead and the age of secondary uranium mineral aggregates in these crusts. Although traces of U may be present in titanite, uranium was not detected in the energy dispersive spectra of the titanite.
5. Pb-rich uranyl-bearing crusts formed from mobilized radiogenic lead and uranium in which Pb/U ratio exceeds 0.16, yield points above the concordia curve and very old apparent $^{206}Pb/^{238}U$ ages.
6. Uraninite from Baie-Johan-Beetz area that is partly replaced by unidentified Pb-rich phases yields Pb/U isotope ratios that fall above the concordia curve.
7. Secondary Pb-U minerals from Baie-Johan Beetz area contain more common lead than those from the Bancroft area.
8. The least stable U, Th, Pb system is in the pyrochlore crystals which yield the lowest points on discordia lines.

Initial $^{87}Sr/^{86}Sr$ ratio, determined on anhydrite concentrate from the Bancroft area is 0.7040[1] and reflects low Rb concentrations of the original evaporite-rich sediments in that area. More detailed discussions on the significance of discordant isotopic ages of minerals from radioactive granitoid rocks are given in previous papers (Rimsaite, 1980a, 1981b).

Unusual Hybrid Petrographic Characteristics of Mineralized Rocks

Radioactive granitoid rocks studied are hybrid and contain partly recrystallized xenoliths (inclusions) of pre-existing mafic, granitic and metamorphic rocks. The older (paleosome) and younger (neosome) portions of a radioactive rock can be recognized in thin sections. Contacts between paleosome and neosome phases and between leucocratic and melanocratic rocks are commonly favourable locations for crystallization of radioactive and accessory minerals. In the three areas studied, hybrid mineralized zones usually grade into relatively homogeneous coarse crystalline pegmatitic phases where feldspars reach several centimetres in diameter. Radioactivity measurements in such coarse crystalline terranes indicate relatively low and uniform distributions of U and Th, and their uranium concentrations determined by the neutron activation method, rarely exceed 50 ppm. Table 3.1 shows differences in uranium and thorium concentrations between mineralized hybrid mica schist/syenite, syenite and adjacent microcline-rich neosome rock. The U and Th concentrations are about 60 and 15 times lower respectively in the feldspar-rich neosome phase than in adjacent syenitic hybrid rocks (Table 3.1, analyses 15, 16, 17; Rimsaite, 1981a, Table 17.1). Mineralized contact zones consist of unusual mineral assemblages (Rimsaite, 1980b) and will be discussed in detail in a separate paper.

Heterogeneous Minerals in Hybrid Mineralized Zones (Table 3.2, Fig. 3.3, 3.4)

The rock-forming, accessory and ore minerals vary in size and exhibit replacement textures. Some minerals, such as feldspars, quartz, pyrite, zircon and some radioactive minerals occur in several generations, and, within a small area of a thin section may vary in size from several microns to more than a centimetre. Starting from the incorporations

[1] All isotope data supplied by Dr. G.L. Cumming of the Department of Physics, University of Alberta; Research contract and report numbers are given in Table 3.3.

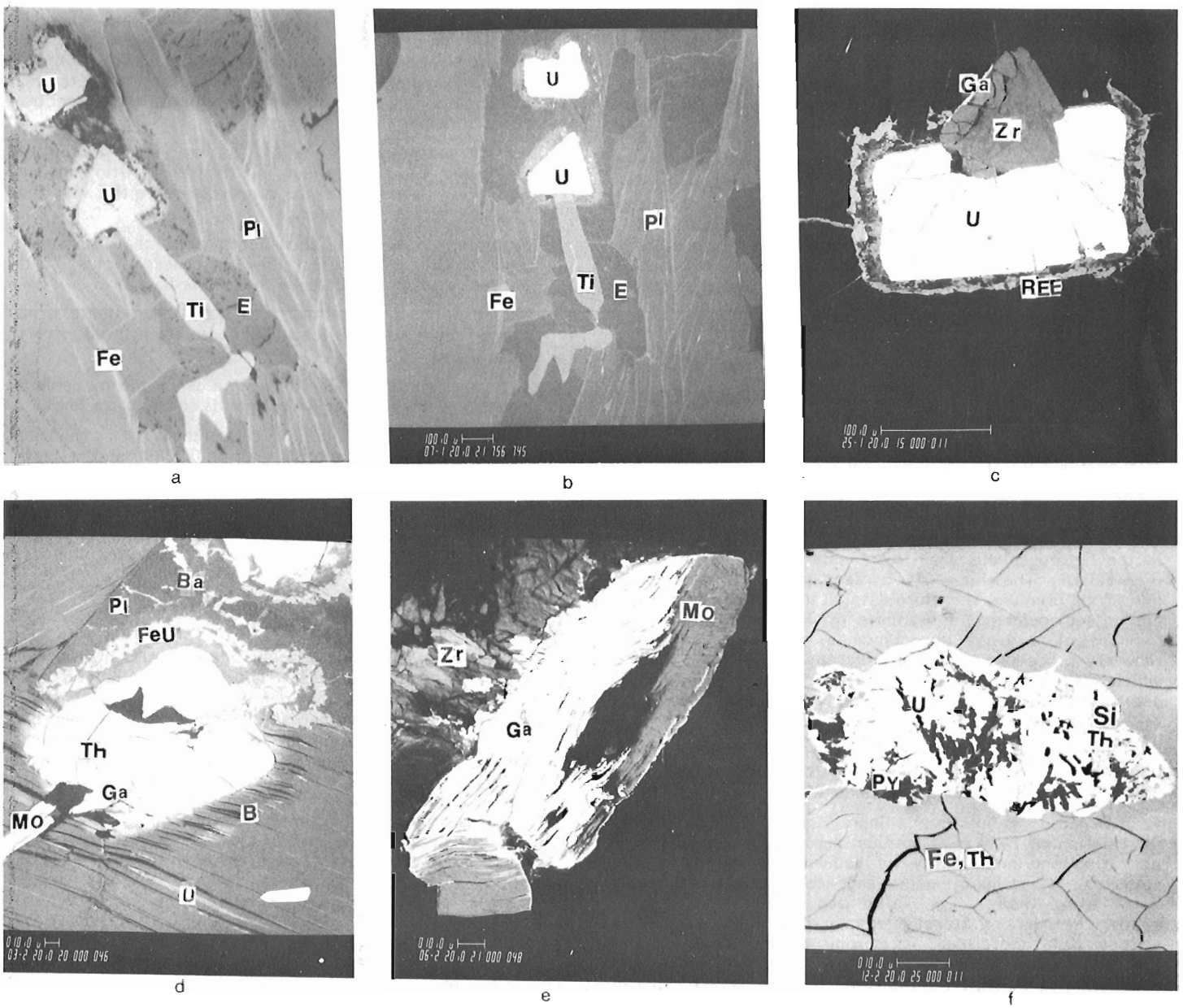

a. *Photomicrograph of uraninite (U) surrounded by prominent chlorite and REE-bearing rims in intergrowths with ilmenite (Ti) and a vug filled with epidote-zoisite (E), all in plagioclase (Pl). Fractures in plagioclase are filled with Fe-rich material (Fe). Reflected light, approximately same magnification as in Figure 3.3b.*

b. *BEI of the same areas as in Figure 3.3a. Because of mass differences, the dense uraninite (U) appears much brighter (white) than less dense ilmenite (Ti, grey).*

c. *BEI of fractured uraninite (U) and associated zircon (Zr). The uraninite has prominent REE-bearing rims (REE) that extend into fractures of adjacent silicates (white lines in black). Zircon grain is coated by white rims of galena (Ga).*

d. *BEI of thorite (Th) with white specks of galena (Ga) enclosed in Fe-U-bearing rims (Fe,U), all in biotite (B) adjacent to plagioclase (Pl) and molybdenite (Mo). Fractures in plagioclase are filled with barite (Ba), whreas basal fractures in biotite are filled with uraniferous mineral aggregates (U).*

e. *BEI of molybdenite (Mo, grey) that is partly replaced by galena (Ga, white) adjacent to shattered zircon (Zr).*

f. *BEI of ferroan thorite (Fe, Th, grey, transected by shrinkage cracks) and uraninite (U, mottled) enclosed in thorite. Fractures in uraninite are filled with Th-Si-bearing phase (Si, Th) and pyrite (Py, black specks).*

Figure 3.3. *Examples of U, Th and associated minerals and of their textures in radioactive granitoid rocks from the Grenville Structural Province (GSC 203414-X).*

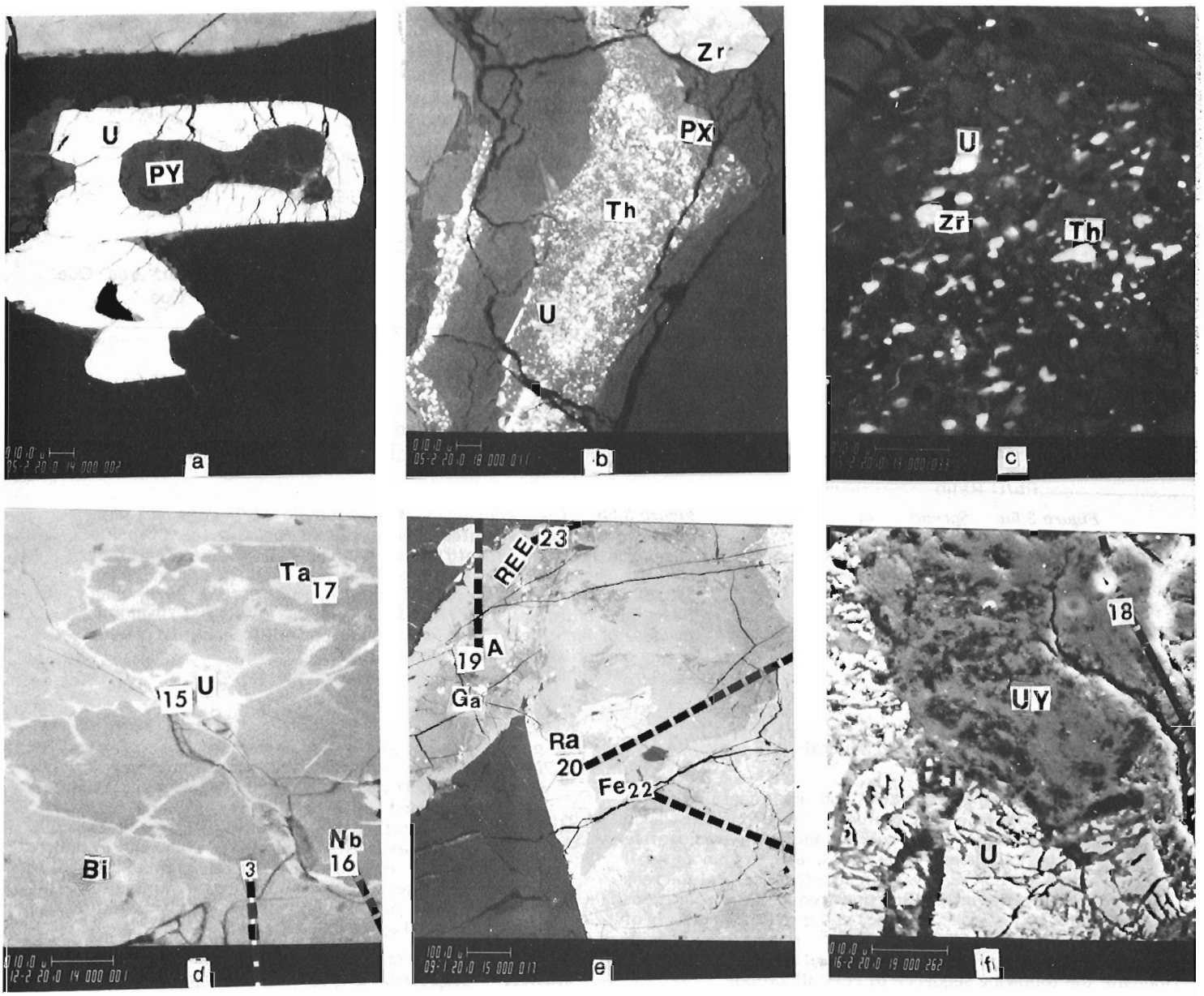

a. *BEI of uraninite (U) overgrowths on pyrite (PY).*

b. *BEI of pyroxene (PX) with small specks of thorite (Th) and uranothorite (U) adjacent to zircon (Zr).*

c. *BEI of a heterogeneous core of a zoned zircon (Zr) with disseminated specks of uraninite (U) and uranothorite (Th). The groundmass is fractured and consists of harder dark grey fragments of pure zircon in a black U-bearing softer phase.*

d. *BEI of metamict pyrochlore with small specks of native bismuth (Bi) and U-rich (U), Ta-rich (Ta) and Nb-rich (Nb) phases. Numbers correspond to analyses in Table 3.2.*

e. *BEI of metamict allanite with disseminated specks of galena (Ga), REE-rich rim (REE), strongly radioactive (Ra) and Fe-rich (Fe) areas. Numbers correspond to analyses in Table 3.2.*

f. *BEI of fractured uraninite (U) in intergrowths with Y-bearing grain (UY). Small circular area above number 18 marks analyzed spot (Table 3.2, analysis 18).*

Figure 3.4. *Associations between radioactive ore and accessory minerals and decomposition of metamict pyrochlore, allanite and U-Y-bearing grains (GSC 203414-W).*

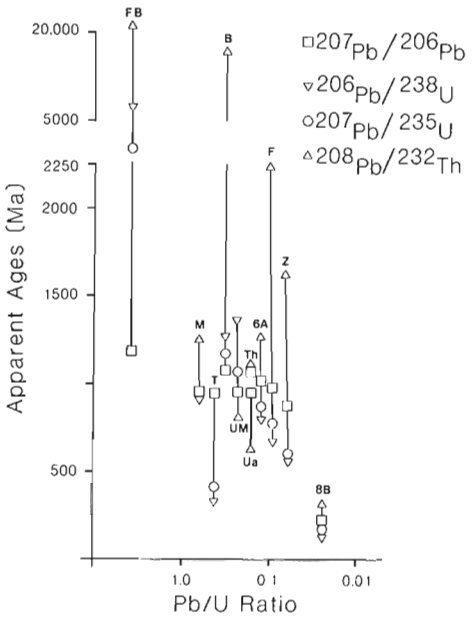

Figure 3.5a. *Spread of discordant apparent ages in relation to Pb/U ratio.*

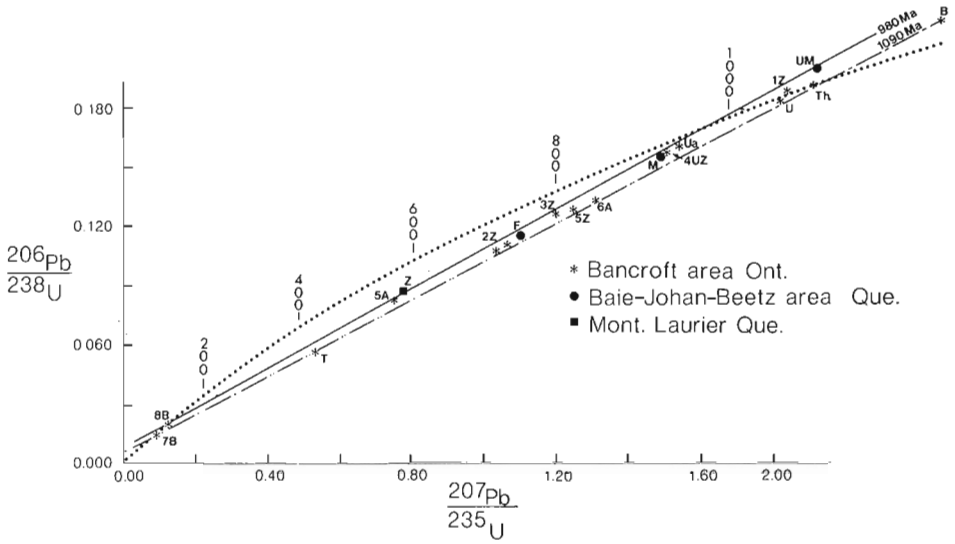

Figure 3.5b. *Concordia diagram for isotopic Pb/U data on radioactive mineral concentrates from granitoid rocks in the Grenville Structural Province. Identification of samples is given in Table 3.3. Data for some points have already been published (Rimsaite, 1980a; 1981a). Isotope analysis from Cumming, reports 1978, 1979, 1980 Research Contracts: 0SU77-00353, 0SU78-00319 and 0SU79-00273. Because of high Pb/U ratios, data for specimen FB cannot be plotted on the concordia diagram presented here.*

Heterogeneous Minerals in Hybrid Mineralized Zones (Table 3.2, Fig. 3.3, 3.4)

The rock-forming, accessory and ore minerals vary in size and exhibit replacement textures. Some minerals, such as feldspars, quartz, pyrite, zircon and some radioactive minerals occur in several generations, and, within a small area of a thin section may vary in size from several microns to more than a centimetre. Starting from the incorporations of paleosome mafic rocks, gneisses and quartzite, textures of rock-forming minerals and their relationships with radioactive minerals imply 4 periods of U mineralization and indicate the following sequence of crystallization:

a) garnet, pyroxene, hornblende, biotite, zircon, with first stage of crystallization of disseminated uraninite and uranothorite (Fig. 3.4b, c);

b) continuing growth of pyroxene and zircon, then plagioclase, pyrite, magnetite, rutile, apatite, monazite, xenotime, with formation of melanocratic ore as second or main stage of crystallization of thorianite, uranothorite and uraninite in and around mafic minerals;

c) continuing growth of plagioclase and zircon, then ilmenite, titanite, allanite, microcline, quartz, muscovite, epidote, hematite, sulphates, calcite and fluorite, with formation of leucocratic ore as third or deuteric stage of crystallization of uraninite, thorite and pyrochlore in prominent rims of mica, calcite, hydrous Fe-rich silicates, oxides and/or sulphides (Fig. 3.3a, b, c, d);

d) overgrowth of albite on plagioclase and formation of myrmekite, and molybdenite, galena, chlorite, sericite, secondary Fe, Ti and Pb oxides and sulphates, carbonates, clay minerals and vein quartz, with fourth or late deuteric stage mineralization as U, Pb, Th, REE complexd with other ions and as crusts along quartz veins and in biotite fractures, and coatings on mineral grains, mainly on titanite, apatite, fluorite and micas. Minerals of the earlier stages of crystallization locally alterated to hydrous mineral aggregates.

The complex mineralogy was observed in all three areas studied. However, proportions of these minerals are different. Pyroxene, anhydrite, calcite and fluorite are most abundant in the Bancroft area. Ti-bearing minerals and epidote are common in Mont-Laurier and Baie-Johan-Beetz areas and phosphates are abundant in Baie-Johan-Beetz area. Local variations are also present in all three areas studied. Some mineralized zones contain abundant apatite and epidote; other zones may contain xenotime, monazite and allanite.

Heterogeneity of minerals is interpreted to result from overgrowths, replacements, decomposition and alterations. The most common are porphyroblastic and poikilitic growth of microcline; perthitization of feldspars; veining by quartz and formation of quartz-albite and quartz-amphibole myrmekites; replacements of pyroxene by amphibole and serpentine-like minerals, and of biotite by chlorite and muscovite; replacement of uraninite by REE-Pb-rich and

Th-Si phases and by fine grained hydrous mineral aggregates; and replacement of molybdenite by galena (Fig. 3.3e). Decomposition of metamict pyrochlore and allanite and separation of U-REE-rich and other phases are illustrated in Figures 3.4d and 3.4e; and replacement of uraninite by U-Y veins is shown in Figure 3.4f.

Radioactive minerals commonly occur as discrete grains and crusts filling fractures at the contact between recrystallized mafic minerals of paleosome domains and neosome phases (Fig. 3.2a, b). Pyroxene, amphibole, titanite, pyrite, magnetite, ilmenite, allanite, zircon and biotite-muscovite intergrowths are the most favourable hosts for uraninite, uranothorite, zircon and other accessory minerals (Rimsaite, 1980a, Fig. 38.1, 38.2 and 1981a, Fig. 17.3).

Fracturing and Associated Alterations

In addition to being fractured by cooling and tectonic activity, radioactive rocks are shattered and fractured as a result of radiation. Distribution of the latter fractures and shattered zones is irregular, being related to heterogeneous and patchy distribution of radioactive minerals. Fractured zones are commonly altered and consist of various secondary minerals. In the samples studied, most uraninite and uranothorite grains are partly replaced by Si-, Pb-, REE-, and Fe-bearing phases and estimated remnants of the original mineral vary between 80 and 20% (Rimsaite, 1981a). The relationship between chemistry of the fresh and altered portions of uraninite, uranothorite, pyrochlore and allanite grains is given in Table 3.2. The altered grains usually retain 10 to 45% of the uranium. In the Mont-Laurier area, uraninite and uranothorite grains are commonly replaced by iron-rich gummite and secondary Ti-bearing minerals that retain some Th but lose much of the uranium (Fig. 3.3; Table 3.1, analyses 30 and 31). Feldspars commonly alter to patches of saussurite and sericite and contain numerous fractures filled with iron-rich and uraniferous compounds. Baie-Johan-Beetz area contains numerous secondary uranyl phosphates, such as autunite, torbernite and phosphuranylite. In the Bancroft area, uraninite grains alter to uranophane, kasolite, coffinite and rutherfordine.

Summary and Conclusions

The petrochemical, mineralogical and isotopic studies reveal a complex geological history of radioactive granitoids. The ore grade occurrences are characterized by erratic distributions of U, Th and REE and the hybrid petrographic nature of host rocks. In contrast, vast areas of relatively more anhydrous granitic rocks and graphic quartz-albite-microcline pegmatites have relatively uniform radioactivity with U values rarely exceeding 30 ppm.

This paper presents data on concentrations and distributions of U, Th, Pb and REE in uraninite, uranothorite, pyrochlore, allanite and in other accessory minerals and in their alteration products. Because high proportions of Th in uranium ore (Th>U) may cause problems in extracting uranium, the data on the abundance and variation of U and Th in fresh and altered minerals provide useful information for planning mining and recovery operations for the uranium. On the basis of her optical work, the author distinguished four stages of mineralization in the three areas studied: an early stage represented by disseminations of uraninite and uranothorite in rock-forming and accessory minerals of paleosome phases; the main stage associated with mafic minerals; and early and late deuteric stages in neosome phases. Locally U, Th and REE minerals are affected by weathering and oxidation, and partly replaced by secondary uranyl-bearing mineral aggregates.

A comparison based on preliminary data in Tables 3.1, 3.2, and 3.3 can be summarized as follows:

1. The early uraninite and uranothorite in melanocratic and syenitic phases are followed by crystallization of deuteric radioactive minerals enclosed in rims of fluorite, hydrous silicates, oxides or sulphides. Increasing silica content with the progressing evolution of radioactive pegmatites is illustrated for the three areas in Table 3.1 (analyses 1, 3, 2, 6, 5, 4 for the Bancroft area; 15, 16, 18, 19 for the Baie-Johan-Beetz area; and 27, 25, 31, 28 for the Mont-Laurier area);
2. Ore grade samples taken from ore zones underground in the Bancroft area contain about ten times higher uranium, thorium and calcium concentrations and ten times lower H_2O/F ratios than mineralized samples from the Baie-Johan-Beetz and Mont-Laurier areas.
3. The U/Th ratio for the ore samples of the Bancroft area is lower in melanocratic samples (0.42 to 3.3) than in leucocratic samples (1.7 to 5.0), the average being 1.4. For mineralized samples of the Baie-Johan-Beetz area (with >1000 ppm U), the U/Th ratio is high, partly as a result of the presence of uranyl-bearing phosphates. In the Mont-Laurier area, the U/Th ratio is high in radioactive mica pegmatites (5.0) and low in an oxidized syenite and K-feldspar pegmatite (0.25) in which primary uranium minerals have been destroyed by oxidation. The thorium is present in thorite and the less abundant uranium is in secondary uranyl-bearing minerals in fractures.
4. Isotopic data supplied by the University of Ablerta are summarized in figure 3.5. Two discordia lines intersect the concordia curve at approximately 980 Ma and 1090 Ma at the upper intersections and at 80 Ma and 120 Ma at the lower intersections respectively. The U-Th-Pb system appears to be least stable in the pyrochlore grains, which yield the lowest points on the discordia lines, and most stable in the uraninite that is enclosed in fluorite and yield Pb/U ratios that fall on the concordia curve near the upper intersection. Most of the samples were from the Bancroft area but the few data on samples from the Baie-Johan-Beetz and one zircon from the Mont-Laurier area yield points between the two discordia lines obtained on the Bancroft material.

Distribution of radioactive spots in autoradiographs indicate that mineralized granitoid rocks in the Grenville Structural Province represent an inital transitional stage from primary disseminated type to the vein-type granite deposit and provide excellent examples of natural chemical reactions that accompany mobilization and redeposition of uranium and other associated ions. The radioactive granitoid rocks studied locally contain ore grade uranium concentrations and, during alteration, can become an important source of U, Th and REE for the formation of other types of U, Th and REE deposits.

References

Cooper, G.E.
1957: Johan Beetz area, Electoral District of Saguenay; Department of Mines Quebec, Geological Report 74, 54 p.; map no. 1099.

Hewitt, D.F.
1957: General geology; in Satterly, J.: Radioactive mineral occurrences in the Bancroft area, Ontario; Ontario Department of Mines, 65th Annual Report, v. 65, pt. 6, 1956, p. 5-26.

Kish, L.
1977: Patibre (Axe) Lake area. Preliminary Report; Ministère des Richesses Naturelles, Service des Gîtes Minéraux, DPV-487, 13 p. and geological map 1:20 000 of DPV-487. (Placed on open file in January, 1977).

Pringle, G.J. and Thorpe, R.I.
1980: Bohdanowiczite, junoite and laitakarite from the Kidd Creek Mine, Timmins, Ontario; Canadian Mineralogist, v. 18, p. 353-360.

Rimasite, J.
1978: Mineralogy of radioactive occurrences in the Grenville Structural Province Ontario and Quebec; a preliminary report; in Current Research, Part B, Geological Survey of Canada, Paper 78-1B, p. 49-58.

Rimasite, J. (cont.)
1980a: Mineralogy of radioactive occurrences in the Grenville Structural Province, Bancroft area, Ontario: a progress report; in Current Research, Part A, Geological Survey of Canada, Paper 80-1A, p. 253-264.

1980b: Selected mineral suites and evolution of radioactive pegmatites in the Grenville Structural Province, Canada; 26e Congrès Géologique International (Paris), Résumés III, p. 999.

1981a: Petrochemical and mineralogical evolution of radioactive rocks in the Baie-Johan-Beetz area, Quebec: a preliminary report; in Current Research, Part A, Geological Survey of Canada, Paper 81-1A, p. 115-131.

1981b: Isotope, scanning electron microscope and energy dispersive spectrometer studies of heterogeneous zircons from radioactive granites in the Grenville Structural Province, Quebec and Ontario in Current Research, Part B, Geological Survey of Canada, Paper 81-1B, p. 25-35.

Satterly, J.
1957: Radioactive mineral occurrences in the Bancroft area, Ontario; Ontario Department of Mines, 65 th Annual Report, v. 65, pt. 6, 1956, 178 p. and geological map 1957b, Haliburton-Bancroft area.

4. URANIUM IN ALKALINE INTRUSIONS, SOUTHEASTERN BRITISH COLUMBIA

R.A. Burwash and K.A. Berndt[1]
University of Alberta

Burwash, R.A. and Berndt, K.A., Uranium in alkaline intrusions, southeastern British Columbia; in Uranium in Granites, ed. Y.T. Maurice; Geological Survey of Canada, Paper 81-23, p. 31-36, 1982.

Abstract

Six small Coryell (Tertiary) stocks have been sampled along an 80 km profile trending southwestward across the strike of the eastern part of the Omineca Crystalline belt. The profile extends from Mt. McGregor, near Kootenay lake, to Rossland. From field, petrographic and chemical data, all samples seem to belong to a single magmatic event.

The rocks range from shonkinite to leucocratic biotite syenite, with biotite augite monzodiorite the dominant phase volumetrically. Quartz appears in the norms of only 2 of 50 analyzed samples. Olivine, fresh or pseudomorphed, appears in most thin sections. The inferred parental magma is an alkaline olivine basalt.

U/Th values for the Coryell stocks are, on average, twice those of the Simpson Islands dyke, Northwest Territories, also of alkaline olivine basalt parentage. Along the Coryell profile, values of U/Th and K_2O/Na_2O decrease progressively from northeast to southwest. This decrease corresponds to a thinning of the sialic crust westward from the Purcell Arch. The U and K_2O changes can be explained as a function of crustal assimilation, controlled by crustal thickness.

Résumé

Six petits intrusifs de Coryell (datant du tertiaire) ont été échantillonnés sur une section de 80 km en direction sud-ouest, en travers de la direction de la partie est de la ceinture cristalline de l'Omineca. La section s'étend à partir du mont McGregor, près du lac Kootenay, jusqu'à Rossland. D'après des données pétrographiques et chimiques obtenues sur le terrain, tous les échantillons semblent appartenir au même événement magmatique.

Les roches varient de la shonkinite à la syénite à biotite leucocrate, avec la monzodiorite à augite et biotite comme phase dominante volumétriquement. Le quartz apparaît dans les normes de seulement 2 des 50 échantillons analysés. L'olivine, fraîche ou pseudomorphe, apparaît dans la plupart des sections minces. Le magma primaire probable est un basalte alcalin à olivine.

Les valeurs des rapports U/Th pour les intrusifs de Coryell sont, en moyenne, deux fois plus élevés que ceux du dyke des îles Simpson, des Territoires du Nord-Ouest appartenant aussi à la famille des basaltes alcalins à olivine. Le long de la section de Coryell, les valeurs des rapports U/Th et K_2O/Na_2O diminuent progressivement à partir du nord-est jusqu'au sud-ouest. Cette diminution correspond à un amincissement de la croûte sialique en direction ouest à partir de Purcell Arch. Les changements dans les concentrations de U et de K_2O peuvent être une fonction de l'assimilation de la croûte, contrôlée par l'épaisseur de celle-ci.

Introduction

In the Omineca Crystalline Belt of southeastern British Columbia a regional metamorphic/plutonic complex developed during Jurassic to Cretaceous time. The Nelson batholith and its satellitic stocks are the most voluminous representation of this plutonic event. In Early Tertiary time renewed deformation and metamorphism were accompanied by the intrusion of a series of alkaline batholiths and stocks, the Coryell plutonic rocks.

A series of small Coryell stocks along a profile across the regional trend of the Omineca Crystalline Belt are being studied by K.A. Berndt as an M.Sc. thesis project. Petrographic and petrochemical data are essentially complete, but isotopic studies are still in progress. Some of the conclusions presented here must be regarded as tentative. For the purpose of studying U-Th variation we have selected six stocks, all of which are 1 km or less in maximum dimension. By using plutons of almost uniform size it was hoped that we could eliminate petrological variations caused by differences in scale in any model we might derive.

Sample Profile

The most easterly identified Coryell stock is exposed on the summit of Mt. McGregor, 4 km west of Kootenay Lake (Fig. 4.1). Our profile extends 80 km southwest from Mt. McGregor to Rossland. The stocks sampled were chosen on the basis of geographical position and quality of exposure. Five of the six have blasted road and/or railway cuts.

At the present level of erosion most of the stocks are intrusive into units other than Nelson plutonic rocks. The host rocks and maximum dimensions of the stocks are given in Table 4.1. Approximately 100 samples were collected, from which 50 were selected for analysis for major elements (by XRF) and U and Th (by delayed neutron activation).

Petrology

The mineralogy of the Coryell stocks has been described by many workers (Rice, 1941; McAllister, 1951; Little, 1960). The most mafic rocks sampled in our fieldwork were shonkinites, forming a significant part of the core of Mt. McGregor and a minor phase of the rim of the Jersey

[1] Department of Geology, Edmonton, Alberta, T6G 2E3

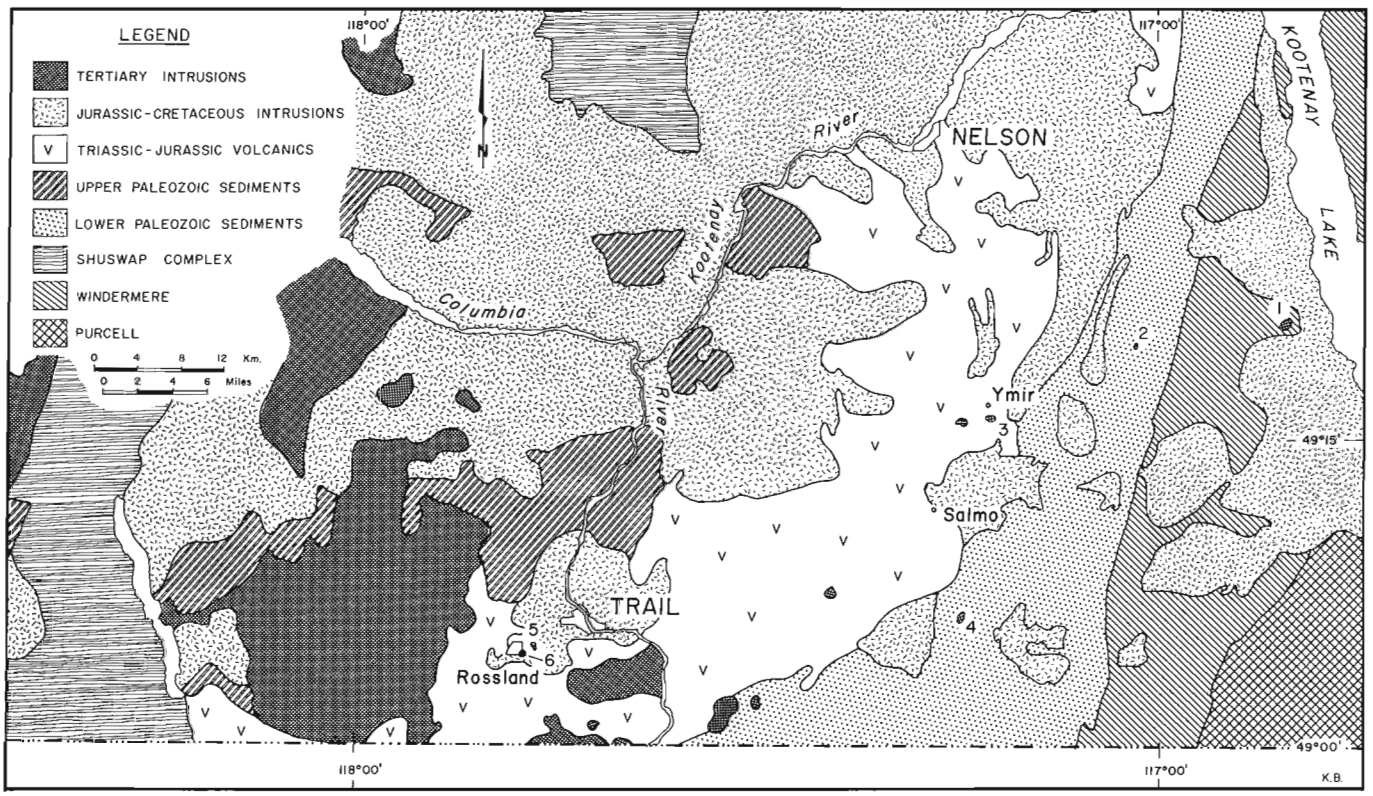

Figure 4.1. *Geological setting of Coryell plutons in the southern part of Nelson map-area (after Rice, 1941; Little, 1960). Sampled plutons numbered: 1 - Mt. McGregor, 2 - Cultus, 3 - Ymir, 4 - Jersey, 5 - Rossland (highway) and 6 - Rossland (railway cutting).*

pluton. Genetically, the shonkinites are classed as cognate inclusions. The 'average' Coryell intrusive rock of our profile is a biotite-augite monzodiorite of medium to coarse grain size. The persistence of olivine, the strongly perthitic orthoclase and the pyroxene hornfels contact metamorphic aureoles suggest relatively rapid fluid emplacement. Biotite-augite syenite, with a marked trachytoid texture, forms the core of the Ymir pluton. Late magmatic leucosyenite dykes fill minor fractures (1 to 5 cm) in the rims of the Ymir and Rossland plutons.

Table 4.1. Maximum dimension and host rock of sampled Coryell plutons

Pluton name and number*	Maximum Dimension (km)	Host Rock (Formation / Age)
1. McGregor	1.0	Horsethief Creek / Hadrynian
2. Cultus	0.5	Laib / Lower Cambrian
3. Ymir	1.0	Rossland / Jurassic
4. Jersey	1.0	Laib / Lower Cambrian
5. Rossland (highway)	0.6	Rossland / Jurassic and Nelson Pluton / Cretaceous
6. Rossland (railway)	0.4	Nelson Pluton / Cretaceous

* Locations plotted on Figure 4.1.

The petrochemistry of the Coryell rocks is best summarized on an AFM diagram (Fig. 4.2). Analyzed samples from each pluton are represented by a field, which encloses all points represented by one rock type or a continuously variable series of rocks (e.g. Mt. McGregor). A trend line fitted to the plotted fields resembles that of many other gabbroic differentiation series. However, Fe enrichment is a minor effect in the Coryell rocks (Fig. 4.3). From textural studies it appears that biotite forms early in the crystallization sequence, reducing the accumulation of Fe.

U-Th Variation

In studying the U-Th variation of the Coryell plutons it seemed desirable to find comparative data for an intrusive body of similar bulk chemical composition with a relatively simple tectonic setting. The Simpson Islands dyke, Great Slave Lake, is a composite body, resulting from an inferred gravitational differentiation of potassic olivine basalt magma within the upper mantle (Burwash and Cavell, 1978). The tectonic setting at the time of intrusion (2200 Ma) was the dilatant phase of the Athapuscow Aulacogen (Hoffman, 1973). The dyke cuts upper amphibolite to granulite facies Archean basement, probably restricting assimilation of U and Th from the wall rocks. The analytical methods used for the Simpson Islands and Coryell samples were the same.

Graphs of K_2O, U and Th vs. SiO_2 (Harker diagrams) for Simpson Islands rocks (Fig. 4.4) show parallel trends during differentiation, with a ten-fold enrichment of all three elements. The correlation coefficient between U and K_2O is +0.985. The U vs. SiO_2 plot for the 50 Coryell samples shows a much more complex pattern (Fig. 4.5). A separation of two divergent trends seems possible. One, with a gentle slope, converges with the Simpson Islands line near 4 ppm U and 60 per cent SiO_2. This could be considered a normal gabbro-syenite differentiation trend, with initial U values twice as high as Simpson Islands.

A different explanation must be sought for the steeply dipping line of points, most of which represent samples from Ymir and McGregor. The terminal point of this array best explains its significance. The lake dyke contains abundant poikilitic biotite flakes up to 2 cm in diameter. The dyke, 3 to 5 cm wide, is a late magmatic intrusive phase, emplaced in a shrinkage crack in the monzodiorite. Similar narrow veins were observed in the Rossland railway cut.

While most of the Coryell data for U shown in Figure 4.5 fall above the Simpson Islands trend line, the same is not true for Th (Fig. 4.6). If analytical error is considered, there is little difference between the main differentiation trends of Th in the Coryell and Simpson Islands suites. The late magmatic residual trend is defined by the same pair of samples as in Figure 4.5.

A plot of U vs. Th for the Ymir stock and the Simpson Islands dyke (Fig. 4.7) shows the consistency of U/Th ratios in comagmatic samples with extended compositional ranges.

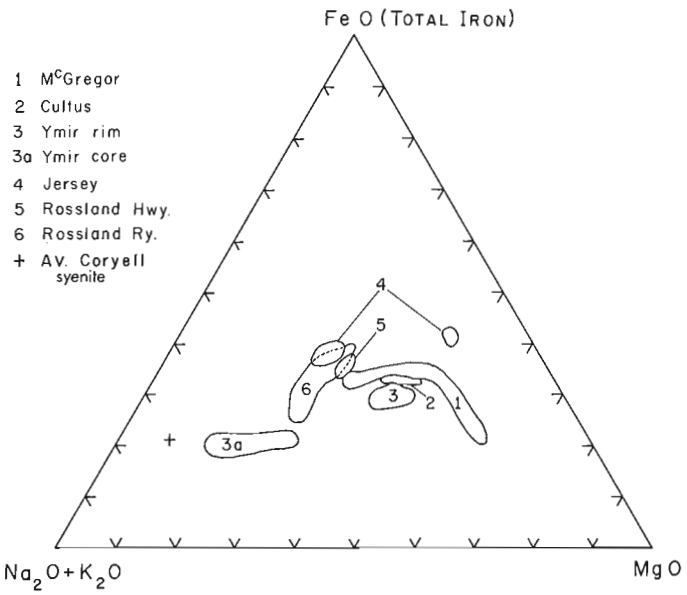

Figure 4.2. *Compositional ranges of Coryell plutons plotted on AFM diagram. Average Coryell syenite is a composite sample prepared by Little (1960, p. 91, sample 1).*

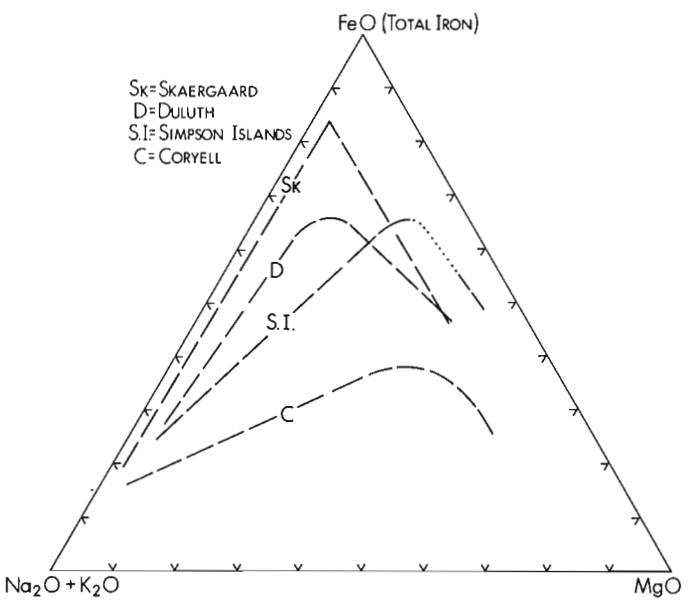

Figure 4.3. *Differentiation trend of Coryell plutons compared with other bodies of basaltic parentage, plotted on AFM diagram (Burwash and Cavell, 1978).*

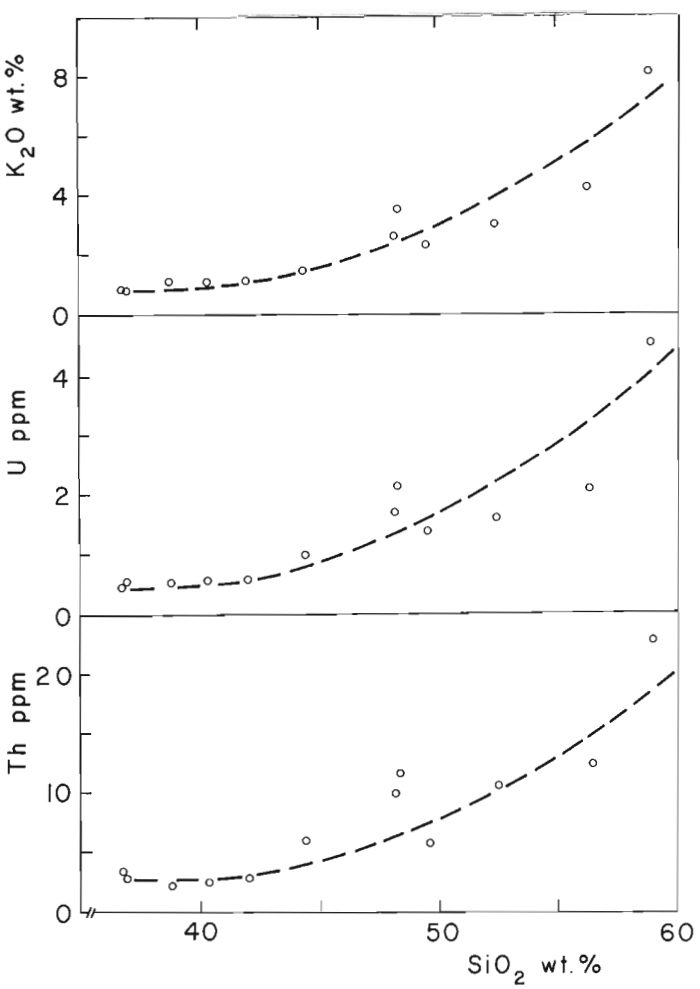

Figure 4.4. *Harker diagram of K_2O, U and Th data for the Simpson Islands dyke, Great Slave Lake, N.W.T. (Burwash and Cavell, 1978).*

For a given Th value the Ymir suite contains twice as much U as Simpson Islands. This is confirmed by the late pegmatitic phases of each intrusive; 4.51 ppm U in Simpson Islands, 8.78 ppm U in Ymir.

Average U/Th ratios of the six Coryell stocks studied (Table 4.2) range from 0.40 at Mt. McGregor to 0.27 at Rossland (highway). The change of ratio is consistent in a geographic sense, decreasing in a southwestward direction. When the ratio K_2O/Na_2O is tabulated, the potassic nature of the stocks is also seen to decrease to the southwest.

Processes of U-Th Enrichment

On the basis of the data from the Coryell plutons and the magmatically comparable Simpson Islands dyke, three main causes of U-Th enrichment are suggested in plutons derived from potassic olivine basalt magma:

1. In the mantle, the depth and degree of partial melting will control the composition of the juvenile magma with respect to incompatible elements, especially the large ion lithophile elements such as U, Th and K (Wyllie, 1971; Ringwood, 1975). We have no specific mineralogical data

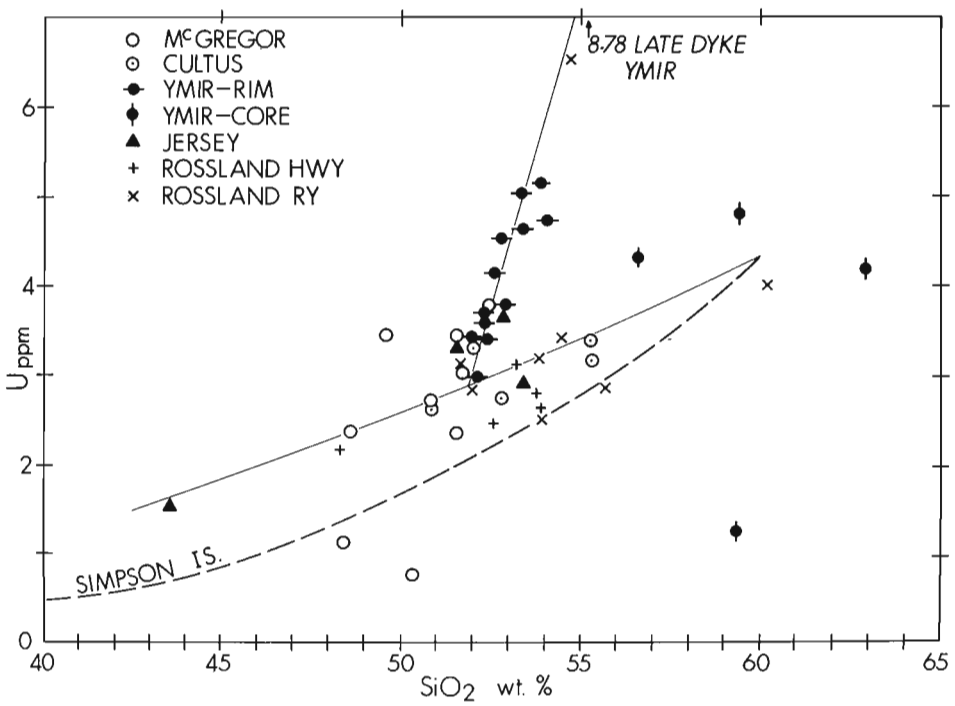

Figure 4.5

Harker diagram of U data for the Coryell plutons. Heavy dashed trend line taken from Figure 4.4.

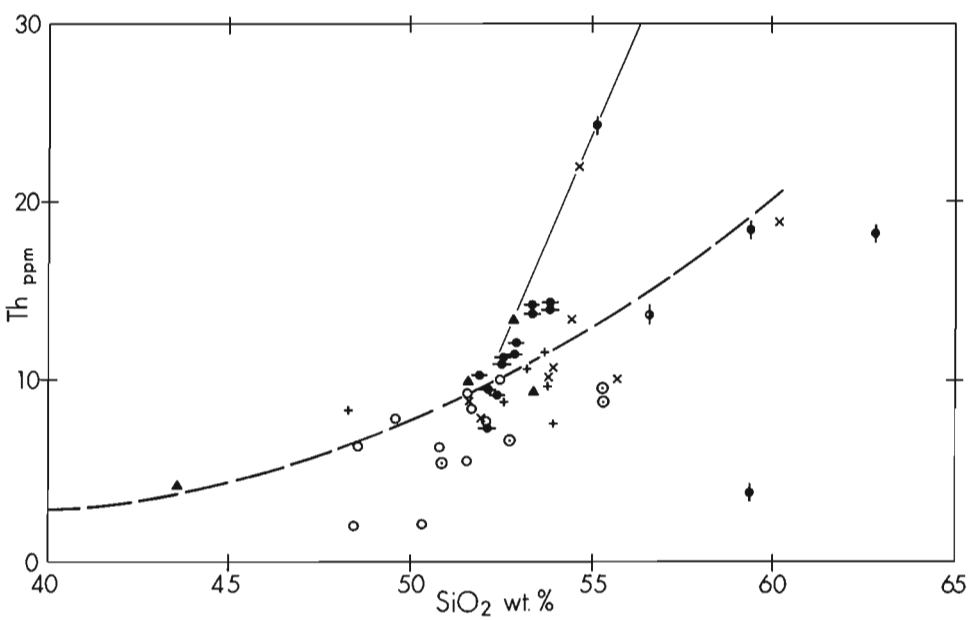

Figure 4.6

Harker diagram of Th data for the Coryell plutons. Heavy dashed line taken from Figure 4.4.

which will permit determination of depth of magmatic source for the Coryell rocks. However, the Simpson Islands model of Burwash and Cavell (1978) of <5 per cent partial melting at a depth of 100 km or less seems applicable.

2. Contamination of basaltic melt by older sialic crust is a strong possibility, either during a temporary residence at the base of the crust or during upward movement through the crust. If the crust is thick and has recently been involved in a major metamorphic episode the possibility of contamination would be enhanced. This is the model invoked for the Coryell stocks in the next section of this paper.

3. Differentiation of magma appears to concentrate U and Th in two stages (Figs. 4.5, 4.6). A progressive increase in both elements takes place throughout the range of SiO_2 values until a critical point is reached. This point appears to coincide with the crystallization of narrow pegmatite dykes, presumably from a melt with a volatile-rich fluid phase in equilibrium with the K-feldspar and biotite crystals. The steeply inclined trend lines on Figures 4.5 and 4.6 are the reflection of the late dykes.

Crustal Thickness

The Bouguer gravity anomaly map of Canada (Dominion Observatory, 1967) shows a marked negative anomaly (less than -200 mgal) along the Rocky Mountain Trench in southeastern British Columbia. This anomaly is associated

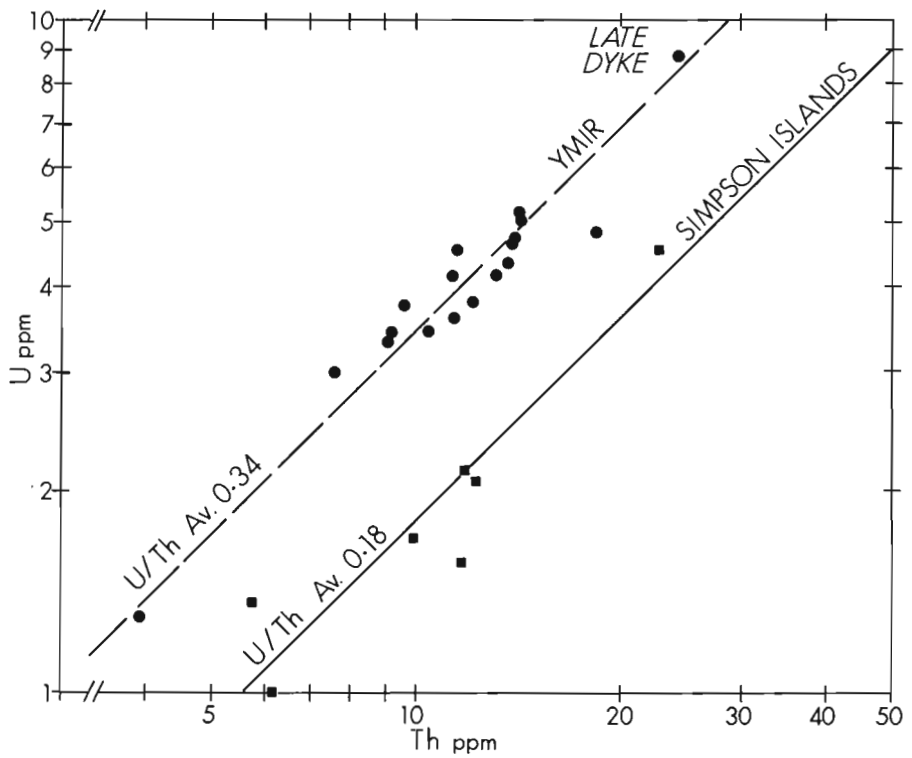

Figure 4.7

Plot of U vs. Th data for the Ymir pluton and Simpson Islands dyke. U/Th average of Simpson Islands based on 12 analyses; 5 less than 1 ppm not plotted.

Table 4.2. U, Th and K_2O/Na_2O values for the Coryell plutons

Pluton name and number	No. of Samples (n)	U (ppm. av.)	Th (ppm. av.)	U/Th	K_2O/Na_2O
1. McGregor	9	2.6	6.5	0.40	2.93
2. Cultus	5	3.1	7.7	0.40	2.52
3. Ymir	17	4.3	12.5	0.34	2.15
4. Jersey	5	2.7	8.9	0.30	1.87
5. Rossland (highway)	6	2.6	9.5	0.27	1.32
6. Rossland (railway)	8	3.6	12.8	0.28	1.34
7. Simpson Islands	12	(Variable)	(Variable)	0.18	0.67

Precision of U determinations is approximately 5 per cent for samples with <2 ppm U and averages 2 per cent for samples with >2 ppm U. Mass spectrometric analyses of samples with 15 and 23 ppm U give results closely comparable to those determined by delayed neutron activation, suggesting no consistent bias in the accuracy of our data (Burwash and Cumming, 1976; Burwash, unpublished).

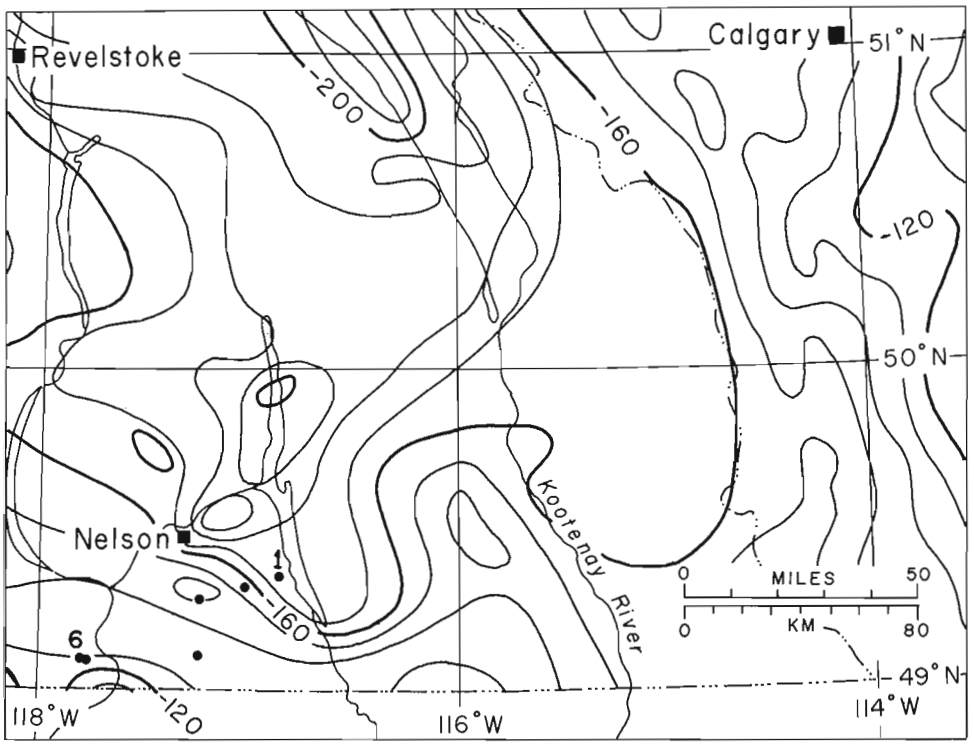

Figure 4.8

Bouguer gravity anomaly map of south-eastern British Columbia (from Dominion Observatory, 1967). Most negative areas (<-200 mgal) along Rocky Mountain Trench at about 51° N and near north end of Kootenay Lake. Coryell plutons of this study plotted in Nelson map-area. Bouguer anomalies range from about -175 mgal at Mt. McGregor to about -130 mgal at Rossland.

with crustal thicknesses in excess of 50 km (Berry et al., 1971). Our sample profile of six Coryell stocks extends southwestward from the margin of this gravity high toward the centre of the Omineca Crystalline Belt, where crystal thicknesses are in the order of 30 to 35 km (Fig. 4.8). When the data presented in Table 4.2 are assessed in relation to Figure 4.8, a strong argument can be made that changes in U/Th and K_2O/Na_2O are directly related to crustal thickness. If this is so, assimilation of older sialic crust was very likely responsible for augmenting U and K in the Coryell magmas.

Acknowledgments

Uranium and thorium analyses were made at the McMaster Nuclear Reactor with the co-operation of E. Hoffman. Whole-rock XRF analyses were done in the Department of Geology, McMaster University, with the co-operation of R.H. McNutt.

References

Berry, M.J., Jacoby, W.R., Niblett, E.R., and Stacey, R.A.
1971: A review of geophysical studies in the Canadian Cordillera; Canadian Journal of Earth Sciences, v. 8, p. 788-801.

Burwash, R.A. and Cavell, P.A.
1978: Uranium-Thorium enrichment in alkali olivine basalt magma-Simpson Islands dyke, Northwest Territories, Canada; Contributions to Mineralogy and Petrology, v. 66, p. 243-250.

Burwash, R.A. and Cumming, G.L.
1976: Uranium and Thorium in the Precambrian Basement of Western Canada. I. Abundance and distribution; Canadian Journal of Earth Sciences, v. 13, p. 284-293.

Dominion Observatory
1967: Bouguer Gravity Anomaly Map of Canada; Department of Energy, Mines and Resources, Ottawa.

Hoffman, P.F.
1973: Evolution of an Early Proterozoic continental margin: the Coronation Geosyncline and associated aulacogens, northwest Canadian Shield; Royal Society of London, Philosophical Transactions, Series A, v. 273, p. 547-581.

Little, H.W.
1960: Nelson Map-Area, West Half, British Columbia; Geological Survey of Canada, Memoir 308, 205 p.

McAllister, A.L.
1951: Ymir Map-Area, British Columbia; Geological Survey of Canada, Paper 51-4, 58 p.

Rice, H.M.A.
1941: Nelson Map-Area, East Half, British Columbia; Geological Survey of Canada, Memoir 228, 86 p.

Ringwood, A.E.
1975: Composition and Petrology of the Earth's Mantle; McGraw Hill, New York, 618 p.

Wyllie, P.J.
1971: The Dynamic Earth; John Wiley, New York, 416 p.

5.

CHARACTERISTICS OF THE OKANAGAN HIGHLANDS INTRUSIVE COMPLEX AS A SOURCE FOR BASAL-TYPE URANIUM DEPOSITS, SOUTH-CENTRAL BRITISH COLUMBIA

D.R. Boyle[1]
Geological Survey of Canada

Boyle, D.R., Characteristics of the Okanagan Highlands Intrusive Complex as a source for basal-type uranium deposits, south-central British Columbia; in Uranium in Granites, ed. Y.T. Maurice; Geological Survey of Canada, Paper 81-23, p. 37-47, 1982.

Abstract

Sedimentary hosted uranium deposits in the Okanagan region of British Columbia occur in unconsolidated, carbonaceous-rich, late Miocene fluvial channel sediments overlying Tertiary fault zones within the Okanagan Highlands Intrusive Complex. The complex consists of Cretaceous quartz monzonite, granodiorite and related pegmatites and Eocene monzonite and related dyke rocks. The deposits, classed as 'basal type', are at the basement-sediment contact and are capped by Pliocene valley basalts. All of the mineralization discoverd to date is in the form of uranous (ningyoite) or uranyl (saleeite, autunite) phosphates. The formation of these deposits is considered to be the result of structurally controlled, deep seated groundwater leaching of the basement complex with eventual infiltration into the fluvial channel sediments and precipitation of uranium phosphate minerals.

Geochemical studies of the Okanagan Highlands Intrusive Complex have been carried out to determine characteristics of favourable source rocks. The average uranium contents of quartz monzonite, granodiorite and Coryell monzonite (4.8, 2.3 and 6.2 ppm respectively) are in good agreement with world averages. Uranium displays significant positive correlations with the K_2O and SiO_2 contents of these rocks and marked negative correlations with mafic indicators such as MgO, CaO, FeO and MnO. Of the trace elements analyzed to date (F, Rb, Sr, Ba, V, Zr, U, Th) only Sr shows an increase above the norm for these rock types. The major element chemistries of the rock types in the complex are similar to world averages with the notable exception that all are enriched in CO_2, a feature which may be related to widespread carbonitization during Eocene volcanism. High CO_2 rock concentrations, together with the fact that recent, structurally controlled groundwaters draining fault zones in the intrusive complex have anomalously high U, HCO_3^- and P contents, may be diagnostic features of favourable source rocks.

Laboratory leaching experiments reveal that the intrusive rocks in the Okanagan Complex and many igneous counterparts elsewhere in the Cordillera contain similar amounts of labile uranium. The levels of labile uranium decrease in the order pegmatite-quartz monzonite-Coryell monzonite-granodiorite. Large volume percentages of medium- to coarse-grained, mica-bearing, leucocratic igneous rocks are a prerequisite for determining fertile source areas.

A sound knowledge of the sequence of tectonic events affecting an intrusive complex would appear to be more important in determining source potential than geochemical parameters, although all are interactively significant. Uranium deposits in the Okanagan region formed after a period of extensional tectonism (Late Miocene to Early Pliocene), leading to optimum groundwater leaching of a 'fabric loosened' intrusive basement complex, and prior to a period of epeirogenesis (Late Pliocene to Early Pleistocene), which resulted in cessation of the ore-forming hydrologic regime.

Résumé

Les gisements d'uranium dans les roches sédimentaires de la région d'Okanagan en Colombie Britannique se rencontrent dans des sédiments fluviaux non consolidés, riches en carbone, de la fin du Miocène, qui recouvrent des zones faillées du Tertiaire, à l'intérieur du complexe de roches intrusives des 'Highlands d'Okanagan'. Ce complexe est constitué de monzonite quartzifère du Crétacé, de granodiorite et de pegmatites associées, de monzonite de l'Eocène et de roches filoniennes associées. Les gisements, classés comme 'type basal', sont situés au contact entre les roches du socle et les sédiments et sont recouverts de basaltes de vallée du Pliocène. Toute la minéralisation découverte à ce jour est sous la forme de phosphates uraneux (ningyoite) ou uranyles (saléite, autunite). La formation de ces dépôts est considérée comme étant le résultat d'un lessivage contrôlé structuralement du socle par des eaux souterraines profondes suivie d'une infiltration éventuelle dans les sédiments fluviaux et une précipitation des minéraux de phosphate d'uranium.

On a effectué des études géochimiques du complexe de roches intrusives des 'Highlands d'Okanagan' afin de déterminer les caractéristiques des roches-mères favorables. Les teneurs moyennes en uranium de la monzonite quartzifére, de la granodiorite et de la monzonite de Coryell (soient 4.8, 2.3 et 6.2 ppm respectivement) sont cohérentes avec les moyennes mondiales. L'uranium montre des corrélations positives importantes avec les teneurs en K_2O et SiO_2 de ces roches et des corrélations négatives marquées avec des indicateurs ferromagnésiens comme MgO, CaO, FeO et MnO. Parmi les éléments traces analysés à ce jour (F, Rb, Sr, Ba, V, Zr, U, Th), seul le Sr présente

[1]601 Booth Street, Ottawa, Ontario, K1A 0E8

une augmentation supérieure à la norme pour ces type de roches. La composition en éléments majeurs des types de roches formant le complexe sont semblables aux moyennes mondiales, sauf que toutes sont enrichies de CO_2, une caractéristique remarquable qui peut être reliée à la carbonatisation très répandue survenue pendant le volcanisme de l'Eocène. Des concentrations élevées en CO_2 dans les roches, ainsi que des eaux souterraines possédant des teneurs anormalement élevées en U, HCO_3 et P, résultant d'un drainage récent, contrôlé structuralement, des zones faillées à l'intérieur du complexe de roches intrusives, peuvent être des indices caractéristiques de roches-mères favorables.

Des expériences de lessivage faites en laboratoire révèlent que les roches intrusives du complexe d'Okanagan et plusieurs roches ignées équivalentes de la Cordillère renferment des quantités semblables d'uranium lessivable. Les niveaux d'uranium lessivable décroissent dans l'ordre suivant: pegmatite, monzonite quartzifère, monzonite de Coryell, granodiorite. Des pourcentages élevés, en volume, de roches ignées leucocrates, micacées, de grain moyen à grossier, sont un prérequis pour être en présence de régions de roches-mères fertiles.

Une connaissance approfondie de la séquence des événements tectoniques reliés à la formation d'un complexe de roches intrusives semble plus importante, pour la détermination du potentiel des roches-mères, que des paramètres géochimiques, bien qu'ils soient tous interreliés. Les gisements d'uranium de la région d'Okanagan se sont formés d'une part après une période de tectonisme étendue (de la fin du Miocène au début du Pliocène), ce qui a conduit à un lessivage maximal par les eaux souterraines d'un socle composé de roches intrusives 'à texture lâche', et d'autre part, après une période de mouvements épirogéniques (de la fin du Pliocène au début du Pléistocène), ce qui a amené la cessation du régime hydrologique responsable de la formation du minerai.

Introduction

A number of Pliocene sedimentary hosted uranium deposits have been discovered in the Okanagan region of south-central British Columbia (Fig. 5.1). These deposits occur within unconsolidated fluvial paleochannel sediments which overlie fault zones and small grabens within the Okanagan Highlands Intrusive Complex. Prior to formation of mineralization during middle to late Pliocene times, paleovalleys were flooded by Pliocene valley basalts of the Plateau Basalt Formation. Five uranium deposits have been outlined to date, of which the Blizzard (4,020t U) and Tyee (650t U) are the largest. The geological setting of the Blizzard deposit serves as a type example for this area and is illustrated in Figure 5.2.

The mineralized host sediments comprise a complex sequence of interfingering conglomerates, sandstones and mudstones. The conglomerate represents reworked fault breccia material and is confined to basement depressions along the fault controlled paleovalleys. Organic material is abundant in many, but not all, mineralized beds. Uranium mineralization is present in the form of uranous (ningyoite) or uranyl (saleeite, autunite) phosphates coating clastic grains and filling intergranular spaces. Because of very high reducing conditions related to large concentrations of marcasite and organic material, ningyoite is the only uranium mineral in the Tyee deposit whereas the Blizzard deposit contains a more complex assemblage of minerals (saleeite, autunite, ningyoite; Boyle et al., 1981). The only elements significantly enriched in these deposits are U, Ca, Mg and P.

As part of a more detailed examination of the genesis of the Okanagan basal-type deposits, detailed investigations have been carried out on the possible source of the ore-forming elements U, Ca, Mg and P. The present work is confined to an examination of source rocks but it is important to realize that a successful genetic interpretation of the formation of infiltration-type uranium deposits, of which the basal-type deposits of the Okanagan are a subdivision, is dependent upon a sound understanding of the interrelationsips between source of ore-forming elements, mechanism(s) of migration, paleoclimatology, environment of deposition and preservation, all of which have to be operative within a favourable and decipherable tectonic framework. These factors, of which source is only one, form the basis of research on the Okanagan deposits.

Geology

The geology of the Okanagan region as outlined in Figure 5.1 has been compiled from regional mapping programs by Little (1957, 1961) and Jones (1959) as well as more detailed local studies by Church (1973, 1977), Monger (1968), Okulitch (1974), Preto (1970), Christopher (1978) and the author. The area lies within the southern portion of the Omineca Crystalline Belt.

The oldest rocks in the Shuswap Metamorphic Complex, are gneisses, quartzites, schists and limestones. This complex forms a large northern mass having a southern embayment fronting on the northern edge of the Okanagan Highlands Intrusive Complex. Smaller block faulted segments also occur in the southern half of the area.

Paleozoic-Mesozoic metavolcanic-metasedimentary rocks comprising greenstone-quartzite-argillite-limestone and andesite-shale-limestone assemblages occur as isolated block faulted roof pendants on the Shuswap Metamorphic Complex and Mesozoic intrusive basement.

The first major intrusive activity began in early to middle Jurassic time with the emplacement of the West Okanagan intrusions (Okanagan, Oliver, Shorts Creek and Salmon Arm bodies) and continued into the early to middle Cretaceous with the intrusion of the Nelson granitoids. The early intrusions of this period consist mainly of granite and monzonite; later intrusions are mainly granodiorite and diorite.

A probable period of quiescence was followed by emplacement of middle to late Cretaceous granitoids. These form a central core in the southern half of the area and consist mainly a quartz monzonite, porphyritic granite and pegmatite.

Eocene volcanic-sedimentary rocks form isolated basins in the southwestern half of the region. This sequence consists mainly of basal sediments and alkali, intermediate, and acid volcanics with lesser amounts of intraformational sediments. The Coryell intrusions which comprise porphyritic augite monzonite, alkaline syenite, and rare shonkinite and granite are coeval with the Eocene volcanics and occur mainly as necks, and elongated bodies and dykes of predominantly NE and NW orientation.

The central area underlain mainly by late Cretaceous and Eocene granitoids has been given the name Okanagan Highlands Intrusive Complex by the author because it represents a discrete segment of crustal rocks in the Omineca Crystalline Belt characterized by intrusive and extrusive activity varying in age from Jurassic to late Pliocene. It is on this complex that the basal-type uranium deposits have formed.

The structural mosaic observed in Figure 5.1 is largely the result of Tertiary tectonism characterized by three peaks of activity, one, accompanied by calc-alkaline volcanism during the Eocene, another in late Miocene to early Pliocene followed by basaltic volcanism, and the final one in late Pliocene to early Pleistocene times. The tectonic activity which accompanied and followed Eocene volcanism led to the formation of major N-S fault lineaments (e.g. Okanagan Valley Lineament). The late Miocene represents a period of tectonic activity leading up to the formation of early Pliocene plateau basalts. Unconsolidated fluvial sediments, which are host to uranium mineralization, were rapidly deposited in NW-SE and NE-SW fault controlled Tertiary valleys and in turn were covered by fissure extruded valley basalts of the Plateau Basalt Formation. It is along the NW-SE fault set that sedimentary-hosted uranium deposits have formed. Finally, during the late Pliocene-early Pleistocene period, the entire area was subjected to regional uplift.

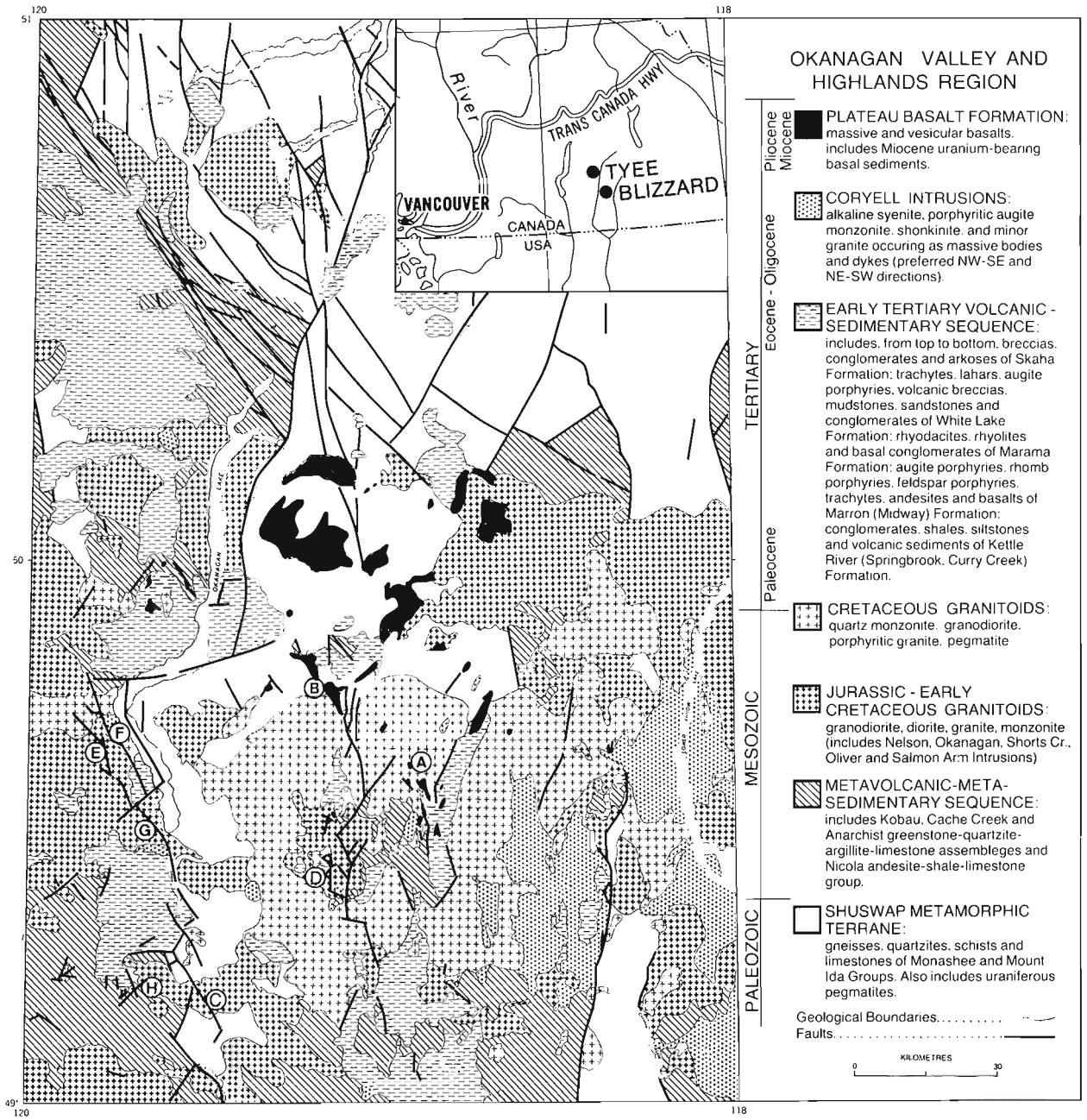

Figure 5.1. *Location and generalized geology of the Okanagan Valley and Highlands region. Geological features and study areas referred to in the text are A) Blizzard deposit, B) Tyee deposit, C) Inkaneep, D) Eugene Creek, E) Darke Creek, F) Eneas Creek, G) Nkwala and H) Blind Creek. Geology after Little (1957, 1961) and Jones (1959).*

Source of Uranium

Essentially, the many sources advocated for the formation of sandstone-type uranium deposits are a reflection of local or regional geological environments. Such sources may be grouped under four main classifications:

a) leaching of an intrusive basement complex or adjacent uplifted block,

b) leaching of volcanic rocks generally overlying the deposits,

c) leaching of host sediments ranging from arkosic to tuffaceous in composition, and

d) hydrothermal activity associated with intrusive and volcanic processes or tectonic events (e.g. taphrogeny, epeirogeny).

For the Okanagan region all of these sources were considered during initial investigations. Only the first, that of leaching of an intrusive basement complex, was found to conform to the observations made on geological and tectonic

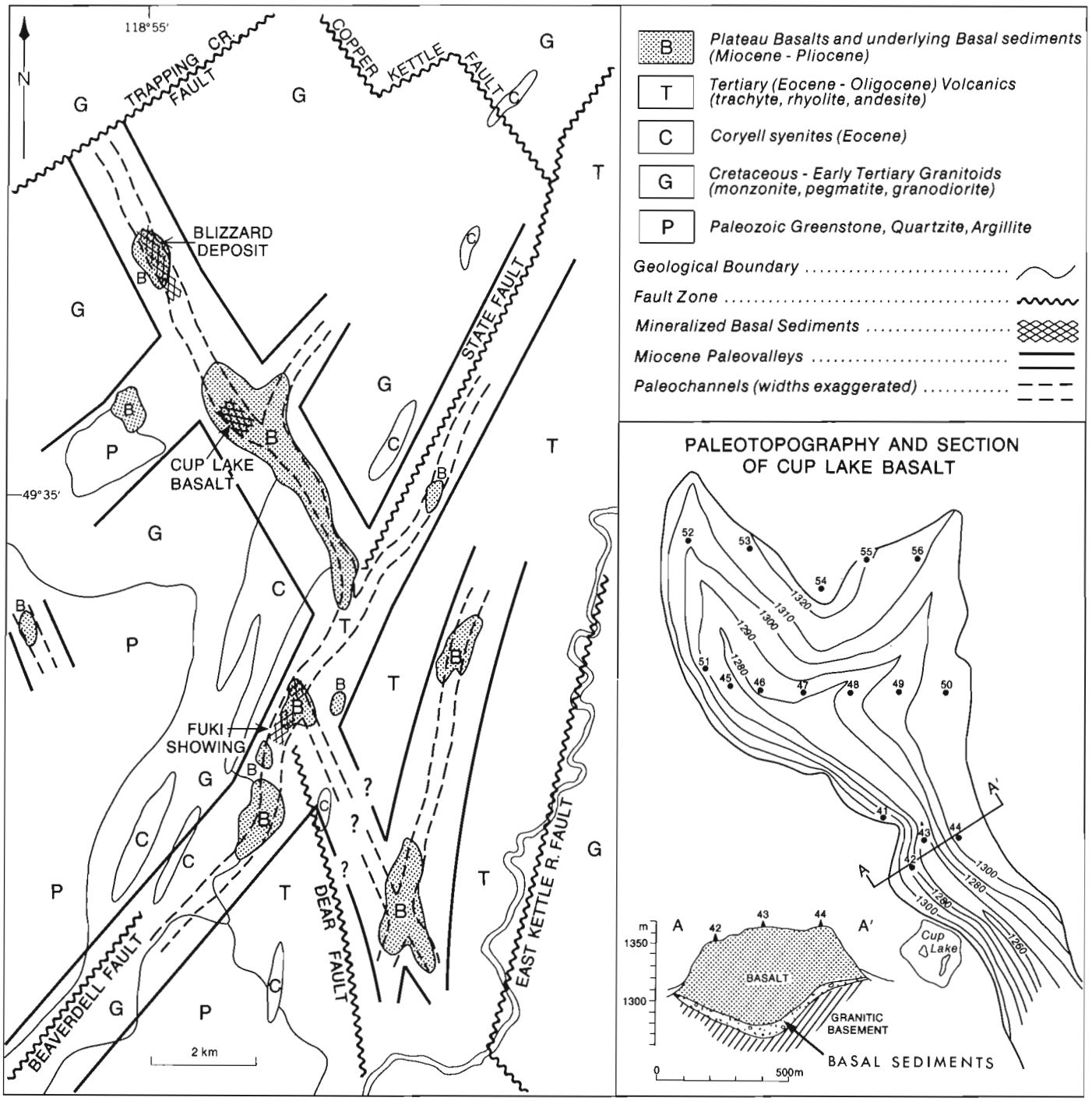

Figure 5.2. *Geological setting of the Blizzard basal-type uranium deposit and associated uranium occurrences. Geology compiled from company assessment reports and mapping by author.*

Table 5.1. Chemistry of intrusive phases in the Okanagan Highlands Intrusive Complex (arithmetic mean and one standard deviation)

	Quartz monzonite (n=79)	Porphyritic Granite (n=20)		Granodiorite (n=14)		Coryell* Monzonite (n=57)	
			Av. Granite(a)		Av. Granodiorite(a)		Av. Hbl-Biot-Qtz-Monzonite(b)
SiO_2	71.80(3.06)	71.40(2.50)	71.30	65.10(4.35)	66.09	65.70(6.39)	65.88
Al_2O_3	15.10(1.06)	15.14(0.97)	14.73	16.20(0.98)	15.73	15.80(1.60)	15.07
FeO	0.60(0.37)	0.72(0.32)	1.64	2.09(0.95)	2.73	1.24(1.02)	2.73
Fe_2O_3	0.88(0.45)	0.95(0.49)	1.21	1.74(0.76)	1.38	1.82(0.88)	1.74
MnO	0.04(0.03)	0.05(0.04)	0.05	0.09(0.04)	0.08	0.06(0.04)	0.08
TiO_2	0.21(0.12)	0.25(0.11)	0.31	0.51(0.22)	0.54	0.50(0.27)	0.81
CaO	1.25(0.81)	1.28(0.89)	1.84	3.74(1.24)	3.83	2.02(1.65)	3.36
MgO	0.37(0.25)	0.44(0.25)	0.71	1.76(1.11)	1.74	1.21(1.17)	1.38
K_2O	4.34(1.12)	4.72(1.39)	4.07	3.63(1.26)	2.73	5.06(0.94)	4.64
Na_2O	3.78(0.74)	3.50(0.74)	3.68	3.60(3.75)	3.75	3.81(0.76)	3.53
P_2O_5	0.08(0.05)	0.10(0.05)	0.12	0.22(0.17)	0.18	0.25(0.24)	0.26
CO_2	0.13(0.08)	0.16(0.11)	0.05	0.29(0.60)	0.08	0.84(0.86)	-
S	0.01(0.00)	0.01(0.00)	-	0.01(0.00)	-	0.01(0.01)	-
F(ppm)	321(465)	385(511)	810	237(202)	500	483(307)	-
Rb(ppm)	212(95)	180(50)	190	125(46)	110	255(85)	-
Sr(ppm)	572(385)	576(266)	150	812(552)	659	919(815)	-
Ba(ppm)	1290(760)	1348(467)	732	1850(624)	888	1570(881)	-
V(ppm)	35(24)	40(15)	72	101(53)	99	59(42)	-
Zr(ppm)	102(72)	143(53)	175	177(71)	140	258(151)	-
U(ppm)+	4.8(4.5)	5.4(4.3)	4.8	2.3(3.6)	2.3	6.2(4.4)	-
Th(ppm)+	16.3(10.5)	22.3(2.1)	21.5	11.8(11.0)	9.0	26.7(13.0)	-
Th/U Ratio	4.5(3.2)	4.3(1.7)	4.5	3.5(3.3)	4.0	5.1(1.9)	-

* does not include dyke rocks
\+ n=79, 20, 43, 76 respectively
(a) average major element compositions from LeMaitre (1976), trace element averages from numerous sources in Handbook of Geochemistry, Springer Verlag Publ.
(b) average major element compositions from Nockolds (1954), trace element averages from numerous sources in Handbook of Geochemistry, Springer Verlag Publ.

Major elements Rb and Sr by X-ray fluorescence; Ba, V, Zr by emission spectrometry; F by ion electrode; U by neutron activation; Th by gamma ray spectrometry.

setting; chemical composition and mineralogy of deposits; availability of uranium, phosphate, calcium, and magnesium; proximity of source to ore, and groundwater hydrology as a transport mechanism. Evidence for this is discussed under these features.

Structure

The entire Okanagan Highlands Intrusive Complex has a very well developed fault and fracture system, the signatures of which are present on both mega and micro scales. Two major sets of fault zones having preferred azimuths of 30° and 330° and a minor N-S fault set developed after the emplacement of the granodiorite and quartz monzonite phases. Post-Eocene reactivation is evidenced by dislocation of phases of the Coryell. High angle normal or reverse fault zones may have a width of up to 1 km; small graben structures enclosing down dropped slices of the basement rocks are also evident. The more massive portions of the complex are well jointed and have undergone extensive fracturing as a result of repeated intrusive activity, extensional tectonism and uplift. Hand specimens and thin sections commonly display microfractures, many of which show radioactive concentrations on alpha and fission track autoradiographs. Shattering along grain boundaries is also evident in thin sections of rocks taken from fault zones. A structural analysis of the complex leads to the conclusion that it is a 'fabric-loosened' body of interconnecting fault and fracture systems capable as a whole of sustaining well developed intermediate and regional groundwater flow systems. Most of the major fault zones examined in the complex were found to be major loci for groundwater discharge.

Petrology and Chemistry

The Okanagan Highlands Intrusive Complex consists of diorite, granodiorite, monzonite, quartz monzonite, porphyritic granite, pegmatite and the Coryell 'monzonite' suite. Although detailed age dating is not available the above order is closely representative of an older to younger generation of intrusions. All of the rock units, with the exception of those of the Coryell, are considered to be late Jurassic to Cretaceous in age. Quartz monzonite accounts for the largest volume in the complex, and is typically coarse grained, consisting of plagioclase (30-35 per cent), potash feldspar (25-35 per cent), smoky quartz (25-30 per cent), biotite and/or muscovite (5-10 per cent), hornblende (less than 1 per cent) and accessories (sphene, rutile, allanite, apatite). The chemical composition as shown in Table 5.1 is very similar to Le Maitre's (1976) average granite, but the quartz monzonite is slightly less calc-alkaline and the lack of hornblende is reflected by a lower ferromagnesian content. It is important to note that the phosphate content is normal or even slightly below average and the CO_2 content is significantly elevated compared to average concentrations

for granite. Of the trace elements shown in Table 5.1 only Sr and Ba display concentrations much above world averages. Both the U (4.8 ppm) and Th (16.3 ppm) contents and resultant Th/U ratio are normal for this type of rock.

The porphyritic granite phase, which is a minor component of the complex, has a chemistry very similar to the quartz monzonite phase (Table 5.1).

The average of 4.8 ppm U for quartz monzonite represents sampling carried out over the entire central Okanagan Complex. Twenty-two and fourteen representative samples of the quartz monzonite phase taken around the Blizzard and Tyee deposits show ranges of 0.9 to 23.6 and 2.5 to 15.0 ppm U and averages of 4.7 ppm and 4.4 ppm respectively. These averages are very close to the regional average for quartz monzonite (4.8 ppm U) and it would appear, therefore, that there is no lithospheric enrichment of uranium in the intrusive phases within the immediate vicinity of the deposits.

The granodiorite and diorite phases are the oldest rocks in the complex, diorite being a very minor component. The granodiorite is typically a medium grained, slightly foliated rock containing more biotite and hornblende than the quartz monzonite. Its composition (Table 5.1) is very similar to the average granodiorite of Le Maitre (1976) with the notable exception of K and CO_2 enrichment. Of the trace elements shown in Table 5.1, Sr and Ba show some increase over normal concentrations. Like the quartz monzonite, average U and Th contents are similar to world averages.

The Coryell intrusions represent a wide variety of rock types consisting of porphyritic augite monzonite, alkali syenite, and rare shonkinite and granite. In Table 5.1 only those rocks classed as monzonites and syenites have been grouped for average composition. The higher standard deviations observed compared to other intrusive rocks of the complex demonstrate their chemical complexity. Their composition may vary from trachyte to alkali syenite but their overall average composition (Table 5.1) best approximates the average hornblende-biotite-quartz monzonite of Nockolds (1954). Notable chemical characteristics are K, CO_2, Rb and Sr enrichment. The U content of these rocks may vary from 2.0 to 36.6 ppm and although there is a scarcity of worldwide data on the U content of rocks of this composition the average values for U (6.2 ppm) and Th (26.7 ppm) do not appear to be above normal.

For all intrusive phases uranium displays significant positive correlations with K_2O and SiO_2 and marked negative correlations with mafic indicators such as MgO, CaO, FeO and MnO.

Alteration is evident in all rock types of the complex. Carbonitization, epidotization and especially kaolinization along fault and fracture zones are characteristic of the quartz monzonite and granodiorite phases while carbonitization and zeolitization are typical of the Coryell rocks. These processes are also reflected chemically as an enrichment of CO_2 for all rock types in the complex (see Table 5.1). Concentrations of carbonate, together with a well developed tectonic fabric, lead to the observed formation of bicarbonated (and uraniferous) structurally controlled groundwaters within the complex.

Assuming that the specific gravities of each of the major rock types are similar, it is possible to estimate the average U abundance of the crustal segment underlying the mineralized region to a depth at which groundwaters can circulate. Quartz monzonite makes up approximately 70 per cent of the complex while granodiorite, Coryell rocks and Eocene volcanics comprise approximately 15, 10, and 5 per cent respectively. The average crustal abundance of U is, therefore, 4.5 ppm which is not unusual for large intrusive basement complexes in the North American Cordillera (see summary in McNeal et al., 1981). On a worldwide basis it is slightly lower than the average for granitic (4.8 ppm, Rogers and Adams, 1969) and silicic plutonic rocks (4.7 ppm, n = 4754; Peterman in McNeal et al., 1981).

A final point to be made concerning the composition of the basement rocks is their compositional relationship to the ore deposits. All of the mineralization found to date is in the form of (Ca,Mg)-U-PO_4 minerals (ningyoite, saleeite, autunite). It should be noted that PO_4 is not enriched above normal concentrations in any of the rocks forming the complex. It is evident from the results in Table 5.1 that the supply of PO_4 to the deposits comes chiefly from the Coryell rocks and the granodiorite phase. To a lesser extent these two phases would also be the main source of Ca and Mg. On the other hand quartz monzonite and the Coryell rocks would be the chief sources of uranium.

Labile U, Ca, Mg and PO_4

Although the concentration of total uranium in rocks may be used as a rough guideline for determining fertile source areas for sandstone-type uranium deposits it is the amount of labile uranium that is the most important factor when assessing source potential. Labile uranium in source rocks can be determined, on a relative basis, by a number of methods. The use by Stuckless and Nkomo (1978) of U-Pb systematics to evaluate U loss in the Precambrian Granite Mountains complex of Wyoming is notable; rocks in the Okanagan region are, however, much too young for application of this technique. Other studies have generally relied upon experimental leaching to show that igneous rocks, and granites in particular, release considerable amounts of uranium when leached (Krylov and Atrashenok, 1959; Szalay and Samsoni, 1969; Kovalev and Malyasova, 1971). Two methods used in this study to determine labile U content include the leaching of rock powders and a comparison of the U contents of groundwaters draining the Okanagan Highlands Intrusive Complex with those draining similar types of lithology elsewhere.

Rock powders representing the various rock types in the region of the deposits, as well as those of other Cordilleran intrusive complexes, were leached for 20 hours using a solution composed of 300, 220, 30, 20, 400, 45 and 20 ppm of HCO_3, Na, Ca, Mg, F, Cl and SO_4 respectively with a pH of 7.5 and a conductivity of 580. The U content of the leaching solution was undetectable (less than 0.05 ppb) and with the exception of a higher Na content the leaching solution approximates that found for many groundwaters draining the intrusive rocks of the Okanagan region. The leaching solution and sample (20 ml to 1 gm) were continuously aerated by allowing air to pass through the funnel holding the sample and solution. Precision for this method was better than 20 per cent. The results of this experiment are shown in Table 5.2. For the various rock types within the area of influence of the deposits the amount of labile uranium decreases in the order pegmatite - quartz monzonite-granite - Coryell monzonite - Eocene volcanics-granodiorite. This is not the order of decreasing total uranium content and it can be seen that the quartz monzonite phase which has the greatest volume percentage in the complex is also the greatest donor of labile U. The intrusive rocks as a whole contain much more available uranium than the Eocene volcanics despite the fact that the total U contents of the volcanics are often greater.

Comparing the labile U concentrations of the individual intrusive phases in the Okanagan Highlands Intrusive Complex with those of other Cordilleran intrusive complexes one can

readily see that the observed levels for the Okanagan rocks are not unique (Table 5.2). In some cases even the granodiorites of other intrusive bodies possess significant amounts of labile U. The best that can be said of these data is that the Okanagan Highlands Intrusive Complex is a good source of labile uranium but the observed levels cannot be used as rigid baselines for determining source potential of other regions.

A second and perhaps more representative method of determining source potential based on levels of labile U is to examine the chemistry of present day groundwaters in light of possible ore-forming processes. This is easily justified for the Okanagan region since the paleoclimate during the time of ore formation (Pliocene) and the present day climate are very similar (Mathews and Rouse, 1963). Analyses for groundwaters draining mineralization and major fault zones in basement rocks are given in Table 5.3. It can be seen from these data that groundwaters draining basement rocks,

Table 5.2. Labile uranium in intrusive and volcanic rocks from the Okanagan and other Canadian Cordilleran Intrusive Complexes

Rock Type+	Av. Uranium* in Rock (ppm)	Av. Concentration of Labile Uranium (ppm)
EOCENE VOLCANICS		
Trachyte (Blizzard area)	7.7(4)	23
Rhyolite (Blizzard area)	5.2(4)	10
Rhyolite (Tyee area)	4.0(4)	4
MONZONITES; GRANITES; SYENITES		
Adanac granite	18.8(7)	451
Surprise Lake alaskite	14.6(48)	277
Okanagan pegmatite	5.2(3)	192
Tombstone syenite	18.0(25)	162
Fourth of July granite	5.6(14)	134
Oliver granite	7.3(15)	131
Okanagan qtz. monzonite	4.8(79)	86
Shorts Cr. monzonite	4.0(13)	84
Raft qtz. monzonite	4.6(25)	64
Okanagan granite	5.4(20)	59
McClure granite	2.2(6)	57
Coryell monzonite	6.2(76)	43
Antimony Hill granite	8.6(3)	34
Katsberg qtz. monzonite	4.7(4)	33
Vernon monzonite	5.5(34)	22
Nicola qtz. monzonite	1.6(13)	13
Wildhorse qtz. monzonite	1.5(5)	11
Quilchena qtz. monzonite	1.4(6)	10
Douglas qtz. monzonite	0.4(2)	5
Duckling syenite	1.1(12)	4
GRANODIORITES; DIORITES		
Cantung granodiorite	6.7(5)	47
Meselinka monzo-diorite	9.4(11)	38
Raft granodiorite	2.4(4)	36
Goldway tonalite	2.7(2)	30
Thane tonalite	3.4(4)	24
Nicola granodiorite	2.6(3)	18
Quilchena granodiorite	1.0(9)	15
Wildhorse granodiorite	1.9(10)	11
Frederickson tonalite	3.8(3)	11
Asitka tonalite	1.6(3)	10
Meselinka granodiorite	9.0(5)	9
Okanagan granodiorite	2.3(43)	9
Douglas granodiorite	0.6(4)	8
Lay monzo-diorite	2.2(3)	4
Wildhorse diorite	1.7(3)	3
Jensen tonalite	1.0(12)	3
Fleet diorite	1.8(7)	3
Ingenika tonalite	2.7(2)	3

+ Rock types from Okanagan region underlined
* No. of samples in brackets.
See text for description of laboratory method used

Table 5.3. Chemistry of groundwaters draining mineralization and fault zones in the Okanagan region, British Columbia (average in brackets)

Geological features*	U in waters (ppb)	pH	Conductivity (μ mhos/cm)	HCO_3 (ppm)	SO_4 (ppm)	F (ppb)
MINERALIZATION:						
Blizzard basal-type uranium deposit (A)						
-springs (7)	0.17-18.0(3.6)	6.0-7.6(7.1)	29-148(85)	11-91(41)	2-10(5)	96-570(230)
-drill hole waters (5)	3.30-160.0(62.0)	7.0-7.4(7.2)	148-306(236)	96-207(160)	2-25(6)	98-230(120)
Haynes Lake basal-type uranium deposit (B)						
-drill hole waters (3)	2.60-14.3(9.7)	6.2-6.8(6.5)	442-1200(758)	317-895(604)	12-27(20)	372-410(390)
Carmi Mo(U) porphyry deposit						
-drill hole waters (6)	3.10-48.0(24.6)	7.1-7.7(7.3)	80-250(163)	15-188(120)	50-220(188)	1880-16000(11200)
Blue Spring (uranium) pegmatite						
-streams (5)	3.90-20.0(11.50)	7.6-8.2(7.6)	433-662(543)	37-411(270)	24-188(93)	245-372(310)
FAULT ZONES IN INTRUSIVE BASEMENT						
Darke Creek (D)						
-streams (7)	1.10-54.0(17.4)	7.8-8.2(8.1)	134-447(342)	77-296(163)	2-9(4)	86-405(208)
-well waters (3)	2.80-75.0(37.0)	7.4-7.6(7.5)	304-400(380)	183-257(226)	8-14(12)	156-221(135)
Eneas Creek (F)						
-streams (6)	4.80-14.8(8.6)	8.1-8.4(8.2)	366-439(370)	195-242(198)	2-10(4)	291-389(337)
Nkwala (G)						
-streams (3)	22.0-54.0(35.3)	8.2-8.3(8.2)	504-644(550)	365-386(370)	474-670(540)	520-720(570)
Blind Creek (H)						
-stream (4)	14.00-16.4(15.1)	7.0-8.1(7.8)	366-678(515)	235-294(270)	2-221(112)	105-188(158)
Inkaneep area (C)						
-streams (11)	1.60-11.7(4.5)	7.2-8.3(7.7)	81-649(278)	51-495(188)	2-23(5)	202-1710(585)
-well waters (2)	23.00-50.0(36.5)	7.2-8.1(7.7)	354-748(550)	227-505(416)	2-8(5)	483-1620(1050)
Eugene Creek (D)						
-streams (21)	1.13-23.0(7.8)	7.2-8.1(7.8)	99-289(204)	64-197(142)	2-15(6)	150-660(490)
-springs (9)	4.00-125.0(22.2)	7.7-8.2(7.9)	143-184(215)	87-23(144)	2011(6)	194-930(411)

* See Figure 5.1 for area locations indicated by letters in brackets. Number of samples in brackets.

Table 5.4. Uranium and phosphate content of ground waters and surface waters in the Okanagan region and other areas of British Columbia

Location	U(ppb)	PO_4(ppb)
OKANAGAN REGION:		
Groundwaters draining fault zones in intrusive rocks*		
- Darke Cr. (spring)	54.00	80
- Darke Cr. (spring)	48.00	83
- Darke Cr. (bore hole)	34.00	490
- Darke Cr. (bore hole)	75.00	40
- Nkwala (spring)	54.00	85
- Eugene Cr. (spring)	13.90	83
- Eugene Cr. (stream)	23.00	83
- Eugene Cr. (stream)	10.00	107
- Eugene Cr. (creek)	10.00	408
- Blind Cr. (spring)	14.40	690
- Blind Cr. (stream)	15.60	40
- Inkaneep (well water)	50.00	1971
- Inkaneep (well water)	23.00	245
Groundwaters draining mineralization*		
- Blizzard deposit DDH-4	59.00	408
- Blizzard deposit DDH-20	106.00	325
- Blizzard deposit DDH-24	3.30	331
- Blizzard deposit (spring)	18.00	123
- Haynes deposit DDH-11	12.20	83
- Haynes deposit DDH-15	14.30	83
- Haynes deposit DDH-34	2.60	328
Surface drainage+		
- Trapping Creek (11)	-	41
- Mission Creek (32)	-	37
- Okanagan River (146)	-	23
- Okanagan Lake (48)	-	34
MAJOR RIVERS IN BRITISH COLUMBIA 74 rivers, 916 sites+	-	37

* Author's data
\+ Water quality data, British Columbia 1961-71, Canada Water Quality Branch, Ottawa

especially those issuing along deep seated structures, have uranium levels which are similar to those for groundwaters in equilibrium with mineralization and are well above average concentrations for surface stream waters which are generally in the order of 0.05 to 0.50 ppb (Boyle and Ballantyne, 1980). It should be noted that the various intrusive phases within the fault zones outlined in Table 5.3 are neither enriched nor depleted in U compared to regional averages. Although extensive worldwide data on the U content of groundwaters in crystalline terranes are not yet available there are few reported values that exceed the levels given in Table 5.3. It is evident therefore, that the groundwaters draining intrusive basement rocks in the Okanagan region are able to liberate and mobilize considerable concentrations of uranium.

Besides uranium the other major elemental constituents of these deposits are P, Ca, and Mg. Mineralization in the Tyee deposit is entirely in the form of ningyoite (Ca-U-PO_4) whereas the Blizzard deposit contains perhaps more saleeite (Mg-U-PO_4) than ningyoite in addition to small amounts of autunite (Ca-U-PO_4). It is important, therefore, when examining source rocks to consider the availability of elements such as P, Ca and Mg. Table 5.4 represents a comparison of PO_4 results for groundwaters draining fault zones in the Okanagan intrusive rocks with those in equilibrium with mineralization, as well as values for surface drainage in the Okanagan and a compiled average for all water quality stations in British Columbia. The phosphate contents of groundwaters draining intrusive rocks in the Okanagan are similar and in some cases higher than those for waters in equilibrium with mineralization. They are also significantly higher than the contents observed for surface drainage. It would appear from these data that there is an adequate abundance of PO_4 in groundwaters leaching the Okanagan Highlands Intrusive Complex, thus permitting the formation of U-PO_4 complexes and eventual precipitation of uranous and uranyl phosphate minerals. Accessory apatite is the prime source of PO_4 in the intrusive phases of the complex.

The availability of Ca and Mg has a direct bearing on the formation and stability of the various U-phosphate minerals in these deposits. Saleeite may be considered as the Mg analogue of autunite; there is no known Mg-U^{4+}-PO_4 analogue of ningyoite. The formation of primary saleeite and autunite in these deposits will be governed by the relative abundances of Ca and Mg and the redox potential of the ore-forming groundwaters. In the Tyee deposit conditions are strongly reducing and Mg-U-PO_4 minerals cannot form. In the Blizzard deposit, where there appears to have been a definite drop in the redox potential down the hydrological gradient but still within a slightly oxidizing regime, saleeite can form where there is a relative abundance of Mg over Ca in the ore forming groundwaters. Table 5.5 is a compilation of range and mean values for Ca and Mg and Ca/Mg ratios of means for groundwaters draining intrusive rocks in the Okanagan and similar areas for which data are readily available. Garrels (1967) has shown that waters draining feldspathic igneous rocks should have a dominance of Ca over Mg. The data in Table 5.5 for groundwaters draining granitic terranes other than the Okanagan confirm his results; Ca/Mg for these waters are rarely less than 3.0. For the Okanagan waters, however, the Ca/Mg ratios are generally much lower and in some cases Mg is present in excess of Ca (e.g. Nkwala fault zone). The Eugene Creek fault zone is the only structure where the Ca/Mg ratio agrees with most of the world data. In terms of ore-forming processes the range of Ca/Mg ratios observed for the Okanagan (0.6 to 7.3) would be represented by deposits containing variable proportions of saleeite, autunite and ningyoite and in some cases no saleeite (e.g. Eugene Creek). The main donors of Mg during weathering of feldspathic igneous rocks are biotite and hornblende (Garrels, 1967), two minerals which reach their highest percentages in the granodiorite and Coryell monzonites. As in the case of phosphate, it would appear that these two phases of the Okanagan Highlands Complex are the main source of Mg and in areas where they are present in significant volume percentages, such as the area around the Blizzard deposit, saleeite should be the dominant uranyl phosphate mineral formed.

Conclusions

Extensive investigations of the source of the ore-forming elements (U, Ca, Mg, PO_4), including leaching of the intrusive basement complex, volcanics rocks (Eocene) and host sediments, as well as emplacement of ore by hydrothermal activity has led to the conclusion that these elements were derived almost entirely from groundwater leaching of the Okanagan Highlands Intrusive Complex. Laboratory leaching experiments and investigations of present day structurally controlled groundwaters associated

Table 5.5. Calcium and magnesium contents of groundwaters draining intrusive terranes

Area*	Ca (ppm) Range	Ca (ppm) Mean	Mg (ppm) Range	Mg (ppm) Mean	Ca/Mg of Means
Okanagan (fault zones)+					
Nkwala (4)	17.8-32.1	23.5	30.0-45.3	37.7	0.6
Darke Creek (5)	15.3-31.1	21.2	3.4-20.1	13.8	1.5
Blind Creek (3)	42.9-51.8	46.4	13.4-37.6	26.4	1.8
Inkaneep (9)	6.7-36.6	15.4	2.6-31.9	8.4	1.8
Eneas Creek (4)	20.2-29.9	23.7	6.4-11.6	9.0	2.6
Eugene Creek (37)	8.8-50.1	29.6	2.3-12.5	4.7	7.3
Granitic massifs					
Norway (28)	-	1.7	-	0.6	2.8
Vosges (51)	-	5.8	-	2.4	2.4
Brittany (7)	-	4.4	-	2.6	1.7
Central Massif (10)	-	4.6	-	1.3	3.5
Alrance Spring F (77)	-	1.0	-	0.4	2.5
Alrance Spring A (47)	-	0.7	-	0.3	2.3
Corsica (25)	-	8.1	-	4.0	2.0
Senegal (7)	-	8.3	-	3.7	2.2
Chad (2)	-	8.0	-	2.5	3.2
Ivory Coast (54)	-	1.0	-	0.1	10.0
Malagasy (2)	-	0.4	-	0.12	3.3
Silicic rocks, Finland (60)	2.4-37.4	9.3	0.7-9.7	3.8	2.4
Moolyala granite, Australia (4)	29-62	46.0	9-26	16.0	2.9
Lac Du Bonnet granite, Ont. (5)	25-119	76	6-46	29	2.6
Bohemian granites, Germany (8)	8.0-62.5	26.1	0.1-20.7	7.7	3.4
North Carolina					
Granite (29)	1.8-12.0	5.0	0.6-4.5	2.0	2.5
Diorite (23)	13.0-174.0	49.0	2.6-40.0	12.0	4.0
Granite and Diorite (10)	6.8-37.0	20.0	2.4-7.6	5.0	4.0
Maine granites, U.S.A. (4)	1.1-62.4	33.4	1.8-9.0	4.6	7.2
Colorado granitic terrain (11)	25-473	152	3-105	35	4.3
Sierra Nevada Batholith					
Ephemeral springs (15)	0.8-7.0	3.1	0.0-2.9	0.7	4.4
Perennial springs (56)	1.0-26.0	10.4	0.0-6.3	1.7	6.0
Crystalline rocks, Italy (15)	1.0-18.0	4.9	0.1-5.2	1.0	4.9
Surprise Alaskite, B.C. (24)	0.9-5.0	3.3	0.1-0.8	0.4	8.3
North Caucasus granites U.S.S.R. (?)	-	10.0	-	1.2	8.3
Mont-Blanc Granite, France (13)	9.2-32.8	18.2	0.0-2.4	0.6	30.0

* No. of samples in brackets
\+ Author's data; all other data by various authors collated in Johnston (1981)

with this complex show that its constituent rocks contain much higher concentrations of labile uranium than other rocks in the region. The PO_4 contents of groundwaters draining this complex are sufficient to promote uranium precipitation in host sediments under even mildly reducing conditions. The low Ca/Mg ratio, resulting from high Mg contents of groundwaters draining the complex, correlates well with the dominance of saleeite ($Mg\text{-}U\text{-}PO_4$) over autunite ($Ca\text{-}U\text{-}PO_4$) in the Blizzard deposit. The Okanagan Highlands Intrusive Complex, with its well developed interconnecting high angle normal and reverse fault systems and its open structure is capable of sustaining well developed intermediate and regional groundwater flow systems.

Detailed major and trace element analyses of the rock phases in the Okanagan Highlands Intrusive Complex show that this complex with the exception of high CO_2 contents is not chemically unique as a source area when compared to similar complexes in the North American Cordillera and throughout the world. The average U contents of the various rock phases and the complex as a whole compare very well with world averages for similar intrusive massifs. High CO_2 rock concentrations, together with the fact that recent structurally controlled groundwaters draining fault zones in the intrusive complex have anomalously high U, HCO_3^- and P contents, may be diagnostic features of favourable source rocks.

A sound knowledge of the sequence of tectonic events affecting an intrusive complex would appear to be more important in determining source potential than geochemical parameters, although all are interactively significant. Uranium deposits in the Okanagan region formed after a period of extensional tectonism (Late Miocene to Early Pliocene), leading to optimum groundwater leaching of a 'fabric loosened' intrusive basement complex, and prior to a period of epeirogenesis (Late Pliocene to Early Pleistocene uplift), which resulted in cessation of the ore-forming hydrologic regime. The maximum period of formation is estimated to be between 4 and 1 Ma.

Acknowledgments

I thank D. Sawyer and T. Turner of Norcen Energy Resources Ltd. and L. Trenholme of New Tyee Resources Ltd. whose support initiated this work. Mineralogical investigations have been carried out in collaboration with A.L. Littlejohn of the Geological Survey of Canada. Analytical work was carried out largely in the laboratories of the Resource Geochemistry Subdivision, of the Geological Survey of Canada under the direction of Ms. G.E.M. Hall. Uranium analysis was by delayed neutron activation in the laboratories of Atomic Energy of Canada Ltd.

References

Boyle, D.R. and Ballantyne, S.B.
1980: Geochemical studies of uranium dispersion in south-central British Columbia; Canadian Institute of Mining of Metallurgy, v. 73, no. 820, p. 89-108.

Boyle, D.R., Littlejohn, A.L., Roberts, A.V., and Watson, D.M.
1981: Ningyoite in uranium deposits of south-central British Columbia - First occurrence in North American uranium deposits; Canadian Mineralogist, v. 19, p. 325-331.

Christopher, P.A.
1978: East Okanagan uranium area (Kelowna to Beaverdell), south-central British Columbia; British Columbia Ministry of Energy, Mines and Petroleum Resources, Preliminary Map 29.

Church, B.N.
1973: Geology of the White Lake Basin; British Columbia Ministry of Energy, Mines and Petroleum Resources, Bulletin 61, 120 p.

1977: Tertiary stratigraphy in south-central British Columbia; in Geological Fieldwork for 1976, B.C. Ministry of Energy, Mines and Petroleum Resources, 1977, p. 7-11.

Garrels, R.M.
1976: Genesis of some ground waters from igneous rocks, in Researches in Geochemistry, v. 2, ed. P.H. Abelson; John Wiley and Sons, New York, p. 405-420.

Johnston, L.M.
1980: Geochemistry of groundwater in crystalline rocks: a review; Progress report on hydro-geochemical research activities, Contaminant Hydrogeology Section, National Hydrology Research Institute, Inland Waters Directorate, Environment Canada, 101 p., (unpublished).

Jones, A.G.
1959: Vernon map area, British Columbia; Geological Survey of Canada, Memoir 296, 186 p.

Kovalev, V.P. and Malyasova, Z.V.
1971: The content of mobile uranium in extrusive and intrusive rocks of the eastern margin of the south Minusink Basin; Geochemistry International, no. 7, p. 541-549.

Krylov, A.Ya. and Atrashenok, L.Ya.
1959: The mode of occurrence of uranium in granites; Geochemistry, no. 3, p. 307-313.

Le Maitre, R.W.
1976: The Chemical Variability of Some Common Igneous Rocks; Journal of Petrology, v. 17, pt. 4, p. 580-637.

Little, H.W.
1957: Geology of the Kettle River (East Half) area, British Columbia; Geological Survey of Canada, Map 6-1957.

McNeal, J.M., Lea, D.E., and Millard, H.T. Jr.
1981: The distribution of uranium and thorium in granitic rocks of the Basin and Range Province, Western United States; Journal of Geochemical Exploration, v. 14, p. 25-40.

Mathews, W.H. and Rouse, G.E.
1963: Late Tertiary volcanic rocks and plant-bearing deposits in British Columbia; Geological Society of America, Bulletin, v. 74, p. 55-60.

Monger, J.W.H.
1968: Early Tertiary stratified rocks, Greenwood map-area (82E12), British Columbia; Geological Survey of Canada, Paper 67-42, 39 p.

Nockolds, S.R.
1954: Average chemical composition of some igneous rocks; Geological Society of America, Bulletin, v. 65, p. 1007-1032.

Okulitch, A.V.
1974: Stratigraphy and structure of the Mount Ida Group, Vernon (82L), Seymour Arm (82M), Bonaparte Lake (92P) and Kettle River (82E) map areas, British Columiba; Geological Survey of Canada, Paper 74-1A, p. 25-30.

Preto, V.A.
1970: Structure and petrology of the Grand Forks Group, British Columbia; Geological Survey of Canada, Paper 69-22, 80 p.

Rogers, J.J.W. and Adams, J.A.S.
1969: Uranium in Handbook of Geochemistry, v. II/1; ed. K.H. Wedepohl, Springer-Verlag, Berlin, p. 90-1 to 90-0-1.

Stuckless, J.S. and Nkomo, I.T.
1978: Uranium-lead isotope systematics in uraniferous alkali-rich granite from the Granite Mountains, Wyoming: Implications for uranium source rocks; Economic Geology, v. 73, p. 427-441.

Szalay, S. and Samsoni, Z.
1969: Investigation of the leaching of uranium from crushed magmatic rocks; Geochemistry International, v. 6, no. 3, p. 613-623.

6.

THE BEHAVIOUR OF U, Th AND OTHER TRACE ELEMENTS DURING EVOLUTION OF THE GUICHON CREEK BATHOLITH, BRITISH COLUMBIA

W.J. McMillan[1]
Ministry of Energy, Mines and Petroleum Resources

McMillan, W.J., The behaviour of U, Th and other trace elements during evolution of the Guichon Creek batholith, British Columbia; in Uranium in Granites, ed. Y.T. Maurice; Geological Survey of Canada, Paper 81-23, p. 49-53, 1982.

Abstract

Island arc series granitic rocks exemplified by the calc alkalic Guichon Creek batholith in south-central B.C. have primitive Sr isotopic ratios and mantle affinities. Uranium and thorium levels in these primitive intrusions tend to be very low. Differentiation trends during evolution of such intrusions tend to concentrate uranium and thorium into more acidic phases. However, if a fluid phase evolves, uranium and thorium are partitioned into it and the acidic phases become depleted in these elements.

Résumé

Les roches granitiques des séries de chaînes d'îles représentées par le batholite calco-alcalin de Guichon Creek dans le sud de la Colombie Britanique présentent des affinités entre les rapports isotopiques de Sr initial et le manteau. Les teneurs en uranium et en thorium dans ces intrusions primitives tendent à être très basses. La différenciation au cours de l'évolution de telles intrusions tend à concentrer l'uranium et le thorium dans des phases plus acides. Toutefois, lorsqu'une phase fluide évolue, l'uranium et le thorium s'y concentrent et les phases acides s'appauvrissent en ces éléments.

Introduction

Although preliminary work showed very low uranium and thorium abundances, a geochemical study of the behaviour of these elements was undertaken for the Guichon Creek batholith. The batholith was previously systematically sampled for major and trace element analyses, and a suite of these samples was selected for this study. The idea behind the work was to see how uranium and thorium changed as the batholith evolved; to see if later phases became enriched in U and Th.

General Setting

The Guichon Creek batholith lies at the south end of the Intermontane Belt in British Columbia (Fig. 6.1). It is associated with late Triassic island arc volcanism. Volcanic rocks in the Belt range from calc alkalic to alkalic in composition.

The batholith intrudes and metamorphoses Karnian sedimentary and volcanic rocks of the Nicola Group. The batholith is 202 ± 8 Ma by K-Ar methods (Northcote, 1969) and 205 ± 10 Ma by the Rb-Sr method (Armstrong, personal communication). That is, it is Norian on the geological time scale (Armstrong, 1978). Rocks of the Nicola Group range from Karnian to Norian in age and dykes originating from the batholith seem to have extrusive equivalents in the volcanic pile.

The batholith and the Nicola volcanic rocks have initial $^{87}Sr/^{86}Sr$ of about 0.7034; that is, they have ratios similar to those found for modern island arcs and are probably mantle-derived (Preto et al., 1979).

Geology and Evolution

The batholith is a dome shaped, composite intrusion (Fig. 6.2). Many mappable phases exist, but, in general, they represent two major evolutionary events. In the older event,

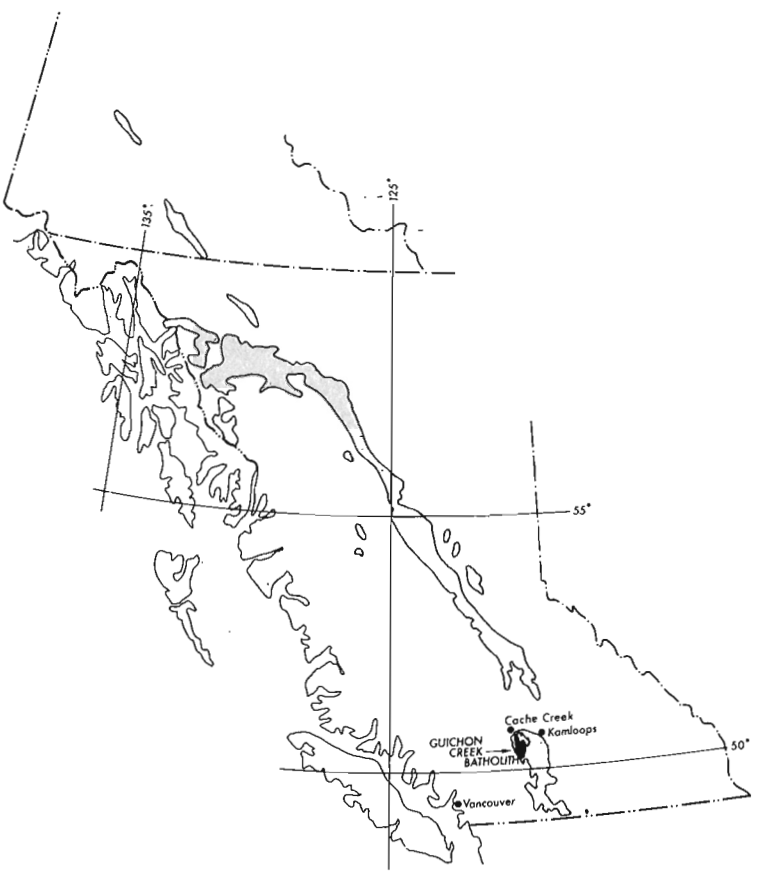

Figure 6.1. *Location map of the Guichon Creek batholith. Shaded area shows the distribution of late Triassic volcanic rocks in British Columbia.*

[1]Parliament Buildings, Victoria, B.C. V8V 1X4

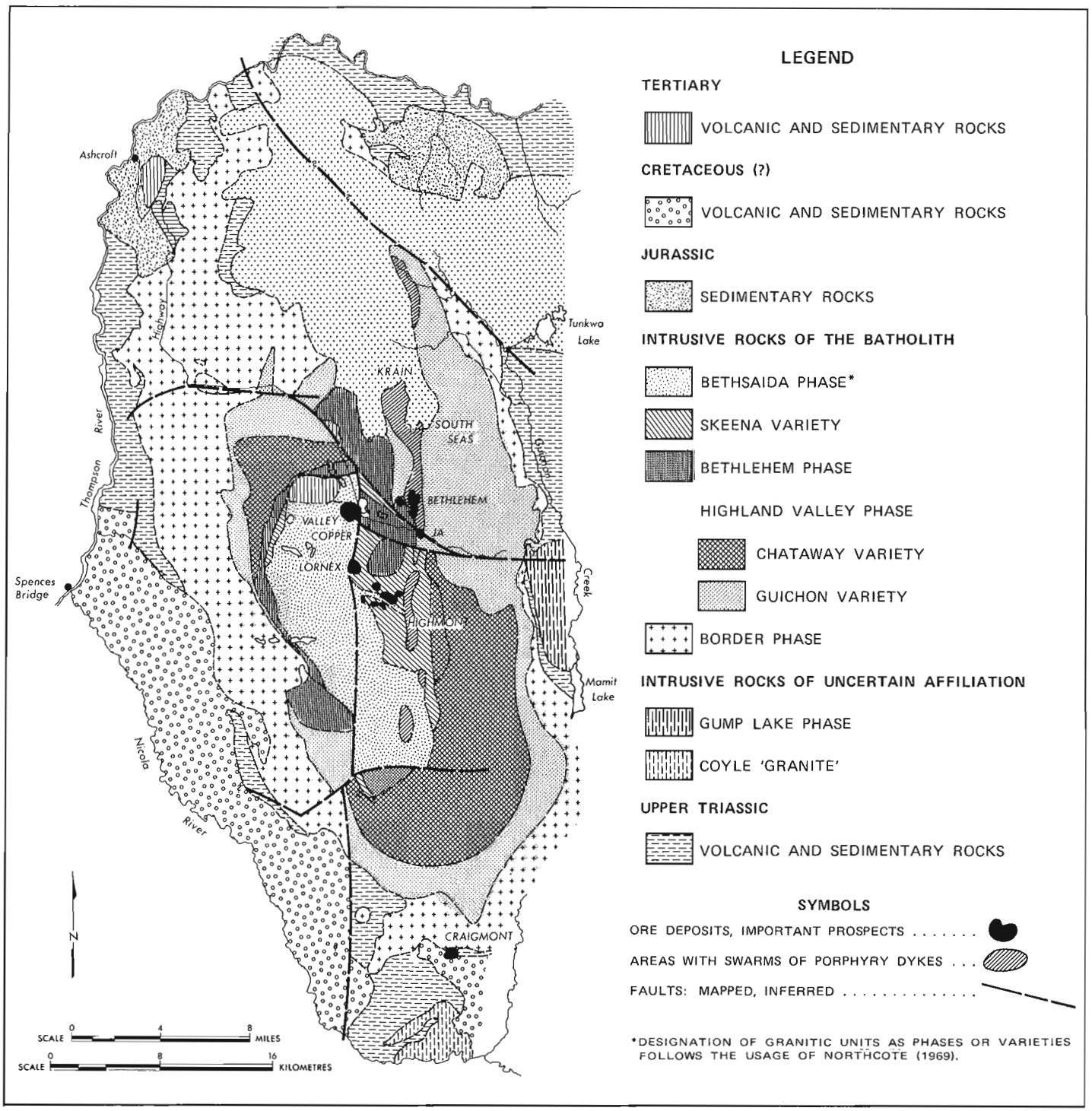

Figure 6.2. *General geology of the Guichon Creek batholith.*

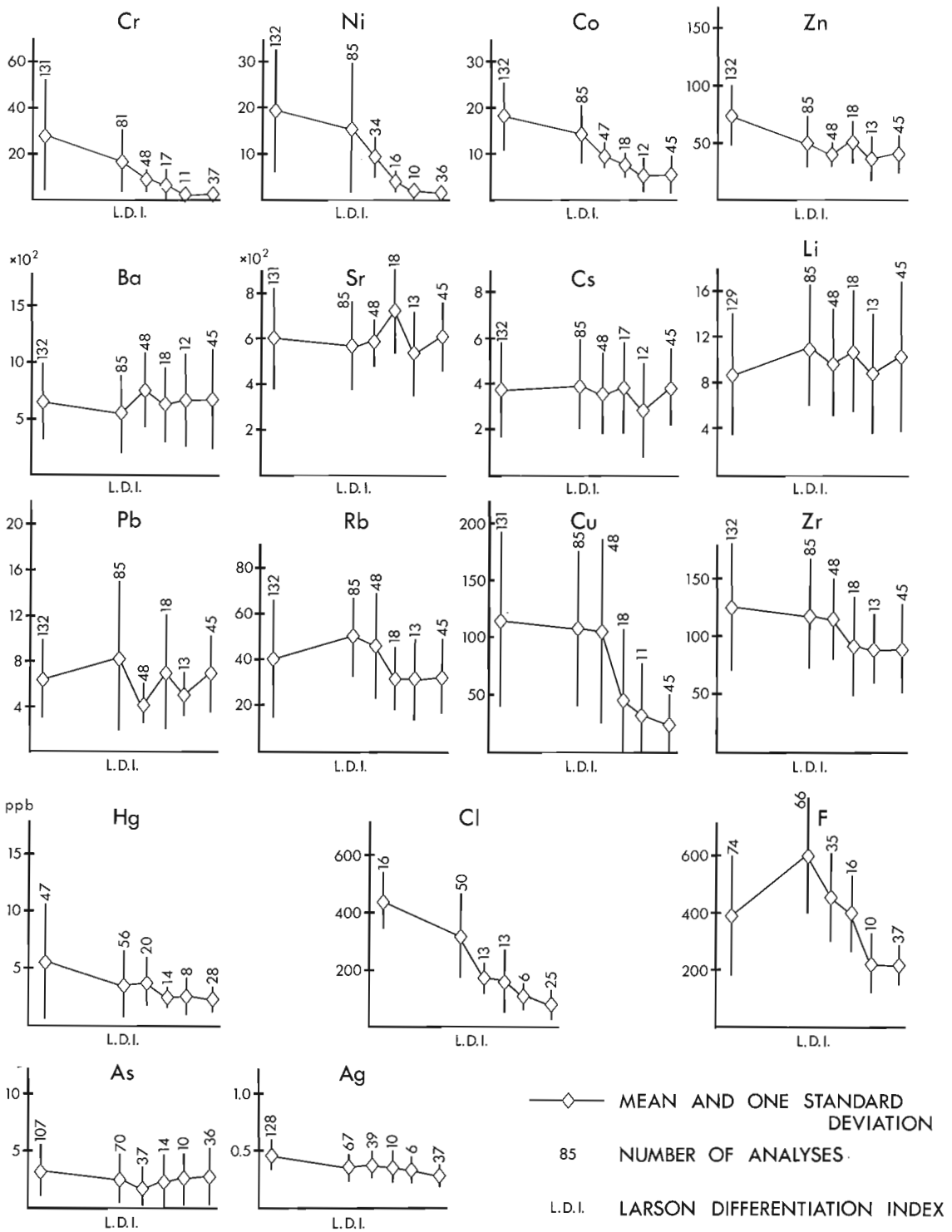

Figure 6.3. *Trace element evolution in rocks of the Guichon Creek batholith. L.D.I. increases to the right; from left to right phases are Border (B) quartz diorite, Guichon (G) granodiorite, Chataway (C) granodiorite, Bethlehem (Bm) granodiorite, Skenna (S) granodiorite and Bethsaida (Ba) quartz monzonite. Concentrations in ppm except Hg in ppb.*

quartz dioritic crystal-liquid mush was emplaced, cooled, crystallized and evolved to granodiorite. The younger event is characterized by renewed magma injection and volatile saturation followed by separation of a fluid phase; in this event granodiorite evolved to quartz monzonite. Apparently, the calc alkalic evolution of the batholith was controlled by cumulate crystallization (McMillan and Johan, 1981; Johan et al., 1980) from a single source magma. There are simple evolutionary curves for less mobile major elements, such as Ca, Mg, Mn, Fe and Ti but more mobile elements show a discontinuity that marks the fluid phase separation.

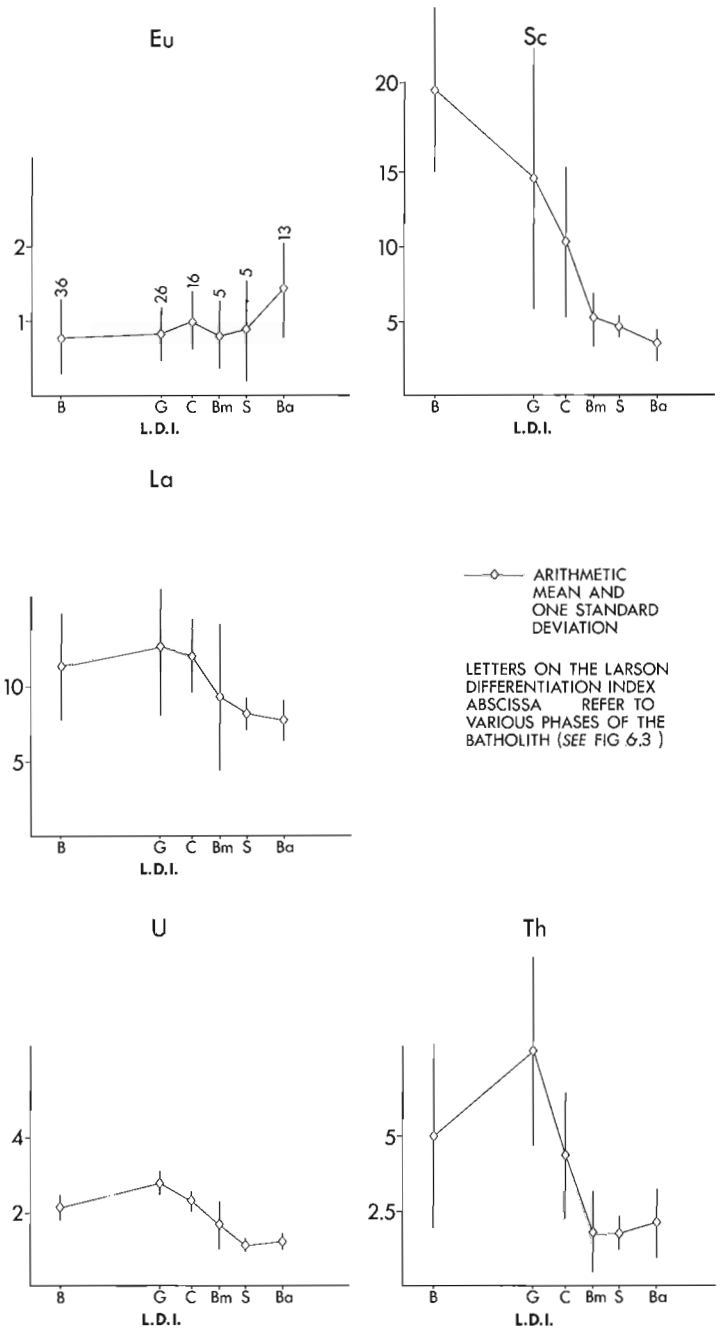

Figure 6.4. *Eu, Sc, La, U and Th evolution in rocks of the Guichon Creek batholith. Concentrations in ppm.*

Trace elements show similar patterns (Fig. 6.3). Chromium, Ni and Co have simple evolutionary curves; elements influenced by the distribution of Na, K and Ca have complex evolutionary paths that were apparently controlled by cumulate crystallization; Rb, Cu and Zr have discontinuities reflecting preferential partioning into the fluid phase.

For the present study approximately one hundred samples of the batholith were analyzed by neutron activation analysis for europium, scandium, lanthanum, uranium and thorium (Fig. 6.4). Europium abundance gradually increased from the most primitive to the most acidic phases. Scandium behaved like most of the major elements and gradually decreased with magma evolution. Both Eu and Sc show a slight discontinuity (break in slope) corresponding to evolution of the fluid phase. Lanthanum concentrations changed little with early evolution then dropped as it was preferentially partitioned into the fluid phase. Thorium concentration rose during the early stages of evolution, then dropped sharply as it also concentrated into the fluid. Uranium shows a pattern similar to that of Th but is less pronounced.

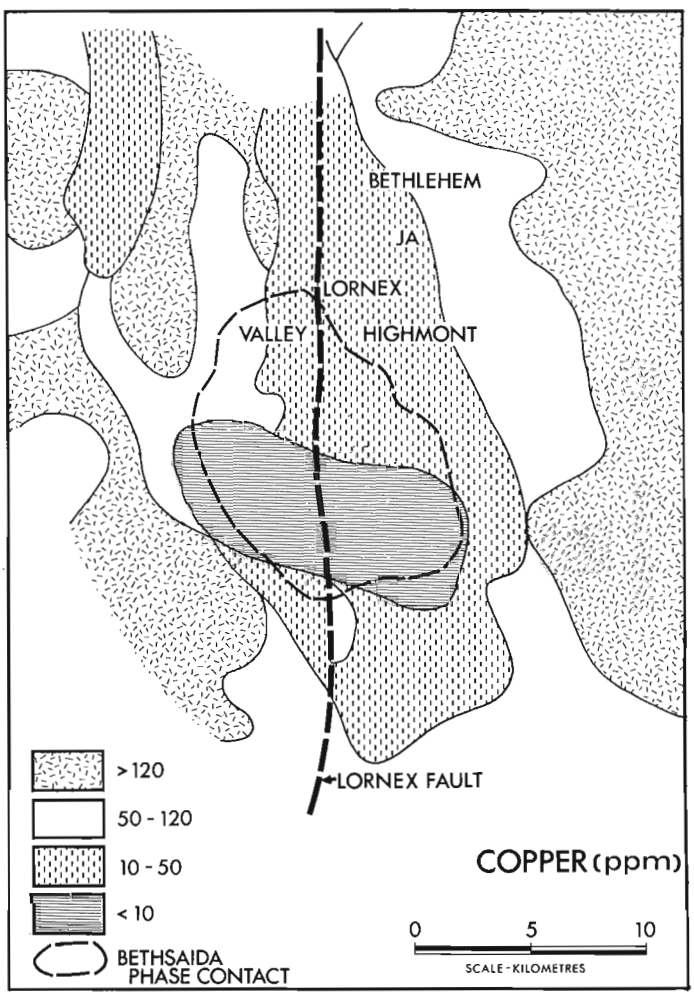

Figure 6.5. *Copper distribution in rocks of the Guichon Creek batholith. Post-mineralization offset on the Lornex Fault has been removed to clarify distribution patterns. The depleted area apparently outlines a former cupola in the youngest phase of the batholith.*

A central area, interpreted to have been a cupola, in the youngest phase of the batholith contains rocks that are strongly depleted in copper (Fig. 6.5) and also in uranium. Late stage potassic porphyry dykes adjacent to and in the cupola area have relatively high thorium and higher uranium concentrations than granitic rocks in the cupola zone. This phenomenon is very common in batholithic complexes regardless of age or derivation of magma; that is, concentration of U in aplitic, pegmatitic and porphyry dyke phases.

Conclusion

Granitic rocks in the Guichon Creek batholith have a common source magma. Evolution from quartz diorite to quartz monzonite was driven by cumulate crystallization at epizonal levels. Relatively mobile major and trace elements show a discontinuity midway through the crystallization history. This discontinuity is interpreted to have been caused by evolution of a hydrothermal phase from the magma. Thorium and uranium concentrations in the rock increased during the early, undersaturated stages of crystallization but both were preferentially partitioned into the hydrothermal phase when it developed. If no hydrothermal phase had developed it appears that both uranium and thorium would have become more concentrated in the later, more acid, phases of the differentiated complex.

Acknowledgments

Permission to publish the report was given by the Chief Geologist, B.C. Ministry of Energy, Mines and Petroleum Resources. The writer acknowledges discussions with and information from his French colleagues Z. Johan and L. LeBel; the manuscript was improved by suggestions from T. Hoy of B.C. Ministry of Energy, Mines and Petroleum Resources and two anonymous external readers. Most of the analytical data comprising the foundation of the interpretation were determined at the Ministry's Analytical Laboratory; U, Th, La, Sc and Eu were analyzed by neutron activation techniques by Novatrack Analysts of Vancouver.

References

Armstrong, R.L.
1978: Pre-Cenozoic Phanerozoic time scale. Computer file of critical dates and consequences of new and in progress decay constant revisions; American Association of Petroleum Geologists, Studies in Geology no. 6, p. 73-91.

Johan, Z., LeBel, L., and McMillan, W.J.
1980: Evolution géologique et pétrologique des complexes granitoïdes fertiles; in Z. Johan, coordinateur, Minéralisations Liées Aux Granitoïdes, France, Bureau de Recherches Géologiques et Minières, Bulletin 99, p. 21-70.

McMillan, W.J. and Johan, Z.
1981: Geochemistry of the Guichon Creek Batholith, British Columbia, Canada; in Proceedings of the Symposium on Mineral Deposits of the Pacific Northwest, 1980, eds. M. Silberman, C. Fuld, and A. Berry; U.S. Geological Survey Open File report 81-355.

Northcote, K.E.
1969: Geology and Geochronology of the Guichon Creek Batholith, B.C.; B.C. Ministry of Energy, Mines and Petroleum Resources, Bulletin 56, 73 p.

Preto, V.A., McMillan, W.J., Osatenko, M.J., and Armstrong, R.L.
1979: Recent Isotopic Dates and Strontium Isotopic Ratios for Plutonic and Volcanic Rocks in South Central B.C.; Canadian Journal of Earth Sciences, v. 16, no. 9, p. 1658-1672.

7.

GEOCHEMISTRY OF GRANITOID PLUTONS OF CAPE BRETON ISLAND, NOVA SCOTIA

Sandra M. Barr[1]
Acadia University

Barr, S.M., Geochemistry of granitoid plutons of Cape Breton Island, Nova Scotia; in Uranium in Granites, ed. Y.T. Maurice; Geological Survey of Canada, Paper 81-23, p. 55-59, 1982.

Abstract

Granitoid plutonic rocks in ten areas of Cape Breton Island have been mapped and sampled for petrological studies. These plutons range in age from late Hadrynian to Carboniferous, and include four with known occurrences of Cu, Mo, and/or W mineralization. They range from diorite to leucogranite in composition, and show typical calc-alkalic chemical trends. With the exception of one muscovite-bearing S-type pluton, all show characteristics of I-type granitoid rocks. They generally do not show chemical features typical of specialized (Sn-U) granites. Mineralized phases are generally lower in SiO_2 compared to unmineralized rock types, and high background means and standard deviations in Ba, base metals, and S may be useful in recognizing mineralized rock types.

Résumé

Des roches granitoïdes, dans dix régions de l'île du Cap-Breton, ont été cartographiées et échantillonnées en vue d'études pétrologiques. Ces intrusifs datent de la fin de l'Hadrynien jusqu'au Carbonifère et quatre d'entre eux contiennent des minéralisations connues en Cu, Mo ou W. Leurs compositions varient de la diorite au leucogranite et présentent des tendances chimiques typiques calco-alcalines. A l'exception d'un intrusif de type S, contenant de la muscovite, ils presentent tous des caractéristiques de roches granitoïdes du type I. Ils ne présentent généralement pas les caractéristiques chimiques typiques des granites spécialisés (Sn-U). Les phases minéralisées ont en général une faible teneur en SiO_2, comparées aux types de roches non minéralisées. Les valeurs de fond et des écarts types pour le Ba, les métaux de base et le S peuvent faciliter l'identification des types de roches minéralisées.

Introduction

Granitoid plutons are abundant in Cape Breton Island and yet few data were previously available concerning their geology, geochemistry, or economic potential. In 1978, a study of these plutons was initiated in co-operation with the Nova Scotia Department of Mines and Energy. To date, plutons in ten areas (Fig. 7.1) have been mapped and sampled, and petrographic studies and chemical analyses for major elements and selected minor and trace elements are completed or in progress. The main purpose of this project is to investigate aspects of the petrology and/or geochemistry which may be indicative of the presence of economic mineralization. In addition, information is being obtained concerning age and petrogenesis of these plutons, about which little was previously known.

This report summarizes some of the petrological and geochemical results of this study to date. Preliminary maps of the plutons showing the distributions of the various rock types have already been published (Barr et al., 1979; Barr, 1980; Campbell, 1980; Barr and Setter, 1980; Barr and O'Beirne, 1981). Detailed petrological descriptions and discussions of sampling and analytical methods are given elsewhere (Barr and O'Beirne, 1981; Barr et al., in preparation).

General Geology

The plutons studied are of late Hadrynian-Cambrian age (Huntington Mountain, Kelly's Mountain, St. Ann's Mountain, Boisdale Hills, Creignish Hills) or Devono-Carboniferous age (White Point, Gillis Mountain, Deep Cove, Petit de Grat), with the exception of the Cape Smoky pluton (Fig. 7.1) which may be Ordovician or Silurian (Cormier, 1972, 1979, 1980). Four have significant occurrences of Cu, Mo, and/or W mineralization associated with them (Fig. 7.1), whereas the others are not known to be mineralized. In the St. Ann's Mountain pluton, Cu-Mo mineralization occurs as disseminations in hornblende-biotite granite, whereas at Gillis Mountain Cu-Mo disseminations are present in all phases of the pluton (Barr and O'Beirne, 1981). At Deep Cove, Mo-Cu-Ag-Bi mineralization is widely distributed in the main granite body and in associated dykes as disseminations and coatings on fractures, as well as in veins and alteration zones. In the Boisdale Hills, W-Cu-Mo mineralization occurs in skarns adjacent to the pluton, and very locally within the granite itself.

With the exception of White Point, the plutons show characteristics of I-type granitoids, as defined by Chappell and White (1974). They typically range from diorite to leucogranite, although granite and leucogranite are the most abundant rock types. Hornblende is the most abundant mafic mineral in all rock types except the most felsic, where biotite is predominant. Accessory sphene is abundant. Primary muscovite occurs only in the White Point pluton. In geochemistry, the rocks are generally metaluminous, containing normative diopside or less than 1 per cent normative corundum. However, the White Point pluton is somewhat peraluminous (consistent with the presence of primary muscovite). The plutons typically have near linear variation diagrams, with concentrations and trends similar to those given by Gribble (1969) for average calc-alkalic plutonic rocks. Initial ratios of $^{87}Sr/^{86}Sr$ are low, typically less than 0.706, except for the White Point pluton where the initial ratio is 0.7097 ± 0.0011 (Cormier, 1972, 1979, 1980, personal communication, 1980).

[1] Department of Geology, Wolfville, N.S. B0P 1X0

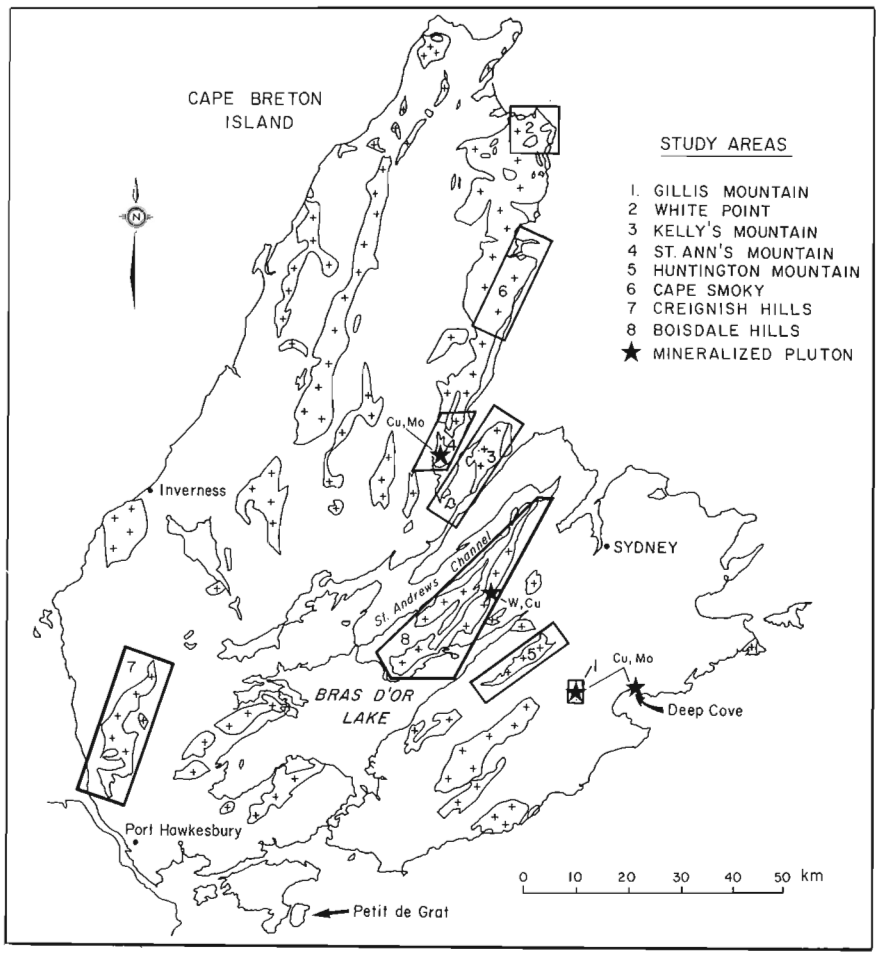

Figure 7.1

Location of areas of granitoid plutons which have been mapped and sampled for petrological studies (1-8, Deep Cove and Petit de Grat).

***Figure 7.2** (below)*

Means (solid vertical lines) and standard deviations (dashed vertical lines) in per cent for major oxides in Cape Breton granitoid rocks containing more than 66 per cent mean SiO_2 (Huntington Mountain, 17 samples; Kelly's Mountain, 30 samples; St. Ann's Mountain, 4 samples and 13 samples; Boisdale Hills, 15 samples; Cape Smoky, 34 samples; White Point, 34 samples; Gillis Mountain, 28 samples and 7 samples; Deep Cove, 9 samples; Petit de Grat, 8 samples). Pluton locations are shown in Figure 7.1. Data for 'specialized' and 'average' (normal) granites are after Tischendorf (1977).

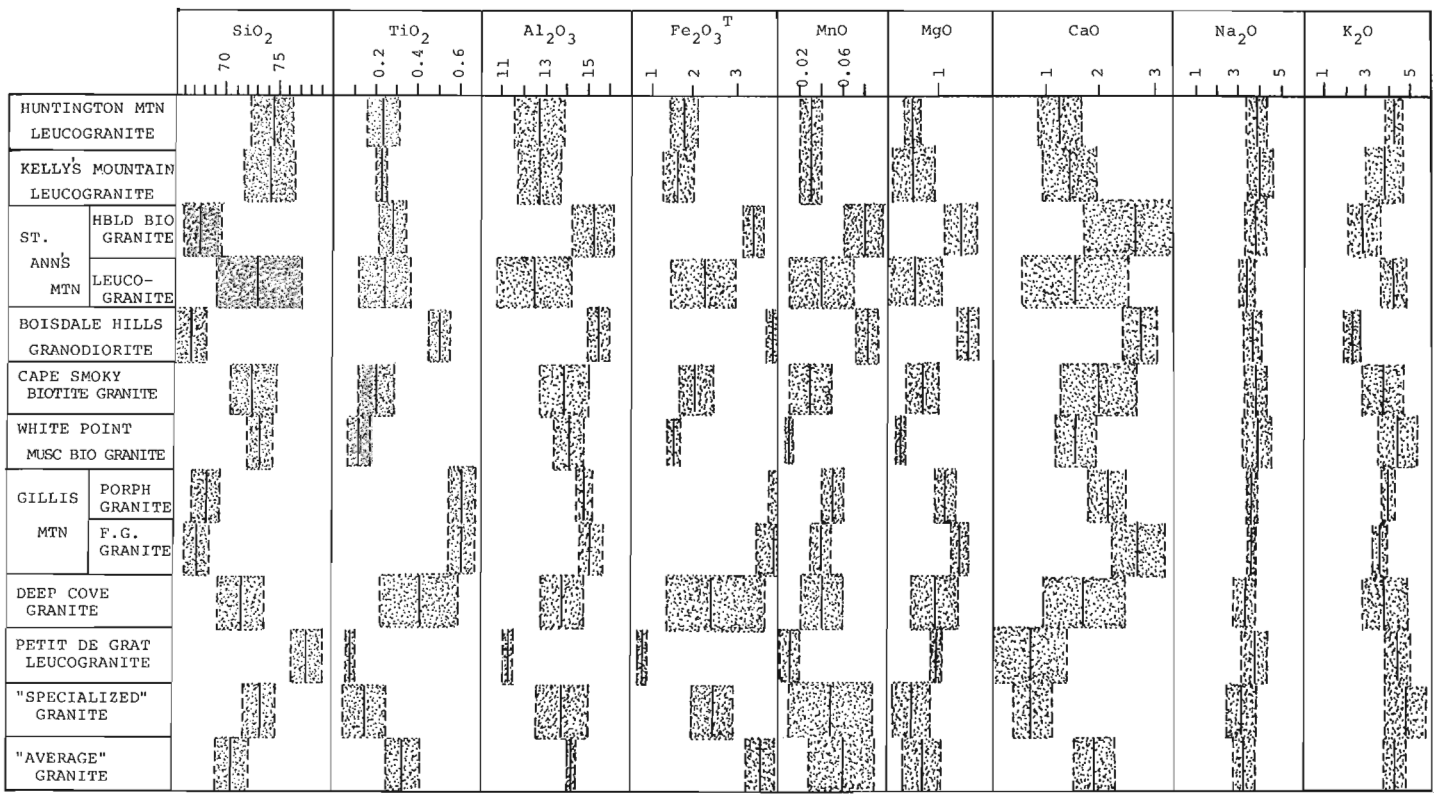

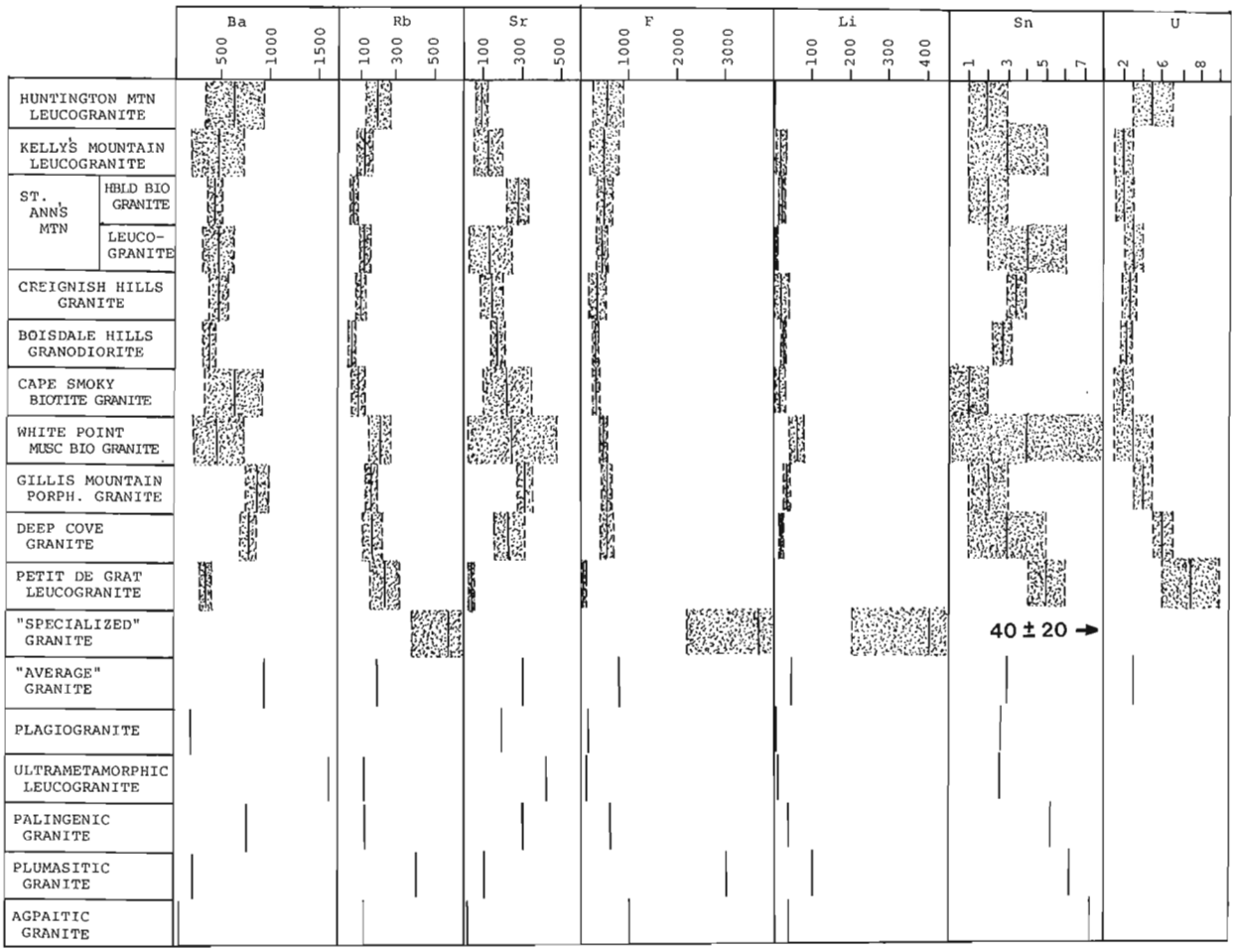

Figure 7.3. *Means (solid vertical lines) and standard deviations (dashed vertical lines) in ppm for selected trace elements in Cape Breton granitoid rocks containing more than 66 per cent mean SiO_2. Numbers of samples as in Figure 7.2, except Creignish Hills, 15 samples. Pluton locations are shown in Figure 7.1. Data for 'specialized' and 'average' (normal) granites are after Tischendorf (1977). Data for the last five granite types in the figure are from Tauson and Kozlov (1973).*

Table 7.1. K/Na, K/Rb, and Mg/Li ratios in granites. Data for 'average' (normal) and 'specialized' granites are after Boissavy-Vinau and Roger (1980), Tischendorf (1977), and Beuss and Stitnin (1968).

	K/Na	K/Rb	Mg/Li
'Average'	1.2	>100	270
'Specialized'	1.6	<100	75
Huntington Mtn.	1.2	176	620
Kelly's Mountain	1.1	229	148
St. Ann's Mtn.	1.3	242	248
Boisdale Hills	0.7	273	310
Cape Smoky	1.1	300	258
White Point	1.3	169	31?
Gillis Mountain	1.1	172	319
Deep Cove	1.2	174	352
Petit de Grat	1.4	153	-

This apparent predominance of I-type granitoid plutons in Cape Breton Island is consistent with the fact that most of the related mineralization is of Cu-Mo-W association, whereas there is an apparent lack of Sn-U mineralization which is generally associated with S-type granitoid plutons (Chappell and White, 1974).

Geochemistry

Because granitoid phases containing more than 66 per cent SiO_2 occur in all the plutons studied, the geochemistries of these rocks are compared in order to characterize both the mineralized and the unmineralized plutons (Fig. 7.2, 7.3, 7.4). These granites (sensu lato) can also be appropriately compared to the average (or normal) and specialized granites of Tischendorf (1977) and the granite classification of Tauson and Kozlov (1973).

In major element geochemistry, the Cape Breton granites (sensu lato) show considerable range compatible with their petrographic variation from granodiorite to leucogranite; generally those with relatively low SiO_2 contain elevated TiO_2, Al_2O_3, total Fe (as Fe_2O_3), MgO, and CaO

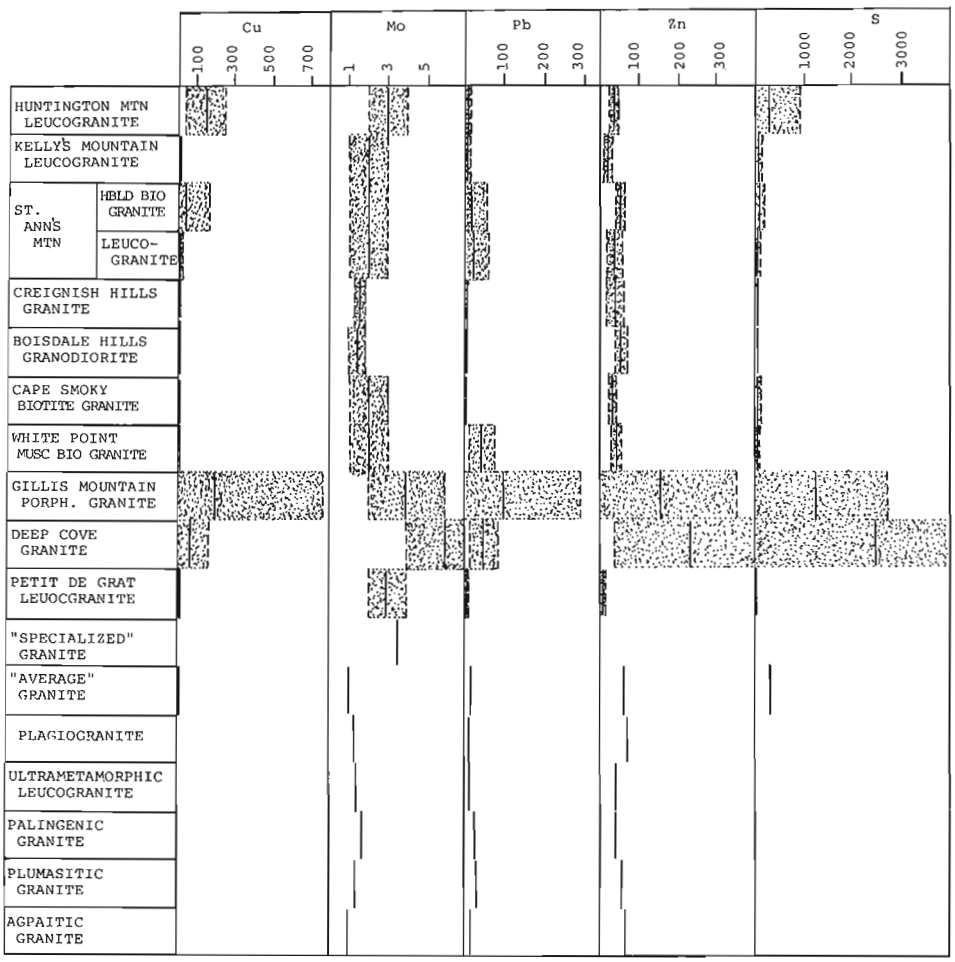

Figure 7.4. *Means (solid vertical lines) and standard deviations (dashed vertical lines) in ppm for selected trace elements in Cape Breton granitoid rocks containing more than 66 per cent mean SiO_2. Numbers of samples are as in Figure 7.2, except Creignish Hills, 15 samples. Pluton locations are shown in Figure 7.1. Data for 'specialized' and 'average' granites are from Tischendorf (1977) and Turekian and Wedepohl (1961). Data for the last five granite types in the figure are from Tauson and Kozlov (1973).*

(Fig. 7.2). The mineralized phases (St. Ann's hornblende-biotite granite, Gillis Mountain granite, Boisdale Hills granodiorite) are generally less felsic than the unmineralized phases, with the exception of the Deep Cove granite which may represent a related but more evolved phase than those at Gillis Mountain (Barr et al., in preparation).

Distinction between average and specialized granites on the basis of major elements is tenuous due to overlap in the ranges of most elements (Fig. 7.2). However, of the Cape Breton granites (sensu lato), only that of the Petit de Grat pluton, with its low CaO and TiO_2 and high SiO_2, resembles a specialized granite.

Trace element data more clearly demonstrate that, with the possible exception of Petit de Grat, Cape Breton granites (sensu lato) are not specialized in the sense of Tischendorf (1977). In particular, Rb, F, Li, and Sn are all much lower in Cape Breton granites (sensu lato) than in specialized granites, and are generally more in line with values for the average granite (Fig. 7.3). Uranium values are also average, with the exception of Petit de Grat which is clearly anomalous. According to the granite classification of Tauson and Kozlov (1973), the Cape Breton granites (sensu lato) are most similar to palingenic granites (Fig. 7.3) and show little similarity to plumasitic ('tin-bearing') or agpaitic ('rare-metal') granites, which are more or less equivalent to the specialized granites of Tischendorf (1973). Elemental ratios (Table 7.1) also confirm that Cape Breton granites (sensu lato) are not specialized.

The Cape Breton granites (sensu lato) generally contain average amounts of Cu, Pb, Zn, Mo, and S, with the exceptions of two of the plutons known to have associated sulphide mineralization: Gillis Mountain and Deep Cove (Fig. 7.4). These two plutons are also high in Ba (Fig. 7.3). These data suggest that high background means and standard deviations in these elements are indicative of mineralization, but it should be noted that these plutons are relatively small and intensely mineralized. The same pattern is not strongly apparent in the St. Ann's Mountain pluton where mineralization occurs only in the hornblende-biotite granite, a relatively minor phase of restricted extent, from which

sampling may have been insufficient to detect a pattern. No geochemical anomalies are apparent in samples from the Boisdale Hills, perhaps because the mineralization is primarily in skarns rather than in the granitoid rocks themselves.

Conclusions

The granitoid plutons studied in Cape Breton Island do not show the geochemical features typical of specialized granites which are generally associated with Sn, U, and related mineralization. Most are I-type granitoid plutons and hence more likely to have potential for Cu-Mo-W mineralization. However, those plutons which are known to have this type of mineralization in Cape Breton Island apparently do not show consistent geochemical indicator patterns, although Ba, base metals, and S may be useful in characterizing mineralized phases.

Acknowledgments

The data presented in this paper are taken primarily from a major report to be published by the Nova Scotia Department of Mines and Energy. G.A. O'Reilly of the Nova Scotia Department of Mines and Energy and A.M. O'Beirne, R.M. Campbell, and J.R.D. Setter, of Acadia University, made major contributions to acquisition and interpretation of the data. Petrographic and geochemical interpretations are included in M.Sc. theses completed or in progress by the latter three persons. However, the interpretations presented here are those of the writer, who thanks the Nova Scotia Department of Mines and Energy for field, technical, and financial support. This project is also funded in part by grant number A4230 from the Natural Sciences and Engineering Research Council of Canada.

References

Barr, S.M.
1980: Geochemistry of granitoid plutons of Cape Breton Island; Nova Scotia Department of Mines and Energy, Report 80-1, p. 127-129.

Barr, S.M. and O'Beirne, A.M.
1981: Petrology of the Gillis Mountain pluton, Cape Breton Island, Nova Scotia; Canadian Journal of Earth Sciences, v. 18, p. 395-404.

Barr, S.M. and Setter, J.R.D.
1980: Plutonic rocks of the Boisdale Hills, central Cape Breton Island; Nova Scotia Department of Mines and Energy, Information Series no. 3, p. 65-68.

Barr, S.M., O'Reilly, G.A., and O'Beirne, A.M.
1979: Geochemistry of granitoid plutons of Cape Breton Island; Nova Scotia Department of Mines and Energy, Report 79-1, p. 109-141.

Barr, S.M., O'Reilly, G.A., and O'Beirne, A.M. (cont.)
Geology and geochemistry of selected granitoid plutons of Cape Breton Island; Nova Scotia Department of Mines and Energy Report. (in press)

Beuss, A.A. and Stitnin, A.A.
1968: Geochemical specialization of magmatic complexes as criteria for the exploration of hidden deposits; XXIII International Geological Congress, Prague; Geochemistry, v. 6, p. 101-105.

Boissavy-Vinau, M. and Roger, G.
1980: TiO_2/Ta ratio as an indicator of the degree of differentiation of tin granites; Mineralium Deposita, v. 15, p. 231-236.

Campbell, R.M.
1980: Creignish Hills pluton; Nova Scotia Department of Mines and Energy, Report 80-1, p. 111-115.

Chappell, B.W. and White, A.J.R.
1974: Two contrasting granite types; Pacific Geology, v. 8, p. 173-174.

Cormier, R.F.
1972: Radiometric ages of granitic rocks, Cape Breton Island, Nova Scotia; Canadian Journal of Earth Sciences, v. 9, p. 1074-1086.

1979: Rubidium/strontium isochron ages of Nova Scotian granitoid plutons; Nova Scotia Department of Mines and Energy, Report 79-1, p. 143-147.

1980: New rubidium/strontium ages in Nova Scotia; Nova Scotia Department of Mines and Energy, Report 80-1, p. 223-233.

Gribble, C.D.
1969: Distribution of elements in igneous rocks of the normal calc-alkaline sequence; Scottish Journal of Geology, v. 5, p. 322-327.

Tauson, L.V. and Kozlov, V.D.
1973: Distribution functions and ratios of trace-element concentrations as estimators of the ore-bearing potential of granites; in Geochemical Exploration; International Geochemical Exploration Symposium, Proceedings, London, 1972, p. 37-44.

Tischendorf, G.
1977: Geochemical and petrographic characteristics of silicic magmatic rocks associated with rare-element mineralization; in Metallization Associated with Acid Magmatism, ed. M. Stremprok, L. Brunol, and G. Tischendorf; International Geological Correlation Programme, v. 2, p. 41-96.

Turekian, K.K. and Wedepohl, W.H.
1961: Distribution of the elements in some major units of the Earth's crust; Geological Society of America Bulletin, v. 72, p. 175-192.

8.

URANIFEROUS GRANITOID ROCKS FROM THE SUPERIOR PROVINCE OF NORTHWESTERN ONTARIO

F.W. Breaks[1]
Ontario Geological Survey, Toronto, Ontario

Breaks, F.W., Uraniferous granitoid rocks from the Superior Province of northwestern Ontario; in Uranium in Granites, ed. Y.T. Maurice; Geological Survey of Canada, Paper 81-23, p. 61-69, 1982.

Abstract

Recent regional examination of uranium-enriched coarse grained to pegmatitic Archean granitoids in part of the Superior Province of northwestern Ontario has revealed a dichotomy of host lithologies for the mineralization. A provisional classification based upon petrological attributes, geological setting, and U/Pb ages documents Type I uraniferous mineralization derived from migmatization of an extensive metasedimentary belt at 2.68 Ga, and Type II mineralization associated with fractionation of a potassic granitoid suite emplaced at about 2.65 Ga. Type I uraniferous mineralization exhibits a path of U-Th fractionation which trends subparallel to lines of average crustal estimates. Contrastingly, Type II mineralization generally exhibits distinctively different U-Th trends which ultimately manifest in very low Th/U ratios. In general, lower K/Rb, Ba/Rb, and higher K/Ba ratios are expressed by Type II uranium occurrences. One of the major controls on the less fractionated and lower grade Type I uranium mineralization is postulated to be lower fO_2 which may relate to the presence of graphite in a metapelitic precursor. Such conditions of reduced fO_2 are also reflected in the ubiquity of white K-feldspar in the S-type granitoids in contrast to the pink to red K-feldspar characterizing Type II uranium occurrences.

Résumé

Un examen régional récent des granitoïdes, allant des granitoïdes à grain grossier enrichis en uranium jusqu'aux granitoïdes pegmatitiques archéens, dans une partie de la province du Supérieur dans le nord-ouest de l'Ontario, a révélé deux types de lithologies hôtes de minéralisation. Une classification provisoire basée sur des attributs pétrologiques, le contexte géologique et les âges obtenus par le rapport U/Pb décrit la minéralisation uranifère de type I dérivée de la migmatisation d'une ceinture métasédimentaire déposée il y a 2,68 Ga, et la minéralisation de type II reliée au fractionnement d'une suite granitoïde potassique mise en place il y a environ 2,65 Ga. La minéralisation uranifère de type I présente un trajet de fractionnement U-Th orienté de façon subparallèle aux lignes de concentrations moyennes de la croûte. Par contraste, la minéralisation de type II présente généralement des orientations U-Th nettement différentes qui se traduisent finalement par des rapports Th/U très bas. En général, des occurrences d'uranium de type II présentent des rapports K/Rb et Ba/Rb plus bas et des rapports K/Ba plus élevés. On suppose qu'un des principaux facteurs de contrôle de la minéralisation uranifère de type I moins fractionnée et à plus faible teneur est la plus faible fugacité de l'oxygène, qui peut être associée à la présence de graphite dans un précurseur métapélitique. Cette faible fugacité de l'oxygène est aussi reflétés par l'omniprésence d'un feldspath K blanc dans les granitoïdes de type S, ce qui contraste avec la coloration de rose à rouge de ce minéral caractérisant les occurrences d'uranium de type II.

Introduction

The Vermilion Bay-Umfreville Lake area (Fig. 8.1) contains the most prolific development of uranium mineralization in granitoid rocks in the Superior Province of Ontario. Although the occurrence of uranium has been known in this area of the English River Subprovince and adjacent Wabigoon Subprovince since 1948, few data regarding geological/metamorphic settings and geochemical characteristics have been available until recently (Breaks and Bond, in preparation). The multiplicity of uranium occurrences, which in fact represent the largest class of lithophile mineralization in this region, could render this area of future exploration interest with regards to potential low grade, large tonnage mineralization, the 'porphyry uranium' deposits of Armstrong (1974). One particular occurrence at Celyn Lake has an average uranium content (Table 8.1) approximately twice that of the Rossing Deposit of Southwest Africa, currently the lowest grade uranium deposit being mined in the world.

The present study of uranium-enriched granitoid rocks in this region represents one facet of a special project designed to evaluate lithophile mineralization in the Superior Province of northwestern Ontario (Breaks and Bond, in preparation; Breaks, 1979, 1980).

Classification of Uraniferous Granitoids

In general, coarse grained to pegmatitic uranium-enriched granitoids have not been stringently classified in the past. Little (1970), for example, subdivided such rocks into red and white pegmatite categories. In this study, radioactive granitoids of northwestern Ontario have been provisionally classified according to the criteria of geological association, characteristic petrological attributes, and radiometric age.

Two distinctive types of uraniferous mineralization in granitoid rocks have been recognized in this region (Breaks et al., 1978) as indicated in Table 8.2. The provisional classification was also found to be applicable elsewhere in the Superior Province of northwestern Ontario,

[1]Consulting Geologist, 110 Chan Crescent, Saskatoon, Saskatchewan, S7K 5NB

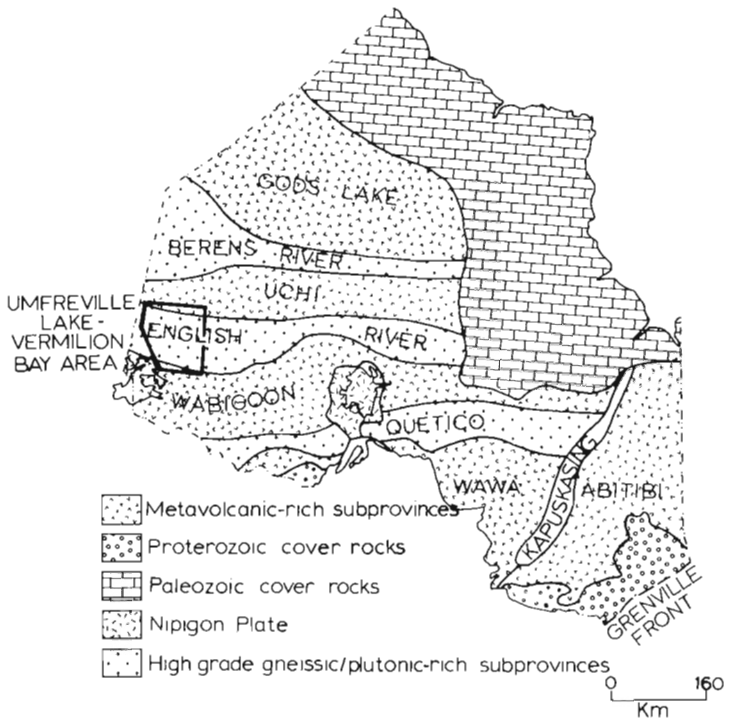

Figure 8.1. *Subprovinces of the Superior Province of northern Ontario (after Goodwin, 1970 and Wilson, 1971).*

where both types of uraniferous granitoid rocks were delineated in the Favourable Lake area (Bond and Breaks, 1978).

Occurrences exemplifying the two distinctive types of uraniferous mineralization are best exposed in the eastern Umfreville Lake area (Fig. 8.2, 8.3).

I. Metasedimentary Migmatite Uranium Association

Uranium mineralization occurring in this environment is principally confined to the Northern Supracrustal Domain of the English River Subprovince (Fig. 8.2). The great majority of known Type I occurrences bears a peripheral relationship to an ovoid shaped, low pressure granulite metamorphic centre positioned over the western part of this domain, between Umfreville and Conifer lakes (Fig. 8.2). Host rocks are white, massive to cataclastic, two-mica, inhomogeneous and homogeneous diatexites (i.e. S-type granitoids of White and Chappell, 1977) derived via advanced stage partial melting of wacke-mudstone metasediments. In the field, these rocks are petrologically distinctive by virtue of a peraluminous accessory mineralogy relating to a metapelitic progenitor (i.e., cordierite, almandine, sillimanite, tourmaline, muscovite, and rarely dumortierite and andalusite) and by variable amounts of melanosome and paleosome 'debris' inherited from the anatectic process.

Model for Derivation of Type I Uraniferous Granitoids

Prior to high grade metamorphism and ambient anatectic conditions, uranium-bearing horizons could have sporadically existed within a regionally extensive clastic sedimentary trough now represented by the Northern Supracrustal Domain of the English River Subprovince. This supposition is, in part, supported by high uranium contents in some metapelitic rocks from the Umfreville Lake area, which contain up to 30 ppm U and 25 ppm Th (Breaks and Bond, in preparation). The initial mode of uranium concentration in this sedimentary environment is, at present, not thoroughly understood. This initial concentration of U and Th may have been achieved via detrital concentration of accessory radioactive minerals and/or absorption by clay minerals within the clastic basin.

During regional anatexis of wacke-mudstone sediments at about 2.68 Ga (Krogh et al., 1976) this initial U and Th would be released to ubiquitous minimum melt systems. Proximity of the Umfreville-Conifer lakes granulite centre to the majority of Type I uranium occurrences is considered significant. Such metamorphic conditions imply relatively extensive partial melting and expulsion of lithophile elements such as U, Th, Rb, Li, Cs, etc. outwards to lower P-T zones. Within these anatectic systems, uranium complexes would fractionate into a residual melt phase which generally exhibits pegmatitic grain sizes.

The Late Archean Sydney Lake Fault Zone truncates the metamorphic sequence in the high grade zone, thus obviating comparison of trace element distribution in high grade and granulite zones with nonmigmatitic equivalents (low and medium grade metawacke and metapelites).

The Lake St. Joseph Facies Series (Breaks et al., 1978; Thurston and Breaks, 1978), situated approximately 190 kilometres east of the Umfreville-Conifer lakes granulite centre, however, contains a complete regional metamorphic progression, and allows for such an analysis. In Table 8.3, average abundance data for Rb, Cs, Li, U and Ba are presented for metawackes and metapelites as a function of metamorphic grade. U, Rb, Li, Cs show significantly lower levels in the Eastern Lac Seul Granulite Centre in comparision to the medium grade zone of this facies progression.

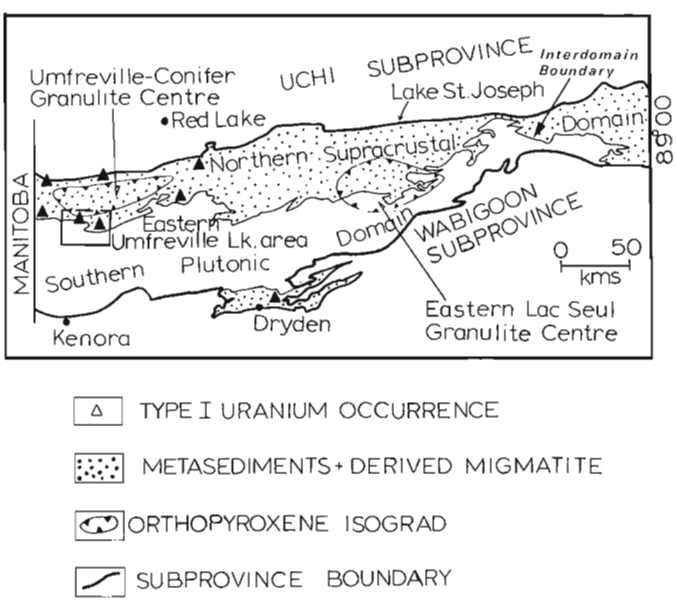

Figure 8.2. *Uranium mineralization associated with metasedimentary migmatite.*

Table 8.1. Average Uranium and Thorium concentrations for selected occurrences from the English River and Wabigoon subprovince

TYPE OF URANIUM MINERALIZATION	U*	Th**	n
Metasedimentary Migmatite Association			
Umfreville Lake Occurrence	52	108	47
Potassic Granitoid Suite Association			
Davidson Occurrence	184	34	50
Celyn Lake Occurrence	708	130	11
Tourist Lake Occurrence			
Porphyritic Syenite	23.5	47.5	2
Porphyritic Biotite Quartz Monzonite	12.5	77.5	8
Quartz-rich, Biotite Trondhjemite	675	335	2
Drope Township Occurrence			
High Grade Zone	427	450	9
Low Grade Zone	25.8	27.5	Bulk Sample
Ena Lake Occurrence	68.4	49	3
Richard Lake Deposit, New Campbell Island Mines Limited***	1000 (U_3O_8)	Not analyzed	Unknown

* Uranium analyses (ppm) by delayed neutron activation at Atomic Energy of Canada Limited, Ottawa.
** Thorium analyses (ppm) by X-ray fluorescence at Ontario Geological Survey Laboratories, Toronto.
n = number of analyses.
*** Analyses for Richard Lake deposit from Pryslak (1976, p. 46).

Table 8.2. Provisional classification of unzoned uraniferous granitoids in Superior Province of northwest Ontario

I. Metasedimentary migmatite association (White Granitoids) Umfreville Lake Occurrence

II. Potassic Granitoid Suite Association (Pink to Red Granitoids).

A. Inequigranular quartz monzonite to granite (sensu stricto) coarse grained to pegmatitic (Davidson Occurrence),

B. Porphyritic (K-feldspar) biotite-quartz monzonite, coarse grained (Tourist Lake Occurrence),

C. Biotite and biotite-hornblende syenite, coarse grained to pegmatitic (Celyn Lake Occurrence).

Table 8.3. Average U, Li, Rb, Cs and Ba contents (ppm) of metawackes and metapelites from Lake St. Joseph metamorphic facies progression

METAMORPHIC/GRADE	Li	Rb	Cs	Ba	U	n
MEDIUM GRADE						
Metapelites	66	91	11	394	2.9	7
Metawackes	45	68	11	326	3.0	9
HIGH GRADE						
Metapelites	25	62	9	332	2.8	17
Metawackes	11	53	6	287	2.7	39
GRANULITE						
Metapelites	14	61	6	558	1.8	9
Metawackes	10	42	5	379	1.0	9

Ba, Rb, Li by atomic absorption spectrophotometry and Cs by X-ray fluorescence at Ontario Geological Survey Geoscience Laboratories, Toronto. U by delayed neutron activation at Atomic Energy of Canada Limited, Ottawa.

n = Number of samples

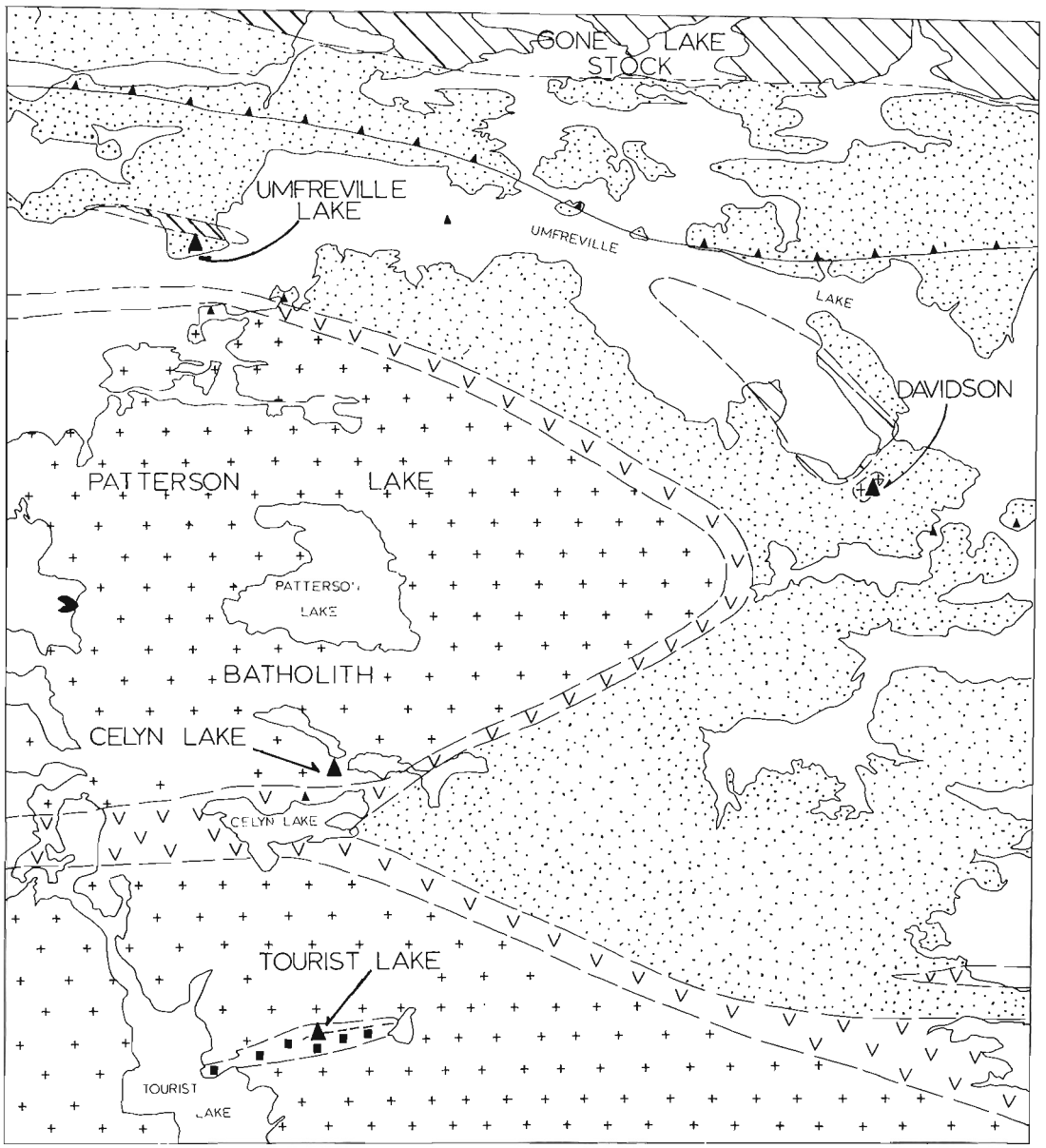

Figure 8.3. *General geology and uranium occurrences of eastern Umfreville Lake area.*

Association of uraniferous mineralization with S-type granitoids in the Northern Supracrustal Domain of the English River Subprovince represents an important new observation. Accordingly, a vast metasedimentary belt, some 1200 kilometres in length, may have future exploration significance with respect to low grade uranium deposits. S-type granitoids are extensively developed throughout the Northern Supracrustal domain, and cumulatively account for an areal extent of about 3400 km^2.

II. Potassic Granitoid Suite Uranium Association

Type II uranium occurrences are associated with distinctively different rocks which represent a prodigious late Archean invasion of potassium-rich granitic melt into the western part of the Southern Plutonic Domain of the English River Subprovince and adjacent Wabigoon Subprovince (Fig. 8.4). This lithological group which consists of massive, pink to red, biotite-bearing, coarse grained to pegmatitic granite (sensu stricto), quartz monzonite, granodiorite and rare syenite was emplaced at approximately 2.65 Ga, postdating the S-type granitoids engendered in the Northern Supracrustal Domain at 2.68 Ga (Krogh et al., 1976). This difference in radiometric age is considered significant in light of crosscutting relations exposed along the interdomain boundary which consistently reveal dykes of potassic granitoid suite rocks postdating S-type granitoids.

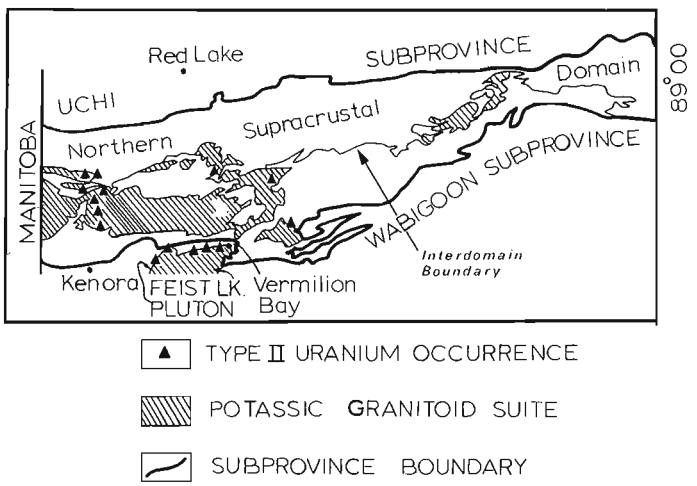

Figure 8.4. Distribution of Type II uranium mineralization associated with potassic granitoid suite rocks of Southern Plutonic Domain (English River Subprovince) and Wabigoon Subprovince.

The most prolific development of uranium mineralization is situated along the interface between the English River and Wabigoon subprovinces in the Vermilion Bay-Willard Lake area, recently investigated by Pryslak (1976) and Beard (1977). The majority of uranium mineralization appears to have evolved as marginal and exocontact residual pegmatitic phases, parental to the Feist Lake Pluton. The largest and highest grade deposit outlined to date here, is owned by New Campbell Island Mines Limited and contains 600 000 tons averaging 0.10 per cent U_3O_8 (Pryslak, 1976, p. 46). The uraniferous mineral phases isolated from this deposit are uraninite, uranothorite, allanite, and beta-uranotile (Robertson 1968, p. 58).

Several salient features serve to discriminate between host rocks of Type I and II uranium occurrences, despite a gross similarity in that both are associated with coarse grained to pegmatitic, leucocratic granitoid rocks:

1. Type II mineralization generally does not contain metasedimentary migmatitic paleosome and/or melanosome components;
2. Type II deposits are frequently found emplaced in amphibolitic mafic metavolcanic rocks or contain inclusions of such lithologies in variable quantities and dimensions; amphibolitic mafic metavolcanic rocks are absent in Type I deposits;
3. Ubiquitous pink to red characterizes host rocks of Type II deposits whereas S-type granitoid host rocks of Type I mineralization are pervasively white;

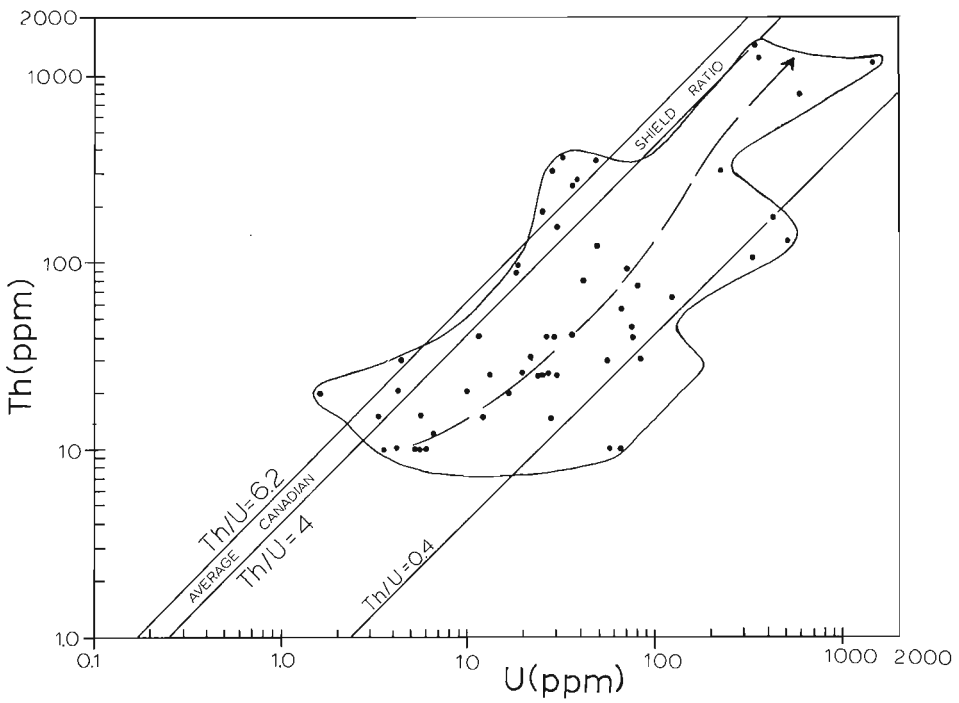

Figure 8.5

Th-U relations in Type I mineralization (Umfreville Lake occurrence). Average Canadian Shield Th/U ratios of 4 and 6.2 respectively from Shaw et al. (1976) and Fahrig and Eade (1968).

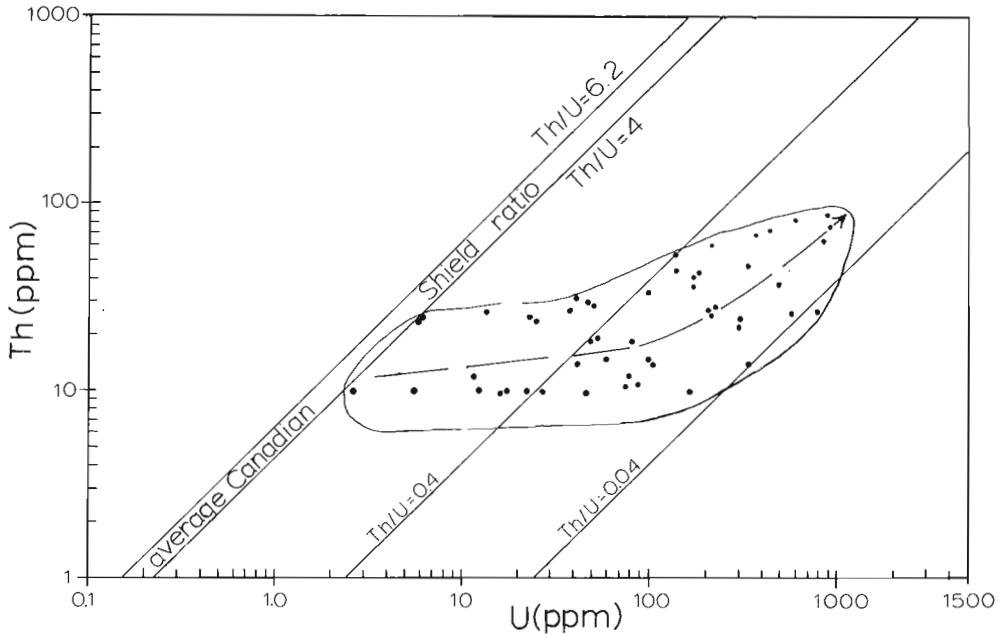

Figure 8.6. *Th-U relations in Type II mineralization (Davidson occurrence). Average Canadian Shield Th/U ratios of 4 and 6.2 respectively from Shaw et al. (1976) and Fahrig and Eade (1968).*

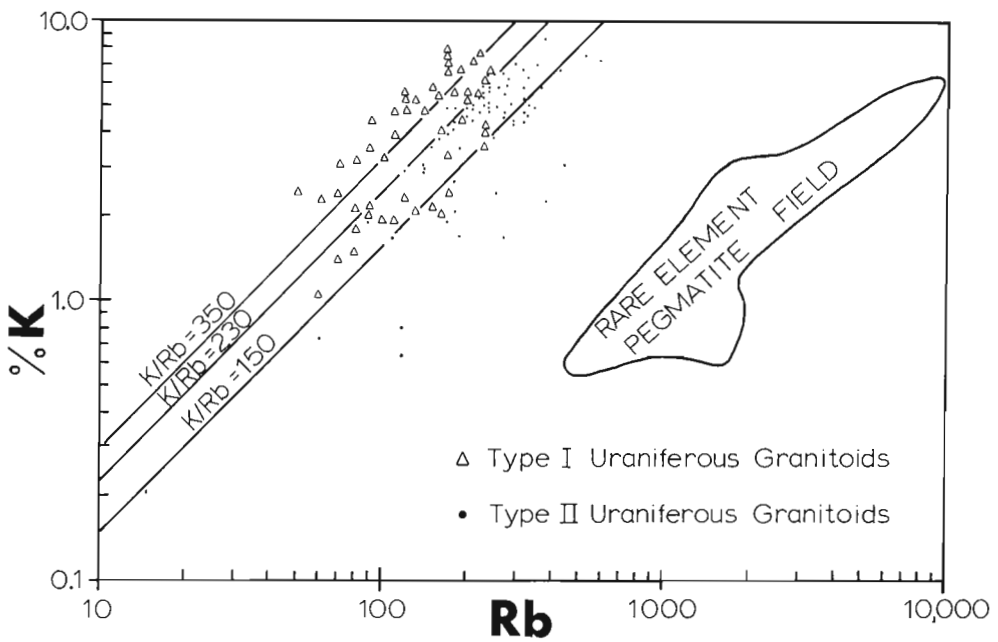

Figure 8.7. *K-Rb petrochemical variation in uraniferous granitoids of English River and Wabigoon subprovinces. Average and range for crustal K/Rb ratios from Taylor (1965).*

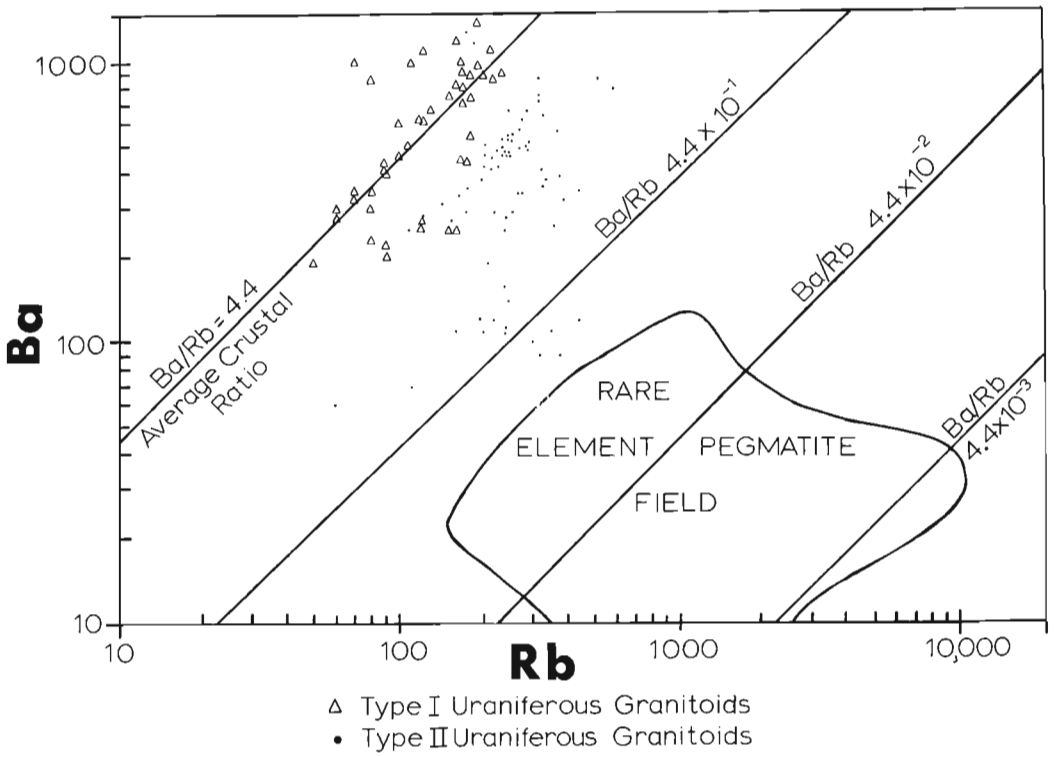

Figure 8.8. *Ba-Rb petrochemical variation in uraniferous granitoids of English River and Wabigoon subprovinces. Average crustal Ba and Rb values from Mason (1966).*

4. Type I uranium host rocks contain an uncommon accessory mineral suite (cordierite, almandine, sillimanite, andalusite, tourmaline, muscovite) for granitoid rocks. In Type II host rocks, biotite usually is the only widespread accessory mineral.

Geochemistry

Preliminary geochemical results indicate that some important differences exist between the two types of uranium mineralization. In terms of Th/U ratios, Type I deposits yield relatively high ratios, which do not substantially depart from the Canadian Shield averages estimated by Fahrig and Eade (1968) and Shaw et al. (1976) as indicated in Figure 8.5. Type II uranium deposits, contrastingly, exhibit fractionation trends characterized by uranium levels increasing at a much greater rate than thorium (Fig. 8.6), ultimately producing very low, distinctive Th/U ratios (commonly 0.4 - 0.04). It is pointed out here that the trend in Type I Th/U ratios in particular, is based only upon one occurrence and results from several others would be required to validate the observed trend. Type II uranium deposits also exhibit increased fractionation with respect to lower K/Rb, Ba/Rb, and higher K/Ba ratios although some overlap in the two data populations is evident (Fig. 8.7, 8.8, 8.9). Both types of uranium mineralization, however, are considerably less fractionated than Li-Be-Cs-Rb rare-element pegmatites also present in the region. According to Shmakin (1971, 1979), pressure has an important bearing on geochemical specialization of a pegmatite. Relatively high pressure (5-8 kbars) favours entry of Ba, Sr, and Pb isomorphously into K-feldspar whereas relatively low pressures, in the order of 2-3 kbars, considered to characterize that of rare-element pegmatites, results in high levels of large cations such as Rb and Cs and depletion of Ba in this mineral. Ba/Rb ratios in particular, have been

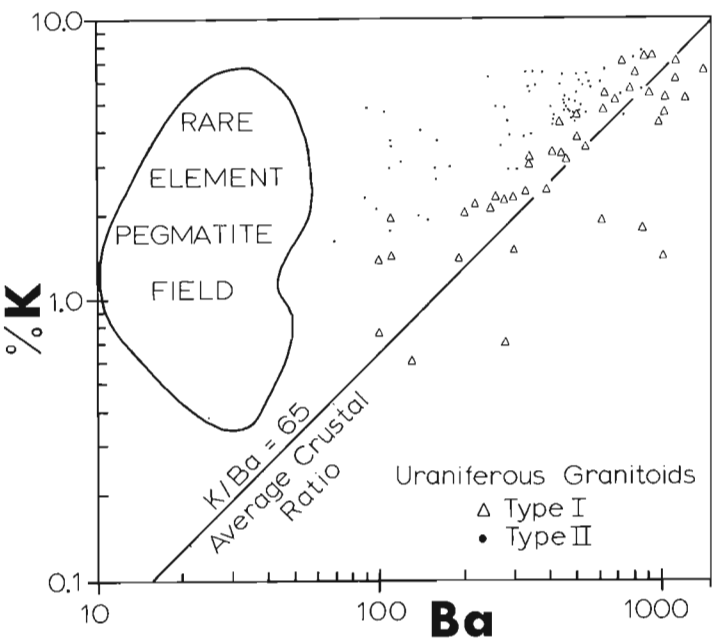

Figure 8.9. *K-Ba petrochemical variation in uraniferous granitoids of English River and Wabigoon subprovinces. Average crustal K and Ba values from Mason (1966).*

proposed as an efficient means of assessing pegmatitic specialization (Shmakin, 1971). Most Ba in the uraniferous granitoids likely resides in K-feldspar, since biotite, the only other major Ba-carrier, represents invariably less than 5 per cent of the rock. Mean Ba values of rare-element pegmatites exhibit a consistent trend of extreme depletion (Tot Lake = 35 ppm, Mavis Lake = 36 ppm, Roadhouse River = 33 ppm, Sandy Creek = 27 ppm) whereas mean Ba values are much higher in both types of uranium-rich granitoids (Umfreville Lake = 572 ppm, Celyn Lake = 435 ppm, Davidson = 405 ppm). This would appear to indicate relatively higher pressure conditions during crystallization of the uranium granitoids, according to the criteria of Shmakin (1971, 1973), although mineral geochemical data for K-feldspar, biotite, and muscovite are needed for more direct comparison.

It is speculated here that Type I uranium mineralization evolved under conditions of relatively lower fO_2, which would effect a lesser degree of concentration of U over Th. One possible controlling influence in the establishment of reduction conditions in Type I magmas may be related to the presence of graphite. Conversion of graphite into CH_4, CO_2, and CO species can have a drastic effect in lowering of fO_2 (Eugster, 1972). Graphite has been recognized in low and medium grade metapelites from the Lake St. Joseph Facies Series.

Summary

Investigation of uranium mineralization evident on a regional scale in part of the Superior Province of northwestern Ontario reveals a general confinement of such mineralization to granitoid rocks of two distinct affiliations. Classification of these uranium-enriched granitoids can be effected utilizing criteria of geological association, petrological idiosyncrasies, and U/Pb zircon ages:

Type I - Uranium associated with metasedimentary migmatite environment, specificially in S-type granitoid magma derived via 2.68 Ga regional anatexis of metawacke-metapelite.

Type II - Uranium associated with differentiation of 2.65 Ga potassic granitoid suite magma (quartz monzonite, granite (sensu stricto), granodiorite).

Geochemically, Type I uranium mineralization is relatively less fractionated than that of Type II, as evidenced by higher ratios of Ba/Rb and Th/U, and generally lower K/Ba and K/Rb. Type II occurrences contain the highest absolute uranium contents (up to 1.0 per cent U_3O_8) and lowest Th/U ratios. If large tonnage – low grade uranium deposits are sought, Type II mineralization is considered to represent a better exploration target, although the potential of Type I mineralization should not be completely discounted until a statistically valid number of occurrences have received systematic investigation. Neither type of uranium mineralization exhibits the advanced degree of fractionation evidenced in the more geochemically specialized rare-element pegmatites which concentrate elements such as Li-Be-Rb and, occasionally, Cs, Ta, and Sn.

The prime controls influencing the observed variation in host rock type to the uraniferous mineralization are considered to be fO_2 and source region for the granitic melt. fO_2 conditions in Type I magmas are reflected in lower $Fe^{3+}/Fe^{2+}+Fe^{3+}$ (Breaks and Bond, in preparation) and white K-feldspar. Type II magmas are generally more oxidized containing higher $Fe^{3+}/Fe^{2+}+Fe^{3+}$ and pink to red K-feldspar. A distinct accessory mineral suite is another important discriminatory feature and reflects differences in source region for the granitoid magmas. Type I uraniferous granitoids are typified by cordierite, almandine, sillimanite, muscovite, biotite, tourmaline and rare andalusite and dumortierite which reflects derivation from a metapelitic progenitor. Type II uraniferous granitoids, which usually contain only biotite (occasionally accompanied by hornblende), are considered to have originated from partial melting of a relatively biotite-rich trondhjemite or quartz diorite.

Although classification of uranium mineralization occurring in various other environments is reasonably well established, that for uranium hosted in granitoid rocks has been extended only cursory attention in the past. As a result, generalization of a manifold of host rocks into one simple category such as 'pegmatite-type' has usually been the case, even though a diversity of granitoid rocks, potentially originating from different environments of magma generation, may be involved. This situation became evident during investigation of uranium-enriched granitoids in the research area. It is hoped that the classification advanced, although provisional, can be expanded through further studies undertaken in uranium-enriched terranes in other shield areas.

References

Armstrong, F.C.
1974: Uranium resources of the future – "Porphyry" uranium deposits; in Formation of Uranium Ore Deposits, International Atomic Energy Agency, Series no. STI/PUB/374, p. 625-634.

Beard, R.C.
1977: Uranium deposits of the Kenora area; in Proceedings of 23rd Annual Meeting of the Institute on Lake Superior Geology, ed. M.M. Kehlenbeck, S.A. Kissin, and R.H. Mitchell, p. 4.

Bond, W.D. and Breaks, F.W.
1978: Ground evaluation of airborne radiometric anomalies in northwestern Ontario, District of Kenora; in Summary of Field Work by the Ontario Geological Survey, ed. V.G. Milne, O.L. White, R.B. Barlow, and J.A. Robertson; Ontario Geological Survey Miscellaneous Paper 82, p. 22-27.

Breaks, F.W.
1979: Lithophile mineralization in northwestern Ontario, rare-element granitoid pegmatites; in Summary of Field Work by the Ontario Geological Survey, ed. V.G. Milne, O.L. White, R.B. Barlow, and C.R. Kustra; Ontario Geological Survey Miscellaneous Paper 90, p. 5-7.

1980: Lithophile mineralization in northwestern Ontario, rare-element granitoid pegmatites; in Summary of Field Work by the Ontario Geological Survey, ed. V.G. Milne, O.L. White, R.B. Barlow, J.A. Robertson, and A.C. Colvine; Ontario Geological Survey Miscellaneous Paper 96, p. 5-9.

Breaks, F.W. and Bond, W.D.
The English River Subprovince, northwestern Ontario – an Archean gneissic belt: geology, geochemistry, and associated mineral deposits; Ontario Geological Survey Report (in preparation).

Breaks, F.W., Bond, W.D., and Stone, D.
1978: Preliminary geological synthesis of the English River Subprovince, northwestern Ontario and its bearing upon mineral exploration; Ontario Geological Survey Miscellaneous Paper 72, 55 p.

Eugster, H.P.
1972: Reduction and oxidation in metamorphism II; 24th International Geological Congress Proceedings, Section 10, p. 4-11.

Fahrig, W.F. and Eade, K.E.
1968: The chemical evolution of the Canadian Shield; Canadian Journal of Earth Sciences, v. 5, p. 1247-1252.

Goodwin, A.M.
1970: Metallogenic evolution of the Canadian Shield; in Geology and Economic Minerals of Canada, Economic Geology Report 1; Geological Survey of Canada, 5th Edition, 838 p.

Krogh, T.E., Harris, N.B.W., and Davis, G.L.
1976: Archean rocks from the eastern Lac Seul region of the English River Gneiss Belt, northwestern Ontario, part 2. Geochronology; Canadian Journal of Earth Sciences; v. 13, no. 9, p. 1212-1215.

Little, H.W.
1970: Distribution of types of uranium deposits and favourable environments for uranium exploration; in Uranium exploration geology, Panel Proceedings Series, International Atomic Energy Agency, STI/PUB/277, Vienna, p. 35-49.

Mason, B.
1966: Principles of Geochemistry; New York, John Wiley, 3rd Edition, 310 p.

Pryslak, A.P.
1976: Geology of the Bruin Lake-Edison Lake area, District of Kenora; Ontario Division of Mines, Geological Report 130, 61 p.

Robertson, J.A.
1968: Uranium and thorium deposits of northern Ontario; Ontario Department of Mines and Mineral Resources, Circular 9, 106 p.

Shaw, D.M., Dostal, J., and Keays, R.R.
1976: Additional estimates of continental surface Precambrian shield composition in Canada; Geochemical et Cosmochimica Acta, v. 40, p. 73-83.

Shmakin, B.M.
1971: The role of pressure in geochemical differentiation of granites and pegmatites; Geochemistry International, v. 8, no. 6, p. 913-918.

1973: Geochemical specialization of Indian Precambrian pegmatites in relation to alkali and ore-element contents of the minerals; Geochemistry International, v. 10, no. 4, p. 890-899.

1979: Composition and structural state of K-feldspars from some U.S. pegmatites; American Mineralogist, v. 64, p. 49-56.

Taylor, S.R.
1965: The application of trace element data to problems in petrology; Physics and Chemistry of the Earth, v. 6, p. 133-213

Thurston, P.C. and Breaks, F.W.
1978: Metamorphic and tectonic evolution of the Uchi-English River Subprovinces; in Metamorphism in the Canadian Shield, ed. J.A. Fraser and W.W. Heywood; Geological Survey of Canada Paper 78-10, p. 49-62.

White, A.J.R. and Chappell, B.W.
1977: Ultrametamorphism and granitoid genesis; Tectonophysics, v. 43, p. 7-22.

Wilson, H.D.B.
1971: The Superior Province in the Precambrian of Manitoba; in Geoscience Studies in Manitoba, ed. A.C. Turnock; Geological Association of Canada, Special Paper 9, p. 41-49.

9. PETROCHEMISTRY OF THE BLACHFORD LAKE COMPLEX NEAR YELLOWKNIFE, NORTHWEST TERRITORIES

A. Davidson[1]
Geological Survey of Canada

Davidson, A., Petrochemistry of the Blachford Lake complex near Yellowknife, Northwest Territories; in Uranium in Granites, ed. Y.T. Maurice; Geological Survey of Canada, Paper 81-23, p. 71-79, 1982.

Abstract

Field studies in 1971 and 1978 outlined a relatively large, subcircular, high-level plutonic complex at the south edge of the Slave Province. Radio-isotope analyses give ages of the order of 2150 Ma. Successive intrusive units range from gabbro (with anorthosite inclusions) through leucoferrodiorite, quartz syenite and granite to peralkaline granite and syenite. Nb and REE mineralization, along with high concentrations of Na, Zr, F and, locally, Y, Th and U, is associated with late pegmatite veining and alteration in the peralkaline rocks. This study documents progressive changes in major and minor element concentrations in the intrusive rocks. Differentiation by fractionation appears to have played a dominant rôle in the development of both the earlier aluminous and later peralkaline rocks. Chemical differences between these two suggest the possibility of different origins, but one unit, the Whiteman Lake Quartz Syenite, has some characteristics of both. High initial $^{87}Sr/^{86}Sr$ ratios in the peralkaline rocks can be as well explained in terms of a lengthy fractionation process as by crustal derivation or contamination of magma. Patterns of element depletion and enrichment throughout the differentiated suite are entirely consistent with the hypothesis that the observed alteration and mineralization are the end-products of magmatic differentiation.

Résumé

Des études effectuées sur le terrain en 1971 et en 1978 ont permis de tracer le contour d'un complexe plutonique relativement étendu, subcirculaire et de haut niveau, à la limite sud de la province géologique des Esclaves. Des analyses radio-isotopiques indiquent des âges de l'ordre de 2150 Ma. Les roches intrusives successives varient du gabbro (avec inclusions d'anorthosite) au granite peralcalin et à la syénite, en passant par la leuco-ferrodiorite, la syénite quartzifère et le granite. La minéralisation de Nb et de terres rares, de même que les concentrations élevées de Na, Zr, F et, par endroits, de Y, Th et U, est reliée à la formation tardive de filons de pegmatite et à l'altération dans les roches peralcalines. Cette étude décrit les changements progressifs dans la concentration des éléments mineurs et majeurs dans les roches intrusives. La différenciation par fractionnement semble avoir joué un rôle dominant dans la formation des roches alumineuses plus anciennes et des roches peralcalines plus récentes. Les différences chimiques entre ces deux types de roches supposeraient des origines différentes, mais une de ces roches, la syénite quatzifère de Whiteman Lake, possède des caractéristiques des deux types. Les rapports initiaux élevés $^{87}Sr/^{86}Sr$ peuvent être expliqués aussi bien par un lent processus de fractionnement que par une dérivation de la croûte ou une contamination du magma. Les configurations d'appauvrissement et d'enrichissement d'éléments pour toute la suite différenciée sont tout à fait cohérentes avec l'hypothèse que l'altération et la minéralisation observées sont le produit final de la différenciation magmatique.

Introduction

Mineralization containing notable concentrations of Nb, Li, Be, Zr, REE, Th, Y and U is associated with altered syenite at Thor Lake, near the north shore of the east arm of Great Slave Lake, 100 km southeast of Yellowknife (Fig. 9.1). The host syenite is part of the youngest unit of a highly differentiated plutonic complex, the Blachford Lake Intrusive Suite. Similarities in mineralogy between the host syenite, its late stage pegmatitic and albitic segregations, and the altered and mineralized rocks suggest that mineralization may be an ultimate product of magmatic differentiation processes. In this paper, petrological and chemical trends are examined in detail to see whether or not they support this hypothesis.

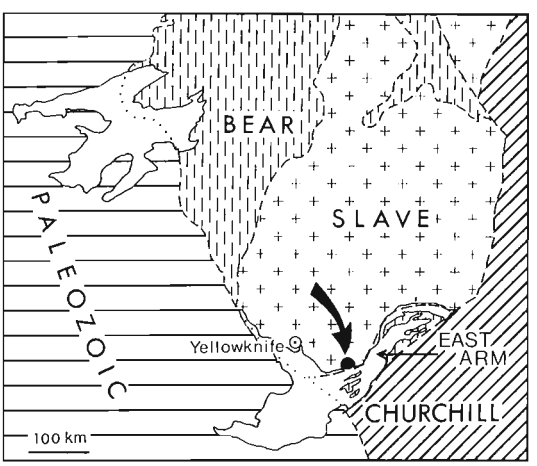

Figure 9.1. *Location of the Blachford Lake complex.*

Geological Setting and Mineralization

The Blachford Lake Intrusive Suite contains gabbro with both ultramafic and anorthositic components, leucocratic ferrodiorite, and syenites and granites of both aluminous and

[1]601 Booth St., Ottawa, Ontario, K1A 0E8

peralkaline type. The mafic rocks were first mapped in the 1930s (Stockwell, 1932; Jolliffe, 1936; Buckham, 1936; Henderson, 1938), but the unusual nature of the granitoid rocks to the east and their relationship to the mafic rocks were not recognized until much later (Davidson, 1972). Together these rocks make up a multiphase, subcircular ring complex some 23 km in diameter, intruded into a terrane of Archean metasedimentary and plutonic rocks in the southern part of the Slave Province (Henderson, 1976; Davidson, 1981). The complex itself has been dated radiometrically by various methods at around 2150 Ma (Wanless et al., 1979), and the regional field relationships suggest that it is older than the Aphebian Great Slave Supergroup that underlies the east arm of Great Slave Lake immediately to the south (Davidson, 1978). A generalized geological map (Fig. 9.2), condensed from 1:50 000 scale maps (Davidson, 1981, Fig. 1), illustrates the setting.

The complex itself is composed of several distinctive and successively intruded plutonic phases, in order: 1) Caribou Lake Gabbro, a unit of marginal gabbro, somewhat varied in composition, that grades inward to a plagioclase-rich phase, leucoferrodiorite, mapped separately; both contain large inclusions of an earlier anorthositic phase; 2) Whiteman Lake Quartz Syenite, a distinctly later intrusion ranging from syenite to granite that forms dykes in the Caribou Lake Gabbro and includes large blocks of it along with numerous xenoliths of country rocks; 3) Hearne Channel Granite and Mad Lake Granite, likely two phases of the same granite magma, both of which are relatively aluminous and contain hornblende and biotite; 4) Grace Lake Granite and Thor Lake Syenite, closely related to one another, with abruptly gradational contact and no obvious intrusive relationship; these units are both peralkaline and contain alkali amphibole but no biotite. The reader is referred to Davidson (1978) for further characterization of the rock types that make up these plutonic units, and for descriptions of their relationships.

It is convenient to consider the Blachford Lake complex in two parts: the earlier, western part including the Caribou Lake Gabbro, Whiteman Lake Quartz Syenite,

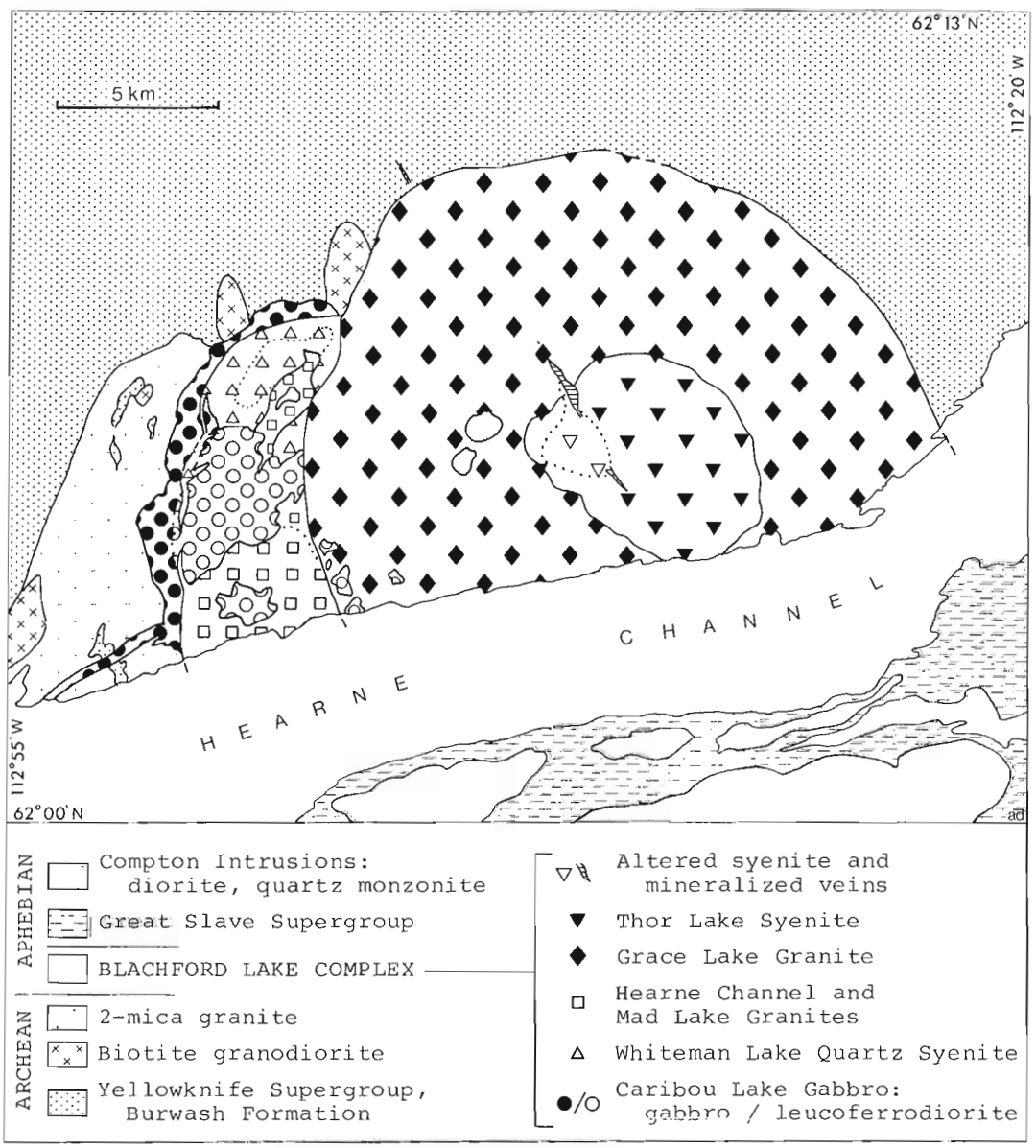

Figure 9.2. *Generalized geological map of the Blachford Lake complex.*

Hearne Channel Granite and Mad Lake Granite, and the later, dominating Grace Lake Granite with its Thor Lake Syenite core. It is within the later peralkaline units that the rare element mineralization is found. Associated with the peralkaline units are dykes and veins of pegmatite whose mineralogy is directly related to the host rocks. These dykes contain coarse acmite, riebeckite and, in places, astrophyllite, and may carry appreciable amounts of zircon, fluorite and bastnaesite. Dykes and veins of sugary to lath-textured albite with similar mineralogy, locally containing phenakite, xenotime and possibly pyrochlore, are spatially related to pegmatites in some areas, or occur alone in others. In the western part of the Thor Lake Syenite, a roughly triangular area of about 2 km^2 has been intensely altered to albite-rich rock with the same lath texture typical of the veins beyond this zone. Patchy mineralization within this zone, and extending both northwest and southeast as vein-like bodies, consists of concentrations of fluorite, carbonate, quartz and very fine grained zircon with rare minerals rich in Nb, Be, Li, Th, Y, U and notable amounts of rare-earth elements.

A small group of mineral claims was staked at Thor Lake for radioactive and rare-earth minerals in 1970, but was allowed to lapse. An airborne radiometric survey carried out by the Geological Survey of Canada in 1971 picked out an anomaly in both U and Th over this occurrence. In 1976, during the boom period in uranium exploration in the Northwest Territories, a much larger group of claims was staked in the vicinity of Thor Lake. To date, trenching and drilling has been unsuccessful in outlining a uranium orebody; in fact, thorium seems to be the main radioactive element. However, the property's chief hope of becoming a mine seems to lie in its notable concentration of niobium and tantalum, perhaps enhanced by Be, Y, Li and the rare-earth elements.

Geochemistry

Once it had been recognized that the Blachford Lake complex displayed features and relationships suggestive of a history of marked differentiation, the chemical part of this study was undertaken to see if concentration of rare elements in the altered zone and veins could be related to the differentiation process. Eighty-five whole-rock analyses, including 11 duplicates, of representative samples of the different units of the complex were made for major, minor and trace elements. The results are available on open file (Davidson, 1981). In addition, patterns of rare-earth element distribution were obtained on 19 samples, and electron microprobe analyses were made on the rock-forming minerals.

Ranges of elemental abundances in the various rock units are portrayed in Figure 9.3. Symbols used in this and subsequent diagrams are explained in Table 9.1. Note that some of the rock units have been subdivided on the basis of internal chemical differences, most of which are found to be areally restricted and thus could be mapped separately. The Hearne Channel and Mad Lake granites, of different aspect and areal distribution, have been included together on account of their essentially identical chemistries. In Figure 9.3, the Whiteman Lake Quartz Syenite has been split into two parts, syenitic and granitic. The rock units in these plots are arranged from left to right in order of decreasing age. It can be seen that, for the most part, continuous trends characterize the units of the earlier, western part of the complex, and that there are discontinuities in trend between the older aluminous granites and the younger peralkaline suite.

Certain predictable trends in the major elements are readily apparent, namely the increases in silica and alkalis, and the decreases in iron, magnesium and calcium towards the younger rocks. Note the peak accumulation of Al_2O_3 in the leucoferrodiorite phase of the Caribou Lake Gabbro, corresponding to a flood of plagioclase precipitation; also note the rather early depletion of Mg, particularly with respect to Fe, and the secondary increase in Fe, Mn and Na in the peralkaline rocks. Among the minor and trace elements, sulphur and heavy metals are depleted early; note, however, the distinct differences in the heavy metal distribution among the various gabbroic phases (Fig. 9.4), supporting the idea that the Caribou Lake Gabbro is itself a composite intrusion. Phosphorus peaks in the plagioclase-rich rocks of the Caribou Lake Gabbro, as does strontium. Ba deposits a little later than Sr. Zr, Rb, REE, Nb, Th and F concentrate, as expected, in the granitic and syenitic rocks. Note particularly that F, Nb and REE peak in the peralkaline suite, whereas U, Th and Rb are slightly more enriched in the aluminous granites. All, however, are concentrated in an albitic dyke (small inverted triangle symbol) that cuts the Thor Lake Syenite, and is likely related to nearby alteration and mineralization.

Harker diagrams for CaO and alkalis (Fig. 9.4), taken together, would signify that this is an alkalic suite, or more specifically, alkali-calcic with an alkali-lime ratio of about 52.5 (Peacock, 1931). The alkali/silica diagram alone, however, shows the gabbroic rocks, including the chilled margin rocks (outlined), to straddle the dividing line (Irvine and Baragar, 1975) between alkaline and subalkaline rocks. By this classification, all the leucodioritic and syenitic rocks, whether peralkaline or not, would be classified as alkaline, but intimately related more quartzose rocks would be subalkaline, including the strongly peralkaline Grace Lake Granite. Probably the best indicator of the nature of the Blachford Lake Intrusive Suite is given by the AFM plot (Fig. 9.5, B) which quite clearly shows the Fe enrichment trend typical of tholeiitic suites. Alkaline suites normally plot close to the dashed line on this diagram, which is the

Table 9.1. Symbols used to distinguish rock units and types Figures 9.3 to 9.7.

SYMBOL	ROCK TYPE	ROCK UNIT
♦	Granite dyke in Grace Lake Granite	
▾	Syenite dyke in Thor Lake Syenite	
◆	Riebeckite granite	- Grace Lake Granite
▼	Varieties of peralkaline syenite	- Thor Lake Syenite
✡	Syenite dyke in ferrogabbro	
□	Biotite-hornblende granite, granophyric or porphyritic	- Hearne Channel and Mad Lake Granites
⧫	Quartz syenite in contact with Grace Lake Granite	- Whiteman Lake Quartz syenite
△	Fayalite-pyroxene syenite to biotite-hornblende granite	
◬	Leuco-ferrodiorite xenolith in Whiteman Lake Quartz Syenite	- Caribou Lake Gabbro
○	Leuco-ferrodiorite	
◉	Sodic anorthosite xenolith in leuco-ferrodiorite	
⊙	Transitional gabbro - leuco-ferrodiorite	
●	Pegmatitic gabbro	
●	Noritic gabbro	
●	Olivine gabbro	
•	Chilled gabbro	
○	Calcic anorthosite xenolith in noritic gabbro	

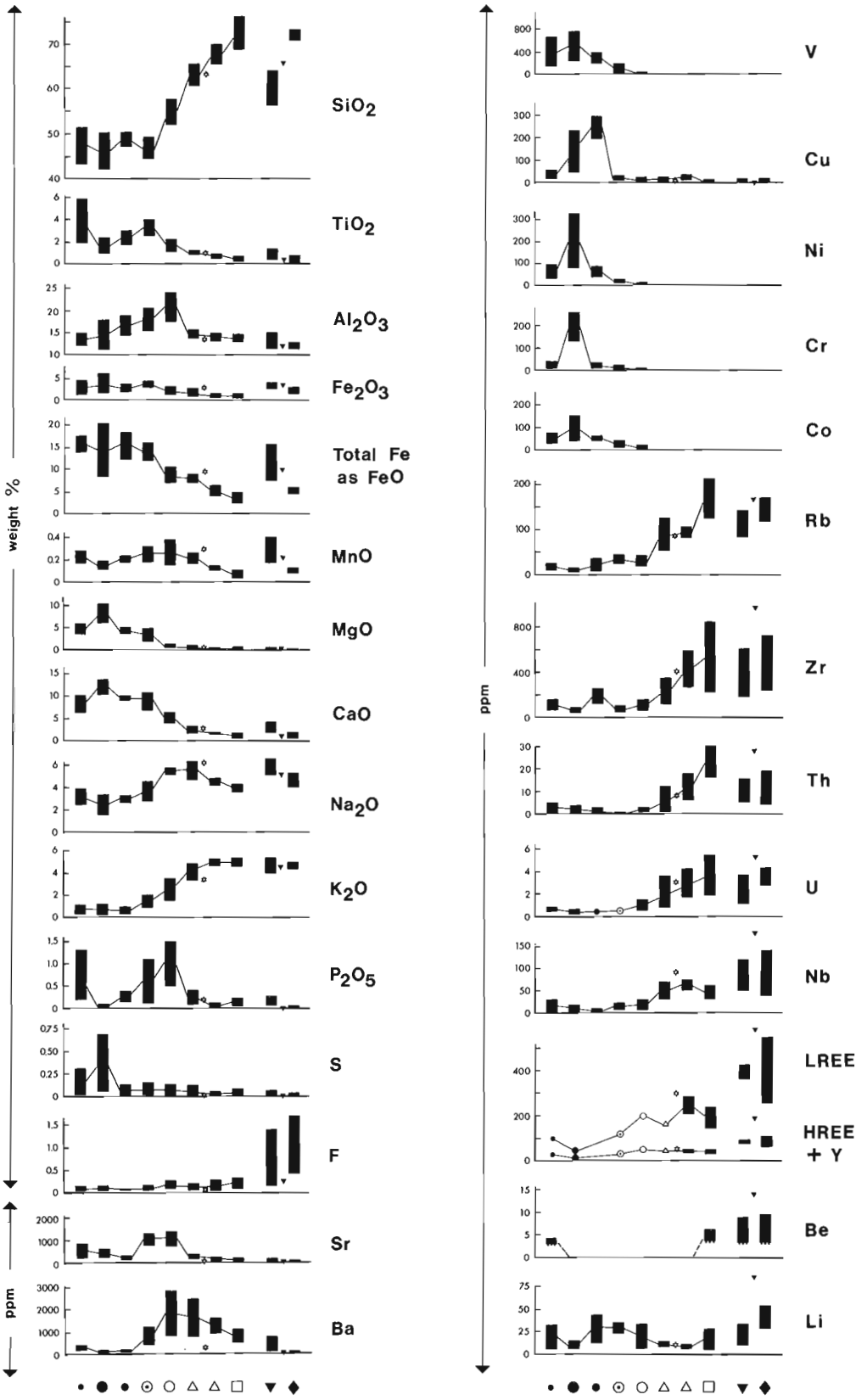

Figure 9.3. *Ranges of element content in units of the Blachford Lake complex. See Table 9.1 for symbols.*

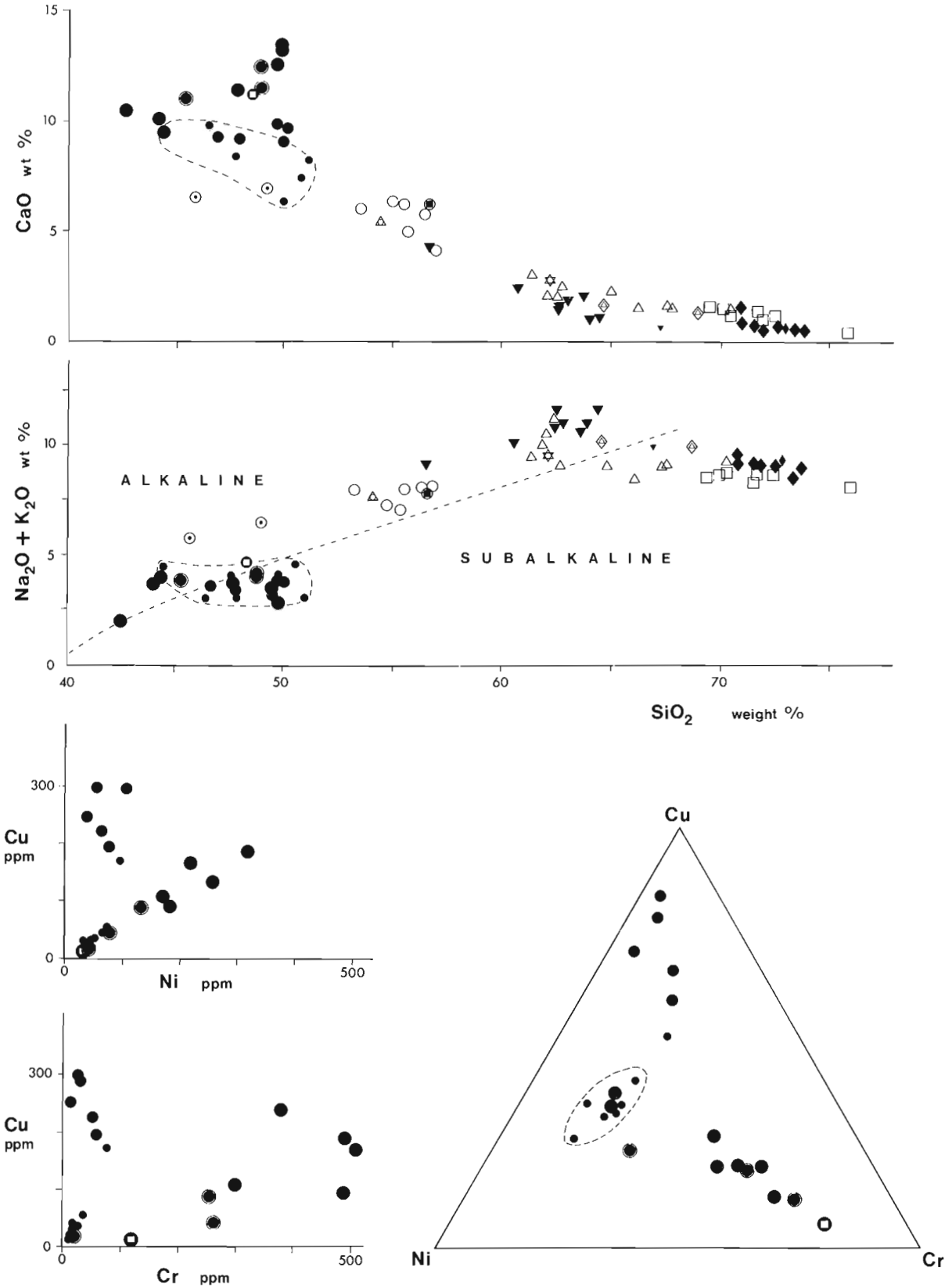

Figure 9.4. *Variation diagrams: variations of lime and of alkalis with silica, and variation of Cu, Ni and Cr in mafic phases of the Caribou Lake Gabbro. See Table 9.1 for symbols.*

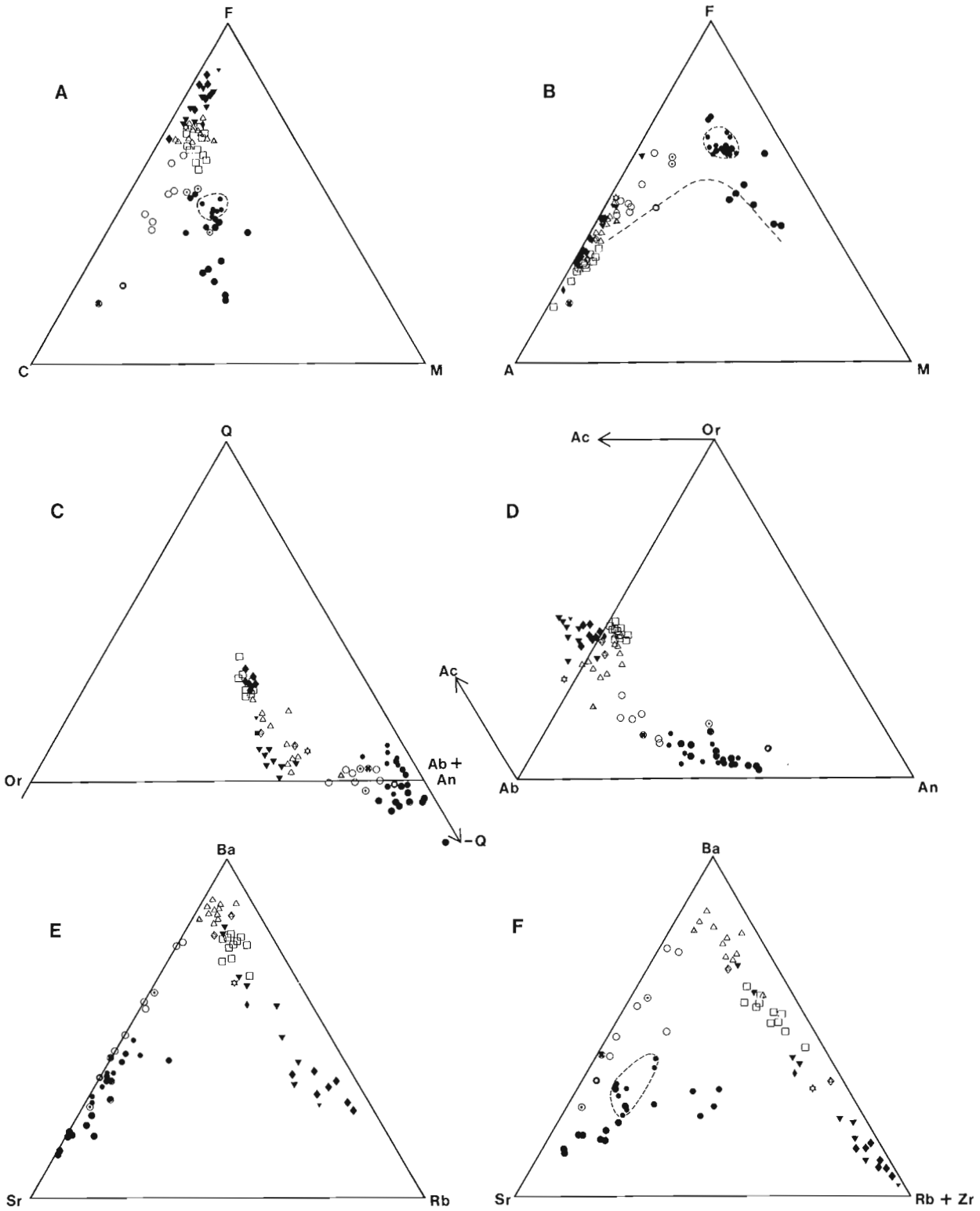

A – *CFM = CaO – Total Fe as FeO – MgO*
B – *AFM = Na_2O + K_2O – Total Fe as FeO – MgO*
C – *Normative Q – Or – Ab+An; normative Ne and Fo+Fa are recalculated to Ab and En+Fs respectively, giving -Q*
D – *Normative Ac – Or – Ab – An; rocks with normative acmite are peralkaline*
E,F – *Sr – Ba – Rb; and Sr – Ba – Rb+Zr.*

Figure 9.5. *Variation diagrams. See Table 9.1 for symbols.*

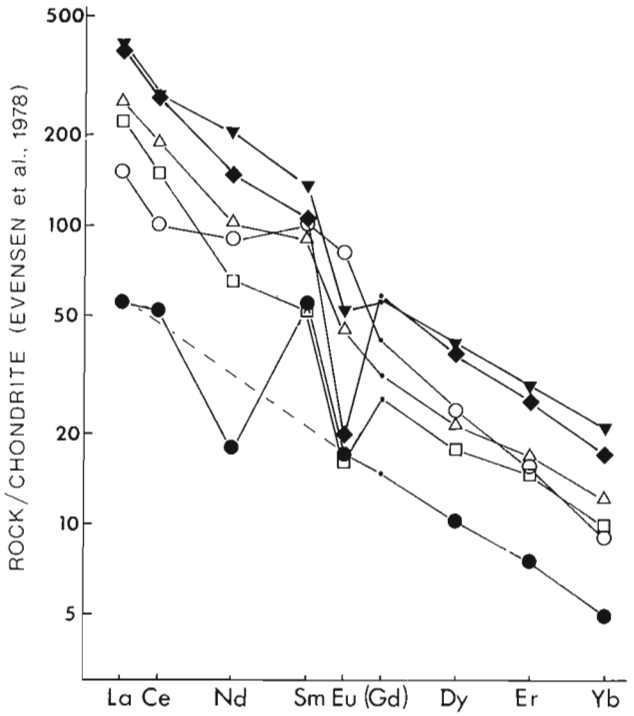

● *Caribou Lake Gabbro, average of 2 gabbros*
○ *Caribou Lake Gabbro, average of 2 leucoferrodiorites*
△ *Whiteman Lake Quartz Syenite, average of 3*
□ *Hearne Channel and Mad Lake granites, average of 2*
▼ *Thor Lake Syenite, average of 3*
◆ *Grace Lake Granite, average of 3*

Figure 9.6. *Chondrite-normalized rare-earth element patterns. Gadolinium was not analyzed.*

divider between tholeiitic and calc-alkaline suites (Irvine and Baragar, 1975). Interestingly, chilled margin gabbros (outlined) show a high degree of iron enrichment with respect to magnesium, a feature also brought out by the CFM plot (Fig. 9.5, A), and suggesting that even the earliest member of the suite, save for the included blocks of anorthosite, had already evolved considerably from a presumed more primitive (magnesian) parental magma.

The plot of normative plagioclase-orthoclase-quartz (Fig. 9.5, C) reveals an interesting distribution. It is quite unlike the normal calc-alkaline trend from gabbro through tonalite and granodiorite to granite; rather, it follows the feldspar trough (Tuttle and Bowen, 1958, Fig. 30) and corresponds to the trend that would be expected had crystal fractionation played an important rôle in the production of this differentiated suite.

Another informative plot is that of normative feldspar components (Fig. 9.5, D), which serves to separate the aluminous from the peralkaline rocks. In the latter, anorthite does not appear in the norm, as alkalis exceed alumina; these rocks, with agpaicity index greater than unity, have normative acmite. The trend shown here is exactly the same as that observed in the highly differentiated transitional – pantellerite volcanic complexes associated with the East African Rift System (Barberi et al., 1975).

The most extended trend, illustrating marked clustering for the different plutonic units, but also an overall continuum for the whole suite, is given by the Sr-Ba-Rb and Sr-Ba-(Rb+Zr) plots (Fig. 9.5, E, F).

Rare-earth element patterns, normalized against chondrites using the values of Evensen et al. (1978), for the six main units of the Blachford Lake Intrusive Suite are given in Figure 9.6. The evolved nature of the early gabbro magma already alluded to is also suggested by the patterns for the mafic rocks; these show a definite enrichment in the light rare-earth elements, whereas a primitive magma would be expected to have a relatively flat profile. Successive members of the suite show greater enrichment in light rare-earth elements, and the progressive development of negative Eu anomalies in the granitic rocks.

Analytical data on the mafic minerals in the Blachford Lake complex also illustrate extreme enrichment in iron with respect to magnesium during differentiation (Fig. 9.7). Clinopyroxenes differentiate to hedenbergite in the Whiteman Lake Quartz Syenite and to sodic hedenbergite in the Thor Lake Syenite. There does not seem to be a continuum to acmite, a pure to somewhat titanian form of which occurs as a late-formed mineral phase in the Grace Lake Granite and in pegmatitic veins. Olivine, nowhere more magnesian than Fo_{67}, becomes remarkably rich in fayalite even in the gabbroic rocks. There seems to be a composition break among the amphiboles: hastingsitic hornblende characterizes all but the peralkaline members of the suite, which contain ferrorichterite that is either zoned to or overgrown by riebeckite. The only exception, providing a link between the aluminous and peralkaline parts of the suite, is zoned amphibole found in the syenitic phases of the Whiteman Lake Quartz Syenite. In the earlier, aluminous part of the suite, biotite develops to almost pure annite.

Age Determinations

Unequivocal field evidence that the peralkaline rocks are younger than the various plutonic units of aluminous nature to the west led to a radiometric dating program for which one aim was to determine if this age difference is significant. K-Ar ages determined on minerals from units of both types are identical within the limits of analytical error (Wanless et al., 1979, Fig. 5), and both are indistinguishable from ages defined by whole-rock Rb-Sr isochrons for each of the Whiteman Lake Quartz Syenite, Mad Lake Granite and Hearne Channel Granite, all three of which have initial $^{87}Sr/^{86}Sr$ ratios between 0.700 and 0.703. The peralkaline units, on the other hand, exhibit enough scatter on the isochron plot that reliable isochrons cannot be constructed; suggested 'ages' are of the order of 200 Ma younger, and initial Sr ratios range from 0.711 to 0.714. Such differences in initial Sr ratio have been taken to support the hypothesis that, for any given igneous complex, rocks with low initial ratios crystallized from mantle-derived magmas whereas those with higher ratios crystallized from either crust-contaminated mantle magmas or lower crust-derived melts (e.g. Emslie, 1978, p. 64). However, this interpretation may not necessarily apply. The Blachford Lake Intrusive Suite has an extremely wide range in Rb:Sr ratio, from 0.003 in gabbro to more than 12 in peralkaline granite. A recent model proposed by McCarthy and Cawthorn (1980) would have initial Sr ratio increase with increase in Rb:Sr ratio during protracted fractionation, and can explain variation in initial Sr ratio without resorting to the idea of crustal contamination or derivation to account for high values. The variation is thus related to time of residence of fractionating magma at depth in the crust.

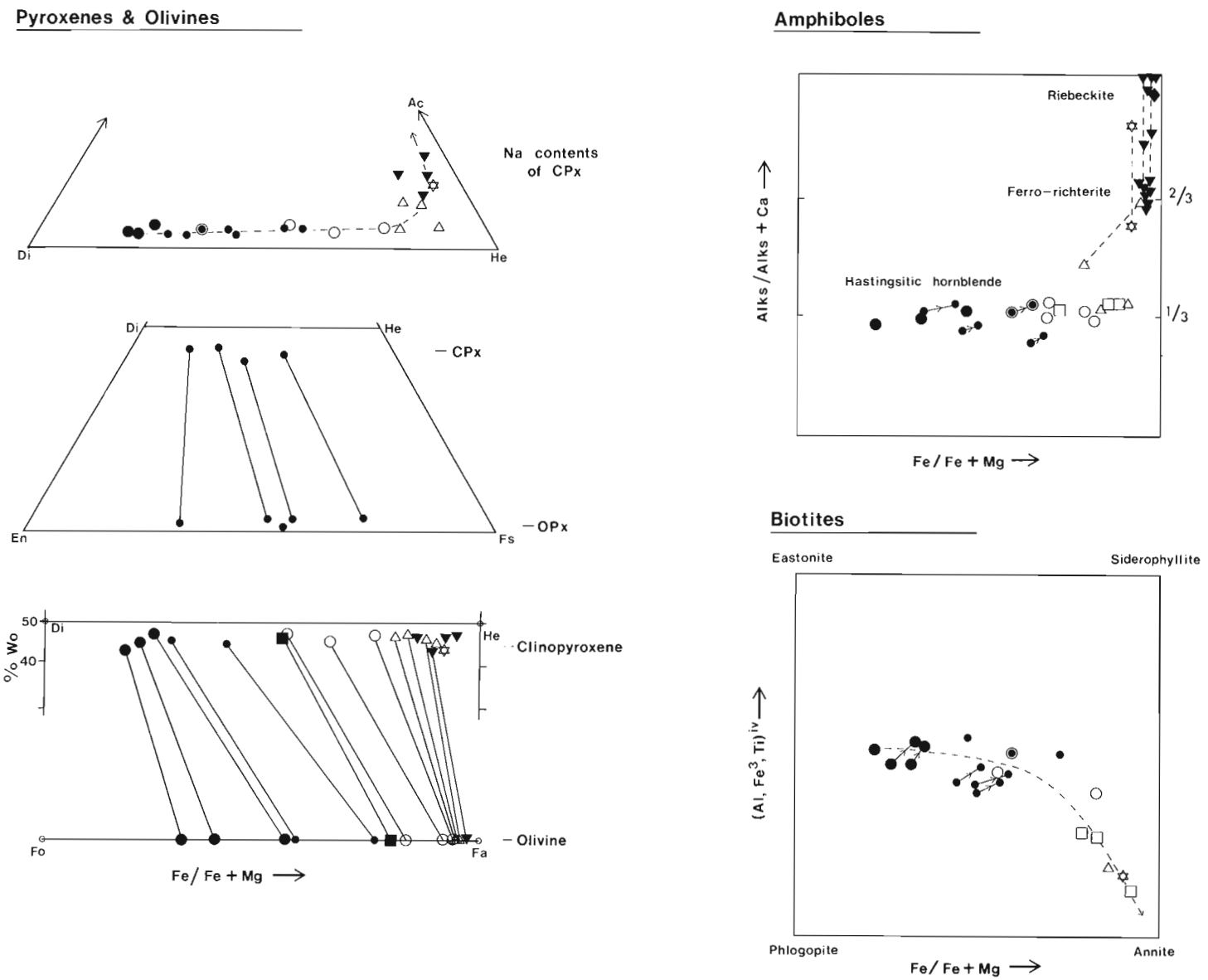

Figure 9.7. *Variation in composition of mafic minerals in the Blachford Lake complex. Black square is mafic ferrogabbro. See Table 9.1 for other symbols.*

Discussion

Apart from the Caribou Lake Gabbro, which has been shown to have been already considerably evolved by the time of its introduction to its present level, and with the possible exception of the contact region between the Grace Lake Granite and the Thor Lake Syenite, none of the units of the Blachford Lake complex show any evidence of in situ differentiation. Thus it would seem that each plutonic unit represents separate intrusion of magma derived by fractionation at some deeper level. The peralkaline rocks, being the most highly fractionated, represent magma that has had the longest residence time lower in the crust before reaching its present high level of emplacement. Hot and dry with respect to H_2O, but relatively highly charged with CO_2 and F, the magma that formed the large Grace Lake – Thor Lake pluton likely rose along a ring fracture system, filling in a tablet-shaped chamber that enlarged as the central block of crust moved down. Cooling against its roof, magma carrying feldspar crystals likely moved inward toward the centre, and then downward, and could have produced a syenitic phase by accumulation of early formed crystals beneath the roof of the central part of the chamber; this is a possible model for the formation of the Thor Lake Syenite. Continued partial exclusion of rare elements from the crystallizing phases allowed build-up of these elements in the residual fluid, which first formed pegmatite and then albitic dykes, followed by localized soda metasomatism and mineralization by the residual elements.

This complex is of a type commonly found to be associated with elevation of isotherms in the crust and upper mantle related to doming in a proto-rift environment. Usually a swarm of such complexes is present, as, for

example, in Nigeria (Jacobsen et al., 1958), where complexes essentially identical to that at Blachford Lake occur. It may be that the Blachford Lake complex is not the only one marginal to the east arm of Great Slave Lake, itself likely the site of rifting in early Proterozoic time (Hoffman et al., 1977). Other complexes, not yet recognized, need not be peralkaline; from an economic point of view, peraluminous ones would be preferable targets for tin and uranium mineralization.

References

Barberi, F., Ferrara, G., Santacroce, R., Treuil, M., and Varet, J.
1975: A transitional basalt-pantellerite sequence of fractional crystallization, the Boina Centre (Afar Rift, Ethiopia); Journal of Petrology, v. 16, p. 22-56.

Buckham, A.F.
1936: Petrology of the Francois River Gabbro; unpublished M. Sc. thesis, University of Alberta, Edmonton, 109 p.

Davidson, A.
1972: Granite studies in the Slave Province; in Report of Field Activities, Part A, Geological Survey of Canada, Paper 72-1A, p. 109-115.

1978: The Blachford Lake Intrusive Suite: an Aphebian alkaline plutonic complex in the Slave Province, Northwest Territories; in Current Research, Part A, Geological Survey of Canada, Paper 78-1A, p. 119-127.

1981: Petrochemistry of the Blachford Lake complex, District of Mackenzie; Geological Survey of Canada, Open File 764.

Emslie, R.F.
1978: Anorthosite massifs, rapakivi granites, and late Proterozoic rifting of North America; Precambrian Research, v. 7, p. 61-98.

Evensen, N.M., Hamilton, P.J., and O'Nions, R.K.
1978: Rare-earth abundances in chondritic meteorites; Geochimica et Cosmochimica Acta, v. 42, p. 1199-1212.

Henderson, J.B.
1976: Yellowknife and Hearne Lake map-areas; Geological Survey of Canada, Open File 353.

Henderson, J.F.
1938: Preliminary report, Beaulieau River area, Northwest Territories; Geological Survey of Canada, Paper 38-1, 20 p.

Hoffman, P.F., Bell, I.R., Hildebrand, R.S., and Thorstad, L.
1977: Geology of the Athapuscow Aulacogen, east arm of Great Slave Lake, District of Mackenzie; in Report of Activities, part A, Geological Survey of Canada, Paper 77-1A, p. 117-129.

Irvine, T.N. and Baragar, W.R.A.
1975: A guide to the chemical classification of the common volcanic rocks; Canadian Journal of Earth Sciences, v. 8, p. 523-548.

Jacobsen, R.R.E., MacLeod, W.N., and Black, R.
1958: Ring complexes in the younger granite province of northern Nigeria; Geological Society of London, Memoir 1, 72 p.

Jolliffe, F.
1936: Preliminary report, Yellowknife River area, N.W.T.; Geological Survey of Canada, Paper 36-5, 10 p.

McCarthy, T.S. and Cawthorn, R.G.
1980: Changes in initial $^{87}Sr/^{86}Sr$ ratio during protracted fractionation of igneous complexes; Journal of Petrology, v. 21, p. 245-264.

Peacock, M.A.
1931: Classification of igneous rock series; Journal of Geology, v. 39, p. 54-76.

Stockwell, C.H.
1932: Great Slave Lake – Coppermine River area, Northwest Territories; Geological Survey of Canada, Summary Report., Part C, p. 37-64.

Tuttle, O.F. and Bowen, N.L.
1958: Origin of granite in the light of experimental studies; Geological Society of America, Memoir 74, 153 p.

Wanless, R.K., Stevens, R.D., Lachance, G.R., and DeLabio, R.N.
1979: Age determinations and geological studies; K-Ar isotopic ages, report 14; Geological Survey of Canada, Paper 79-2, p. 34-38.

10.

COMPARATIVE PETROCHEMISTRY OF TWO COGENETIC MONZONITIC LACCOLITHS AND GENESIS OF ASSOCIATED URANIFEROUS ACTINOLITE-APATITE-MAGNETITE VEINS, EAST ARM OF GREAT SLAVE LAKE, DISTRICT OF MACKENZIE

S.S. Gandhi and N. Prasad[1]
Geological Survey of Canada

Gandhi, S.S. and Prasad, N., Comparative petrochemistry of two cogenetic monzonitic laccoliths and genesis of associated uraniferous actinolite-apatite-magnetite veins, east arm of Great Slave Lake, District of Mackenzie; in Uranium in Granites, ed. Y.T. Maurice; Geological Survey of Canada, Paper 81-23, p. 81-90, 1982.

Abstract

Two cogenetic monzonitic laccoliths, one hosting uraniferous actinolite-apatite-magnetite veins, were sampled for a comparative petrochemical study as an aid to understanding the genesis of the veins and to provide guides for exploration of other similar intrusions in the east arm of Great Slave Lake. The results reveal that the two bodies are very similar in chemical and mineralogical composition. They show a small compositional range and a calc-alkaline differentiation trend. They are subalkaline in character but locally show effects of alkali metasomatism.

Uranium and thorium contents of both intrusions average about 6 and 27 ppm respectively, somewhat above the global average contents for these elements in intermediate igneous rocks. An analysis of variance shows that most of the variation in the contents of uranium and thorium occurs at local rather than regional level in each of the laccoliths and the variance between the laccoliths is negligible. Although the range and mean of uranium values in both laccoliths are similar, the laccolith barren of veins has the values showing a clustered distribution within the range in contrast to the laccolith hosting the veins, which shows a scattered distribution suggesting some uranium mobility. This may have had a bearing on the processes of mineralization.

The occurrence of veins along tensional fractures in the intrusion, and their pegmatoid character led previous workers to suggest a genetic relationship between the veins and the intrusion. The petrochemical results, however, show that the limited in situ differentiation is unlikely to have led to the extreme enrichment of iron and phosphorus necessary to form the veins. This suggests that the fluid that formed the veins was most probably derived from a deep-seated magma chamber, where a melt more mafic than monzonite was undergoing differentiation. The presence of cogenetic dioritic laccoliths to the west and mafic inclusions in the monzonite support this conclusion.

Résumé

Deux laccolithes monzonitiques cogénétiques, l'un contenant des filons uranifères d'actinolite-apatite-magnétite, ont été échantillonnés pour une étude pétrochimique comparative, afin de faciliter la compréhension de la genèse des filons et de fournir des guides pour l'exploration d'autres intrusions semblables dans le bras est du Grand Lac des Esclaves. Les résultats révèlent que les deux intrusifs ont une composition chimique et minéralogique très semblable. Ils présentent une composition peu étendue et une tendance à la différenciation calco-alcaline. Ils sont de caractère subalcalin, mais présentent par endroits les effets d'un métasomatisme alcalin.

Les teneurs en uranium et en thorium des deux intrusions sont en moyenne de 6 et 27 ppm respectivement, soit un peu plus que les teneurs moyennes globales de ces éléments dans les roches ignées intermédiaires. Une analyse des variances montre que la majeure partie de la variation dans les teneurs en uranium et en thorium se rencontre à un niveau local plutôt que régional dans chacun des laccolithes et que les différences entre les laccolithes sont négligeables. Bien que les gammes et les moyennes des teneurs en uranium dans les deux laccolithes soient semblables, le laccolithe exempt de filons présente des valeurs montrant une distribution serrée, par contraste avec le laccolithe contenant les filons, qui présente une distribution éparse, ce qui suggère une certaine mobilité de l'uranium. Il peut y avoir eu une relation entre ce fait et les processus de minéralisation.

L'occurrence de filons le long de fissures de tension dans l'intrusion et leur caractère pegmatoïde ont conduit des chercheurs précédents à proposer une relation génétique entre les filons et l'intrusion. Les résultats pétrochimiques, toutefois, montrent que la différenciation limitée "sur place" est peu susceptible d'avoir mené à un enrichissement important en fer et en phosphore requis pour former les filons. Ce fait laisse croire que le fluide qui a formé les filons a probablement dérivé d'une chambre magmatique en profondeur, où une matière en fusion plus ferromagnésienne que monzonitique subissait une différenciation. La présence de laccolithes dioritiques cogénétiques à l'ouest et d'inclusions ferromagnésiennes dans la monzonite corroborent cette conclusion.

[1] 601 Booth Street, Ottawa, Ontario K1A 0E8

Introduction

Two cogenetic monzonitic laccoliths, each approximately 2.5 km^2 in area, one hosting uraniferous actinolite-apatite-magnetite veins and the other barren of mineralization were sampled to (i) determine the range and mean contents of various elements in them, (ii) estimate chemical variability at four statistical levels within each laccolith and between them, (iii) interpret the trend of differentiation and its bearing on the genesis of the veins, and (iv) provide petrochemical guides to exploration of similar intrusions. An unbalanced nested sampling design was adopted, and a total of 53 and 59 samples were collected from the two laccoliths (Gandhi and Prasad, 1980).

Geological Setting

The two bodies, the Regina Bay and the Meridian Lake laccoliths, belong to a string of more than 20 cogenetic laccolithic intrusions of diorite-monzonite composition that extends along the 225 km length of the east arm of Great Slave Lake (Fig. 10.1). The majority were emplaced along the contact between the Pethei Group limestone and the overlying salt-solution megabreccia of the Stark Formation consisting of red mudstones and shallow water carbonates. The sediments belong to the Aphebian Great Slave Supergroup interpreted as having been deposited in an aulacogen on the southern margin of the Archean Slave Craton (Hoffman, 1968, 1969; Hoffman et al., 1977). The brecciated nature of the Stark Formation apparently permitted bulging of intrusions to form laccoliths (Badham, 1978). The intrusions are well exposed in the glaciated terrain. Their contacts are commonly steep, and the breccia at their margin commonly includes angular fragments of the intrusions. This brecciation is regarded here as post-emplacement, probably related to the movements along major strike-slip faults. Deposition of the Late Aphebian or Early Helikian Et-Then Group that unconformably overlies the laccoliths and the Great Slave Supergroup, started during the faulting and continued after the cessation of movements along the faults.

The laccoliths are predominantly monzonitic east of 111°30'W, and west of this line are predominantly dioritic with more acidic dykes and veins at their borders (Hoffman et al., 1977). The laccoliths exhibit little mappable differentiation although minor variations in the proportion of feldspar, hornblende, biotite and quartz occur in them. Biotite concentrates from samples of two of the laccoliths

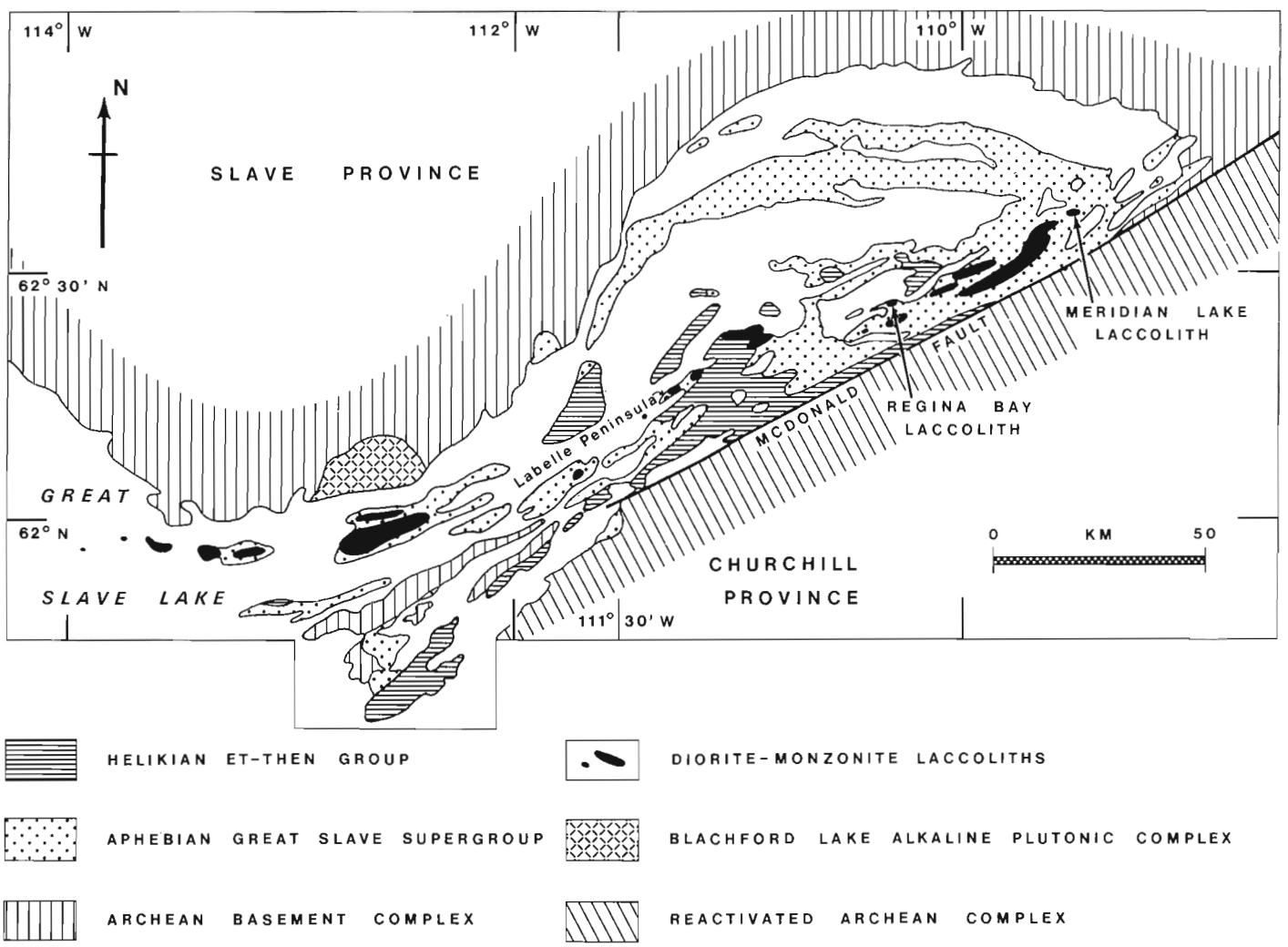

Figure 10.1. *General geology of the east arm of Great Slave Lake and location of the Meridian Lake and Regina Bay laccoliths.*

yielded K-Ar ages of 1845 and 1795 Ma (GSC-61-78 and GSC-67-77; 62°29'45"N, 109°52'W and 62°11'N, 112°06'W respectively; Lowdon et al., 1968 and Wanless et al., 1970). The intrusive event is related in time with the emplacement of the Great Bear Batholith, 250 km northwest of the east arm of Great Slave Lake, which is believed to be related to an eastward subduction in the Wopmay Orogen (Hoffman, 1980, p. 538-539). Intrusions comparable in texture and composition to the east arm laccoliths occur near the east shore of Great Bear Lake; they are the earliest granitic intrusions of the Great Bear Batholith (Hoffman and McGlynn, 1977, p. 176).

Mineralization

Intrusions in the central part of the east arm of Great Slave Lake (between 110°15' and 111°30'W) host veins of actinolite, apatite, magnetite, and hematite, some of which carry minor amounts of uraninite closely associated with the magnetite. Veins, pods and disseminations of pyrite, chlorite, quartz, calcite, dolomite, copper sulphides, and rarely cobalt-nickel arsenides, are noted in places, but these minerals are scarce and their distribution is erratic, and for the most part they are younger in paragenetic sequence (Badham and Muda, 1980). The veins are vertical or steeply dipping, with the majority striking between east and northeast. They range in width from a fraction of a centimetre to a metre, rarely up to two metres, and their lengths range from a few centimetres up to 150 metres. They may pinch and swell along the strike, and some of them bifurcate and coalesce. Growth of crystals is inwards from the walls, with actinolite commonly oriented across the strike. Wider veins exhibit zoning with very coarse crystals of apatite and actinolite in the centre. The veins are more numerous and better explored in the Regina Bay laccolith where one vein was explored by a 150 m long adit (Lang et al., 1962, p. 203).

The close spatial association of the veins with the intrusions, and their pegmatoid character suggested a genetic relationship between the veins and the laccoliths (Lang et al., 1962; Gandhi, 1978; Badham, 1978). This is further emphasized by U-Pb isotopic ratios in uraninite which show good correlation between Pb-Pb and U-Pb plots and yielded ages of 1755 and 1785 Ma respectively (Gandhi, 1978; Bloy, 1979). Although the results are discordant, suggesting lead loss, the ages are close to the time of intrusion, as indicated by the K-Ar age determinations, reflecting the genetic relationship.

Petrography and Petrochemistry

Preliminary petrographic examination of selected samples from the two laccoliths reveals a small range in modal composition within each laccolith and close overall similarities between the two laccoliths. The rocks are quartz-bearing monzonites according to the Streckeisen (1976) classification. Well developed plagioclase laths, 5 to 8 mm long and commonly albite to andesine, form 50 to 65 per cent of the rocks. A few samples are rich in

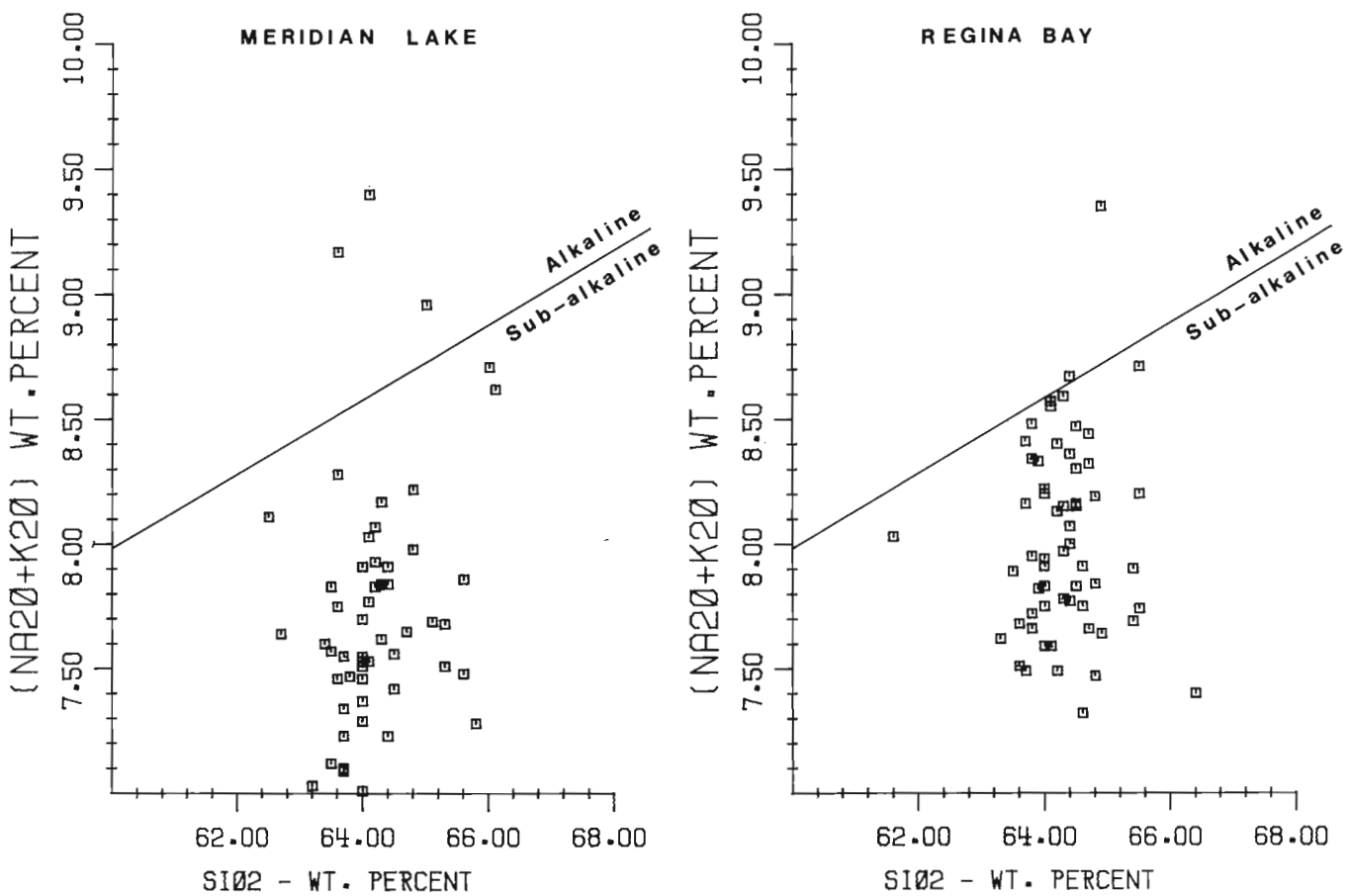

Figure 10.2. *Plot of total alkalis versus silica in samples of Meridian Lake and Regina Bay laccoliths.*

Table 10.1. The range and mean values of chemical components in samples from the Meridian Lake and Regina Bay laccoliths, east arm of Great Slave Lake, District of Mackenzie.

	MERIDIAN LAKE LACCOLITH Number of Samples: 53			REGINA BAY LACCOLITH Number of Samples: 59			Average Monzonite† (from Le Maitre, 1976)
	Minimum	Maximum	Mean	Minimum	Maximum	Mean	
SiO_2	62.50	66.10	64.21	61.60	66.40	64.30	62.60
TiO_2	0.55	0.65	0.59	0.55	0.64	0.59	0.78
Al_2O_3	14.10	16.30	15.09	14.30	16.70	14.93	15.65
Fe_2O_3	0.50	2.20	1.37	0.50	2.80	1.80	1.92
FeO	0.8	4.0	3.06	0.70	3.40	2.15	3.08
MnO	0.03	0.09	0.05	0.01	0.08	0.03	0.10
MgO	0.81	3.19	2.48	1.62	3.68	2.95	2.02
CaO	0.52	3.52	2.32	0.88	3.97	2.33	4.17
Na_2O	2.60	8.50	4.13	2.70	7.70	4.18	3.73
K_2O	0.31	4.74	3.61	0.50	5.27	3.84	4.06
P_2O_5	0.13	0.18	0.16	0.13	0.20	0.15	0.25
H_2O^T	0.7	2.50	1.72	0.80	2.60	1.56	1.09
CO_2	0.10	3.10	0.68	0.00	2.70	0.61	0.08
(Total)			(99.47)			(99.42)	(99.53)
F	0.03	0.06	0.05	0.03	0.08	0.05	
U_{DNC} ppm	2.1	10.3	6.02	3.40	11.60	6.35	
Th_{XRF} ppm	22.0	37.00	27.53	21.00	35.00	27.85	
eU ppm	1.9	10.8	6.17	0.6	11.5	6.64	
eTh ppm	22.6	36.0	28.89	18.2	34.9	27.73	
Specific Gravity	2.600	2.750	2.689	2.630	2.720	2.671	

† Average of 336 analyses

– Oxides and F analyses based on X-ray fluorescence and chemical methods by the Analytical Chemistry Section, Geological Survey of Canada, given in wt. %

– U_{DNC} analyses based on delayed neutron counting by Atomic Energy of Canada Ltd., Ottawa

– Th_{XRF} analyses based on X-ray fluorescence by Bondar-Clegg & Co. Ltd., Ottawa

– eU and eTh based on McPhar Spectra 44 spectrometer readings on outcrop surface

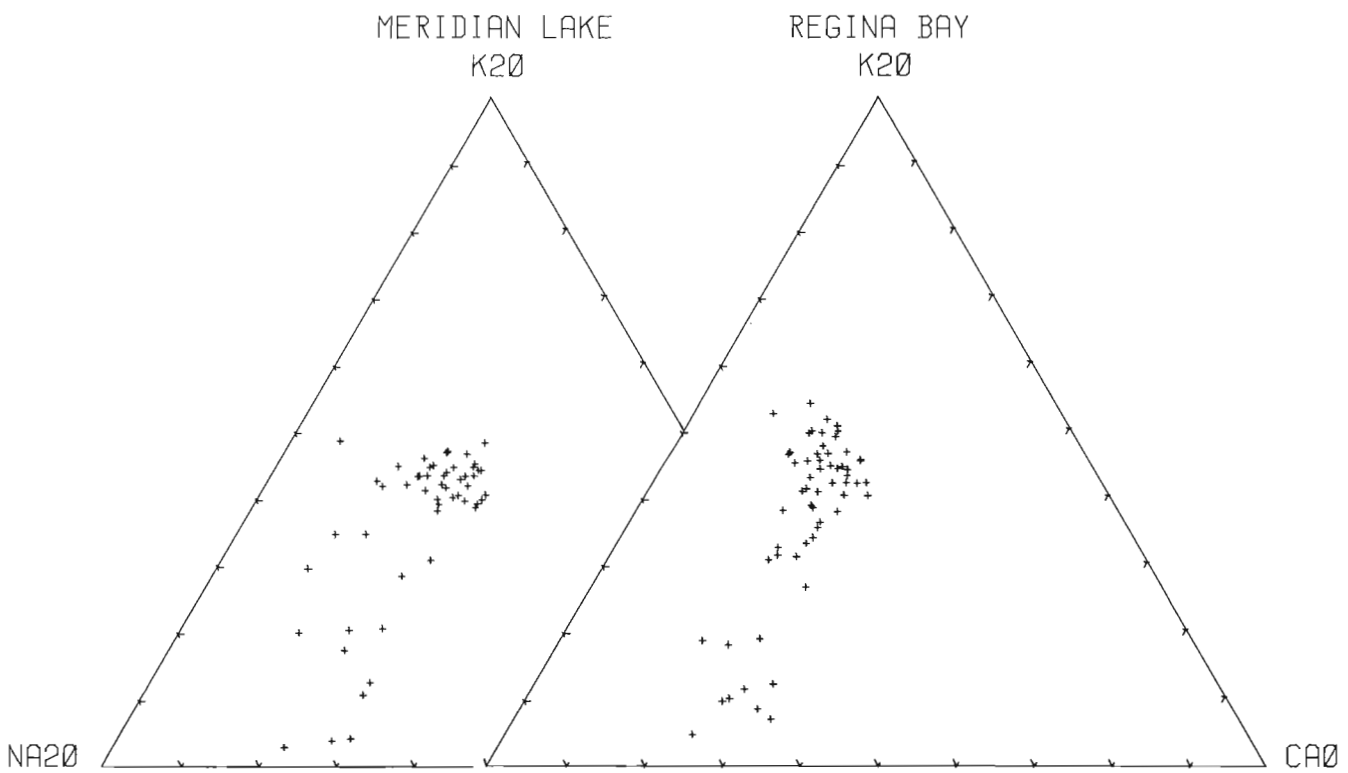

Figure 10.3. *Plot of Na_2O-CaO-K_2O in Meridian Lake and Regina Bay laccoliths.*

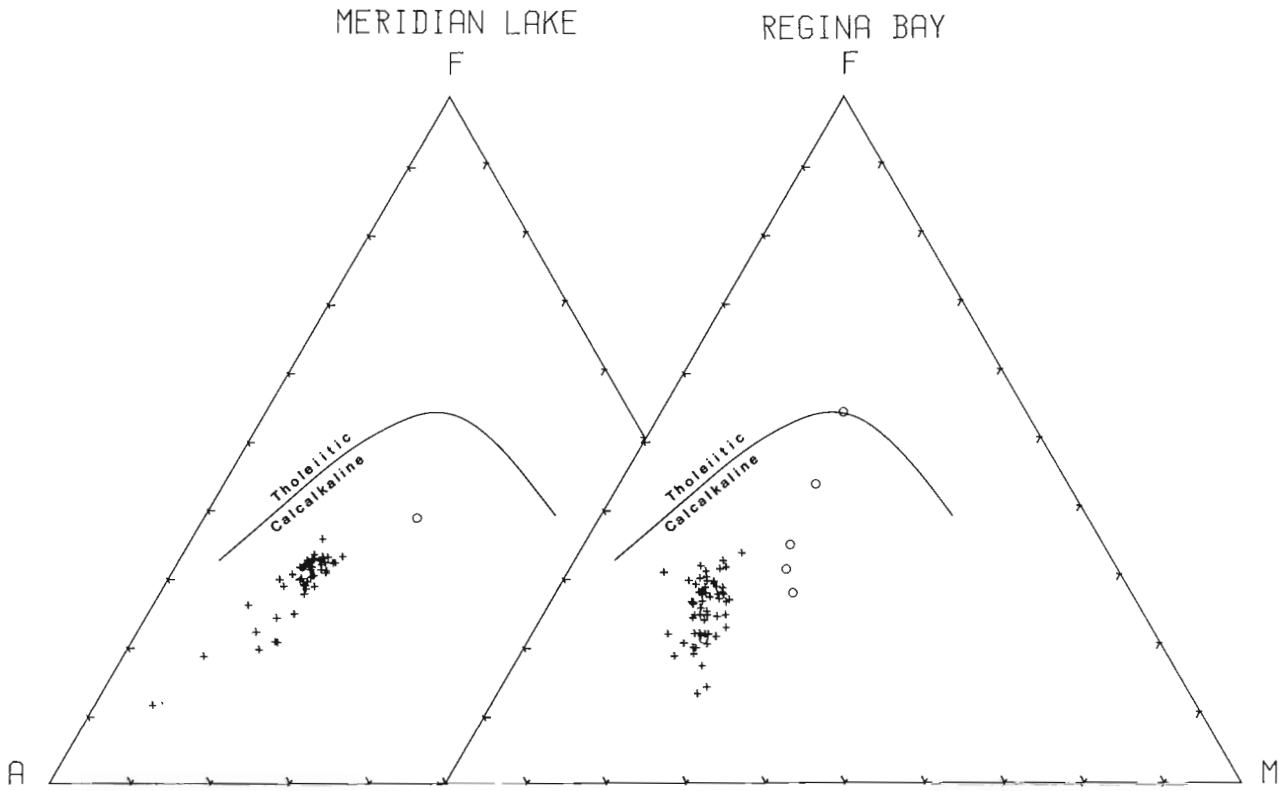

Figure 10.4. *A-F-M plot of samples of Meridian Lake and Regina Bay laccoliths. A = (Na_2O + K_2O), F = (FeO + 0.8998 Fe_2O_3), M = MgO; + = monzonite samples, o = mafic igneous inclusions.*

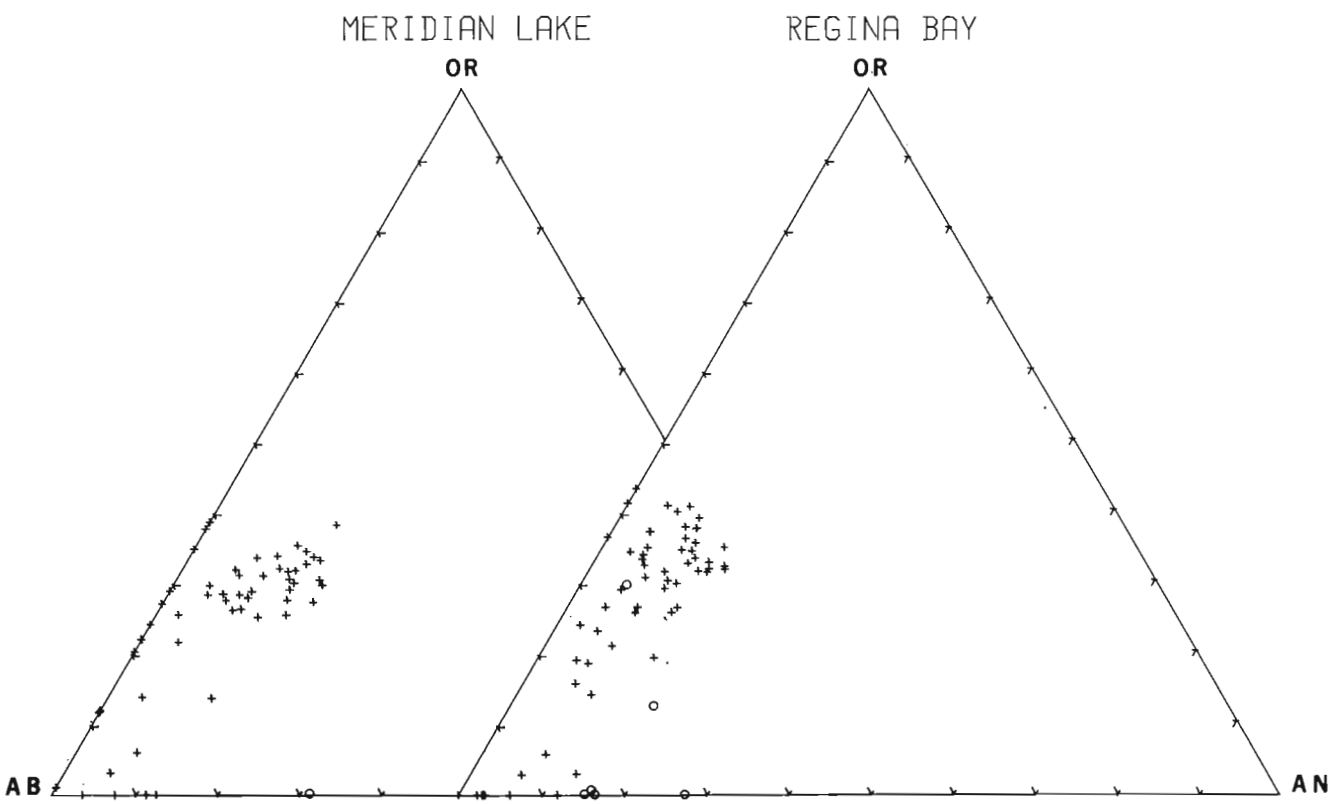

Figure 10.5. *Normative albite-anorthite-orthoclase (AB-AN-OR) plot of samples of Meridian Lake and Regina Bay laccoliths; + = monzonite samples, o = mafic igneous inclusions.*

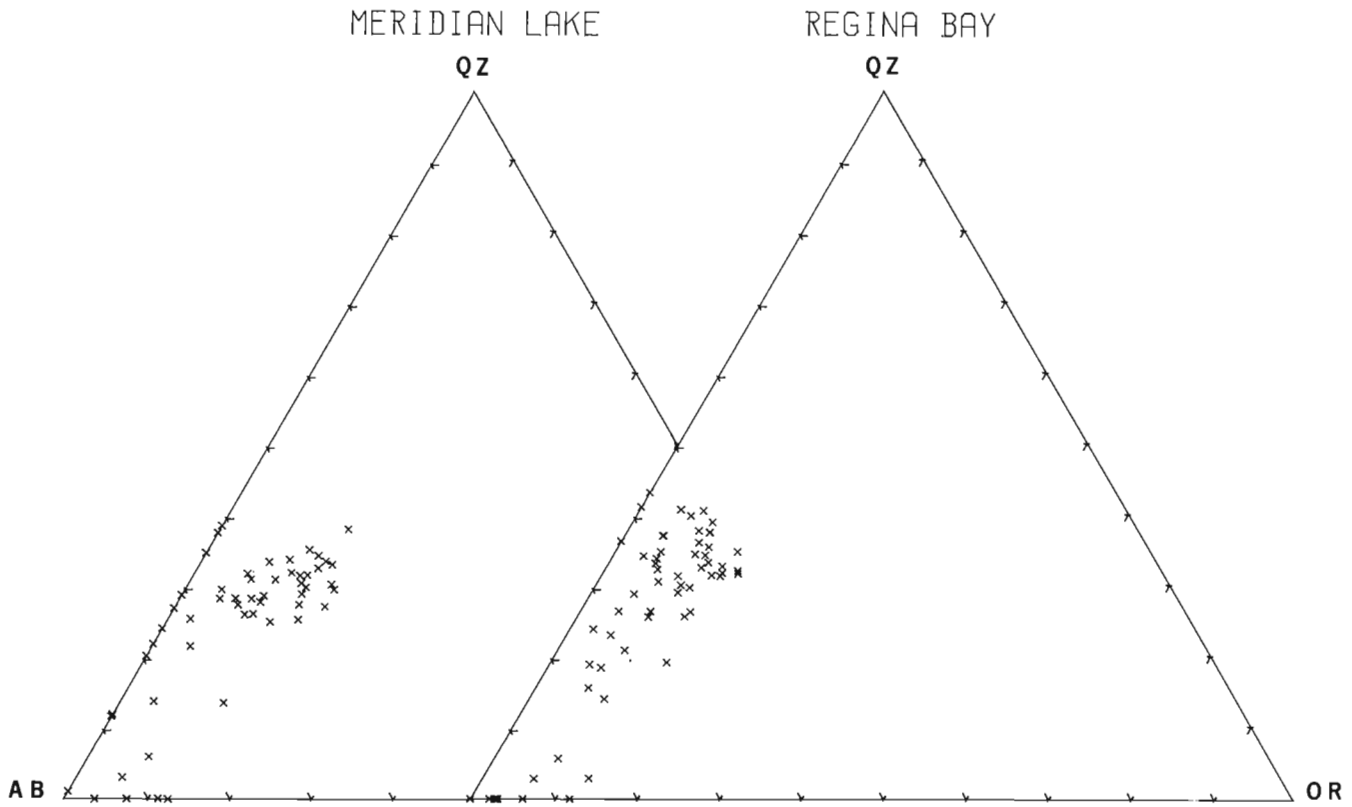

Figure 10.6. *Normative albite-orthoclase-quartz (AB-OR-QZ) plot of samples of Meridian Lake and Regina Bay laccoliths.*

albite and some of the plagioclase laths are zoned. The interstitial material is fine- to medium-grained, composed predominantly of alkali feldspar, commonly perthite, and quartz, each making 5 to 15 per cent of the rock. Quartz grains are generally subhedral, but in the more siliceous rocks subhedral to euhedral phenocrysts are present. The primary mafic silicates are green hornblende and biotite, together making up 10 to 15 per cent of the rock. Hornblende commonly predominates over biotite. In some rocks however, biotite is as abundant as hornblende. The mafic silicates tend to form medium grained aggregates. Accessory magnetite, apatite and zircon form very small euhedral or subhedral crystals, many of them occurring as inclusions in the mafic silicates. Monazite, causing radiogenic haloes in biotite, titanite and calcite are present in some samples. The rocks are altered to a varying degree. Feldspars are saussuritized, and hornblende and biotite are generally altered to chlorite.

The range and mean content of major element oxides, fluorine, uranium, thorium and specific gravity in the two laccoliths are given in Table 10.1, with a global average of monzonite (Le Maitre, 1976) for comparison. The results show that the range in composition for the two laccoliths is rather small, and that they are remarkably similar in overall chemical characters. Plots of total alkalis versus silica for the two laccoliths (Fig. 10.2) show clustering of points in the subalkaline field near the boundary with the alkaline field. Triangular plots of Na_2O-K_2O-CaO (Fig. 10.3) reveal enrichment of Na_2O and corresponding depletion of K_2O in some of the rocks. In the A-F-M plots (Fig. 10.4) a majority of points form a cluster in the calc-alkaline field reflecting limited in situ differentiation; however some of the rocks that lie closer to the alkali end are enriched in soda and reflect soda metasomatism at the late stage of crystallization. The mafic cognate inclusions, shown as circles in the plots, have higher ferromagnesian content than the laccolith samples, suggesting a calc-alkaline differentiation of a parent magma at depth. The normative AB-AN-OR and AB-OR-QZ plots in Figures 10.5 and 10.6 respectively, also demonstrate the soda metasomatism in some of the rocks.

The data on uranium and thorium contents of the samples and specific gravity have been discussed by Gandhi and Prasad (1980). The range and mean values for these are given in Table 10.1. The intermediate igneous rocks in various parts of the world commonly contain 2 ppm U and 7 ppm Th, according to the compilation by Nishimori et al. (1977, p. 7). Thus the two quartz monzonite laccoliths are relatively enriched in uranium and thorium, and even exceed global averages for granites which commonly contain 4 to 5 ppm U, and 15 to 19 ppm Th.

The X-Y diagrams of uranium and thorium values (Fig. 10.7A) show that thorium has the same range and distribution in both laccoliths. Uranium in the Meridian Lake laccolith has a narrow range of values reflected in a horizontal trend, but in the Regina Bay laccolith, uranium shows a scatter of values with no discernible trend. This could indicate redistribution of the uranium in the latter laccolith. The same interpretation can be derived from the plots of U/Th ratios versus uranium (Fig. 10.7B), which show that in the Meridian Lake laccolith a great majority of the points are clustered around the mean and in the Regina Bay laccolith they are evenly distributed over the entire range of values. This difference in the distribution of uranium in the two laccoliths is also apparent from the plot of U/Th ratios versus thorium (Fig. 10.7C).

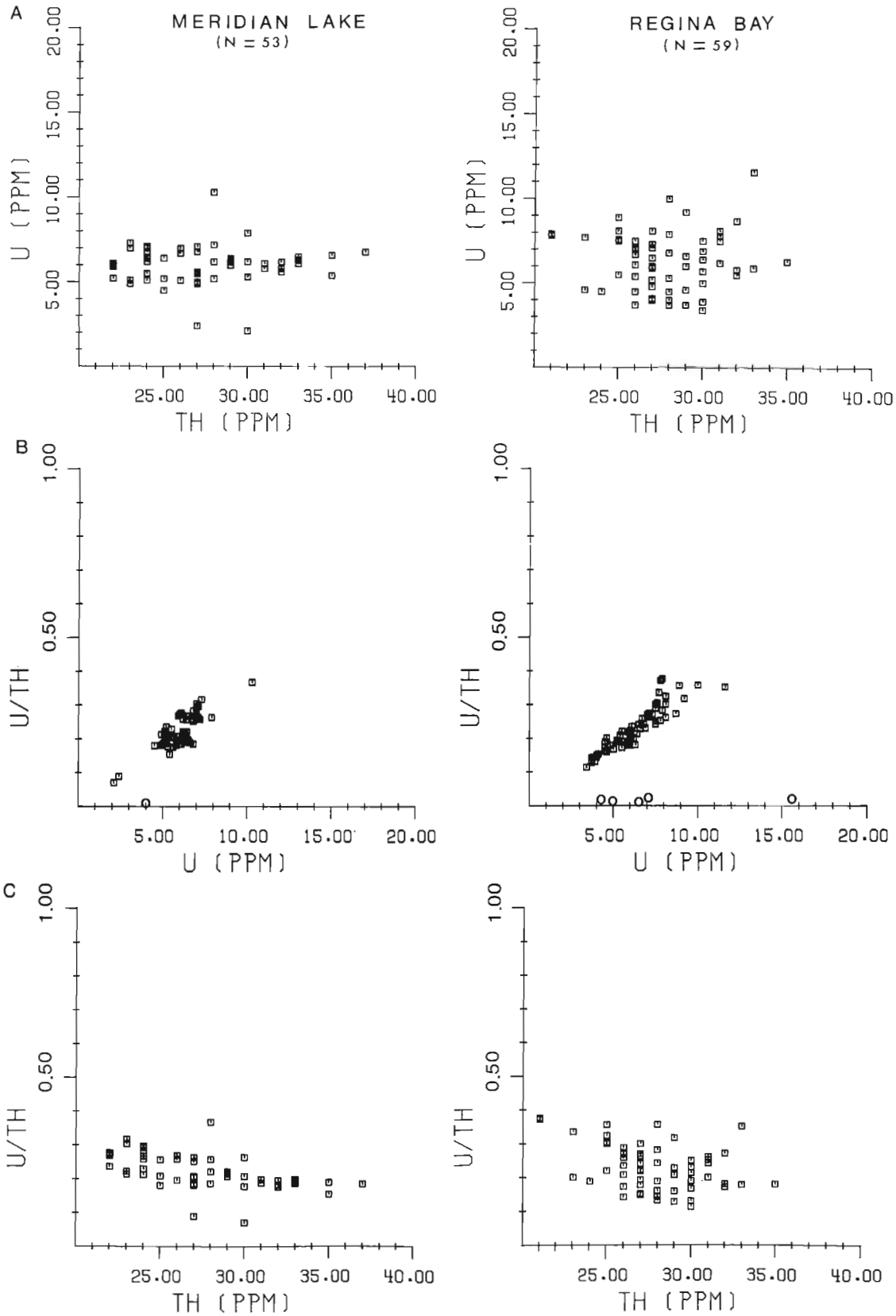

Figure 10.7. *Plot of uranium versus thorium, U/Th ratio versus uranium and U/Th ratio versus thorium in samples of Meridian Lake and Regina Bay laccoliths. Circles in B represent samples of mafic igneous inclusions.*

Table 10.2. Analysis of variance for uranium, thorium and specific gravity in the Meridian Lake and Regina Bay laccoliths

	MERIDIAN LAKE LACCOLITH					REGINA BAY LACCOLITH				
Variable	U_{DNC}	Th_{XRF}	eU	eTh	Sp.Gr.	U_{DNC}	Th_{XRF}	eU	eTh	Sp.Gr.
Total Variance	2.24	18.69	3.19	15.50	0.001	2.97	14.16	9.64	18.18	0.0005
Percentage of total variance at:										
Level 4 (200 m squares)	0.05^N	17.62^N	0.00^N	0.00^N	33.27^N	17.02^N	0.00^N	21.42^N	22.65^N	12.61^N
Level 3 (100 m squares)	0.00^N	0.00^N	26.75^N	0.00^N	21.04^N	3.67^N	29.39*	0.00^N	12.74^N	0.00^N
Level 2 (50 m squares)	87.51*	0.00^N	32.30^N	96.01***	0.00^N	7.77^N	0.00^N	70.61**	0.00^N	14.20^N
Level 1 (outcrop)	12.44	82.38	40.95	3.99	45.69	71.54	70.61	7.97	64.61	73.20

Note: Significance based on computed F-ratios as follows:

* Significant at $\alpha = 0.05$ where α represents level of significance
** Significant at $\alpha = 0.01$
*** Significant at $\alpha = 0.001$
N = Not significant

Table 10.3. Analysis of variance for uranium, thorium and specific gravity between the Meridian Lake and Regina Bay laccoliths

Variable	U_{DNC}	Th_{XRF}	eU	eTh	Sp.Gr.
Total Variance	2.554	15.564	6.270	12.566	0.0008
Percentage of total variance at:					
Level 5 (between laccolith)	0.28^N	0.00^N	0.00^N	3.03^N	17.89**
Level 4 (200 m squares)	9.91^N	10.14^N	15.87^N	9.16^N	25.51*
Level 3 (100 m squares)	0.00^N	8.26^N	0.83^N	3.38^N	2.77^N
Level 2 (50 m squares)	42.79^N	0.00^N	66.74**	35.24^N	0.00^N
Level 1 (outcrop)	47.02	81.60	16.56	49.19	53.82

Note: Significance levels as in Table 10.2.

An analysis of variance, using the method by Garrett and Goss (1980), was performed on the uranium and thorium contents and specific gravity data, and the results are summarized in Table 10.2 (Gandhi and Prasad, 1980, p. 237). It is seen from the table that most of the variation in uranium and thorium contents in the two laccoliths occurs locally rather than regionally, viz. at outcrop level and between outcrops rather than at levels involving greater distances. Specific gravity shows a negligible variance around the mean. When the two laccoliths are compared, the percentage of total variance in the uranium and thorium contents at the 5th level or interlaccolith level, is negligible as seen in Table 10.3.

Discussion and Conclusion

The data presented indicate that the quartz monzonite laccoliths at Meridian Lake and Regina Bay are remarkably similar in their overall mineralogical and chemical characters. Both show a rather small range in chemical composition, indicating limited in situ differentiation along a calc-alkaline trend, leading to slight enrichment in silica and soda, and depletion in calcium, magnesium, and iron. Locally, significant enrichment in soda and corresponding depletion in potash occurred in both intrusions. This can be attributed, in part at least, to soda metasomatism at a late stage of crystallization.

Regarding the genesis of the actinolite-apatite-magnetite veins, it is apparent that the observed trend and degree of differentiation in situ are unlikely to have led to the extreme enrichment of iron, calcium and phosphorus required to form the veins. Other possible mechanisms are differentiation in the magma chamber at depth, or derivation of the components of the vein from suitable country rocks by groundwater circulating in convection cells generated by the heat of the intrusion. The latter mechanism seems unlikely in view of the rather unusual composition of the veins. Furthermore, this mechanism should have operated equally efficiently in both laccoliths which are in identical geological setting, yet no such veins have been found in the Meridian Lake laccolith.

Compositionally, the laccoliths lie near the thermal minima in the system quartz-albite-orthoclase-anorthite, and the magma that formed the laccoliths is itself a differentiation product of more mafic magma that crystallized at depth. Dioritic laccoliths to the west and the presence of mafic cognate xenoliths in the laccoliths are evidence for a mafic parent magma, probably basaltic in composition.

Differentiation at depth thus appears to be the most likely mechanism for generating the fluid that formed the veins. Such a fluid could be generated by magmatic differentiation or liquid immiscibility or volatile transfer. The chemistry of the veins is consistent with a hydrothermal siliceous fluid highly charged with volatiles. This fluid would have migrated to higher levels, and deposited vein minerals along fractures that were formed by cooling and contraction of the laccoliths. With regards to uranium, its scattered distribution in the Regina Bay laccolith (Fig. 10.7) suggests that it was redistributed perhaps as a result of the hydrothermal activity, which may have led to its concentration in the veins.

References

Badham, J.P.N.
1978: Magnetite-apatite-amphibole-uranium and silver-arsenide mineralizations in Lower Proterozoic igneous rocks, east arm, Great Slave Lake, Canada; Economic Geology, v. 73, no. 8, p. 1474-1491.

Badham, J.P.N. and Muda, M.M.
1980: Mineralogy and paragenesis of hydrothermal mineralizations in the east arm of Great Slave Lake; Economic Geology, v. 75, no. 8, p. 1220-1225.

Bloy, G.R.
1979: U-Pb geochronology of uranium mineralization in the east arm of Great Slave Lake, Northwest Territories; unpublished M.Sc. thesis, University of Alberta, 64 p.

Gandhi, S.S.
1978: Geological observations and exploration guides to uranium in Bear and Slave structural provinces and the Nonacho Basin, District of Mackenzie; in Current Research, Part B, Geological Survey of Canada, Paper 78-1B, p. 141-149.

Gandhi, S.S. and Prasad, N.
1980: Uranium and thorium variations in two monzonitic laccoliths, east arm of Great Slave Lake, District of Mackenzie; in Current Research, Part B, Geological Survey of Canada, Paper 80-1B, p. 233-240, 1980.

Garrett, R.G. and Goss, T.I.
1980: UANOVA: A FORTRAN IV Program for unbalanced nested analysis of variance; Computers and Geoscience, v. 6, p. 35-60.

Hoffman, P.F.
1968: Stratigraphy of the Great Slave Supergroup (Aphebian), east arm of Great Slave Lake, District of Mackenzie; Geological Survey of Canada, Paper 68-42, 93 p.

1969: Proterozoic paleocurrents and depositional history of the East Arm Fold Belt, Great Slave Lake, Northwest Territories; Canadian Journal of Earth Sciences, v. 6, p. 441-462.

1980: Wopmay Orogen: a Wilson cycle of Early Proterozoic age in the northwest of the Canadian Shield; in Continental Crust and its Mineral Deposits, ed. D.W. Strangway; Geological Association of Canada, Special Paper 20, p. 523-549.

Hoffman, P.F. and McGlynn, J.C.
1977: Great Bear Batholith: a volcano-plutonic depression; in Volcanic Regimes in Canada, ed. W.R.A. Baragar, L.C. Coleman, and J.M. Hall; Geological Association of Canada, Special Paper 16, p. 169-192.

Hoffman, P.F., Bell, P.R., Hildebrand, R.S., and Thorstad, L.
1977: Geology of the Athapuscow aulacogen, east arm of Great Slave Lake, District of Mackenzie; in Report of Activities, Part A, Geological Survey of Canada, Paper 77-1A, p. 117-129.

Lang, A.H., Griffith, J.W., and Steacy, H.R.
1962: Canadian deposits of uranium and thorium; Geological Survey of Canada, Economic Geology Report 16, 324 p.

Le Maitre, R.W.
1976: The chemical variability of some common igneous rocks; Journal of Petrology, v. 17, p. 589-637.

Lowdon, J.A., Stockwell, C.H., Tipper, H.W., and Wanless, R.K.
1968: Age determinations and geological studies, Report 3; Geological Survey of Canada, Paper 62-17, 140 p.

Nishimori, R.K., Ragland, P.C., Rogers, J.J.W., and Greenberg, J.K.
1977: Uranium deposits in granitic rocks; United States Energy Research and Development Administration, Open File Report GJBX-13 (77), 311 p.

Streckeisen, A.
1976: To each plutonic rock its proper name; Earth Sciences Review, v. 12, p. 1-33.

Wanless, R.K., Stevens, R.D., Lachance, G.R., and Delabio, R.N.
1970: Age determinations and geological studies, K-Ar Isotopic Ages, Report 9; Geological Survey of Canada, Paper 69-2A, 78 p.

11. # RADIOMETRIC STUDY OF THREE RADIOACTIVE GRANITES IN THE CANADIAN SHIELD: ELLIOT LAKE, ONTARIO; FORT SMITH, AND FURY AND HECLA, N.W.T.

B.W. Charbonneau[1]
Geological Survey of Canada

Charbonneau, B.W., Radiometric study of three radioactive granites in the Canadian Shield: Elliot Lake, Ontario; Fort Smith, and Fury and Hecla, N.W.T.; in Uranium in Granites, ed. Y.T. Maurice; Geological Survey of Canada, Paper 81-23, p. 91-99, 1982.

Abstract

Granitic rocks in three areas of the Canadian Shield, Elliot Lake, Ontario, Fort Smith and Fury and Hecla, N.W.T., have been studied with respect to their uranium and thorium contents. These rocks are all associated with various types of radioactive concentrations namely conglomeratic ores at Elliot Lake and vein type and disseminated occurrences at Fury and Hecla and Fort Smith.

The trends defined in the variations of uranium and thorium with their ratios reflect the amount of remobilization of uranium that has occurred within the plutons. An increase in the U/Th ratio with U indicates postmagmatic remobilization of U. A lack of variation indicates no such remobilization. An inverse correlation between U/Th ratio and Th indicates radioelement distributions that were at least partly governed by magmatic processes.

The amount of postmagmatic remobilization that has taken place is indicative of favourability for epigenetic uranium mineralization within or near the intrusion. However, rocks that show a lack of remobilization may be important as a source of clastic mineralization provided that suitable accessory minerals are present.

The relationships between radioelement concentrations and their ratios are detectable on airborne radiometric maps and profiles allowing the users some insight on the uranium potential of granitic terranes.

Résumé

Trois régions de roches granitiques dans le bouclier canadien, Elliot Lake, Ontario, Fort Smith et Fury et Hecla, T.N.O. furent étudiées en rapport avec leur contenu en uranium et thorium. Ces roches sont toutes associées à divers types de concentrations radioactives tel que des minerais conglomératiques à Elliot Lake, et des veines et des dissiminations à Fury et Hecla et Fort Smith.

Les tendances dans les variations entre l'uranium ou le thorium et leurs rapports indiquent l'importance de la remobilisation de l'uranium à l'intérieur des plutons. Une augmentation dans le rapport U/Th avec l'U indique de la remobilisation post magmatique. Une absence de variation indique qu'il ne s'est produit aucune remobilisation. Une corrélation inverse entre le rapport U/Th avec le Th indique que la distribution des radioéléments est contrôlée, en partie au moins, par des processus magmatiques.

Le degré de remobilisation post magmatique est un indicateur du potentiel en minéralisation epigénitique d'uranium à l'intérieur ou à proximité de l'intrusion. Toutefois, les roches qui ne montrent aucune rémobilisation peuvent être importantes comme source de minéralisation clastique pourvu que des minéraux accessaires appropriés soient présents.

La relation entre les concentrations des radioéléments et leurs rapports est détectable à partir des cartes et profils radiométriques ce qui donne aux usagers quelques renseignements sur le potentiel en uranium des terrains granitiques.

Introduction

Approximately 2 000 000 km^2 of Canada, largely over the Precambrian Shield, have been surveyed by reconnaissance airborne gamma ray spectrometry. A contour map of the uranium distribution compiled from the survey results (Fig. 11.1) indicates areas of uranium enrichment, many of which relate to granitic bodies.

Figure 11.1 shows the locations of the three granitic areas discussed in this paper. Results of the airborne spectrometer surveys over these areas have been published previously as Geological Survey of Canada Open Files No. 101 (Fort Smith) and No. 262 (Elliot Lake), and Geophysical Series Map No. 35647G (Fury and Hecla).

These surveys were flown at 5 km line spacing and a mean terrain clearance of 120 m, using spectrometer systems having approximately 50 000 ml of NaI(Tl) detectors. The spectrometers were calibrated and results presented in units of radioelement concentration (Darnley, 1970; International Atomic Energy Agency, 1976). These results give a measure of the average surface concentration of radioelements for an area along the aircraft flight path, but there is attenuation due to the effect of overburden, biomass, and surface water.

Much of the surveyed areas are overlain by glacial till, the composition of which generally reflects that of the underlying bedrock. Papers by Shilts (1976) and Perttunen (1977) indicate that much of the material in glacial till has not moved far from its bedrock source. The biomass and surface water attenuate the radioactivity from the

[1] 601 Booth Street, Ottawa, Ontario K1A 0E8

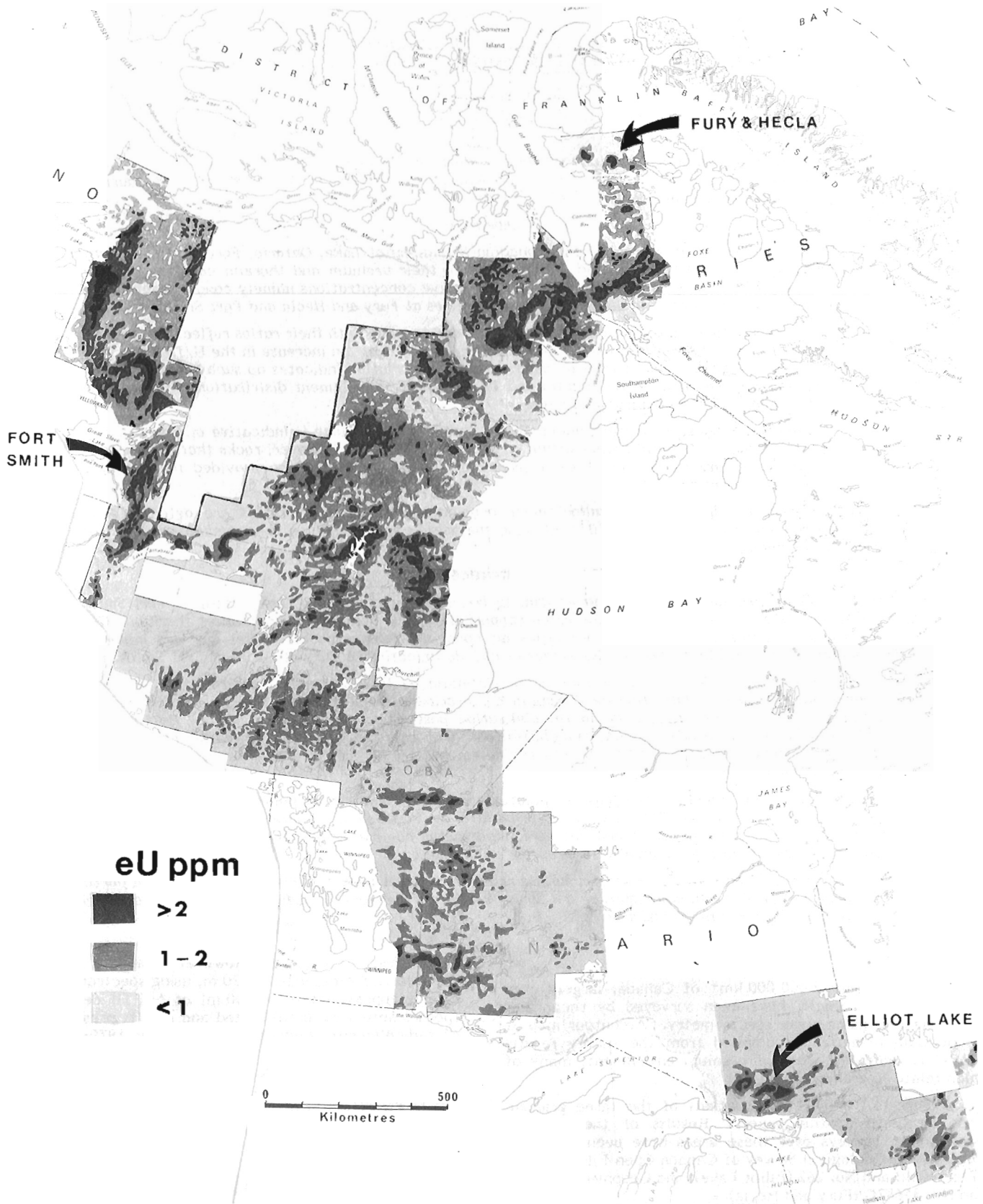

Figure 11.1. *Airborne eU (in ppm) over part of the Canadian Shield showing location of Fury and Hecla, Fort Smith, and Elliot Lake areas.*

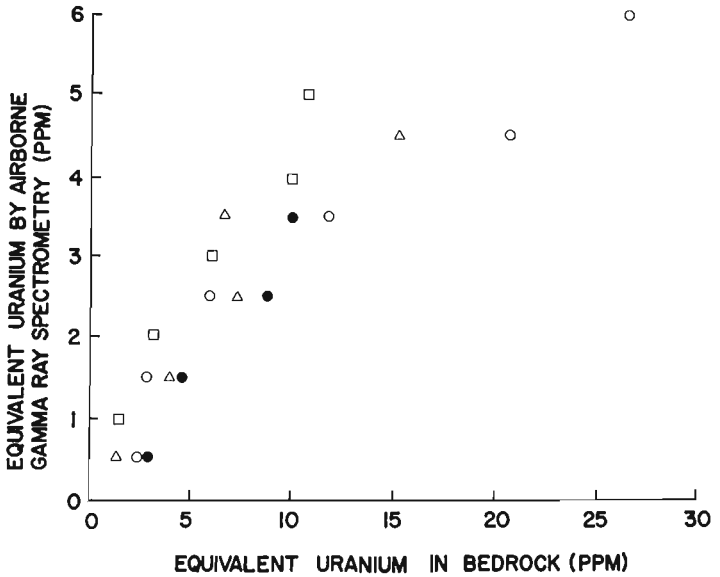

Figure 11.2. Relationship between gamma ray spectrometric determination of uranium concentration from airborne data and from bedrock for four areas of the Canadian Shield. Squares represent an area north of Great Slave Lake; open circles – Baffin Island north of Fury and Hecla Strait; solid circles – north of Elliot Lake, Ontario; triangles – Mont Laurier, Quebec.

underlying bedrock and overburden. Consequently, the airborne measurements will generally indicate radioelement concentrations somewhat lower than those in the bedrock.

The relationship between equivalent uranium values shown on the airborne contour maps and equivalent uranium concentrations in bedrock (determined by in situ gamma ray spectrometry or laboratory gamma ray spectrometric analysis of rock samples) is illustrated in Figure 11.2. Many of the 850 uranium analyses represented in Figure 11.2 have been previously reported by Charbonneau et al. (1976). This illustration was compiled by plotting the average equivalent uranium concentration for all of the sites located within each of the contour intervals on the airborne maps. The results show that over the range of concentrations normally found in rocks, the uranium content of bedrock is approximately 2 to 4 times greater than the value determined by the airborne method. A similar factor applies to the thorium measurements. The airborne determination of the eU/eTh ratio, however, is generally much closer to the bedrock value. Based on the results from four widely separated areas of the Canadian Shield, it appears that airborne spectrometric determinations of 3 to 4 ppm eU over granitic bodies are indicative of significantly enriched rocks having uranium concentrations of the order of 10 ppm.

The gamma ray spectrometric determination of equivalent uranium is based on the measurement of gamma rays emitted by bismuth-214 and assumes that the radioactive decay series of uranium-238 is in equilibrium (Rosholt, 1959 and Ostrihansky, 1976). Comparison of direct uranium determinations by delayed neutron counting with equivalent uranium determinations by gamma ray spectrometry for 50 granite samples from the Fury and Hecla area (Fig. 11.3) and for several hundred samples of crystalline rocks from other parts of Canada (Charbonneau et al., 1981) indicates that individual samples may have considerable uranium excess or deficiency relative to the ^{214}Bi (eU), but on average the uranium concentration is similar to the equivalent uranium value. These results are based on the analyses of small samples (about 1 gm for delayed neutron counting, about 400 gm for laboratory gamma ray spectrometric analysis). It is thought that the averaging effect of the large samples analyzed by in situ portable gamma ray spectrometry and the very large sample analyzed in airborne surveys (Darnley and Grasty, 1971) should result in equivalent uranium determinations which are closer to the actual uranium concentration than the individual sample results shown in Figure 11.3.

The previous discussion was aimed at showing that the relationship between U and Th determinations obtained using portable spectrometers on the ground or by radiometric or chemical analyses of selected samples should be, under normal circumstances, visible on airborne radiometric maps and profiles. This in turn should allow the user to select granite bodies that have favourable characteristics as defined in the remainder of this paper.

Geological Description of the Three Study Areas

The granitoid bodies in the three areas investigated differ significantly in their petrological nature.

In the Elliot Lake area, the granitoid rocks studied extend over an area of about 30 km by 20 km. These rocks of Archean age range from granodiorite to granite with an average composition of quartz monzonite. The intrusion is one of a string of similar bodies surrounded by gneissic rocks, lying to the north of the Huronian Quirke Lake syncline which

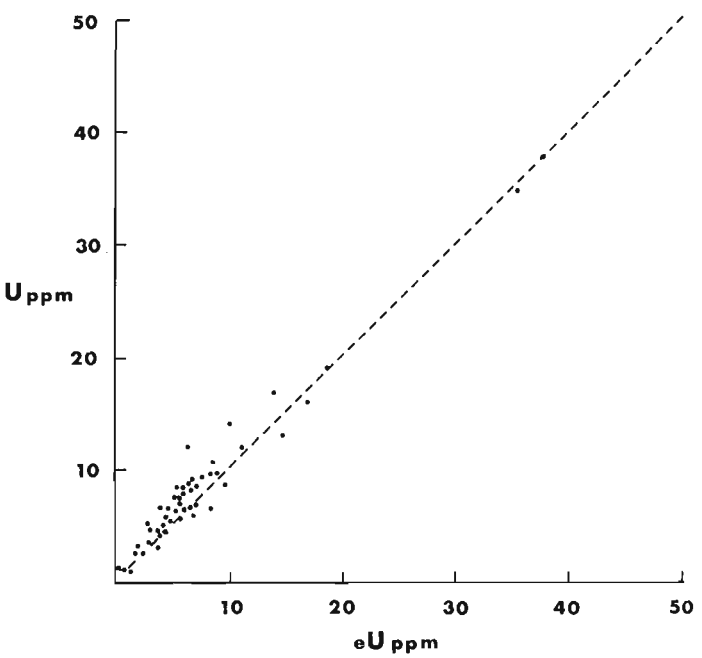

Figure 11.3. Uranium in ppm (delayed neutron counting) versus equivalent uranium ppm (laboratory gamma ray spectrometry) for fifty samples of granite from Fury and Hecla area.

contains conglomeratic uranium deposits (Darnley et al., 1977). This granitoid is medium to coarse grained, massive to porphyritic, and in places faintly gneissic. Colour varies from grey to bright pink.

Microcline, perthite, oligoclase, quartz, hornblende and biotite are the major minerals in the Elliot Lake rocks. In most specimens the mafic minerals are altered to chlorite, epidote, leucoxene, and iron oxides. The plagioclase has been extensively altered to white mica. Other minerals present are magnetite, hematite, ilmenite, pyrite, apatite, and radioactive accessories.

Table 11.1. Principal radioactive accessory minerals in Elliot Lake, Fury and Hecla, and Fort Smith granites

Elliot Lake	thorite, allanite, zircon, monazite, sphene
Fury and Hecla	thorite, allanite, zircon (minor), sphene (rare)
Fort Smith	monazite, zircon (minor), uraninite (very rare)

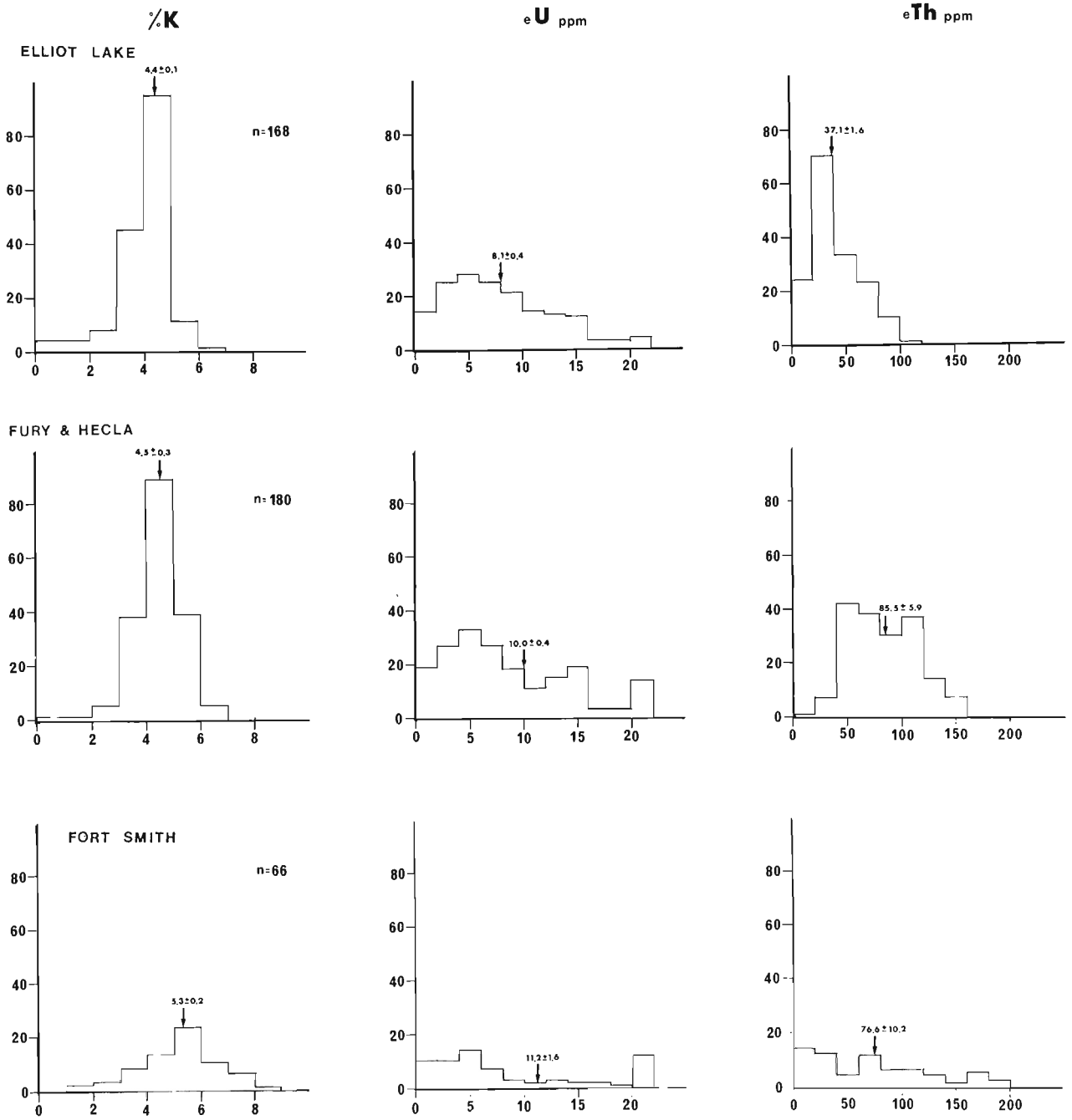

Figure 11.4. Histograms showing K %, eU ppm, and eTh ppm by gamma ray spectrometry for Elliot Lake, Fury and Hecla, and Fort Smith granites. Uranium values greater than 20 ppm have been grouped in the last class interval.

The Fury and Hecla investigation covered a well defined granitic body, 30 km in diameter. The age of this intrusion, presently being dated, is either Archean or Hudsonian. The rocks cut a gneissic terrane and are relatively undeformed, suggesting that they may be late Hudsonian. They are medium- to coarse-grained, equigranular to subporphyritic, and vary from red to pink. They are composed of microcline, somewhat sericitized oligoclase or albite, quartz, biotite, magnetite, hematite, and radioactive accessory minerals. A sequence of Helikian redbed sediments overlies part of the granite.

The Fort Smith study area is a north-trending belt, approximately 50 km wide and 200 km long intruded diapirically by an early Hudsonian megacrystic granitic to quartz monzonitic batholith (Bostock, 1981). These rocks are generally pink, coarsely porphyritic and foliated, and consist of microcline or microcline perthite phenocrysts, calcic oligoclase, quartz, biotite and accessory garnet, muscovite, ilmenite, anatase, rutile, hematite, fluorite, pyrite, and radioactive minerals. The potassium feldspars are deformed, usually crushed at their margins, and range up to 5 cm in length. Some microcline occurs in the groundmass in addition to forming the phenocrysts. The plagioclase grains are somewhat altered to epidote and sericite. Quartz occurs as isolated grains and in sutured patches. Both plagioclase and quartz are strained. Biotite is brown to greenish and commonly altered to chlorite but is relatively undeformed.

More detailed accounts of the geology of these three areas are given by Roscoe (1969) for the Elliot Lake area; Chandler et al. (1980) and Ciesielski and Maley (1980) for Fury and Hecla; and Charbonneau (1980), Bostock (1981) and Cape (1977) for the Fort Smith area.

Table 11.1 lists the main radioactive minerals in the three granitoids. These were identified optically in thin section and confirmed by microprobe analysis of autoradiograph sources. Both the Fort Smith and Fury and Hecla granites are thoriferous and contain thoriferous accessory minerals, whereas the Elliot Lake granite, which has a uranium/thorium ratio of about 1:5 (near crustal average), contains in addition more uraniferous radioactive minerals (zircon, sphene). For these three granitoids, the radioelement concentrations and ratios of the whole-rock generally reflect the uranium and thorium contents of their accessory mineral suites. The ranges of uranium and thorium concentrations expected in radioactive accessory minerals have been published by Hounslow (1976).

Uranium and Thorium Contents of the Three Granitoids

Results of gamma ray spectrometric analyses of the three granitoids are illustrated in the form of histograms in Figure 11.4 and summarized in Table 11.2. Data for the Elliot Lake and Fury and Hecla areas were obtained by in situ analyses with a portable spectrometer; data for the Fort Smith area are from laboratory analyses of a suite of samples collected over the entire Fort Smith belt.

Correlations between uranium and thorium concentrations within the three granitoids are illustrated in Figure 11.5. In this illustration, in situ measurements were used for all three areas. In situ analyses for the Fort Smith area are derived from two detailed study areas, near the eastern and western margins of the batholith (Charbonneau, 1980). The eastern area falls within the less evolved root zone and the western area falls within the more evolved head of the diapir as described by Bostock (1981). The large dots represent the arithmetic means for each plot and error bars are shown. In the discussion that follows it is realized that some redistribution of uranium, which could have affected its correlation with thorium and their ratio, may have occurred due to weathering or paleoweathering (surface related) phenomena. However the large sample volume of the in situ measurements would tend to average out small scale redistribution effects.

It can be seen from Figure 11.5 that in the Elliot Lake area, the uranium/thorium ratio tends to increase somewhat with uranium concentration and is independent of thorium concentration. In the Fury and Hecla granite, the uranium/thorium ratio shows a much stronger increase with increase in uranium concentration and no change with thorium. In the Fort Smith granite, the uranium/thorium ratio varies directly with uranium concentrations and inversely with thorium concentrations. These trends are also evident on airborne spectrometer profiles across each of the areas (Fig. 11.6).

A tentative interpretation of the trends shown on Figure 11.5 is that there has been only limited redistribution of uranium in the Elliot Lake granite with the uranium having been absorbed onto altered mafic minerals and iron oxides. This granite may have been the source rock for the Elliot Lake conglomeratic deposits (Roscoe, 1969) but no occurrences of any type have been found within the granite and its margins. In the case of the Fury and Hecla granite, the redistribution has been strong and the uranium has been reconcentrated in sericitic alterations, in biotite grains, and in fractures (Maurice, 1982). Granites showing strong mobilization of uranium are expected to host epigenetic uranium occurrences because more uranium is available in labile sites. Fracture controlled mineralization was located in the Fury and Hecla area both in shear zones within the granite and in fractures cutting overlying late Helikian sediments. The relationships between uranium/thorium ratio and uranium and thorium in the Fort Smith granite suggest that thorium was fixed in the early stages of magmatic evolution. Another possibility, similar to that proposed by Nash (1979) in relation to rocks in northwest U.S.A. is that thorium remained relatively immobile in an original sedimentary rock. According to this model, the rock is melted and thorium is concentrated mainly in the primitive phases of magmatic evolution and is present in lesser concentrations in the more differentiated phases. Uranium, on the other hand, is concentrated in the less thoriferous, more evolved portions of the granite. In the Fort Smith belt, some uranium was expelled outwards to the edge of the intrusion and into the wall rocks creating a flanking uranium/thorium ratio anomaly. This marginal anomaly may relate to the escape of volatiles (plus uranium) with pressure release related to upward movement of the diapir (Bostock, 1981). Uraninite associated with fluorite has been located along the margins of the intrusion and discrete radioactive sources, tentatively identified as uraninite, have been found in the older charnockitic wall rocks (Charbonneau, 1980).

Comparison with Other Granites

For comparison with the three granitic areas studied, the variations of eU and eTh concentrations in two other areas are illustrated in Figure 11.7. Data for deep (400 m) borehole samples from the Archean Granite Mountains, Wyoming, U.S.A., are taken from Stuckless et al. (1977). The eU/eTh ratio shows a strong positive correlation with uranium suggesting uranium mobilization as in the Fury and Hecla granite. Fission track studies (Stuckless et al., 1977) have shown that in the Granite Mountains uranium has been strongly concentrated along fractures. Figure 11.7 also

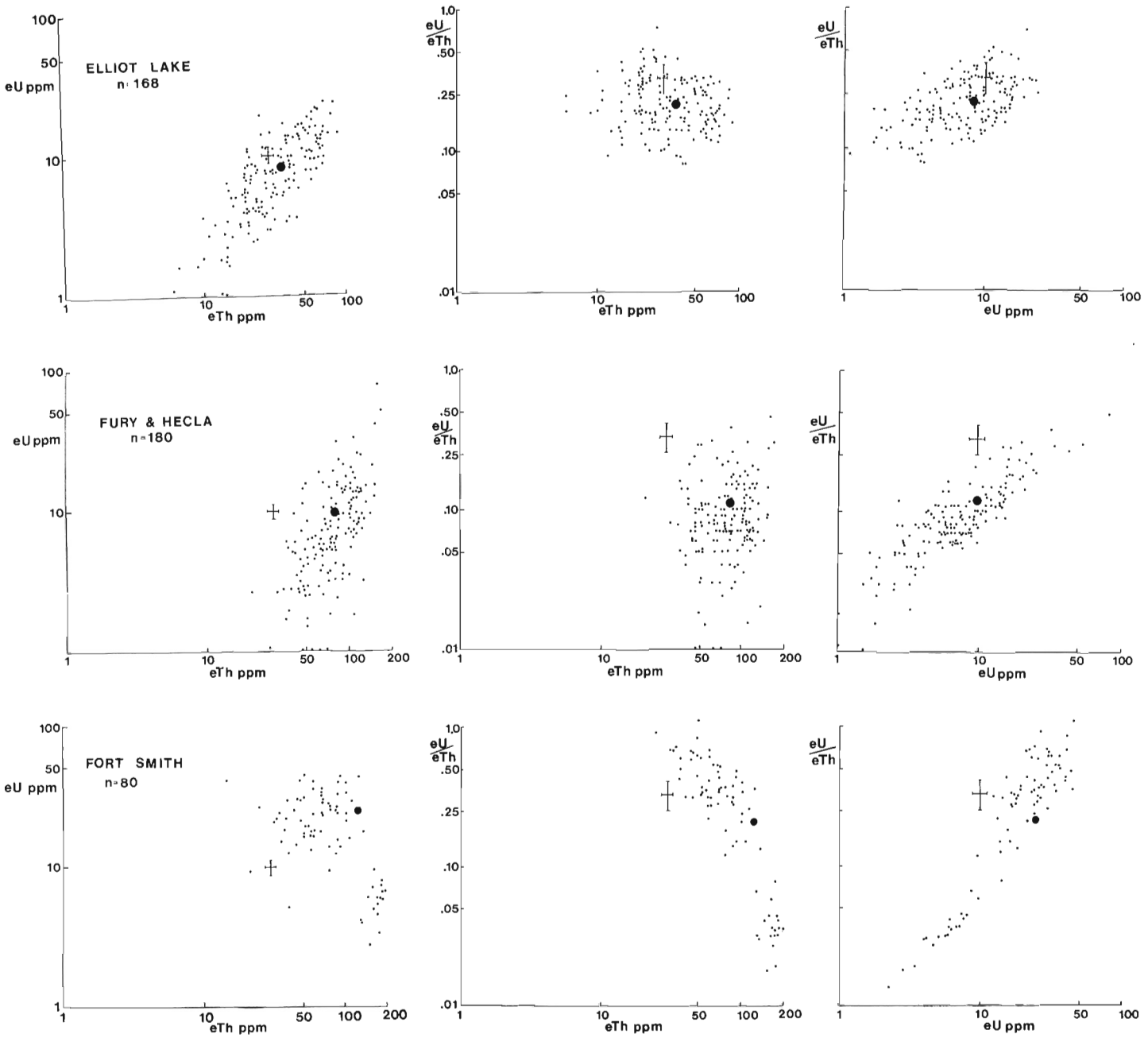

Figure 11.5. eU/eTh ratio versus eU and eTh for Elliot Lake, Fury and Hecla, and Fort Smith granites.

Table 11.2. Average K (%), eU (ppm), eTh (ppm), and total count (Ur) for Elliot Lake, Fury and Hecla, and Fort Smith granites

	No. Det.	K%*	eU ppm*	eTh ppm*	Ur**
Elliot Lake	168	4.4 ± 0.1	8.1 ± 0.4	37.1 ± 1.6	36
Fury and Hecla	180	4.5 ± 0.3	10.0 ± 0.4	85.5 ± 5.9	62
Fort Smith	66	5.3 ± 0.2	11.2 ± 1.6	76.6 ± 10.2	60

* Arithmetic Means ± Standard Error of Mean
** IAEA Technical Report 174, 1976

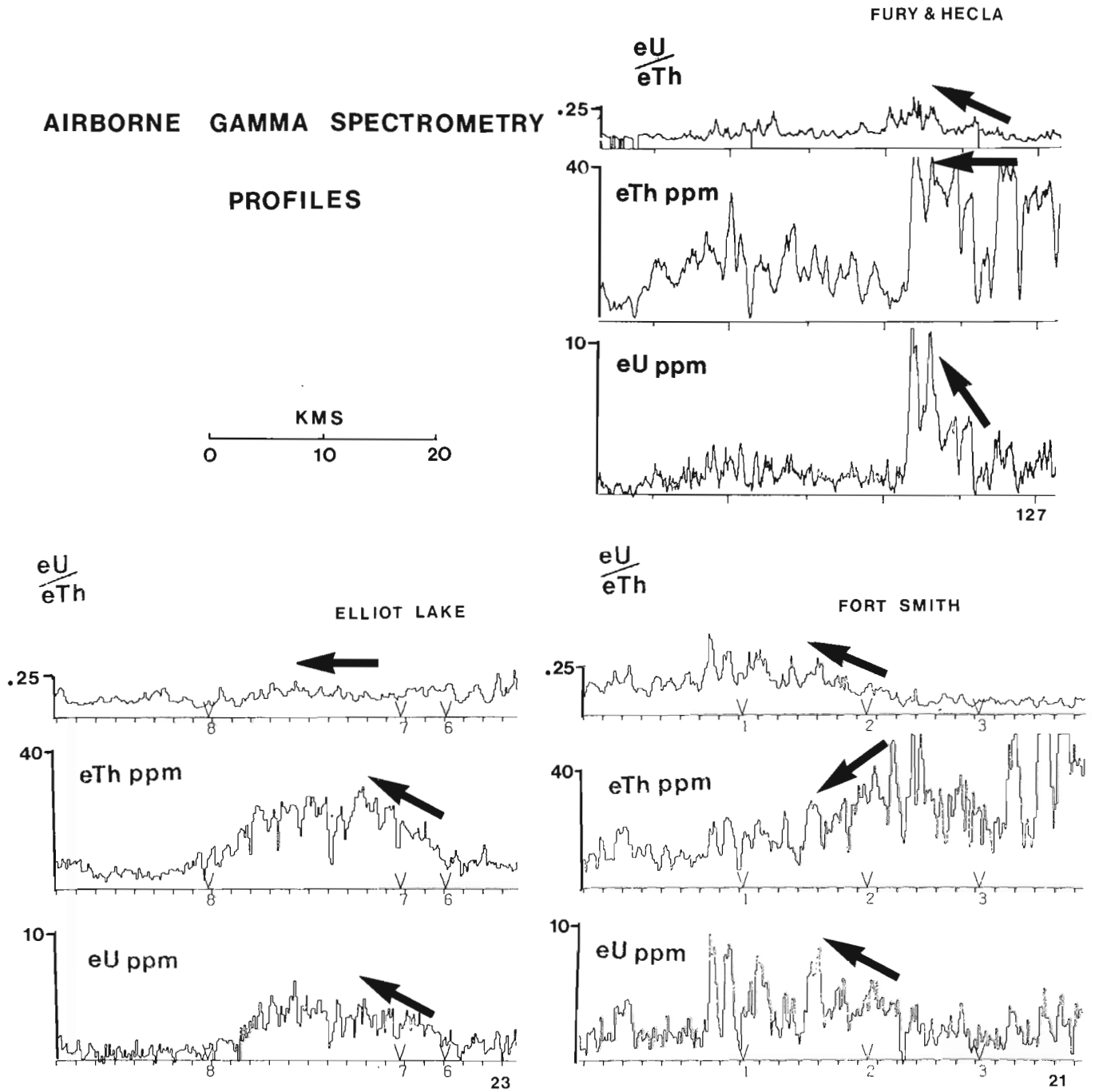

Figure 11.6. *Airborne gamma ray spectrometric profiles over Elliot Lake, Fury and Hecla, and Fort Smith granites showing eU, eTh, and eU/eTh ratio profiles. Arrows are included to accentuate the significant variations.*

shows in situ gamma ray spectrometric analyses for the Devonian South Mountain batholith (two mica granite) of Nova Scotia (K.L. Ford, personal communication). The positive correlation between the ratio and uranium, and the negative correlation between the ratio and thorium are apparent. These correlations again relate to differentiation trends within the batholith with more differentiated rocks having higher uranium/thorium ratio, more uranium and less thorium (Chatterjee and Muecke, 1982). Similar correlations between uranium, thorium, and their ratio have also been described in French granites (Cuney, 1978). It should be noted that although uranium and thorium trends are similar to those found in the Fort Smith belt, the flanking uranium/thorium ratio anomaly, so prominent there, is not seen in the Nova Scotia granites.

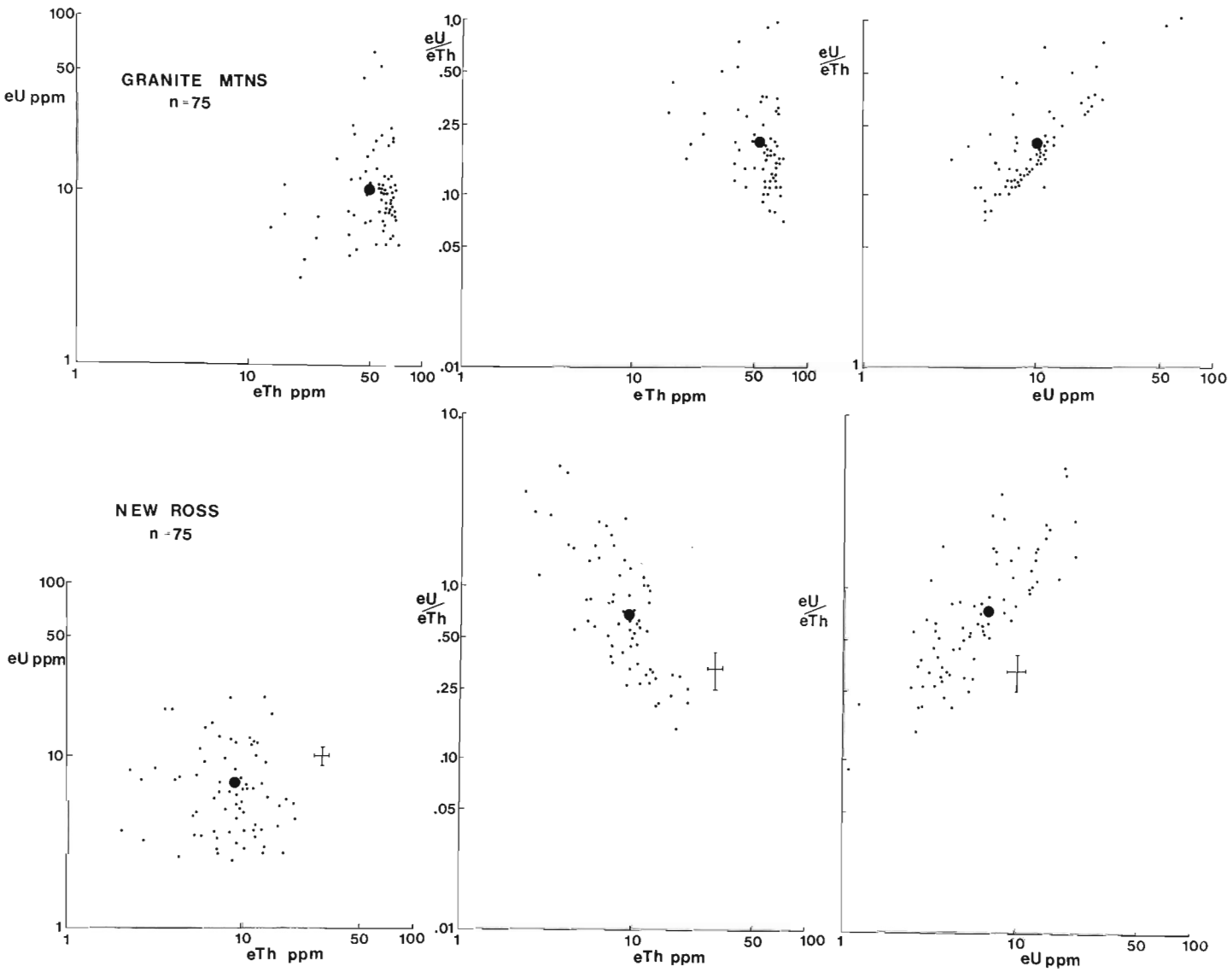

Figure 11.7. eU/eTh ratio versus eU and eTh for Granite Mountains, Wyoming and New Ross granite, Nova Scotia.

Summary

Ground investigations of three granitic bodies having radioelement enrichment indicate relationships between uranium and thorium concentrations which may be useful in assessing their uranium potential. If the uranium/thorium ratio increase strongly with uranium but not thorium, post magmatic redistribution of uranium is suggested and this could be a favourable economic criterion because uranium may have concentrated into deposits within or near the granite. If uranium versus uranium/thorium ratio does not show appreciable variation within the intrusion, it indicates that uranium has not been redistributed after the intrusive event either because there was no percolation of fluids to mobilize the uranium or because the bulk of the uranium is located within stable accessory minerals. If the uranium/thorium ratio is inversely correlated with thorium, the radioelement distribution is at least in part governed by magmatic processes. This situation may also be favourable if the end product of differentiation is a rock with high uranium/thorium ratio, high uranium and low thorium. Rocks with these characteristics would also be expected to have a significant percentage of labile uranium (Nash, 1979).

Further work on these granites, which will include whole-rock chemistry, trace element determinations, and fission and alpha track studies is being completed. This work should enable better understanding of the significance of the results discussed in this paper. Of particular interest is whether the uranium redistribution trends evident at Elliot Lake and particularly at Fury and Hecla are surface or paleosurface related or of deeper seated (primary/hydrothermal/metamorphic) origin.

Acknowledgments

The paper was critically read by K.A. Richardson and Y.T. Maurice, both of whom made many helpful changes that led to its final format. Radioactive mineral identification was provided by A.L. Littlejohn and G.J. Pringle, airborne gamma spectrometric surveys by P.B. Holman, and laboratory gamma ray spectrometry by G.W. Cameron, all of the Geological Survey of Canada. A number of people including K.L. Ford, G.R. Bernius, G.W. Cameron, R.B. Shives, L. Jones, and I. Garat were involved in various segments of the fieldwork.

References

Bostock, H.H.
1981: A granitic diapir of batholithic dimensions at the west margin of the Churchill Province; in Current Research, Part B, Geological Survey of Canada, Paper 81-1B, p. 73-82.

Cape, D.F.
1977: An investigation of the radioactivity of the Pilot Lake area, N.W.T.; unpublished M.Sc. thesis, University of Alberta, 156 p.

Chandler, F.W., Charbonneau, B.W., Ciesielski, A., Maurice, Y.T. and White, S.
1980: Geological studies of the late Precambrian supracrustal rocks and underlying granitic basement, Fury and Hecla Strait area, Baffin Island, District of Franklin; in Current Research, Part A, Geological Survey of Canada, Paper 80-1A, p. 125-132.

Charbonneau, B.W.
1980: The Fort Smith radioactive belt, Northwest Territories; in Current Research, Part C, Geological Survey of Canada, Paper 80-1C, p. 45-57.

Charbonneau, B.W., Ford, K.L., and Cameron, G.W.
1981: Equilibrium between U and eU (^{214}Bi) in surface rocks of Canada; in Current Research, Part C, Geological Survey of Canada, Paper 81-1C, p. 45-50.

Charbonneau, B.W., Killeen, P.G., Carson, J.M., Cameron, G.W., and Richardson, K.A.
1976: Significance of radioelement concentration measurements made by airborne gamma-ray spectrometry over the Canadian Shield; in Exploration for Uranium Ore Deposits; International Atomic Energy Agency, Ser. No. STI/PUB/434, p. 35-53.

Chatterjee, A.K. and Muecke, G.K.
1982: Geochemistry and the distribution of uranium and thorium in the granitoid rocks of the South Mountain Batholith, Nova Scotia: some genetic and exploration implications; in Uranium in Granites, ed. Y.T. Maurice; Geological Survey of Canada, Paper 81-23, report 2.

Ciesielski, A. and Maley, J.
1980: Basement of Agu Bay area and Gifford River area, Baffin Island, Northwest Territories; Geological Survey of Canada Open File 687.

Cuney, M.
1978: Geologic environment, mineralogy, and fluid inclusions of the Bois Noirs-Limouzat uranium vein, Forez, France; Economic Geology, v. 73, p. 1567-1610.

Darnley, A.G.
1970: Airborne gamma-ray spectrometry; Canadian Mining and Metallurgical Bulletin, v. 63, no. 694, p. 145.

Darnley, A.G. and Grasty, R.L.
1971: Mapping from the air by gamma-ray spectrometry; in Geochemical Exploration, ed. R.W. Boyle and J.I. McGerrigle; Canadian Institute of Mining and Metallurgy, Special Volume 11, p. 485-500.

Darnley, A.G., Charbonneau, B.W., and Richardson, K.A.
1977: Distribution of uranium in rocks as a guide to the recognition of uraniferous regions; in Recognition and Evaluation of Uraniferous Areas; International Atomic Energy Agency, Ser. No. STI/PUB/450, p. 55-86.

Hounslow, A.W.
1976: Mineralogy of uranium and thorium: a tabular summary; Mineralogical Laboratories, Mining Division, Colorado School of Mines Research Institute, Golden, Colorado.

International Atomic Energy Agency
1976: Radiometric reporting methods and calibration in uranium exploration; STI/DOC/10/174, 57 p.

Maurice, Y.T.
1982: Uraniferous granites and associated mineralization in the Fury and Hecla Strait area, Baffin Island, N.W.T.; in Uranium in Granites, ed. Y.T. Maurice; Geological Survey of Canada, Paper 81-23, report 12.

Nash, J.T.
1979: Uranium and thorium in granitic rocks of northeastern Washington and northern Idaho, with comments on uranium resource potential; United States Department of the Interior, Geological Survey, Open File Report 79-233, 39 p.

Ostrihansky, L.
1976: Radioactive disequilibrium investigations, Elliot Lake, Ontario; Geological Survey of Canada, Paper 75-38, Pt. 2, p. 21-48.

Perttunen, M.
1977: The lithological relation between till and bedrock in the region of Hameenlinna, Southern Finland; Geological Survey of Finland, Bulletin 291, 68 p.

Roscoe, S.M.
1969: Huronian rocks and uraniferous conglomerates in the Canadian Shield; Geological Survey of Canada, Paper 68-40, 205 p.

Rosholt, J.N.
1959: Natural radioactive disequilibrium of the uranium series; United States Geological Survey Bulletin 1084-A, 30 p.

Shilts, W.W.
1976: Glacial till and mineral exploration; in Glacial Till, an Interdisciplinary Study, ed. R.F. Legget; Royal Society of Canada, Special Publication no. 12, p. 205-224.

Stuckless, J.S., Bunker, C.M., Bush, C.A., Doering, W.P., and Scott, J.H.
1977: Geochemical and petrological studies of a uraniferous granite from the Granite Mountains, Wyoming; U.S. Geological Survey Journal of Research, v. 5, p. 61-81.

12.

URANIFEROUS GRANITES AND ASSOCIATED MINERALIZATION IN THE FURY AND HECLA STRAIT AREA, BAFFIN ISLAND, N.W.T.

Y.T. Maurice[1]
Geological Survey of Canada

Maurice, Y.T., Uraniferous granites and associated mineralization in the Fury and Hecla Strait area, Baffin Island, N.W.T.; in Uranium in Granites, ed. Y.T. Maurice; Geological Survey of Canada, Paper 81-23, p. 101-113, 1982.

Abstract

Two well defined circular airborne radiometric anomalies, each about 30 km in diameter and separated by some 50 km in an east-west direction, were outlined in Archean and/or Lower Proterozoic basement rocks north of Fury and Hecla Strait in northern Baffin Island. Systematic mapping and rock analyses show that the main radioactive unit underlying both anomalies is a homogeneous calc-alkali granite averaging 8 ppm U and 80 ppm Th. A 0.1 km^2 portion of the granite underlying the eastern anomaly averages 30 ppm U and 120 ppm Th and is heavily jointed with some fractures showing wall rock alteration and uranium concentrations up to 90 ppm.

Analyses of 44 granite samples show no apparent correlation between the regional variation of uranium and of any of the major elements. Of the minor and trace elements, only slight increases in Pb, Th and F are noticed in the more uraniferous parts of the granite.

The basement rocks are unconformably overlain by 6000 m of unmetamorphosed Upper Proterozoic (Neohelikian to Early Hadrynian) sediments. Radioactivity was found in an oligomictic hematitic quartz-cobble conglomerate at the base of the sequence but it is not intense and is due mostly to thorium.

Most promising from an economic standpoint are radioactive veins in shear zones within the eastern granite and, occasionally, within the Upper Proterozoic sediments. These veins contain a fine recticulated quartz stockwork and are enriched in Cu and Mo as well as uranium. Wall rock alteration involves enrichment in K_2O and MgO and depletion in Na_2O and CaO.

Other radioactive rocks in the region include pegmatites in basement gneisses near the western granite. These are widespread but do not follow any obvious structural pattern and are seldom traceable for more than a few metres. They may be consanguineous with the granite and could represent a late intrusive phase.

A process of removal of uranium from the granite mass and its concentration in zones of fractures is suggested to explain the origin of the radioactive veins as well as the more uraniferous parts of the eastern granite. It is not known whether this took place under supergene or hydrothermal conditions but the proximity of the veins to the unconformity and a relatively simple element assemblage favours a supergene origin. However, the presence of radioactive veins within the Upper Proterozoic sediments is indicative that at least some mineralization formed after deposition of the sediments.

Résumé

Deux anomalies radiométriques aéroportées circulaires et bien définies, ayant un diamètre de 30 km chacune et séparées par quelque 50 km en direction est-ouest furent définies dans une région de roches archéennes ou du début du Protérozoïque, au nord du détroit de Fury et Hecla, dans le nord de la terre de Baffin. Une cartographie systématique et des analyses de roches montrent que la principale unité radioactive formant les deux anomalies est un granite rose calco-alcalin homogène, présentant des concentrations moyennes de 8 ppm d'uranium et 80 ppm de thorium. Une portion de 0,1 km^2 du granite dans l'anomalie de l'est présente des concentrations moyennes de 30 ppm d'uranium et de 120 ppm de thorium et est fortement fracturée présentant une altération des murs et des concentrations d'uranium allant jusqu'à 90 ppm.

Les analyses de 44 échantillons de granite ne montrent aucune corrélation apparente entre les variations régionales d'uranium et de l'un ou l'autre des éléments majeurs. En ce qui concerne les éléments mineurs et les éléments traces, on n'a remarqué que de légères augmentations en Pb, Th et F dans les portions les plus uranifères du granite.

Les roches de base sont recouvertes de façon discordante par une suite de sédiments non métamorphisés datant de la fin du Protérozoïque (du Néohélicien au début de l'Hadrynien), d'une épaisseur de 6 000 m. On a trouvé des traces de radioactivité dans un conglomérat de galets quartzifères oligomictique hématitique à la base de la série de sédiments, mais cette radioactivité n'est pas intense et est due principalement au thorium.

[1]601 Booth Street, Ottawa, Ontario K1A 0E8

Les gisements les plus prometteurs, d'un point de vue économique, sont les filons radioactifs qu'on retrouve dans les zones de cisaillement dans le granite de l'est et, occasionellement, dans les sédiments du Protérozoïque. Ces filons contiennent un stockwerk quartzifère à maille fine et sont enrichis en cuivre et en molybdène, aussi bien qu'en uranium. L'altération de la roche des murs comporte un enrichissement en K_2O et MgO et un appauvrissement en Na_2O et CaO.

On retrouve à proximité du granite de l'ouest, des pegmatites radioactives dans les gneiss du socle. Celles-ci sont très répandues, mais ne semblent avoir aucune configuration structurale apparente et sont rarement détectables pour plus de quelques mètres. Elles peuvent être apparentées au granite et pourraient représenter une phase tardive de l'intrusion.

On croit que l'origine des filons radioactifs, de même que les parties les plus uranifères du granite de l'est, pourrait s'expliquer par un processus de lixiviation de l'uranium de la masse granitique et de sa concentration dans les zones de fractures. On ne sait pas si ce processus s'est produit dans des conditions supergènes ou hydrothermales, mais étant donné que les filons se trouvent à proximité de la discordance et qu'il y a un assemblage relativement simple d'éléments, on croirait plutôt à une origine supergène. Cependant, la présence de filons radioactifs dans les sédiments de la fin du Protérozoïque indique qu'au moins une partie de la minéralisation s'est formée après la déposition des sédiments.

Introduction

A multidisciplinary project was undertaken in the summer of 1979 to investigate basement rocks and overlying Late Precambrian supracrustals of the Churchill Province in the region of Fury and Hecla Strait in northern Baffin Island. A detailed account of the work is given by Chandler et al., (1980).

Part of the interest in these rocks derives from a federal government sponsored airborne radiometric survey which indicated unusually high levels of radioelements over a wide area (Geological Survey of Canada, 1979). The survey revealed two well defined anomalies, each about 30 km in diameter and separated by some 50 km in an east-west direction (Chandler et al., 1980, Fig. 20.2). Geological mapping established that the main radioactive unit in both anomalies is a medium grained pink biotite granite that intrudes a variety of mesocratic basement gneisses. Neither the gneisses nor the supracrustals show anomalous radioactivity but the proximity of the radioactive granites to a major unconformity adds considerable interest to the region from an economic standpoint. Chandler and Stevens (1981) established that sedimentation of the supracrustals began around 1100 Ma ago, closely following the deposition of the Athabasca Formation (1350 Ma ago, Ramaekers and Dunn, 1977) that is related to major uranium deposits. Detailed prospecting in the Fury and Hecla area has uncovered several radioactive prospects, some with characteristics suggesting a genetic relation to the unconformity.

Geology and petrology

The granite underlying the eastern radiometric anomaly (Fig. 12.1) forms a massive and homogeneous batholith, well exposed over an area of approximately 500 km^2. It is unconformably overlain by, and often in fault contact with, the younger Proterozoic sediments. The rock shows a lack of structural features except along the margins and in shear zones where a mild foliation is locally visible. The major components seen in thin section are microcline, quartz, partly sericitized plagioclase, and biotite. From microprobe analysis, the composition of the plagioclase was found to average An_{15-16}. Zircon, apatite, magnetite, allanite, and thorite are the common accessories. Allanite is ubiquitous and quite abundant in some sections. It usually occurs in or adjacent to biotite grains and is generally altered to a mixture of chlorite, clay minerals and bastnaesite. Thorite is generally altered (thorogummite?) and present in biotite grains or with the allanite. Sphene, often altered to anatase, occurs sparsely and fluorite was seen in one section.

The western granite (Fig. 12.2) is not as well exposed as its counterpart in the east. Its southernmost exposure is located about 12 km north of the unconformity. The granites in the east and west are very similar except that the western granite is somewhat finer grained and often contains small amounts of primary muscovite.

Mineralization

The radioactive mineralization discovered in the Fury and Hecla area falls into two main categories:

a. fracture-controlled within the eastern granite and adjacent Upper Proterozoic sediments and,

b. pegmatites near the western granite.

In addition, radioactivity was encountered in hematitic quartz-cobble conglomerate at the base of the Upper Proterozoic supracrustals. This radioactivity is due mostly to thorium and is not intense.

The fracture-controlled mineralization occurs along fractures and shear zones within the granite (e.g. locality C, Fig. 12.1) and along faults that bring the granite in contact with the supracrustals (e.g. locality D, Fig. 12.1). The veins are characterized by a recticulated quartz stockwork and, in proximity to the fractures, the granite is yellow and soft indicating intense alteration. Such alteration is widespread in the eastern granite particularly near the contact with the supracrustals, but it is not always accompanied by increases in radioactivity, at least, judging from what can be observed at the surface. Some alteration zones measure several kilometres in length but the radioactive zones examined by the writer were only in the order of 10 to 20 m long. One radioactive zone measuring about 100 m has been reported by Dejour Mines Ltd. (The Northern Miner, 1980).

Because the radioactive veins are severely oxidized, samples collected at the surface contain only secondary uranium minerals (uranophane and meta-autunite were identified) and their uranium content is suspected to be severely depleted. Diamond drilling by Dejour Mines Ltd. at locality B (Fig. 12.1) intersected zones containing an unidentified fine grained black radioactive oxide at a depth of about 50 m (D. Fisher, personal communication, 1981). Pyrite and specular hematite were also found in the core.

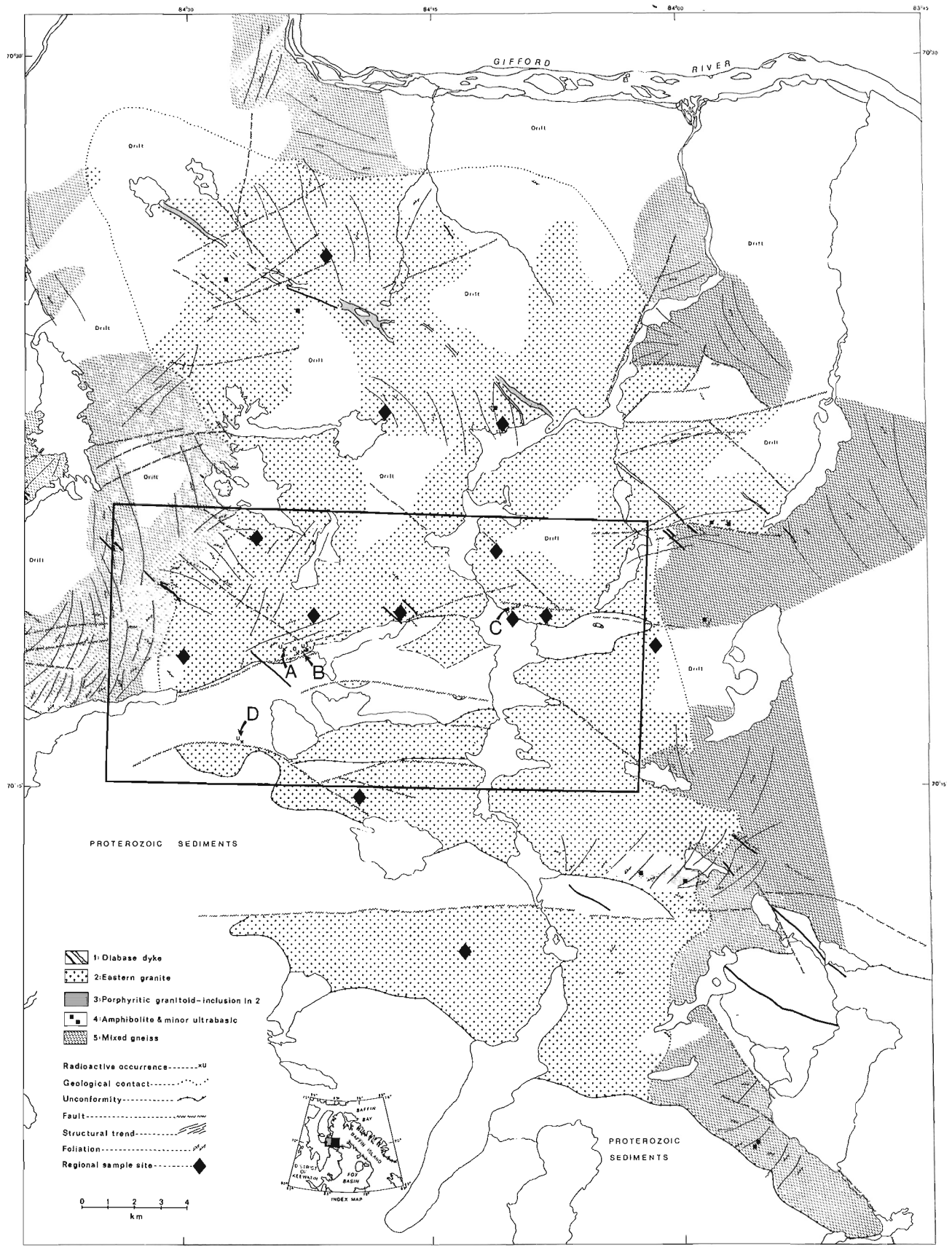

Figure 12.1. *Geology of the eastern granite (after Ciesielski and Maley, 1980), and location of detailed radiometric survey (outlined) and regional samples. Occurrences A to D described in text.*

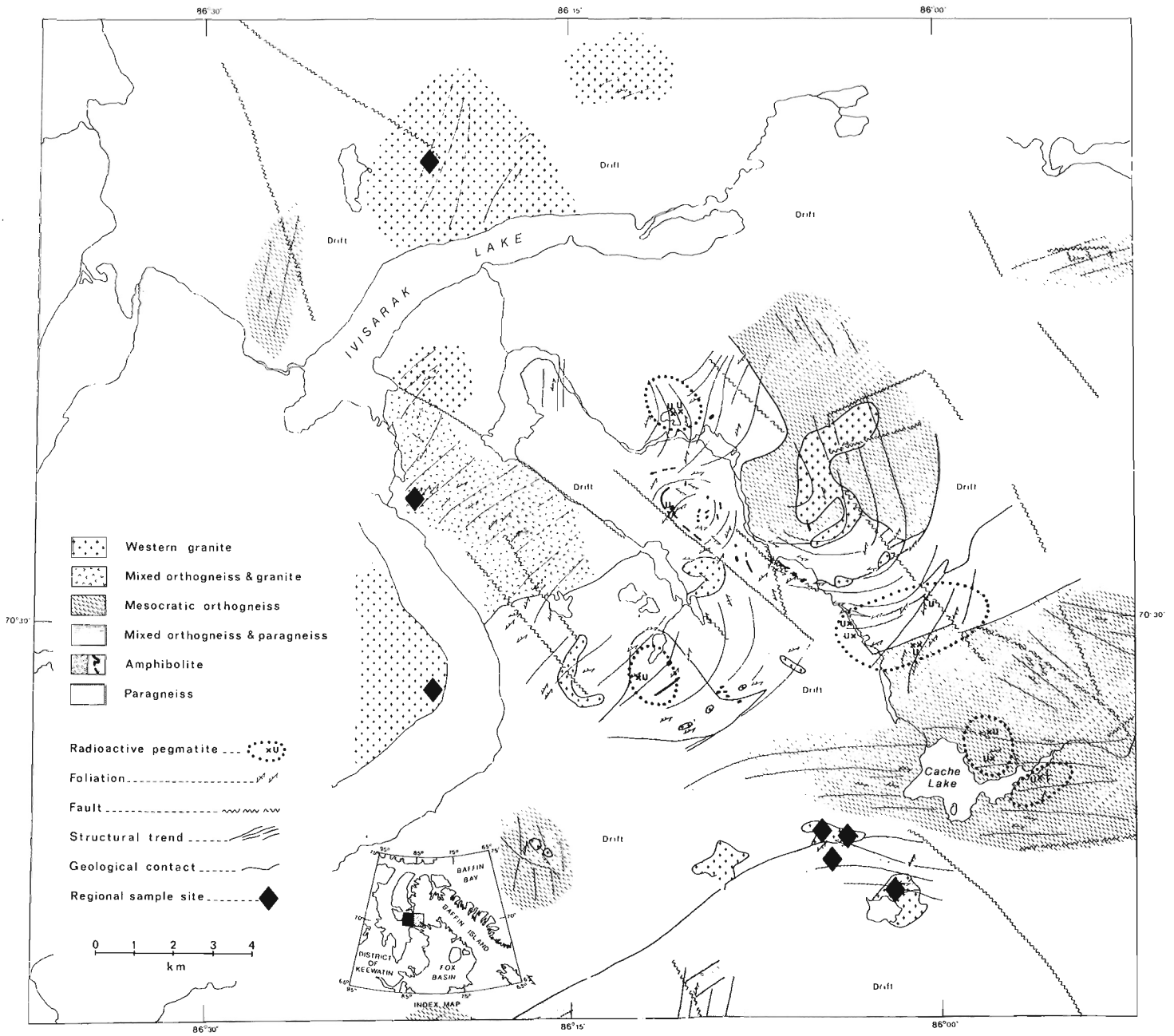

Figure 12.2. *Geology of the western granite (after Ciesielski and Maley, 1980) and location of regional samples.*

Maximum uranium contents in surface exposures of fracture-controlled radioactive zones reached 300 ppm U at locality C and 1500 ppm U at locality D (Fig. 12.1), the two most interesting occurrences examined by the writer (locality B was not visited). However, in the writer's opinion, these values are not representative of uranium concentrations at depth because of the likelihood of severe surface leaching.

Fracture-controlled radioactivity was not found in the west but radioactive pegmatites occur within the gneisses in proximity to the western granite. They conform broadly to the foliation and tend to occur in separate groups as indicated in Figure 12.2. Individual pegmatites are seldom traceable for more than a few metres.

The pegmatites are granitic in composition with a medium to coarse texture. Their radioactivity often increases with biotite content and the most radioactive outcrops are stained with secondary uranium oxides. The primary radioactive minerals were identified as uraninite and altered allanite, generally as inclusions in biotite.

Nonradioactive pegmatites, similar in appearance to the radioactive ones, occur throughout the western region. They are found in the gneisses and, unlike the radioactive ones, also in the granite. Pegmatites are uncommon in the east and were never found to be radioactive.

Geochemistry

The rectangle in Figure 12.1 outlines the area of a detailed helicopter-borne radiometric survey over the most intense part of the regional anomaly in the east. Survey specifications were given in Chandler et al. (1980). Figure 12.3 shows the distribution of U in that area using contour intervals expressing concentrations in relation to an arbitrary background measured over barren Upper Proterozoic sandstone.

The lowest contour corresponds approximately to the outline of the granite pluton. The anomaly peaks at 'A' with readings exceeding 5X the levels found over the sandstone. The eastern granite was sampled using the following scheme:

1. 11 samples collected in an area of 0.1 km^2 in zone 'A' (Fig. 12.3).
2. 13 samples collected in a 1 km^2 area within the 3X background contour line enclosing zone 'A' – intermediate zone.
3. 13 samples from the remainder of the granite (sample locations shown in Figure 12.1) – regional sampling.

In addition, three samples were obtained from a zone of altered granite close to a fracture-controlled radioactive occurrence within zone 'A', and seven samples were collected at various locations within the western granite (see Figure 12.2 for locations). All are single, fist-size grab samples, free of any visible impurities.

The major, minor, and trace element composition of the various parts of the granite, including the western granite and various mineralized outcrops is shown in Table 12.1. The major element composition of the granite is very uniform and approaches the composition of an average calc-alkali granite as determined by Nockolds (1954; column F in Table 12.1). With an overall (regional) concentration of 8 ppm U and about 75-80 ppm Th, both the eastern and western granites are anomalous in their radioelement content, as the normal concentration of these metals in granitic rocks is closer to 4 ppm U and 20 ppm Th. There is a steady increase in the U content towards zone 'A' where it averages 30 ppm U. There is also an increase in Th but it is less pronounced. None of the major elements show similar variations (compare columns A, B, and C, Table 12.1). Of the minor and trace elements, only slight increases in F, and to a lesser extent in Pb are observed. These variations, however, are very minor compared to that of U.

In the altered granite (column D, Table 12.1), U reaches 90 ppm averaging 60 ppm; there is a significant increase in K_2O and MgO and a decrease in CaO, Na_2O and, to a lesser extent, in Fe and Mn compared to the unaltered granite. Of the minor and trace elements, F, Cu, and Pb increase, and Sr decreases slightly. In thin section, the altered granite shows complete sericitization of the plagioclase (hence the decrease in Ca and Na, and the increase in K) and 50 to 75 per cent replacement of the biotite by quartz (decrease in Fe and Mn). The allanites remain only as relics and thorite is rare.

Elemental variations in the vicinity of the radioactive veins are illustrated further by a geochemical profile obtained across the mineralized vein at locality C (Fig. 12.1). Variations in the major elements and U and Th are shown in Figure 12.4, and variations in Cu, Pb, Zn, and Mo are shown in Figure 12.5.

Note that the amount of feldspar, as reflected in Al_2O_3, remains constant throughout the granite (sample nos. 1, 2, 3, 6, 7, 8, 9 and 10 in Fig. 12.4) and is low in the vein (sample nos. 4 and 5). Uranium increases sharply in the vein and in the adjacent altered granite. Thorium is somewhat erratic but follows a pattern similar to that of Al_2O_3 pointing to its presence in the granite rather than in the vein. The diagram does, however, suggest a slight increase in Th in the altered granite.

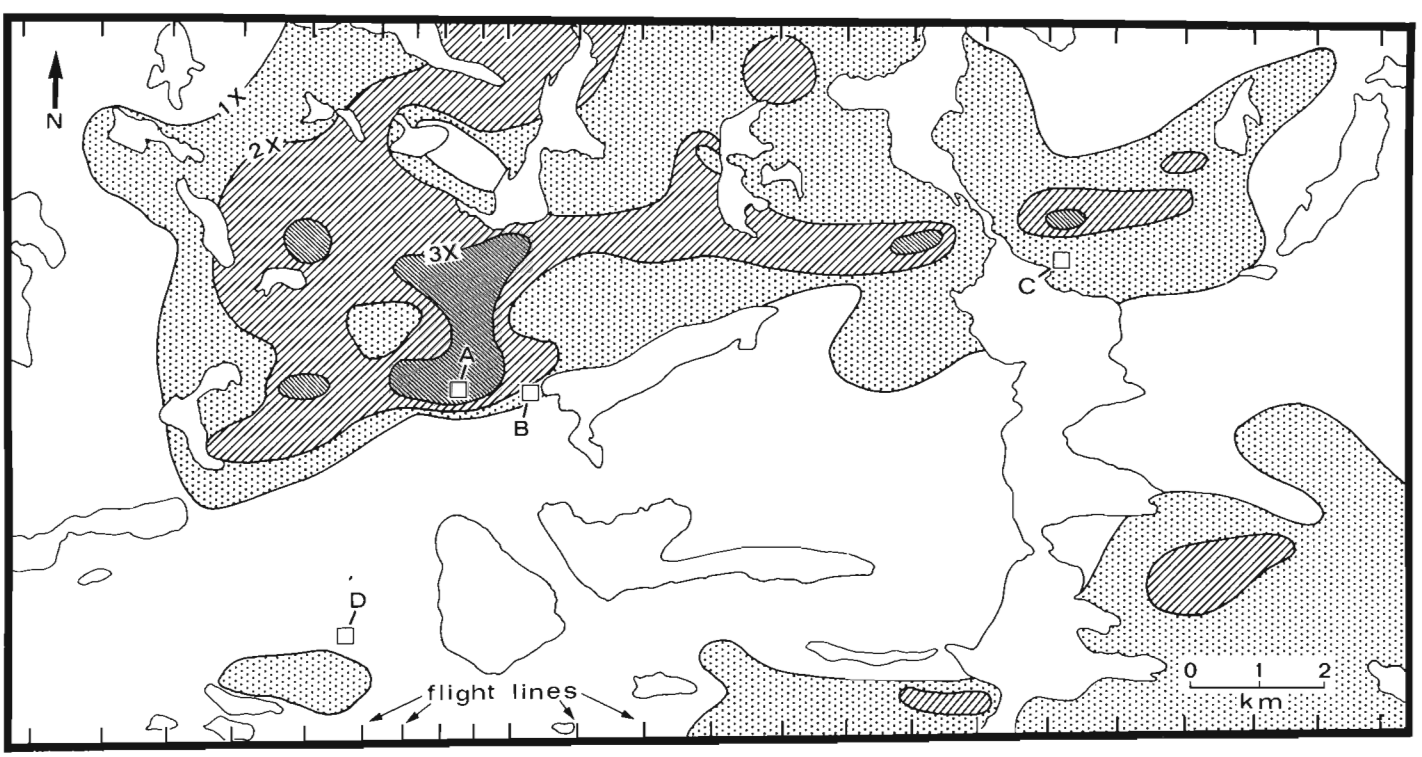

Figure 12.3. *Detailed uranium distribution pattern of central part of eastern granite. Area located in Figure 12.1.*

Table 12.1. Major, minor, and trace element composition of granitic rocks and associated mineralization, Fury and Hecla Strait area

		A	B	C	D	E	F	G	H	I	J	K
SiO_2	(%)	71.9	72.5	72.2	72.8	72.6	72.1	86.0	95.4	74.2	71.9	76.1
Al_2O_3	"	14.6	14.3	14.2	14.0	14.2	13.9	7.3	1.9	11.3	14.5	14.6
K_2O	"	5.8	5.6	5.9	7.4	5.1	5.5	3.5	0.07	6.72	1.51	1.02
CaO	"	0.65	0.75	0.62	0.08	0.98	1.33	0.05	0.02	0.22	2.46	2.62
Na_2O	"	3.3	3.2	3.1	0.9	3.2	3.1	0.3	0.1	0.9	4.0	4.8
MgO	"	0.50	0.37	0.34	0.79	0.28	0.52	0.39	0.00	1.52	0.87	0.00
FeO	"	0.7	0.6	0.6	0.4	0.6	1.7	0.1	0.1	1.6	1.8	0.0
Fe_2O_3	"	1.1	1.2	1.2	1.0	1.1	0.9	0.9	0.7	1.3	0.9	0.2
MnO	"	0.02	0.03	0.03	<0.01	0.03	0.06	0.01	0.01	0.04	0.04	0.01
TiO_2	"	0.19	0.17	0.19	0.19	0.17	0.37	0.08	0.03	0.37	0.30	0.01
P_2O_5	"	0.07	0.06	0.05	0.06	0.06	0.18	0.10	0.20	0.11	0.03	0.02
H_2O	"	0.7	0.4	0.8	1.5	0.7	0.5	0.6	0.4	0.9	1.2	0.2
Total		99.53	99.18	99.23	99.12	99.02	100.16	99.33	98.93	99.18	99.51	99.58
U	(ppm)	7.9	13.5	30.2	58.8	8.1	3.5	302	1490	6240	536	2.1
Th	"	84	73	120	137	67	18	28	16	235	203	8
F	"	218	221	277	357	139	800	185	98	200	140	50
Sr	"	91	140	91	49	77	300	40	69	158	213	171
Rb	"	260	300	300	330	230	400	170	40	260	100	80
Ba	"	800	780	720	640	570	830	390	430	2280	180	120
Sn	"	3.4	5.0	6.5	5.0	8.6	3.5	<1.0	4.0	2.0	4.0	<1.0
Zr	"	202	187	209	218	199	200	93	123	87	47	17
Mo	"	2	5	3	5	2	2	61	2	560	118	2
Cu	"	6.9	7.6	2.6	12.0	2.7	16.0	198	30	47	121	3.0
Pb	"	32	38	48	69	44	30	48	69	1830	329	23
Zn	"	32	35	32	25	34	30	21	9	57	65	4
S	"	300	520	250	370	230	400	700	200	1800	2200	100
U/Th		0.094	0.185	0.252	0.429	0.121	0.194	10.8	93.1	26.6	2.64	0.263

A – Eastern granite; ≈500 km^2 – Regional sampling (13 samples)
B – Eastern granite; ≈1 km^2 – Intermediate zone (13 samples)
C – Eastern granite; ≈0.1 km^2 – Zone 'A' (11 samples)
D – Eastern granite; Altered granite within zone 'A' (3 samples)
E – Western granite; ≈100 km^2 – Regional sampling (7 samples)
F – Average calc-alkali granite; major elements from Nockolds (1954) – minor and trace elements from Granier (1973)
G – Radioactive vein; locality C, Figure 12.1 (1 sample)
H – Radioactive vein; locality D, Figure 12.1 (1 sample)
I – Strongly radioactive pegmatite, western anomaly (1 sample)
J – Moderately radioactive pegmatite, western anomaly (1 sample)
K – Nonradioactive pegmatite, western anomaly (1 sample)

Analytical techniques:

1 Major element oxides (except FeO), Rb, and Ba: XRF using fused disc
2 F: Selective ion electrode following carbonate fusion
3 FeO: dichromate titration following cold acid decomposition
4 H_2O and S: fusion in resistence furnace and determination by infrared spectroscopy
5 Sn, Th, Zr: XRF using compressed disc
6 U: neutron activation/delayed neutron counting
7 Sr, Mo, Cu, Pb, and Zn: atomic absorption following Hf acid sample decomposition

Analyses by:

1,2,3 and 4 Analytical Chemistry Section, Geological Survey of Canada
5 Bondar Clegg and Co. Ltd.
6 Atomic Energy of Canada Ltd.
7 Resource Geochemistry Subdivision, Geological Survey of Canada

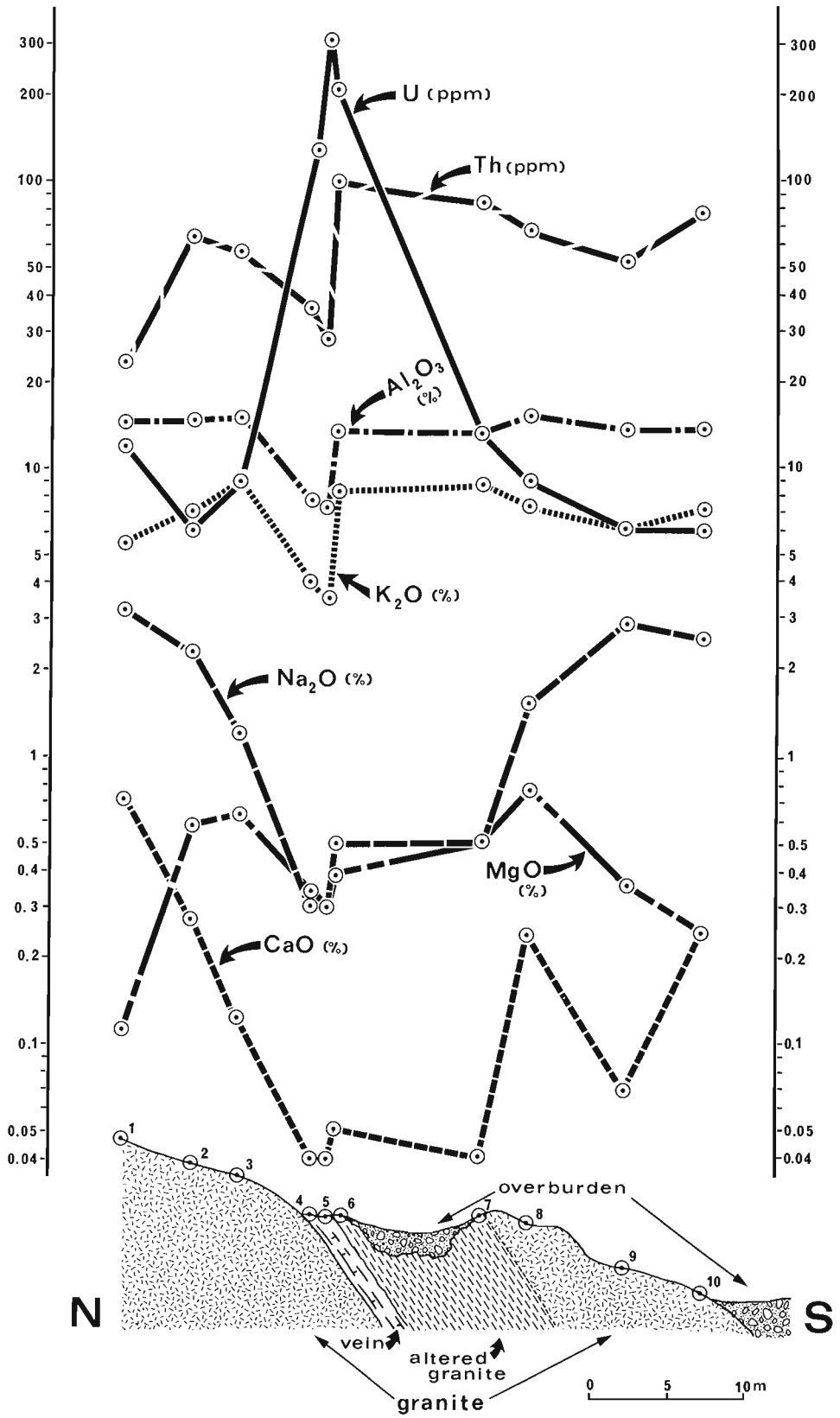

Figure 12.4. *Geochemical profile across mineralized vein (locality C, Fig. 12.1). Distribution of U, Th, Al_2O_3, K_2O, Na_2O, MgO, and CaO.*

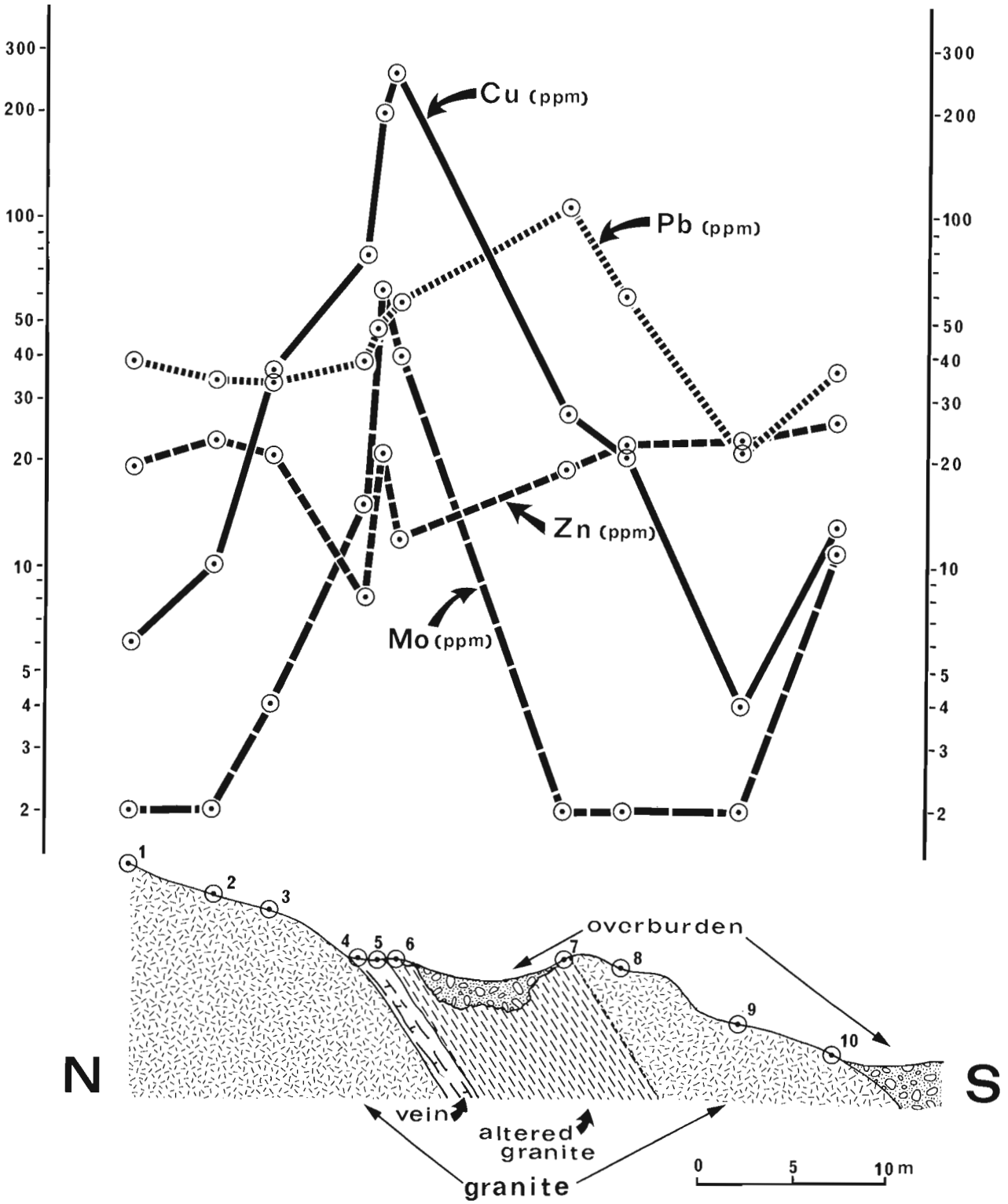

Figure 12.5. Geochemical profile across mineralized vein (locality C, Fig. 12.1). Distribution of Cu, Pb, Zn, and Mo.

Calcium and sodium both show a constant decline towards the vein which commences beyond the zone of alteration. Potassium and magnesium show an increase towards the vein. It is curious that Mg is highest in the samples of unaltered granite nearest the alteration zone and appears to decline in the altered granite towards the vein.

Of the trace elements, both Cu and Mo show well defined anomalies over the vein and the alteration zone. The decline of these elements in the unaltered granite is progressive particularly in the case of Cu. Zinc appears to be depleted in both the alteration zone and the vein. Lead is only slightly enhanced in the vein but is higher in the altered granite.

Particle Track Analyses

Eleven samples from different parts of the eastern granite were submitted to fission and α-track analyses as a means of micromapping the radioelement distribution. Uranium concentrations were estimated by comparing track densities with those produced by two glass standards containing respectively 12 and 150 ppm equivalent natural uranium. The principle and the techniques of particle track analyses have been described by Thiel et al. (1979).

In eastern granite samples containing average concentrations of uranium (6 to 10 ppm), the radioelements are contained mostly in allanite, thorite, and zircon (Plate 12.1). Microprobe analyses of samples from the eastern granite indicate that the U content of allanite is in the order of 0.1 per cent and from less than 0.1 per cent to about 8.0 per cent in thorite. No measurements were made on zircon. When present, sphene contains from 100 to 150 ppm U (Plate 12.2).

In samples from zone 'A' (≈30 ppm U), some of the U is located in microfractures and along grain boundaries in addition to being contained in allanite, thorite, and zircon (Plate 12.3). Often, biotite is considerably enriched in U (several hundred ppm) in these samples, particularly where microfractures intersect the biotite grains. Where this occurs, the biotite may be enriched throughout the grain or, more commonly, the enrichment is greater in the vicinity of the microfracture. Locally, the biotite grains are enriched along their outer boundaries (Plate 12.4). It appears that biotite acts as a reductant precipitating the uranium.

The sericitized plagioclase in samples from zone 'A' contains about 5 to 10 ppm U but in the altered granite near the mineralized fractures, the uranium content of sericitized plagioclase may reach 100 to 150 ppm. This uranium, as well as that found in microfractures and veinlets (Plate 12.5), represent the bulk of the uranium in the altered granite (about 50 to 100 ppm U) because biotite, allanite, and thorite have largely been replaced and probably contribute little to the total uranium content.

Discussion

The similarity in the chemistries of the eastern and western granites suggests that they both belong to the same intrusion and are probably connected at depth. Present exposure in the eastern granite area, however, probably represents a deeper erosional level than the finer grained western granite. As a result, pegmatites which may have formed over both cupolas are now preserved only in the capping gneisses still found over the western granite.

The origin of the uranium concentrations associated with the eastern granite poses a different problem. Although it has been shown that the uranium content increases with magmatic differentiation (Rogers and Adams, 1969), the lack of variation in the major and trace elements in the Fury and Hecla granite, particularly for the more common indicators of magmatic differentiation, K, Rb, Sr, and Ba, suggests that primary magmatic processes (syngenetic) are not responsible for the uranium enrichment observed in parts of the eastern granite (viz. zone 'A'). Instead, both the analytical results and particle track analysis suggest that the uranium enrichment originates from epigenetic processes.

The question arises as to whether these processes are supergene or hydrothermal. In the first instance, one envisages the primary uranium-bearing minerals of the granite, allanite and thorite, being oxidized within the zone of weathering, the uranium leached and carried downward as soluble uranyl complexes and precipitated under reducing conditions along fractures to form veins. In some cases, the uranium, could have impregnated an area of the granite mass by percolating through microfractures and grain boundaries, perhaps as a result of local hydrostatic pressure conditions, to form more massive zones of uranium enrichment such as zone 'A'. This could have taken place just prior to the deposition of the Upper Proterozoic sediments, or after, perhaps during diagenesis with fluids circulating along the unconformity. The presence of mineralization in Upper Proterozoic sediments (locality D) is indicative that at least some of the mineralization formed after the deposition of the supracrustals.

In the hydrothermal model, aqueous solutions of meteoric or juvenile derivation, perhaps heated by the cooling granite and circulating in convection cells, cause the deuteric alteration of the uranium-bearing minerals, transporting and redepositing the uranium in cooler parts of the granite mass. This could have occurred as a late magmatic phase or during a subsequent tectonically active period.

The proximity of the veins and zone 'A' to the Upper Proterozoic unconformity and the relatively simple element assemblage accompanying the uranium favours a supergene origin. On the other hand, sericitization of the wall rock and the presence of specular hematite may require higher temperatures than those that would normally prevail in the near surface environment. The increase in thorium in zone 'A' and in the altered granite, although slight, remains puzzling. However, considering the abundance of thorium in the source rock and the alteration of the thorite, it is possible that some thorium may have been redistributed with the uranium. Langmuir and Herman (1980) reviewed the conditions under which thorium may be mobilized by natural waters and point out that the formation of certain complexes may increase thorium mobility by several orders of magnitude.

The problem of the origin of the uranium concentrations associated with the eastern granite is a difficult one to resolve. The situation is not unlike that of northern Saskatchewan where several years of intense research have not yet settled the question. At Fury and Hecla, further work, planned or in progress, including isotopic analyses, age determinations, and thermometry may help elucidate this problem.

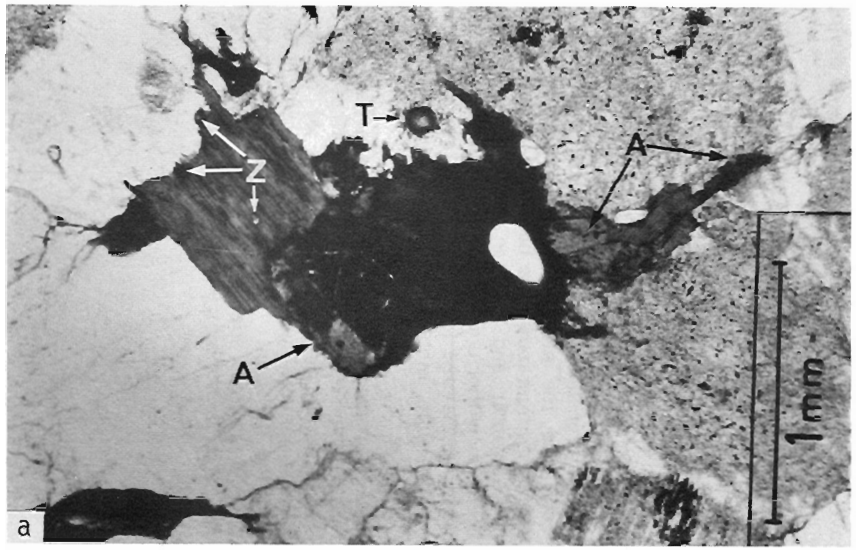

Plate 12.1a. *Photomicrograph showing allanite (A), thorite (T), and zircon (Z) associated with biotite in the eastern granite.*

Plate 12.1b. *Uranium distribution in the same field.*

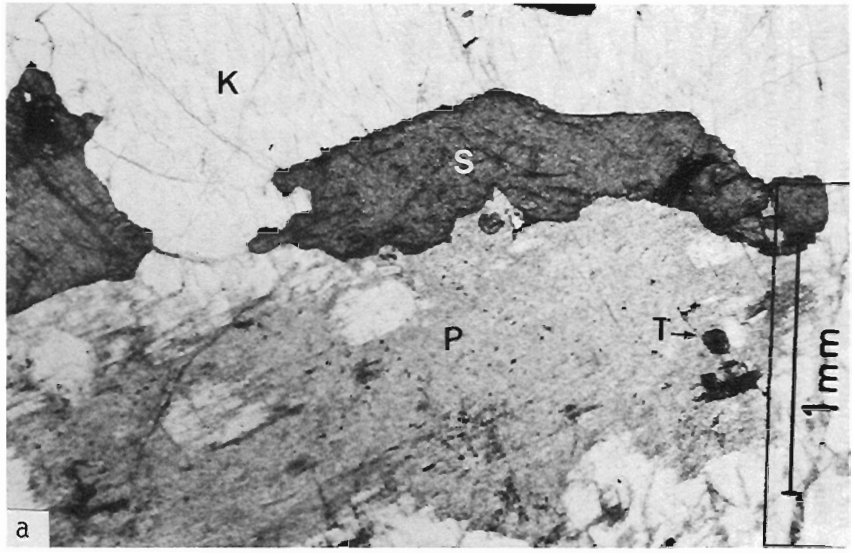

Plate 12.2a. *Photomicrograph showing sphene (S) and thorite (T) between grains of microcline (K) and sericitized plagioclase (P) in the eastern granite.*

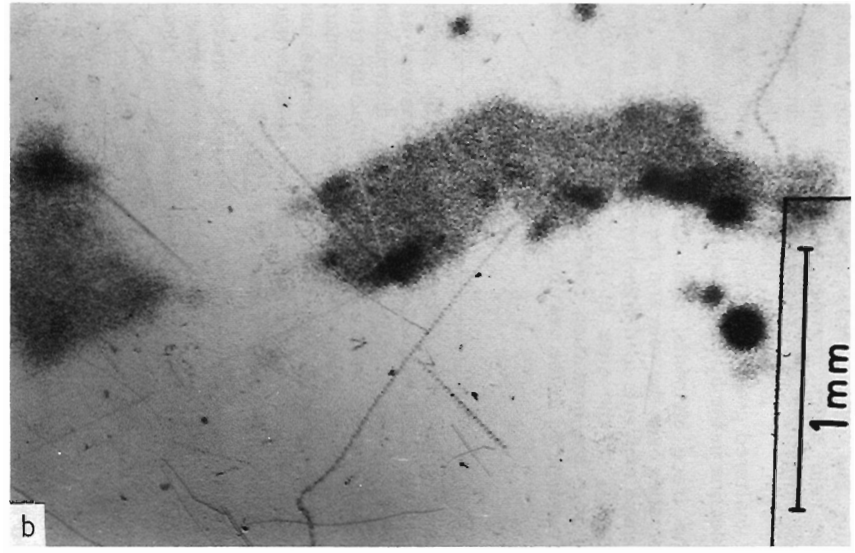

Plate 12.2b. *Uranium distribution in the same field.*

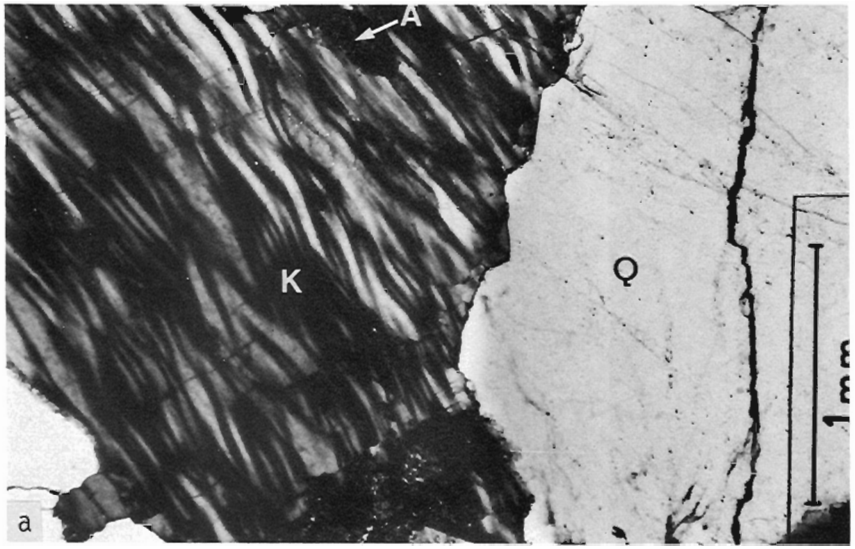

Plate 12.3a. *Photomicrograph (crossed nicols) showing microcline (K) enclosing a grain of allanite (A), and fractured quartz (Q) in zone 'A', eastern granite.*

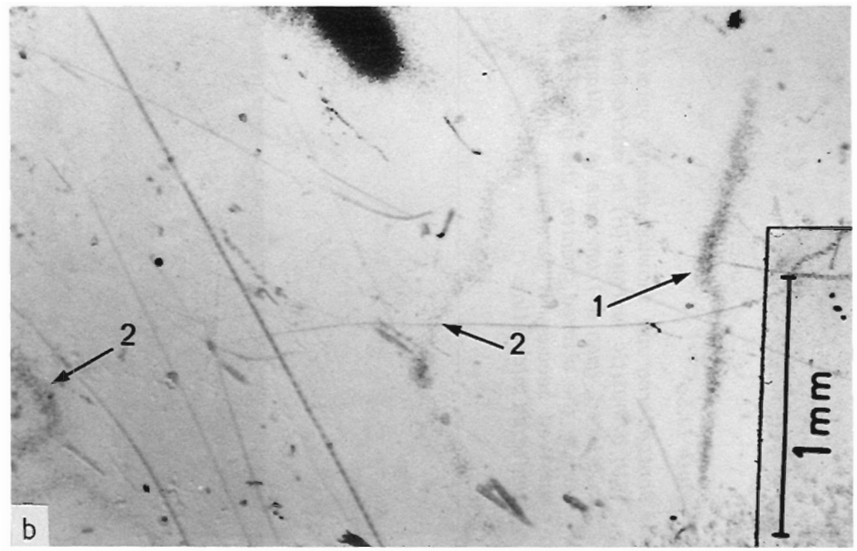

Plate 12.3b. *Uranium distribution in the same field. Note tracks along fracture across quartz grain (1) and along grain boundary (2).*

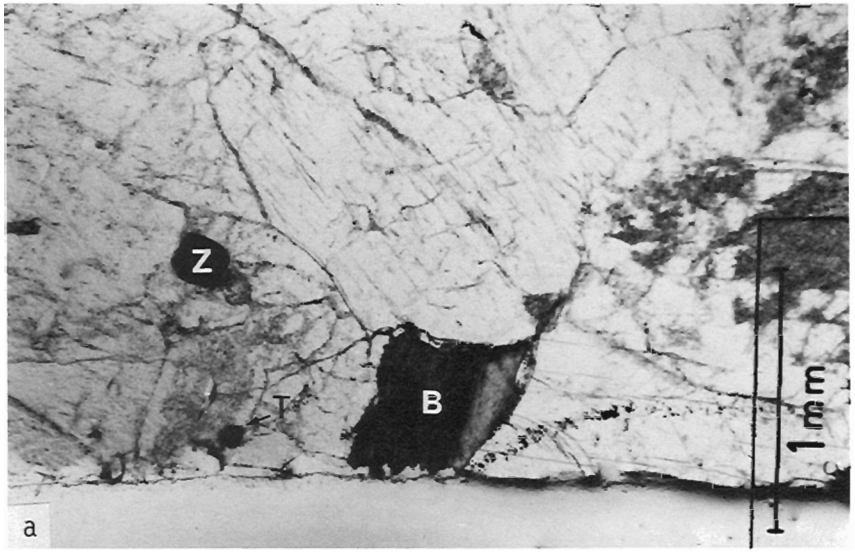

Plate 12.4a. *Photomicrograph showing biotite (B), thorite (T), and zircon (Z) in magnetite grain, with microcline and sericitized plagioclase in zone 'A', eastern granite.*

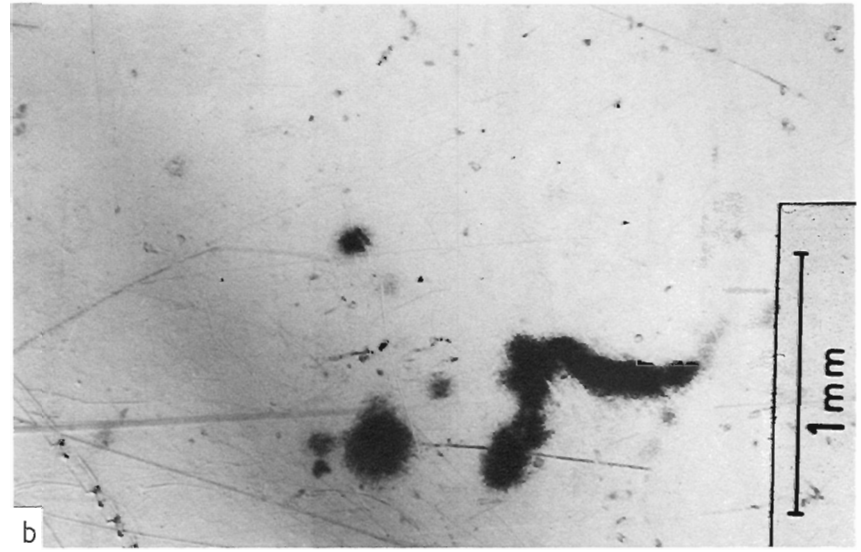

Plate 12.4b. *Uranium distribution in the same field. Note uranium enrichment along two margins of the biotite grain.*

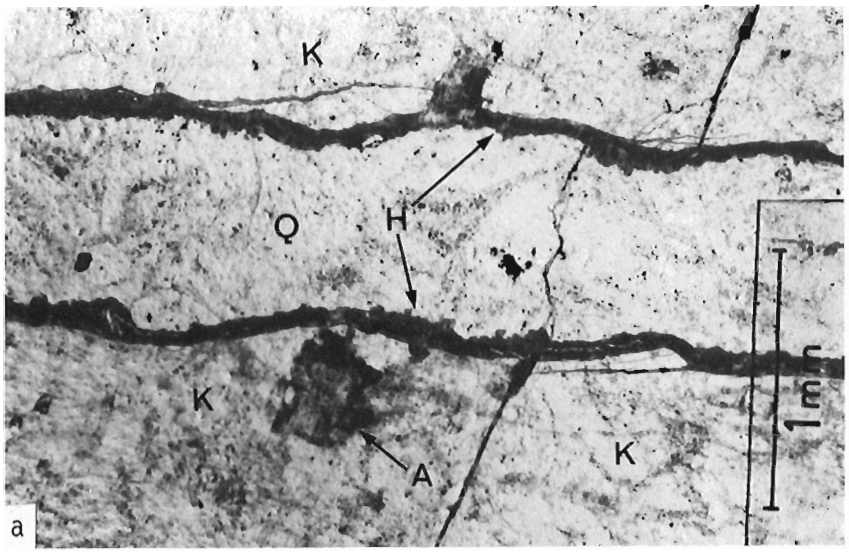

Plate 12.5a

Photomicrograph showing quartz veinlet (Q) with hematitic margins (H) in microcline (K) in altered granite from zone 'A'. Allanite is rare in the altered granite; the grain shown survived because it formed an inclusion in unaltered microcline.

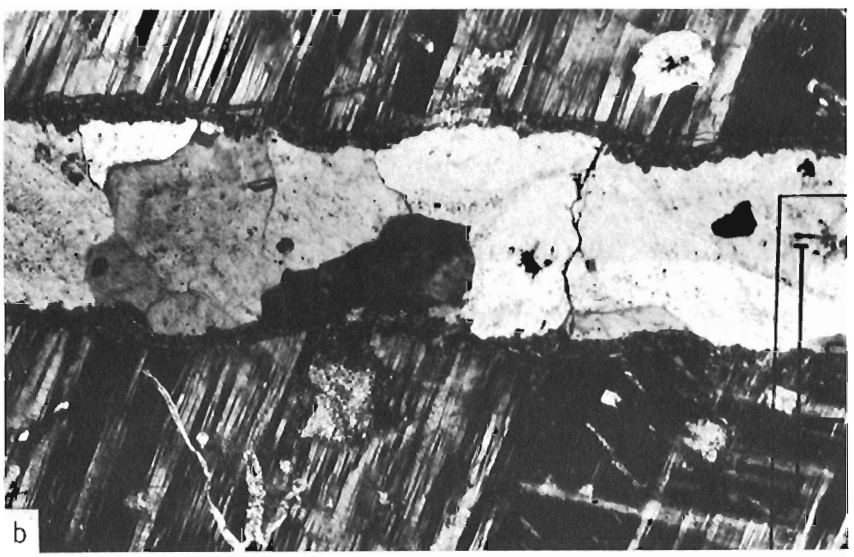

Plate 12.5b

The same field in crossed nicols.

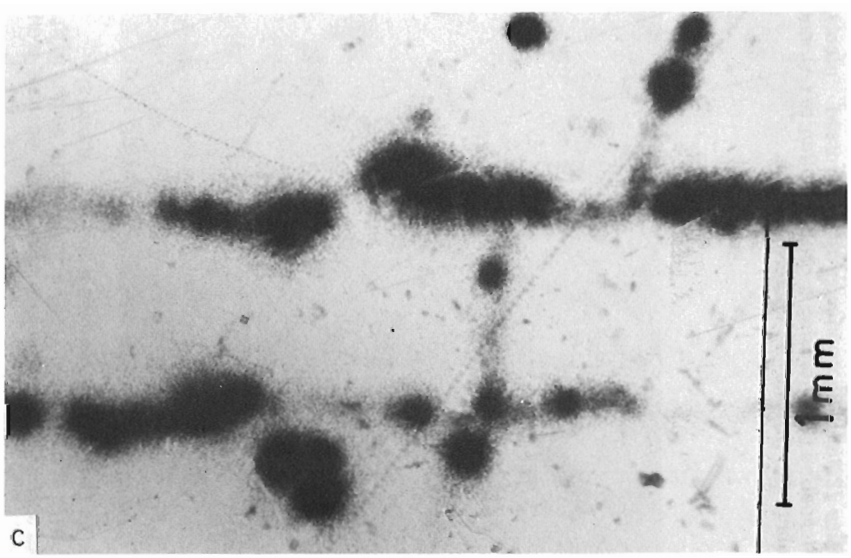

Plate 12.5c

Uranium distribution in the same field. Note uranium concentrations in the margins of the quartz veinlet and in fractures across both quartz and microcline.

Acknowledgments

The writer is indebted to Brian Charbonneau for allowing him to use the radiometric data shown in Figure 12.3 and to Al Littlejohn for performing microprobe analyses and many of the microscopic observations reported in this study. Moire Wadleigh is thanked for her enthusiastic and able assistance in the field.

References

Chandler, F.W., Charbonneau, B.W., Ciesielski, A., Maurice, Y.T., and White, S.
1980: Geological studies of the Late Precambrian supracrustal rocks and underlying granitic basement, Fury and Hecla Strait area, Baffin Island, District of Franklin; in Current Research, Part A, Geological Survey of Canada, Paper 80-1A, p. 125-132.

Chandler, F.W. and Stevens, R.D.
1981: Potassium-argon age of the Late Proterozoic Fury and Hecla Formation, northwest Baffin Island, District of Franklin; in Current Research, Part A, Geological Survey of Canada, Paper 81-1A, p. 37-40.

Ciesielski, A. and Maley, J.
1980: Basement of Agu Bay area and Gifford River area, Baffin Island, Northwest Territories; Geological Survey of Canada, Open File 687.

Geological Survey of Canada
1979: Agu Bay; Geophysical map no. 35647G.

Granier, C.L.
1973: Introduction à la prospection géochimique des gîtes métallifères; Masson et cie, Paris, 143 p.

Langmuir, D. and Herman, J.S.
1980: The mobility of thorium in natural waters at low temperature; Geochimica et Cosmochimica Acta, v. 44, p. 1753-1766.

Nockolds, S.R.
1954: Average chemical composition of some igneous rocks; Geological Society of America, Bulletin, v. 65, p. 1007-1032.

Ramaekers, P.P. and Dunn, C.E.
1977: Geology and geochemistry of the eastern margin of the Athabasca Basin; in Uranium in Saskatchewan, ed. C.E. Dunn; Saskatchewan Geological Society Special Publication 3, p. 297-322.

Rogers, J.J.W. and Adams, J.S.
1969: Uranium; in Handbook of Geochemistry, ed. K.H. Wedepohl; Berlin-Heidelberg – New York.

The Northern Miner
1980: Fury and Hecla uranium project could unearth new producing area; v. 65, no. 47, p. 4.

Thiel, K., Saager, R., and Muff, R.
1979: Distribution of uranium in early Precambrian gold-bearing conglomerates of the Kaapvaal craton South Africa: review of a case study for the application of fission track micromapping of uranium; Minerals Science and Engineering, v. 11, no. 4, p. 225-244.

13.

ANOMALY '60': A URANIFEROUS GRANITIC PLUTON ON MELVILLE PENINSULA, N.W.T.

Michel E. Delpierre[1]
Cominco Ltd.

Delpierre, M.E., Anomaly '60': a uraniferous granitic pluton on Melville Peninsula, N.W.T.; in Uranium in Granites, ed. Y.T. Maurice; Geological Survey of Canada, Paper 81-23, p. 115-118, 1982.

Abstract

The Proterozoic (Aphebian) Penrhyn Group in the Foxe Fold Belt in south-central Melville Peninsula, N.W.T. hosts numerous coarse grained to pegmatitic granitic plutons some of which show a definite enrichment in uranium with a few being significantly anomalous. Anomaly '60' is caused by a strongly radioactive pegmatitic granite intrusion that occurs at the base of the Penrhyn metasediments which rest unconformably on Archean gneisses. The granite is both discordant and concordant with the Proterozoic country rocks (marbles and paragneisses) and exhibits ghost layering at numerous localities. Uranium mineralization as uranophane and other secondary minerals sometimes forming pseudomorphs after uraninite appears to show a strong association with biotite accumulations. Thorium is variably present and may exceed the uranium content. Results from rock geochemistry, ground radiometry, detailed prospecting and a diamond drill program of six short holes conducted in 1979, indicate that although some ore grade mineralization occurs over short sections, the low grade and tonnage potential coupled with logistical difficulties, makes this 'porphyry uranium' occurrence uneconomic at present.

Résumé

Les roches du groupe de Penrhyn d'age Protérozoique (Aphébien) appartenant à la ceinture plissée de Foxe dans le centre-sud de la presqu'île de Melville, T.N.O., sont hôtes de nombreuses intrusions granitiques, allant des roches à grain grossier aux roches pegmatitiques; quelques-unes présentent un enrichissement en uranium et certaines en contiennent des concentrations importantes. L'anomalie '60' est causée par une roche intrusive granitique pegmatitique, fortement radioactive, qui se trouve à la base des roches sédimentaires partiellement métamorphisées de Penrhyn qui reposent de façon discordante sur les gneiss Archéens. Le granite est à la fois discordant et concordant avec les roches encaissantes (marbres et paragneiss) du Protérozoique et présente des couches 'fantômes' à plusieurs endroits. La minéralisation en uranium sous forme d'uranophane et d'autres minéraux secondaires qui forment parfois des pseudomorphes après l'uraninite semble être fortement associée aux accumulations de biotite. La concentration de thorium est variable et excède parfois celle de l'uranium. Les résultats obtenus à partir de la géochimie des roches, de la radiométrie au sol, de la prospection détaillée et d'un programme de forage au diamant de six petits trous effectué en 1979, indiquent que, bien que certaines sections courtes contiennent des teneurs élevées, la faible teneur en général et le faible potentiel de tonnage, en plus des difficultés logistiques, font que cette occurrence d'uranium 'porphyrique' n'est pas économique à l'heure actuelle.

Introduction

In 1978 Cominco Ltd. reassessed all the radiometric data available for Melville Peninsula and checked several regionally anomalous zones using lake water geochemistry, followed up by close spaced airborne radiometry to delineate the anomalous zones more precisely. A similar approach, on a larger scale, was used in 1979 to cover Cominco's holdings which numbered just under 4000 claims (staked in 1978), and other potential areas identified on reconnaissance lake sediment and water geochemical maps by the Geological Survey of Canada (1978a, b). A more sophisticated spectrometric system was used to fly about 2300 line km and was successful in locating 37 significantly anomalous zones which were all ground checked and sampled. Without exception these zones were all related to granitic plutons. Anomaly '60' is a typical example located in the south-central part of Melville Peninsula, N.W.T. at latitude 67°10'32"N and longitude 83°52'06"W.[2]

Geology and Mineralization

The Foxe Fold Belt in which Anomaly '60' occurs (Fig. 13.1), comprises an ENE trending belt of Archean and Proterozoic metasediments and plutonic rocks that extends from southern Melville Peninsula to central Baffin Island, a distance of about 700 km. On Melville Peninsula, the metasediments known as the Penrhyn Group (2500-1800 Ma), unconformably overlie the Archean gneisses, and have undergone polyphase deformation and metamorphism during the Hudsonian Orogeny. The intrusive relationships of the plutonic rocks suggest emplacement before, during and after this tectonism. The Penrhyn rocks have been mapped by Heywood (1967) and later by Henderson et al., (1976) and Okulitch et al., (1977a, b, 1978).

The Archean rocks predominantly comprise grey to orange weathering, tan, white to pink, medium- to coarse-grained biotite and hornblende granodiorite to quartz

[1] 409 Granville Street, Vancouver, B.C. V6V 1T2

[2] The airborne radiometric survey carried out under the Federal Uranium Reconnaissance Program indicated an anomaly of 5.5 ppm eU over a background of 2 to 3 ppm eU in this region (Geological Survey of Canada, 1978c, profile line 4070).

monzonite gneiss. Well developed foliation is common. The basement has been intruded by large plutonic masses which have close compositional similarities with the hosting gneisses resulting in subtle contacts recognized more on regional evidence than on outcrops.

Generally, the base of the Penrhyn is represented by grey to white, relatively clean, recrystallized glassy orthoquartzites which rest on scarce lenticular occurrences of feldspathic metaregolith not noticed around Anomaly '60'. Overlying the orthoquartzite is a white, coarse grained massive to bedded marble unit with very minor biotite paragneiss. Calc-silicate gneisses and marble-quarzite units overlie the marble in a gradational contact passing into predominantly brown to grey, rusty, fine- to medium-grained quartz-feldspar-biotite paragneisses often with garnet and graphite. The relationship between these two major units, as well as their original thicknesses, is totally obliterated by deformational thinning, repetition by folding and dilation by syntectonic plutonism. Correlations are rendered difficult and evidence of the angular discordance at the base of the Penrhyn is effaced. Metamorphism is in the upper amphibolite facies.

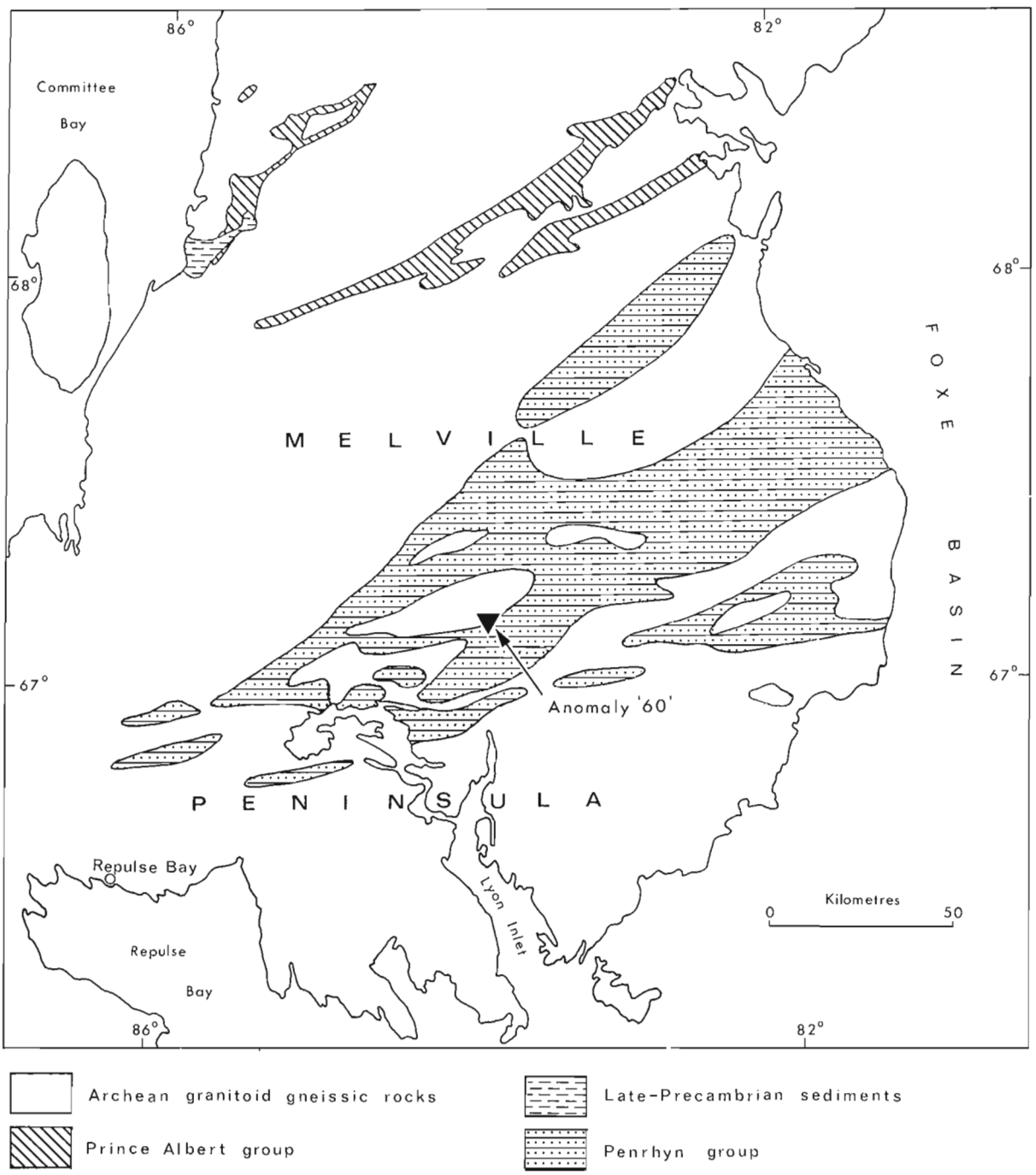

Figure 13.1. *Geology of southern Melville Peninsula and location of Anomaly '60'.*

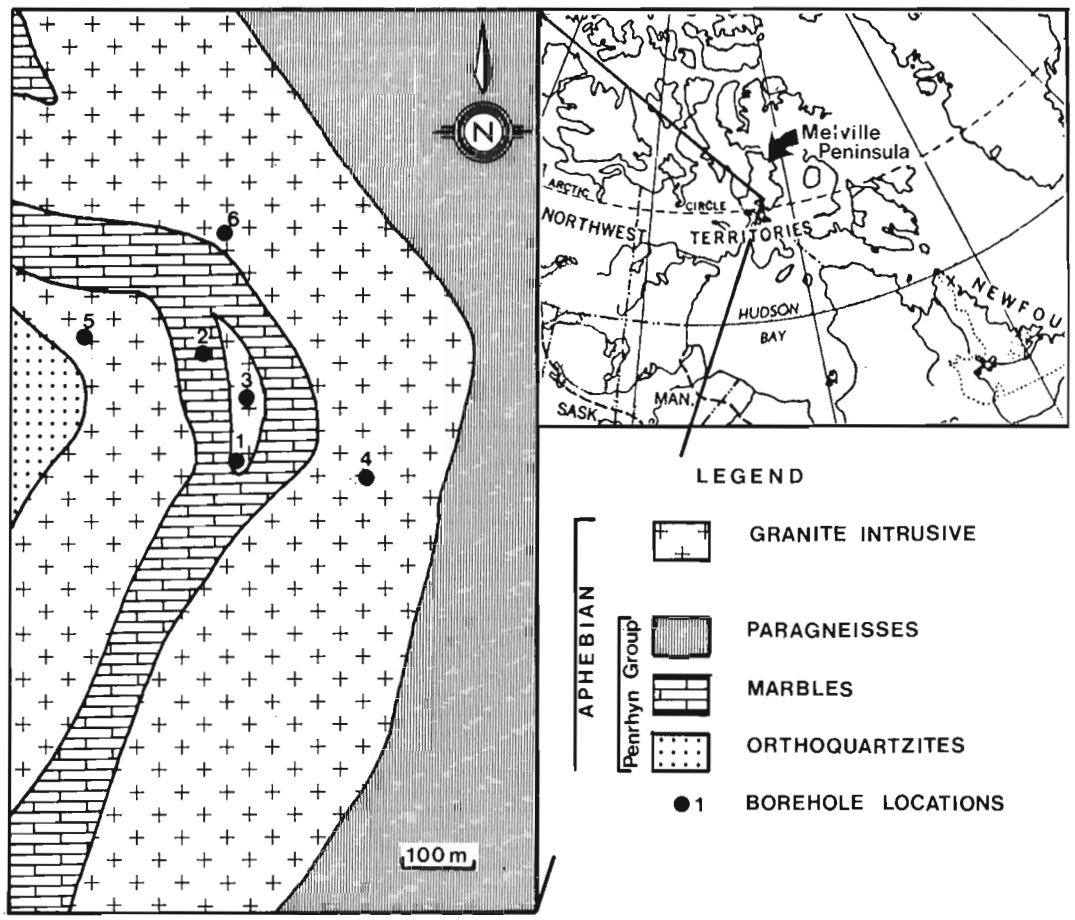

Figure 13.2. *Anomaly '60': generalized geology and borehole locations.*

The granitic rocks intrude both the basement and the Penrhyn as large masses, thick sills and dykes. Numerous screens and xenoliths of basement gneiss, contorted marble and paragneiss occur within the plutons. Mostly they are pink to tan, coarse grained granodiorite to quartz monzonite, locally foliated but generally massive. Some of the granites show porphyroblastic textures suggesting a formation by late syntectonic fusion and recrystallization of pelitic gneiss. A significant number of these plutons show pegmatitic phases that are enriched in uranium.

Figure 13.2 shows the generalized geology of the property. Anomaly '60' is almost entirely underlain by a granitic pluton that intrudes the Archean basement and orthoquartzites, marbles and biotite paragneisses of the Penrhyn Group.

Fieldwork consisted of detailed mapping on a scale of 1:2 000 over an area of 1 km^2 covering the entire zone of interest. A ground spectrometric survey was conducted over this area which was also minutely prospected. In addition, rock sampling on 100 m centres was carried out and a total of 195 m in 6 holes were drilled to test the at-depth potential for uranium concentrations and attempt to construct the geometry of the radioactive unit. The location of the boreholes is shown in Figure 13.2.

Fresh samples show that the generally massive, locally foliated intrusion ranges from pink to grey. It weathers to an orange-buff. Petrologically the rock varies from a medium- to coarse-grained biotite granodiorite to a granite with an average modal composition of approximately 35% plagioclase, 35% K-feldspar, 25% quartz, 4% biotite and 1% muscovite. The feldspars occur as euhedral to anhedral grains up to 5 mm in size with occasional megacrysts up to 10 mm set in a granular quartz groundmass (0.1-2 mm grain size). Graphic intergrowths are common, as are clots of biotite measuring several millimetres in diameter. Iron oxides are present and probably result from the alteration of mafic minerals. Accessory minerals include apatite, garnet, chlorite, xenotime, zircon, sphene, monazite, tourmaline, magnetite and molybdenite. The intrusion which may well be multiphased, exhibits a strong, well defined tabular character. It appears to have a 'boxwork' type structure with both vertical dyke-like bodies and thick to thin coalescing, concordant and disconcordant sills. Large screens and xenoliths of generally strongly folded marble and paragneiss are present in the igneous rocks. Although the granite is pervasive throughout the entire Penrhyn stratigraphy on the property as thin units, a thicker development of the intrusive is found at both the orthoquartzite-marble and marble-paragneiss interfaces.

The ground radiometric survey delineated several zones of high radioactivity caused by both uranium and thorium, and invariably associated with zones of biotite enrichment. The drilling program tested the sills at several locations over an approximate true thickness of 120 m (assuming a 20° dip). Although detailed interpretation of the structure is not possible at this stage, the results suggest that radioelement enrichment occurs in narrow discontinuous biotite

concentrations that make up to 25 per cent of the rock and that these are not correlatable stratigraphically. The better intersections in the granite averaged 0.02 per cent U_3O_8 over a 9 m true vertical thickness. Individual intersections ranged from traces to 0.077 per cent U_3O_8 over 1.22 m. A minor occurrence of remobilized uranium was found in a shear zone in borehole number 2 (Fig. 13.2).

The uranium/thorium ratio is generally greater than 1 and in the better intersection, ranges from 0.9 to 5.6 averaging about 3.0. The uranium minerals found are all secondary (uranophane was identified) sometimes forming cubic pseudomorphs after uraninite.

Conclusion

The generally sporadic nature and overall low grade of the uranium mineralization encountered on Anomaly '60', coupled with a restricted tonnage potential and severe logistical difficulties, make this uranium prospect uneconomic at present.

References

Geological Survey of Canada
1978a: National Geochemical Reconnaissance Release, regional lake sediment and water geochemical reconnaissance data, Melville Peninsula, N.W.T.; NGR 32A-1977 or 32B-1977, NTS 46N and part of 47B; Geological Survey of Canada, Open File 521A or 521B.

1978b: National Geochemical Reconnaissance Release, regional lake sediment and water geochemical reconnaissance data, Melville Peninsula, N.W.T.; NGR 33A-1977 or 33B-1977, NTS 46O, P and part of 47A; Geological Survey of Canada, Open File 522A or 522B.

Geological Survey of Canada (cont.)
1978c: Barrow River, District of Franklin, Northwest Territories; Geophysical Series Map no. 36546G.

Henderson, J.R., Reesor, J.E., Le Cheminant, A.N., Hutcheon, I.E., and Miller, A.
1976: Geological maps of Penrhyn Group, Melville Peninsula, N.W.T. (1:50 000 scale); Geological Survey of Canada Open File 307.

Heywood, W.W.
1967: Geological notes, northeastern District of Keewatin and southern Melville Peninsula, District of Franklin, Northwest Territories (Parts of 46, 47, 56, 57); Geological Survey of Canada, Paper 66-40, 20 p.

Okulitch, A.V., Gordon, T., Henderson, J.R., Reesor, J.E., and Hutcheon, I.E.
1977a: Geology of the Barrow River map area, Melville Peninsula, District of Franklin; in Report of Activities, Part A, Geological Survey of Canada, Paper 77-1A, p. 213-215.

1977b: Geology of the south half of Barrow River map area (46 O, P), N.W.T. (1:50 000 scale); Geological Survey of Canada Open Files 433 to 443.

Okulitch, A.V., Gordon, T., Henderson, J.R., Hutcheon, I.E., and Turay, M.
1978: Geology of the Barrow River and Hall Lake map areas, Melville Peninsula, District of Franklin; in Current Research, Part A, Geological Survey of Canada, Paper 78-1A, p. 159-161.

14.

AIRBORNE RADIOMETRIC ANOMALIES CAUSED BY LATE KINEMATIC GRANITIC ROCKS IN THE MOLSON LAKE-RED SUCKER LAKE AREA, EAST-CENTRAL MANITOBA

Werner Weber[1], David C.P. Schledewitz[1], and Nashir M. Soonawala[2]
Manitoba Mineral Resources Division

Weber, W., Schledewitz, D.C.P., and Soonawala, N.M., Airborne radiometric anomalies caused by late kinematic granitic rocks in the Molson Lake-Red Sucker Lake area, east-central Manitoba; in Uranium in Granites, ed. Y.T. Maurice; Geological Survey of Canada, Paper 81-23, p. 119-124, 1982.

Abstract

Recent geological mapping with simultaneous ground gamma ray spectrometer surveys in an area with a chain of airborne radiometric anomalies of greater than 2 ppm eU indicate uranium enrichment in late kinematic (late Kenoran?) pink leucogranitic rocks including granites, alaskites, and syenites which form dykes, stocks and small plutons in a batholithic tonalite – granodiorite complex.

Field geological evidence suggests that the potassium-rich rocks were formed by hydrothermal solutions and that at least some of them are metasomatic replacement bodies.

Results of a geophysical grid survey over a pronounced anomaly indicate that it is caused by a significant volume of leucogranitic rocks with an unusually high background concentration of uranium averaging 25 ppm eU. The uranium seems to be associated with hematite which coats mineral grains and fills small fractures.

Résumé

Une cartographie géologique récente et des relevés connexes par spectrométrie de rayons gamma, effectués dans une région comportant une chaîne d'anomalies radiométriques aéroportées de plus de 2 ppm d'eU, indiquent un enrichissement en uranium des roches roses leucogranitiques tardives (de la fin du Kénora?) comprenant des granites, des alaskites, et des syénites, qui forment des dykes et de petits intrusifs dans un complexe batholitique formé de tonalites et de granodiorites.

Des preuves géologiques permettent de croire que des roches riches en potassium ont été formées par des solutions hydrothermales et qu'au moins quelques-unes d'entre elles sont d'origine métasomatiques.

Les résultats d'une étude géophysique par méthode de quadrillage sur une anomalie prononcée indiquent qu'elle est causée par un volume important de roches leucogranitiques ayant une teneur de fond anormalement élevée en uranium, atteignant en moyenne 25 ppm d'eU. L'uranium semble être associé à l'hématite qui recouvre les minéraux et remplit les petites fractures.

Introduction

The Uranium Reconnaissance Program (URP; Darnley et al., 1975) conducted between 1975 and 1977 and covering most of Manitoba's Precambrian, outlined in that province three main areas with eU greater than 2 ppm; a) northwestern Manitoba; b) southeastern Manitoba and c) east-central Manitoba.

The anomalies in northwestern Manitoba lie in the Wollaston Fold Belt and have been evaluated since 1975 by various means including drilling (Soonawala et al., 1979). Hudsonian leucogranite stocks which intrude Aphebian metasedimentary rocks (Weber et al., 1975) are characterized by high U contents and high U/Th ratios, whereas Hudsonian granite batholiths display high U and Th contents, but low U/Th ratios. Archean granites have variable U content and consistently low U/Th ratios. Uranium enrichment is most prominent in Hudsonian leucogranites. The highest concentration drilled was 0.1 per cent U over 1 m (Soonawala et al., 1979). Uranium is present as uraninite, generally associated with biotite. The mineralization is too erratic to be of economic value at present (Soonawala et al.,1979). As in the case of the uraniferous pegmatites in the Wollaston belt in Saskatchewan, the uranium is thought to have been mobilized from uranium-enriched metasediments overlying an Archean granitoid crust. This crust is the primary source of the uranium.

The airborne radiometric anomalies in southeastern Manitoba are related to uraniferous pegmatites in the English River Subprovince, similar to those described by Breaks (1982) in Ontario.

In east-central Manitoba, the anomalies form a distinct chain between the Cross Lake-Red Sucker Lake and the Stevenson Lake-Island Lake greenstone belts, in a granitoid terrane which was poorly known before it was mapped in 1979 and 1980.

Based on our previous experience with URP anomalies and on the basis of a reconnaissance geological survey (Soonawala, 1978) it was tentatively assumed that these anomalies were probably related to leucogranites similar to those in northwestern Manitoba. It was thus decided to undertake a geological mapping project to study the area between latitude 54°N and the Cross Lake-Red Sucker Lake

[1] 993 Century Street, Winnipeg, Manitoba R3H 0W4
[2] Now with Atomic Energy of Canada Ltd., Whiteshell Nuclear Research Establishment, Pinawa, Manitoba. R0E 1L0

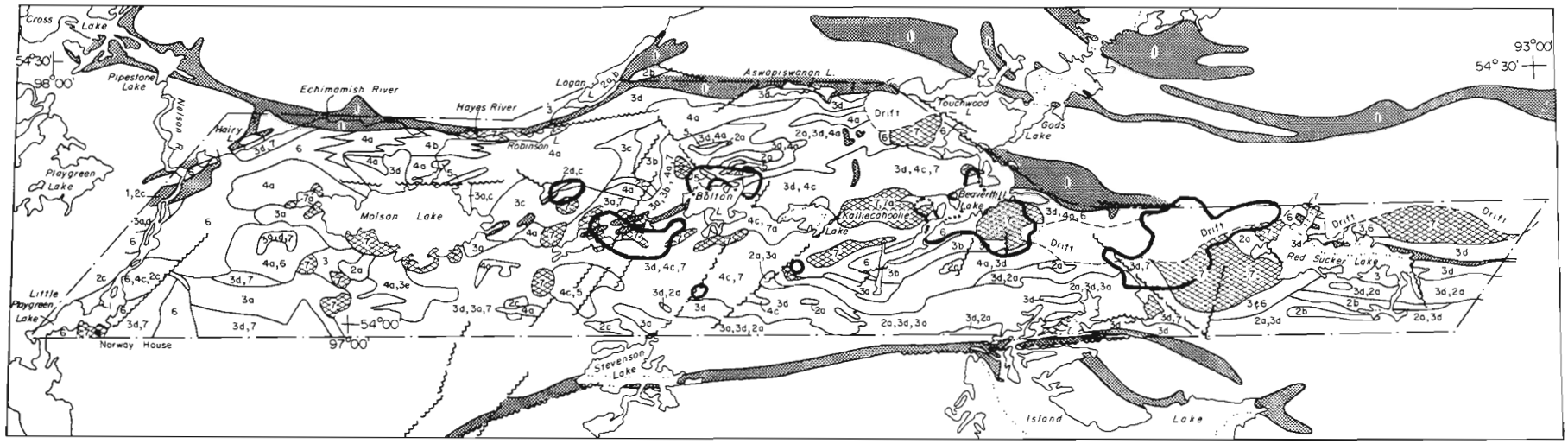

Late – tectonic Granite

Metavolcanic and Metasedimentary Rocks (Greenstones)

URP Anomaly > 2ppmeU

Miles
10 0 10 20 30 40
10 0 10 20 30 40 50 60
Kilometres

Fault

Geological contact

Boundary of Molson Lake – Kalliecahoolie Lake Project

Figure 14.1. *Geology of the Molson Lake Area, east-central Manitoba, compiled from preliminary maps (Schledewitz, 1980; Weber and Chase, 1980), and showing URP anomalies >2 ppm eU (Geological Survey of Canada, 1978). The rock units are numbered as in Table 14.1.*

greenstone belt (Weber and Schledewitz, 1979, 1980). One prominent anomaly was evaluated in detail with a gamma ray spectrometer, a magnetometer, and a very low frequency electromagnetic survey on a grid of about 1 km^2 (Soonawala, 1979).

Geology

With the exception of the western and eastern margin, the area is underlain by well exposed bedrock (up to 80 per cent exposure). Table 14.1 lists the main rock units; the geological map (Fig. 14.1) shows their distribution, and Table 14.2 indicates the recognized geological events.

The supracrustal rocks in unit 1 make up the discontinuous greenstone belt along the northern margin of the area. They also form a chain of lenses from Aswapiswanan Lake towards Molson Lake and Little Playgreen Lake, obviously representing the remnants of a once more continuous west-southwest-trending belt of supracrustal rocks.

Tonalitic gneiss, amphibolites and migmatites (unit 2a, b, c), intruded by tonalites (unit 3), occur predominantly on the flank of the supracrustal belts. The amphibolites appear to be higher metamorphosed equivalents of the metabasalts in unit 1.

Tonalitic plutons (unit 3), comprising various phases (unit 3a, b, c, d, e), and slightly younger granodiorite batholiths (unit 4a), and related units (unit 4b, 4c), underlie about 70 per cent of the area. Leucogabbro and quartz diorite of unit 2c are petrographically similar to unit 3a and probably represent a more basic phase of the plutons. Hornblende in units 3a and 3b shows evidence that it was derived from an original pyroxene. Whereas the tonalites (unit 3) are spatially and genetically closely related to rocks of unit 2 (and unit 1), the megacrystic granodiorites (unit 4) occupy the core of the granitoid terrane between the supracrustal belts.

Recrystallized gabbroic and diabasic dykes (unit 5) are widespread between Molson Lake and Joint Lake. Compositionally, these dykes are similar to the Molson dykes (Scoates and Macek, 1978). Primary structures, such as igneous differentiation, chilled contacts, and primary textures are preserved. The mineralogy is largely recrystallized, however, in contrast to the fresh Molson dykes. The dykes of unit 5 are weakly deformed or cataclastic in places and they may be intruded by rocks of units 7 and 8. It is tentatively assumed that these dykes intruded during a tensional tectonic event (with the majority of the dykes striking in approximately east-northeast direction) which was active probably between 2.7 and 2.5 Ga ago.*

The late granitic rocks include grey-pink metasomatic gneisses (unit 6) which are mainly derived from tonalitic gneisses (unit 2a), pink granite stocks (unit 7) and dykes of pink granite (unit 7), alaskite, pegmatite, aplite and syenite (unit 8). Many of these rocks possess an irregularly developed, distinctly red hematite stain particularly pronounced in the inequigranular alaskite.

Many of the granitic dykes seem to be replacement bodies formed by hydrothermal, increasingly potassium-rich solutions. Associated potassium metasomatism also resulted in lit-par-lit granitic veining and in the growth of interstitial and porphyroblastic potassium feldspar, locally and over large areas.

The major period of deformation and metamorphism (D_1, M_1) preceded the emplacement of the granodiorite batholiths. A second, milder period of deformation and metamorphism (D_2, M_2) coincided approximately with the intrusion of the late granites. A period of dominantly east-trending shearing is contemporaneous with, or postdates, the intrusion of unit 8, but predates the Molson swarm. This shearing is most prominent along the margins of the greenstone belts. An even younger period of faulting strikes in a NNE direction and forms very distinct lineaments, visible on airphotographs, in the granitoid terrane east of Molson Lake.

Table 14.1. Table of Formations, Molson Lake Area

Map unit		
PRECAMBRIAN		
Proterozoic		
	9*	Gabbro and diabase dyke (Molson Swarm)
Archean		
		Late Granitic Rocks (7, 8)
	8	Alaskite, aplite, pegmatite, syenite
	7	Granite, leucogranite, pink, medium- to coarse-grained, massive, locally prophyritic; 7a, white granite.
	6	Hybrid gneiss: porphyritic granodiorite and tonalitic gneiss with mafic inclusions and pink granite sills and dykes.
	5*	Metagabbro dyke
		Early Plutonic Rocks
	4a	Megacrystic granodiorite
	4b	Porphyroclastic and/or gneissic granodiorite, augen gneiss
	4c	Medium- to coarse-grained granodiorite
	4d	White pegmatite
	3a	Medium- to coarse-grained hornblende (biotite) tonalite to granodiorite, partly porphyritic
	3b	Coarse biotite-hornblende monzonite
	3c	Biotite tonalite to granodiorite (metasomatized tonalite)
	3d	Leucotonalite
	3e	Porphyroblastic granodiorite
		Supracrustal and Metamorphic Rocks, Migmatites
	2a	Tonalite, tonalitic gneiss, minor amphibolite (up to 20%), flaser gneiss with minor amphibolite
	2b	Tonalite, tonalitic gneiss inter-layered with amphibolite (20-50%)
	2c	Leucogabbro, quartz diorite, gabbro, amphibolite, generally with agmatitic or lit par lit leucosome
	2d	Magnetiferous quartzofeldspathic gneiss
	1	Metavolcanic and related intrusive rocks, metasedimentary rocks

*not shown on map, Figure 14.1.

* The time frame is based on correlations with similar, but radiometrically dated units in the northwestern Superior Province (Weber and Scoates, 1978).

Table 14.2. Geological events in the Molson lake area

Intrusions, extrusions, depositon	Structure, metamorphism
	Phase IV
Diabase to gabbro dykes of the Molson Swarm	
	Phase III
Late kinematic granites, alaskites, aplites and pegmatites, syenites	D_2 - Major shearing along northwesterly and easterly trends; asymmetric folds vary from open to moderate closure with localized isoclinal upright to steeply overturned folds, with resultant narrow shear zones in areas of tight folding.
	M_2 - Lower to middle amphibolite facies metamorphism in the gneiss terrane. - Potassium metasomatism - Contact metamorphism
	S_2 - Gneissosity to metamorphic layering in narrow shear zones. - Cataclastic foliation - Platy quartz, biotite and amphibole realignment
Gabbro dykes	
Granodiorite dykes	
	Phase II
Granodiorite batholiths, sills and lit-par-lit injections	D_1 - Structure and style within the metavolcanic suite uncertain, considered to be open folds and faulting; within the tonalite gneiss and migmatite, structures are typified by easterly-trending antiforms with moderate plunge and synforms which are upright isoclinal folds of variable plunge.
Tonalite, quartz diorite, monzonite, leucotonalite	M_1 - Greenschist (to amphibolite) facies metamorphism in supracrustal rocks. - Amphibolite facies metamorphism in tonalitic gneiss zones.
	S_1 - Gneissosity and metamorphic layering in tonalite complex.
	Phase I
Clastic sediments*	
Unconformity	
Feldspar porphyry	
Gabbro and ultramafic sills and dykes	
Mafic flows, minor felsic flows, volcanogenic sediments	

* Relationship between clastic sedimentary rocks and intrusive rocks of Phase II is not exposed. Clastic sedimentary rocks might be younger than Phase II (as e.g. in the Island Lake greenstone belt).

Evaluation of the Airborne Anomalies

In addition to the URP anomalies shown in Figure 14.1, the distinct U and U/Th peaks on the individual flight lines were also considered during the evaluation of the airborne survey.

The geological mapping indicated that airborne anomalies and individual peaks coincide generally with areas containing a high percentage of rocks of units 7 and 8. Spectrometer readings, using an Exploranium GR-310 unit, obtained during the geological mapping program, also indicated that eU contents of these rocks, alaskite and syenite in particular, were higher (mean of 13 ppm eU) than for other granitoid rocks (granodiorite, tonalite: mean of 6 ppm eU).

The late kinematic potassic rocks also yielded more frequent and higher, anomalous readings (up to 50 ppm eU). The highest values tend to be localized along fractures.

Two hundred and fifty-three gamma ray spectrometer readings taken over an anomaly (greater than 4 ppm U) near Beaver Hill Lake (Soonawala, 1979*) indicate a bimodal uranium distribution with a background population of around 8 ppm eU (which is about 4 ppm over the normal content for granitic rocks) and an anomalous population of around 25 ppm eU (Fig. 14.2). The thorium histogram is possibly bimodal with a primary grouping around 35 ppm, and a second at about 65 ppm. The uranium-thorium coefficient of correlation at 0.370 is small but still noticeable. Soonawala (1979) concluded that the URP anomalies are caused by a significant volume of granitic rocks having a uranium content of around 25 ppm.

The distinctly pink colour and commonly associated red stain of the late kinematic potassic rocks is caused by hematite which coats mineral grains, fills small hairline fractures and is often associated with altered biotite.

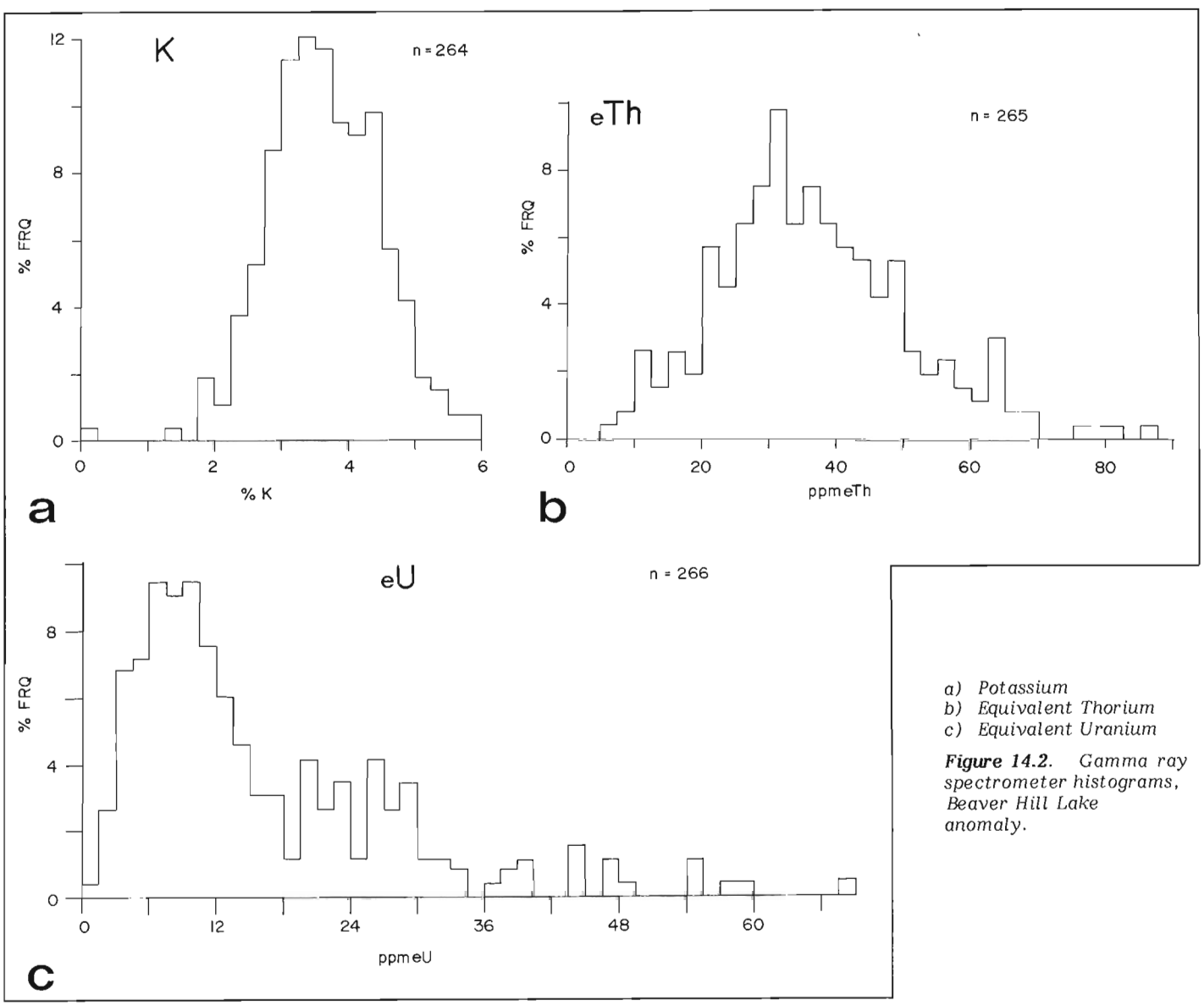

a) *Potassium*
b) *Equivalent Thorium*
c) *Equivalent Uranium*

Figure 14.2. *Gamma ray spectrometer histograms, Beaver Hill Lake anomaly.*

* The URP anomaly with amplitude exceeding 4 ppm equivalent uranium was accurately located by broad-band helicopter scintillometer survey with 0.5 km line spacing (Soonawala, 1978) and subsequently investigated on the ground by a gamma ray spectrometer, a magnetometer, and VLF-EM survey on a geophysical grid with 50 m line spacing (Soonawala, 1979).

Preliminary results of mineralogical studies suggest that radiograph 'hot spots' from polished sections of the uranium-enriched granitoid rocks of the Beaver Hill Lake anomaly are spatially related to hematite which in turn is commonly associated with biotite. In addition, radiograph 'hot spots' from thin sections were produced by synchysite (Ca Ce $(CO_3)F$)* associated with hematite in hornblende tonalite (unit 3a) and by meta-autunite II* in a granite dyke (unit 7). Both minerals are similar to allanite under the microscope.

Alteration of such radioactive carbonates and silicates, and subsequent migration during hydrothermal metasomatic activity might have lead to the observed uranium enrichment in late kinematic granitic rocks (units 7 and 8).

The association of uranium enrichment with late kinematic granites (unit 7) is obvious from the contoured URP maps (Geological Survey of Canada, 1978), especially when the anomalies of greater than 1 ppm eU are considered. Thus, values higher than 1 ppm eU must represent a greater enrichment which might include supergene enrichment in favourable structures, e.g. north-northeast-trending fractures, or east-trending S_2 shear zones.

In part, URP anomalies of greater than 2 ppm eU might also reflect an abundance of granite detritus of unit 7 and 8 in drift cover or boulder fields, e.g. west of Red Sucker Lake. With the exception of minor uranium bloom along a fracture, no uranium mineralization was discovered during the mapping program. More detailed follow-up is required to test possible sites for uranium enrichment to fully evaluate the URP anomalies.

* X-ray determination by K. Albino, Mineralogical-Petrographical Laboratory, Geological Services Branch.

References

Breaks, F.W.
1982: Uraniferous granitoid rocks from the Superior Province of northwestern Ontario; in Uranium in Granites, ed. Y.T. Maurice; Geological Survey of Canada, Paper 81-23, report 8.

Darnley, A.G., Cameron, E.M., and Richardson, K.A.
1975: The Federal-Provincial Uranium Reconnaissance programs; in Uranium Exploration 1975; Geological Survey of Canada, Paper 75-26, p. 49-68.

Geological Survey of Canada
1978: Canada/Manitoba Uranium Reconnaissance Program, Geophysical Series, Airborne Gamma-Ray Spectrometric Maps 35963 G (Cross Lake), 36153G (Oxford Lake), 36253G (Stull Lake).

Schledewitz, D.C.P.
1980: Manitoba Mineral Resources Division, Preliminary Maps 1980K-3 (Oxford House, Southwest), 1980K-4 (Oxford House, Southeast), 1980K-5 (Stull Lake, Southwest).

Scoates, R.F.J. and Macek, J.J.
1978: Molson Dyke Swarm; Manitoba Mineral Resources Division, Geological Paper 1978-1.

Soonawala, N.M.
1978: Regional Geophysical Surveys; in Manitoba Mineral Resources Division, Report of Field Activities 1978, p. 70-82.

1979: Geophysical Investigations; in Manitoba Mineral Resources Division, Report of Field Activities 1979, p. 55-67.

Soonawala, N.M., Garber, R.D., and Whitworth, R.A.
1979: Follow-up of the Uranium Reconnaissance program in Northwest Manitoba; Canadian Mining and Metallurgical Bulletin, Volume 72, no. 804, p. 83-94.

Weber, W. and Chase, K.
1980: Manitoba Mineral Resources Division, Preliminary Maps 1980K-1 (Molson Lake, East Half) and 1980K-2 (Molson Lake, West Half).

Weber, W. and Schledewitz, D.C.P.
1979: Molson Lake-Kalliecahoolie Lake Project; in Manitoba Mineral Resources Division, Report of Field Activities 1979, p. 29-37.

1980: Molson Lake-Kalliecahoolie Lake Project; in Manitoba Mineral Resources Division, Report of Field Activities 1980, p. 33-37.

Weber, W. and Scoates, R.F.J.
1978: Archean and Proterozoic metamorphism in the northwestern Superior Province and along the Churchill-Superior boundary, Manitoba; in Metamorphism in the Canadian Shield, Geological Survey of Canada, Paper 78-10, p. 5-16.

Weber, W., Anderson, R.K., and Clark, G.S.
1975: Geology and Geochronology of the Wollaston Lake Fold Belt in Northwestern Manitoba; Canadian Journal of Earth Sciences, v. 12 no. 10, p. 1749-1759.

15. # URANIFEROUS PEGMATITES OF THE SHARBOT LAKE AREA, ONTARIO

K.L. Ford[1]
Geological Survey of Canada

Ford, K.L., Uraniferous pegmatites of the Sharbot Lake area, Ontario; in Uranium in Granites, ed. Y.T. Maurice; Geological Survey of Canada, Paper 81-23, p. 125-138, 1982.

Abstract

Reconnaissance airborne gamma ray spectrometric data (5 km line spacing) covering the southern Grenville Province clearly indicate four anomalous zones, namely Mont Laurier and Huddersfield Township in western Quebec, and the Bancroft and Sharbot Lake areas in eastern Ontario. These radiometric surveys show that the Sharbot Lake area has a distinctly higher average eU/eTh ratio compared to the other Grenville pegmatite districts. Detailed (1 km line spacing) airborne gamma ray spectrometric surveys in the Sharbot Lake area have been particularly useful in providing a comprehensive picture of the pegmatite distribution. The radiometric patterns clearly show three belts along which the pegmatites are concentrated.

The majority of the pegmatites occur as conformable to semiconformable sill-like bodies ranging from bands less than 1 metre wide to bodies exceeding 500 by 50 metres. They are generally white to pale pink, massive to locally foliated and coarse grained. The principal radioactive mineral is uraninite commonly associated with biotite. Other radioactive phases include allanite, monazite, thorite, uranothorite, zircon and apatite. Average equivalent uranium concentrations measured by in situ gamma ray spectrometry range from a low of 3 ppm (averaging 36 ppm eTh) for pegmatites hosted by pink leucogranite gneiss to amphibolite-hosted pegmatite with an average of 41 ppm (averaging 24 ppm eTh). Locally, equivalent uranium concentrations exceeding 5000 ppm may be found.

Field evidence suggests that the pegmatites may have been developed by partial melting of Grenville Supergroup paragneisses. In places the pegmatites show evidence of mobilization and emplacement into adjacent granite gneisses and metasediments.

Résumé

Les données obtenues par spectrométrie aéroportée des rayons gamma (sur des lignes espacées de 5 km), couvrant la région sud de la province de Grenville, indiquent clairement quatre zones d'anomalies, soit Mont-Laurier et la municipalité de Huddersfield, dans l'ouest du Québec, et les régions de Bancroft et de Sharbot Lake, dans l'est de l'Ontario. Ces levés radiométriques montrent que la moyenne des rapports eU/eTh pour la région de Sharbot Lake est nettement plus élevée que pour les autres régions pegmatitiques du Grenville. Des levés aéroportés détaillés (sur des lignes espacées de 1 km) par spectrométrie des rayons gamma, dans la région de Sharbot Lake, ont été particulièrement utiles pour fournir une image complète de la distribution des pegmatites. Les contours radiométriques indiquent clairement trois ceintures le long desquelles les pegmatites sont concentrées.

La majorité des pegmatites ressemblent à des sills, concordants à semi-concordants, se trouvant en bandes pouvant varier de 1 m de largeur jusqu'à des masses de plus de 500 m par 50 m. Leur couleur varie généralement du blanc au rose pâle et leur texture varie de massive à laminée et à grain grossier par endroits. Le principal minéral radioactif est l'uraninite, souvent associé avec la biotite. D'autres phases radioactives comprennent l'allanite, la monazite, la thorite, l'uranothorite, le zircon et l'apatite. Les concentrations moyennes d'eU, mesurées sur place par spectrométrie des rayons gamma, varient de 3 ppm (avec une moyenne de 36 ppm d'eTh), pour les pegmatites logées dans les gneiss leucogranitiques roses, jusqu'à une moyenne de 41 ppm (avec une moyenne de 24 ppm d'eTh), pour les pegmatites logées dans l'amphibolite. On peut trouver, par endroits, des concentrations d'eU dépassant 5000 ppm.

Des preuves sur le terrain permettent de croire que les pegmatites se sont développées par fusion partielle des paragneiss du supergroupe de Grenville. Par endroits, les pegmatites présentent des signes évidents de mobilisation et de mise en place dans les gneiss granitiques et les roches métasédimentaires adjacents.

[1]601 Booth Street, Ottawa, Ontario, K1A 0E8

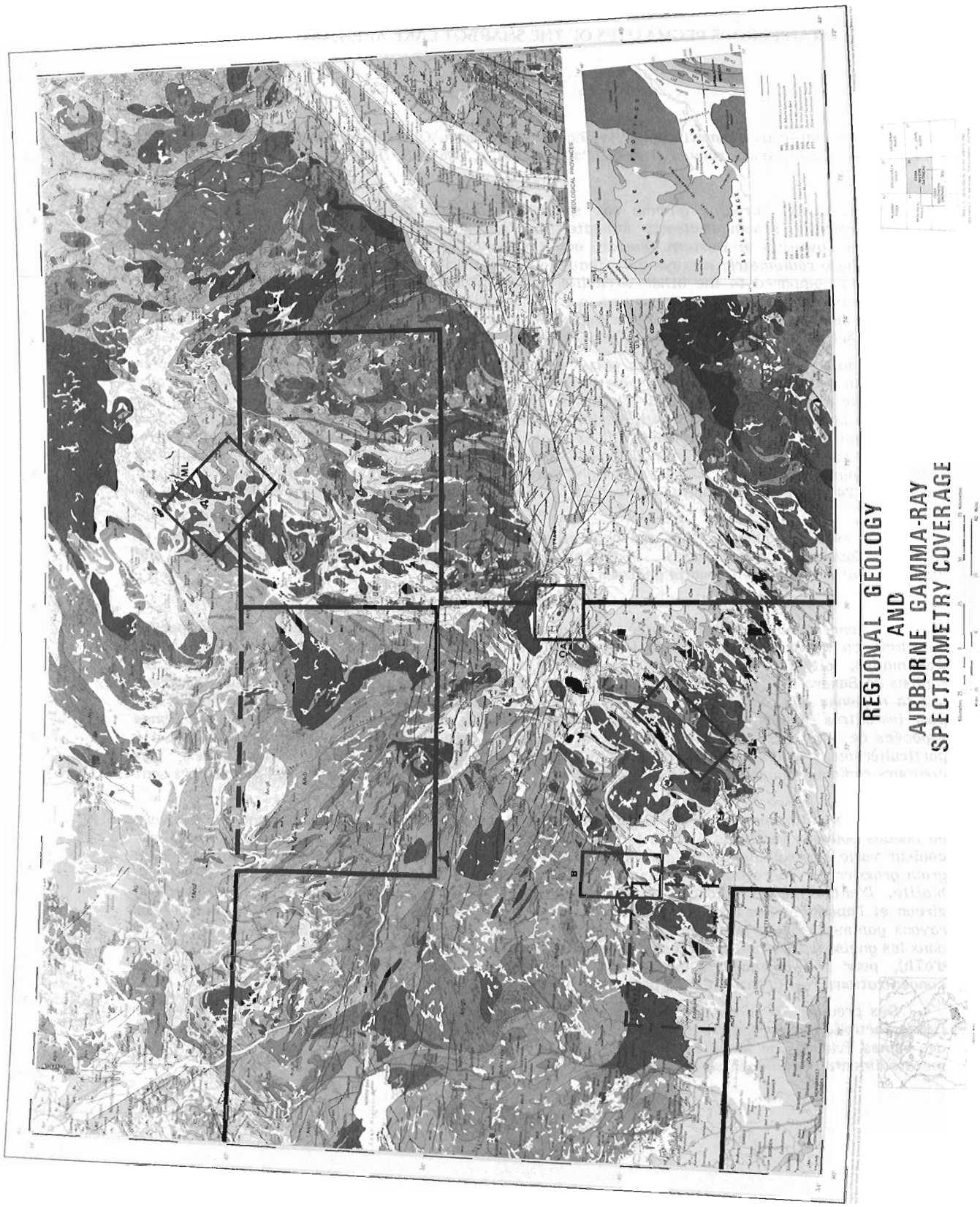

Figure 15.1. *Regional geology and airborne gamma ray spectrometric coverage of southeastern Ontario and southwestern Quebec.*

Introduction

Since 1969 the Geological Survey of Canada has conducted or contracted reconnaissance airborne gamma ray spectrometric surveys with 5 km line spacing followed by more detailed surveys of selected areas. Regional radioelement distribution patterns compiled from the reconnaissance surveys correlate well with areas of known uranium mineralization and are useful in outlining uraniferous geochemical provinces. This is particularly evident for the western portion of the Grenville Province. Figure 15.1 shows the regional geology for N.T.S. Map Sheet 31, Rivière Gatineau, covering a substantial portion of the western Grenville Province.

The extent of airborne gamma ray spectrometric coverage in this region is also shown on Figure 15.1. The reconnaissance surveys published to date include Geological Survey of Canada Open Files 331 (31F) and 428 (31C), and Geophysical Series Maps 35431G (31D); 35531G (31E); 36031G (31J), and 36231G (31L). In addition to these surveys flown with 5 km line spacing, surveys with line spacings ranging from 1/4 mile to 1 km are also indicated on Figure 15.1. These include areas B (Bancroft, GSC Open File 45), ML (Mont Laurier, GSC Open File 110), OA (Ottawa-Arnprior, GSC Open File 264), and SL (Sharbot Lake, GSC Open File 582).

Regional Radioelement Patterns

Figure 15.2 shows the regional distribution of equivalent uranium for the portion of N.T.S. map 31 surveyed to date, covering a varied terrane of Precambrian rocks with bordering areas of Paleozoic rocks. The Ontario Gneiss Belt (Fig. 15.1; OGB in Fig. 15.2), composed mainly of Lower Aphebian (Baer et al., 1971) quartzofeldspathic, pink to grey, well layered gneisses of amphibolite to locally granulite grade of metamorphism, occupies most of the northwest half of Figure 15.2 and is characterized by low equivalent uranium values. The Central Metasedimentary Belt (Fig. 15.1; CMB in Fig. 15.2) on the other hand, includes marble, quartzite, aluminous gneisses and schists, and metavolcanics of the Helikian Grenville Supergroup with metamorphic grade varying from upper greenschist to locally granulite. This belt occupies most of the southeast half of Figure 15.2 and is characterized by northeast-trending zones of elevated equivalent uranium values particularly along its boundary with the Ontario Gneiss Belt. Along this western boundary are situated the Bancroft (B, Fig. 15.2), Huddersfield Township (HT) and Mont Laurier (ML) pegmatite districts. The Sharbot Lake district (outlined in black) is located well within the established limits of the Central Metasedimentary Belt. The Sharbot Lake and Bancroft areas are separated by an area of low equivalent uranium values. This area is commonly referred to as the Hasting Basin Metamorphic Low (HBML, Fig. 15.2), characterized by greenschist grade metamorphism. Metamorphic grade rises rapidly east and west of this low to reach locally granulite grade east of Sharbot Lake in the Frontenac Axis and west of Bancroft in the Ontario Gneiss Belt (Wynne-Edwards, 1972).

Both the Sharbot Lake and Bancroft areas have maximum airborne equivalent uranium values exceeding 3 ppm (Fig. 15.2). However the Sharbot Lake area (Ford and Charbonneau, 1979) has distinctly lower regional equivalent thorium values (<5 ppm) and higher regional eU/eTh ratio values (0.50-0.75) than the Bancroft area (5-10 ppm eTh and <0.50 eU/eTh).

Sharbot Lake Pegmatite District

Figure 15.3 shows the geology for that portion of the Sharbot Lake area surveyed with 1 km line spacing. This area is dominated by felsic intrusive rocks, the oldest of which is the predominantly grey, granodioritic Northbrook Gneiss (NG, Fig. 15.3) and a possible equivalent, the Mellon Lake Gneiss (MLG; Chappell, 1978) dated at 1226 ± 25 Ma (Silver and Lumbers, 1966; Davidson et al., 1979). This grey granite phase is followed by a more potassic quartz monzonitic to granitic phase, the Addington-Lavant Granite Gneiss (ALG) dated at 1104 ± 25 Ma (Lumbers, 1967). This phase is in turn followed by late tectonic intrusions (Wolfe, 1979) of the Mountain Grove Mafic complex (MM), the McLean Granite Pluton (MP), and the Elphin Granite (EG). All these granitoids are intruded into a sequence of Grenville Supergroup rocks composed of mafic to intermediate metavolcanics and metasediments composed of amphibole-rich gneisses and schists, clastic siliceous gneisses and carbonate metasediments. Unconformably overlying these units and the Northbrook Gneiss is the Flinton Group, a clastic metasedimentary sequence (Moore and Thompson, 1972). Age relationships between the Flinton Group and the late tectonic intrusions are uncertain. The Flinton Group has not been defined on Figure 15.3 as most of it lies outside the map area with only minor occurrences west of Kaladar and in the Crotch Lake area. Possible equivalents are found southeast of Kaladar in the Clare River Structure (Chappell, 1978).

The pegmatites are considered the last intrusive phase and are found in all rock types including the Flinton Group. Silver and Lumbers (1966) give a U-Pb date of 1030 ± 20 Ma for the pegmatites in the Bancroft-Madoc area. No attempt has been made to subdivide the pegmatites on the basis of relative age as the majority appear to be late tectonic. The pegmatites hosted by the Addington-Lavant Gneiss appear to be phases of this gneiss and as such may bear no genetic relationship with the main volume of pegmatite hosted by the Grenville Supergroup and Northbrook Gneiss. Other pegmatite dykes are associated with the late tectonic intrusions but these are usually confined to the granitic bodies or occur within short distances from the contacts (Davidson et al., 1979).

Metamorphic grade increases steadily west to east from the high temperature portion of low grade metamorphism west of Kaladar to the low temperature portion of high grade metamorphism east of Sharbot Lake (Wolfe, 1978, 1979, 1980).

Structurally the Sharbot Lake survey area is divided into two domains by a northeast-southwest shear zone (SZ, Fig. 15.3) with domal intrusions prominent east of the shear zone and northeast-trending antiformal-synformal structures prominent west of it.

Figures 15.4 and 15.5 show respectively the equivalent uranium and eU/eTh ratio maps for the Sharbot Lake area at 1 km line spacing and the eastern portion of the area, at 1/2 km line spacing. The radiometric patterns west of the NE-SW shear zone are dominated by well defined belts of elevated equivalent uranium values paralleling the general structural trends (Ford and Charbonneau, 1979). These belts outline the area where uraniferous white pegmatites occur. These are concentrated mainly (1) along the southern boundary of the Northbrook Gneiss, (2) peripheral to the edges of the Mellon Lake Gneiss, and (3) along a linear zone within the central portion of the Northbrook Gneiss. East of

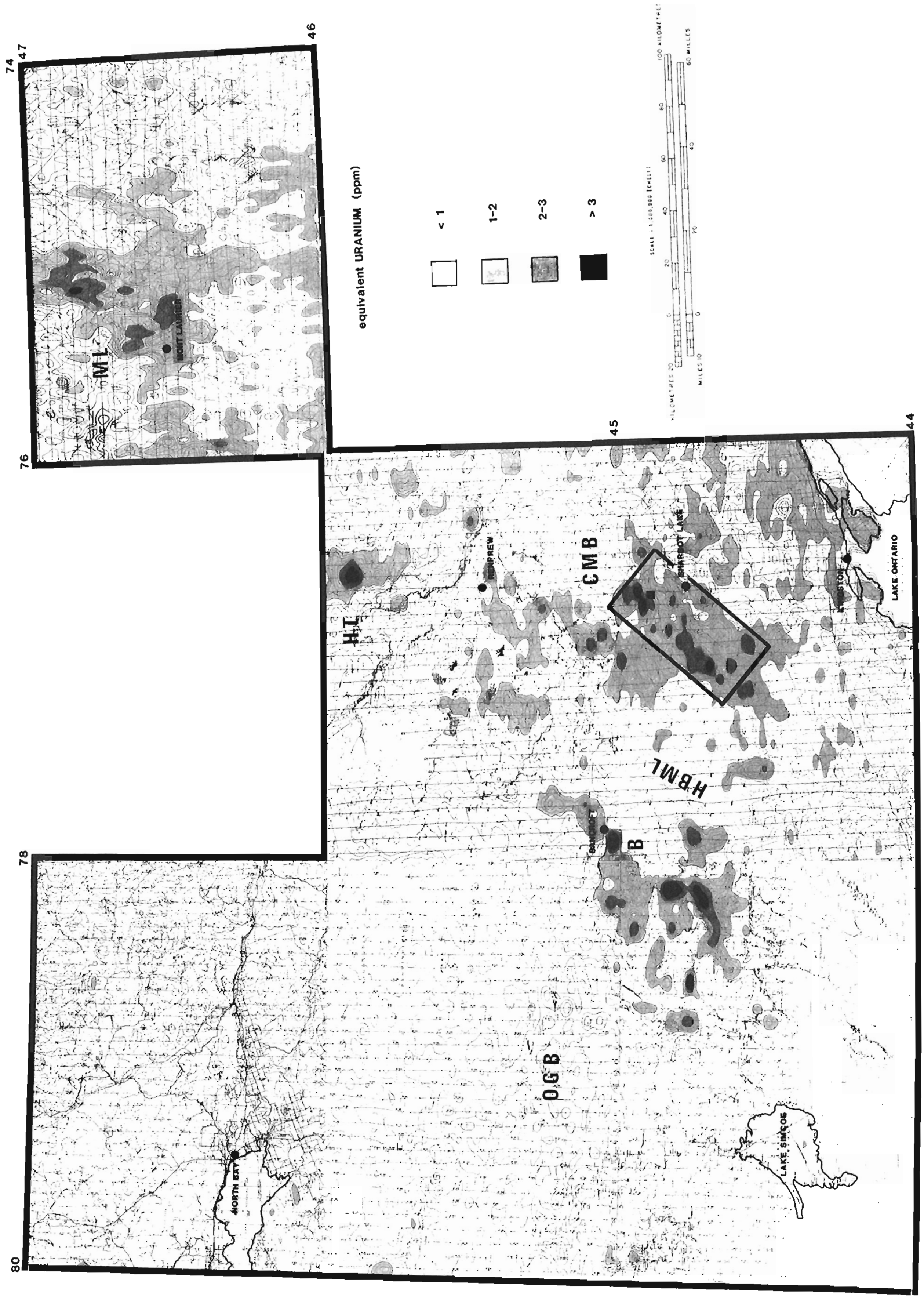

Figure 15.2. Regional equivalent uranium distribution, part of N.T.S. 31.

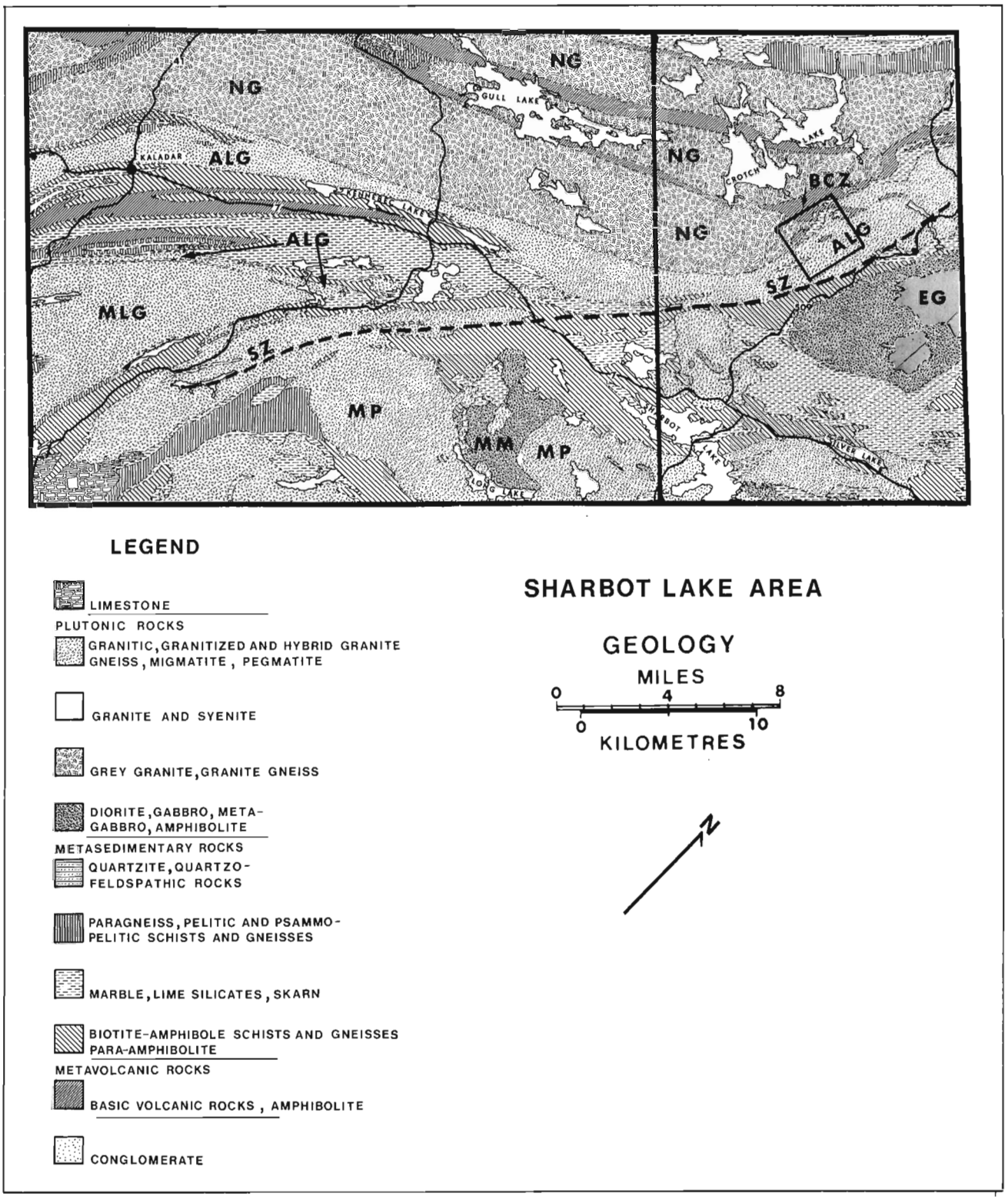

Figure 15.3. Geology of the Sharbot Lake area after Hewitt (1964).

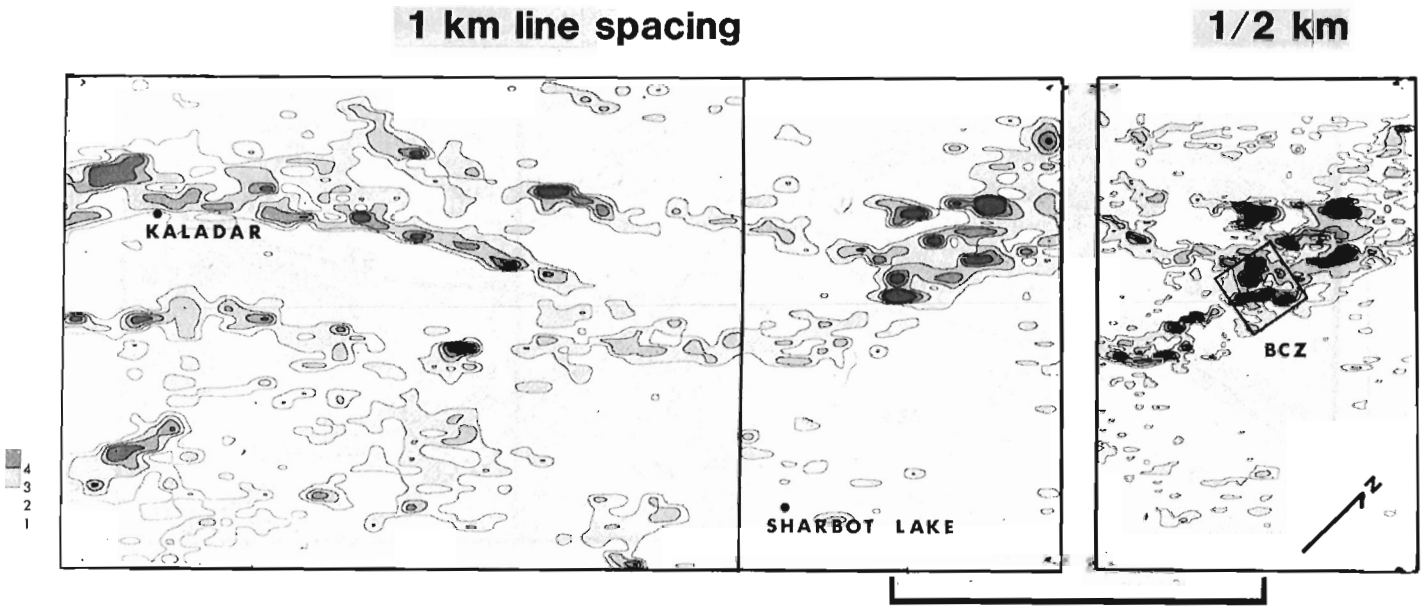

Figure 15.4. *Sharbot Lake, equivalent uranium in ppm (1 and 1/2 km line spacing).*

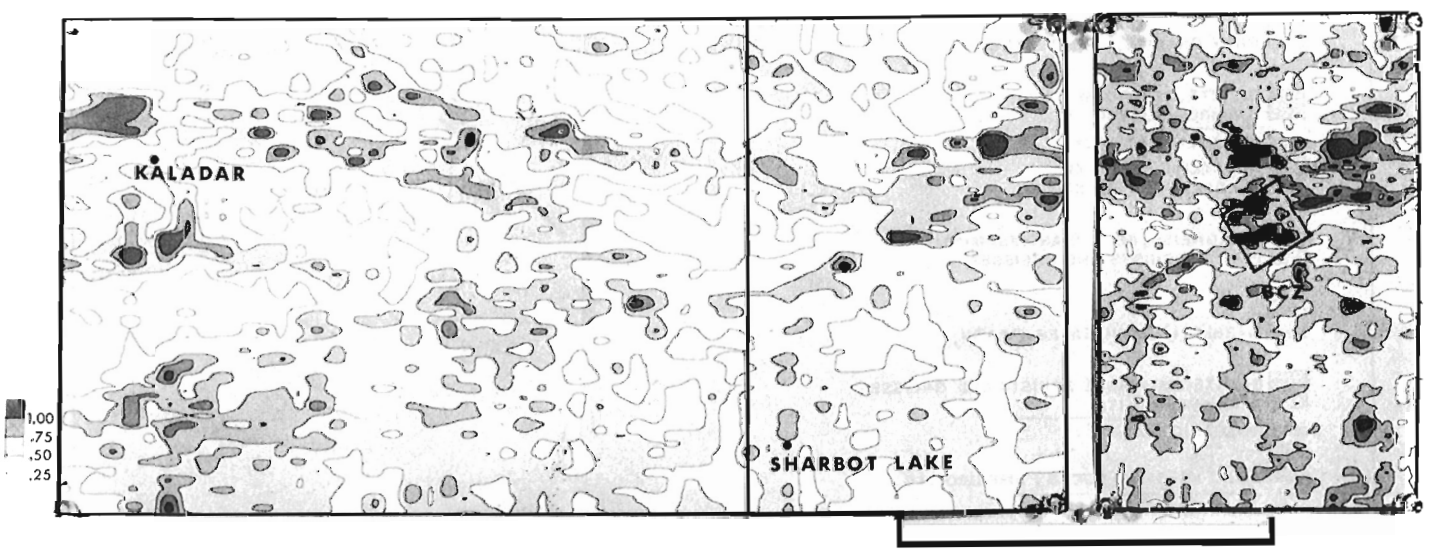

Figure 15.5. *Sharbot Lake equivalent uranium/equivalent thorium ratio (1 and 1/2 km line spacing).*

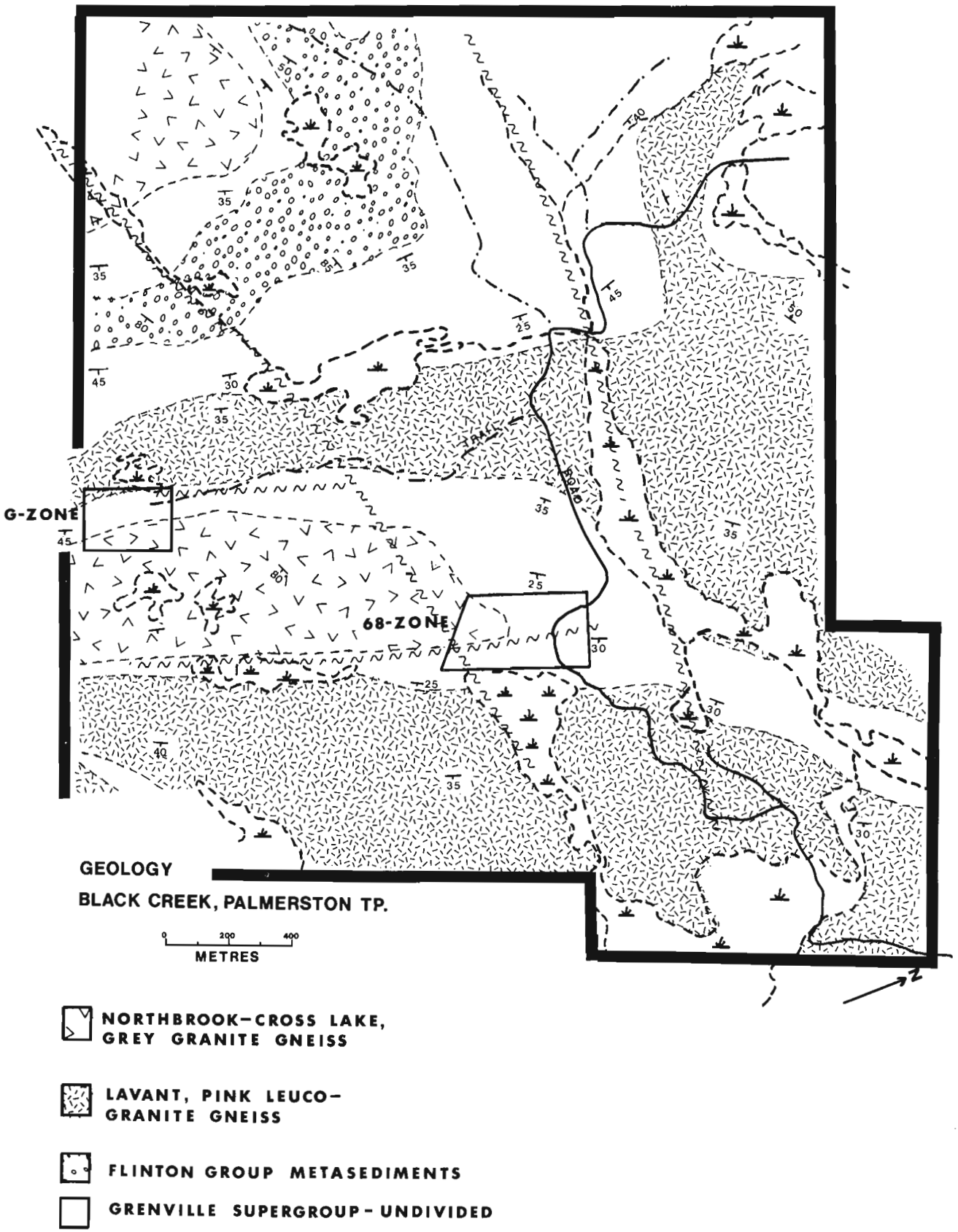

Figure 15.6. *Geology of the Black Creek Zone, Palmerston Township.*

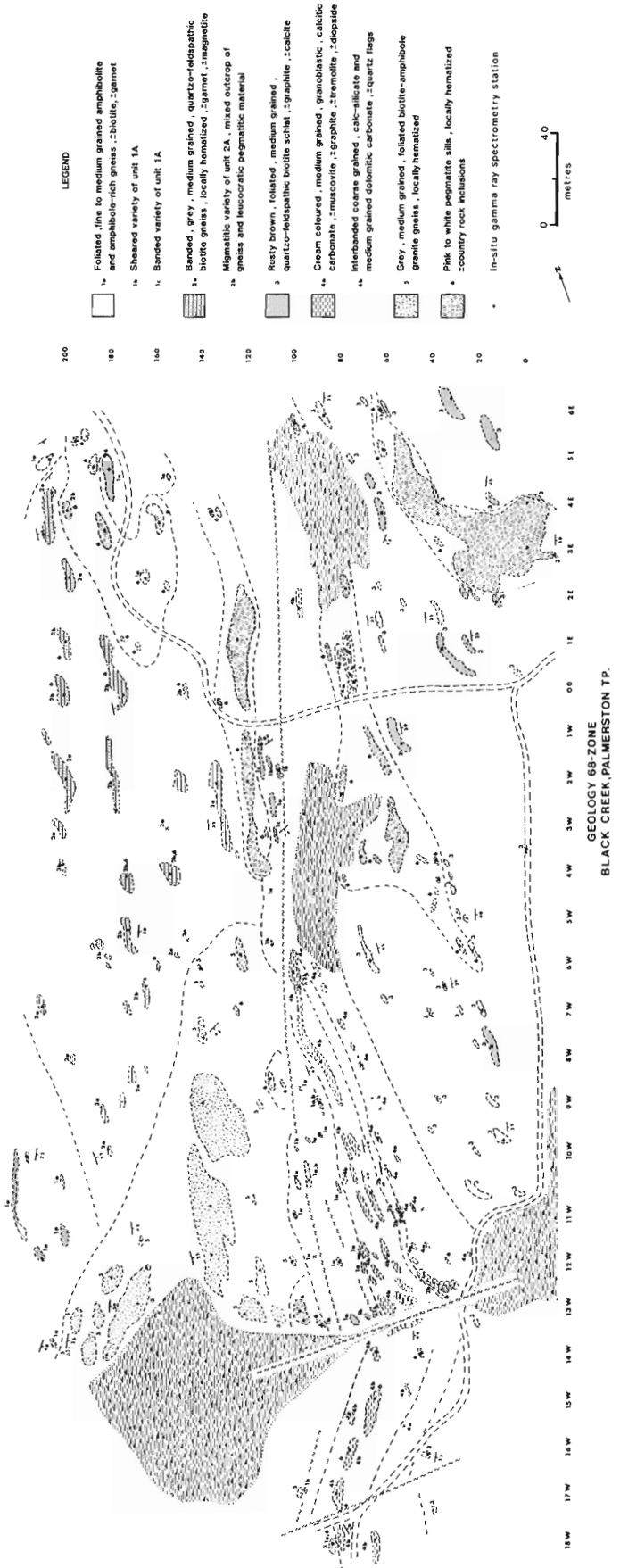

Figure 15.7. Geology, 68-Zone, Black Creek, Palmerston Township.

this shear zone the patterns are less distinct except for two diffuse circular features relating to bodies of the late tectonic McLean Granite. Zones 1 and 2 have been interpreted by various workers (Chappell, 1978; Wolfe, 1978) as zones of major structural weakness and/or faulting. Within these zones, anatexis, metasomatism, and assimilation of Grenville Supergroup paragneisses may have contributed to the formation of pegmatitic material.

Uraniferous Pegmatites of Southern Palmerston Township

Detailed investigations were concentrated mainly in a 10 km^2 area of southern Palmerston Township, the Black Creek Zone (BCZ, Fig. 15.3, 15.4). Figure 15.6 shows the geology of the Black Creek Zone. The dominant lithologies are pink, leucogranite gneiss (Lavant Gneiss) and grey, granodioritic gneiss (Northbrook Gneiss). These units are separated from each other by narrow north-northeast-trending zones of Grenville paragneiss and pegmatite. Foliation and gneissosity in the granitic gneisses are for the most part parallel to the strike of the paragneisses. Shearing is evident in the paragneisses and pegmatites occupying these narrow zones as shown by the local development of augen texture and mylonite (Plate 15.1 A, B, C). Gradational contacts such as shown in Plate 15.2 support the assumption of local derivation of some pegmatitic material from the partial melting of quartzofeldspathic gneisses and schists commonly associated with pegmatite in these zones of structural weakness.

The dominant geological features of the pegmatites in the Black Creek Zone are:

1. They are generally leucocratic, white to pale pink and quartz monzonitic in composition. Red varieties do exist; these are commonly rich in magnetite and strongly hematized.
2. They have a generally massive, coarse granitic texture although aplitic and coarse megacrystic phases (granophyric feldspars >40 cm) can be present in the same outcrop.
3. They vary from thin (1 cm) migmatitic bands or segregations (Plate 15.2A, B) to single bodies with widths greater than 30 metres and lengths in excess of 100 metres.
4. They occur mainly as discontinuous, conformable to semiconformable sill-like bodies with contacts varying from sharp to gradational (Plate 15.2A, B).
5. The principal minerals include quartz, microcline, plagioclase and biotite. Accessory phases include muscovite, magnetite, pyrite, molybdenite, graphite, apatite, garnet, and anatase. Amphibole and pyroxene are rare. Radioactive minerals include uraninite, uranothorite, thorite, allanite, monazite, and zircon (Plate 15.1 and 15.3).
6. Uraninite is the most common ore mineral and is commonly associated with pockets or zones rich in biotite and occasionally apatite (Plate 15.1 and 15.3). These biotite-rich zones can be scattered randomly throughout massive pegmatite or localized in the migmatitic contact zones with quartzofeldspathic gneisses (Plate 15.2A). Occasionally these migmatitic contact zones are cataclastically deformed and can have high apatite and uranium contents (up to 4000 ppm U; Plate 15.1A, B, C).

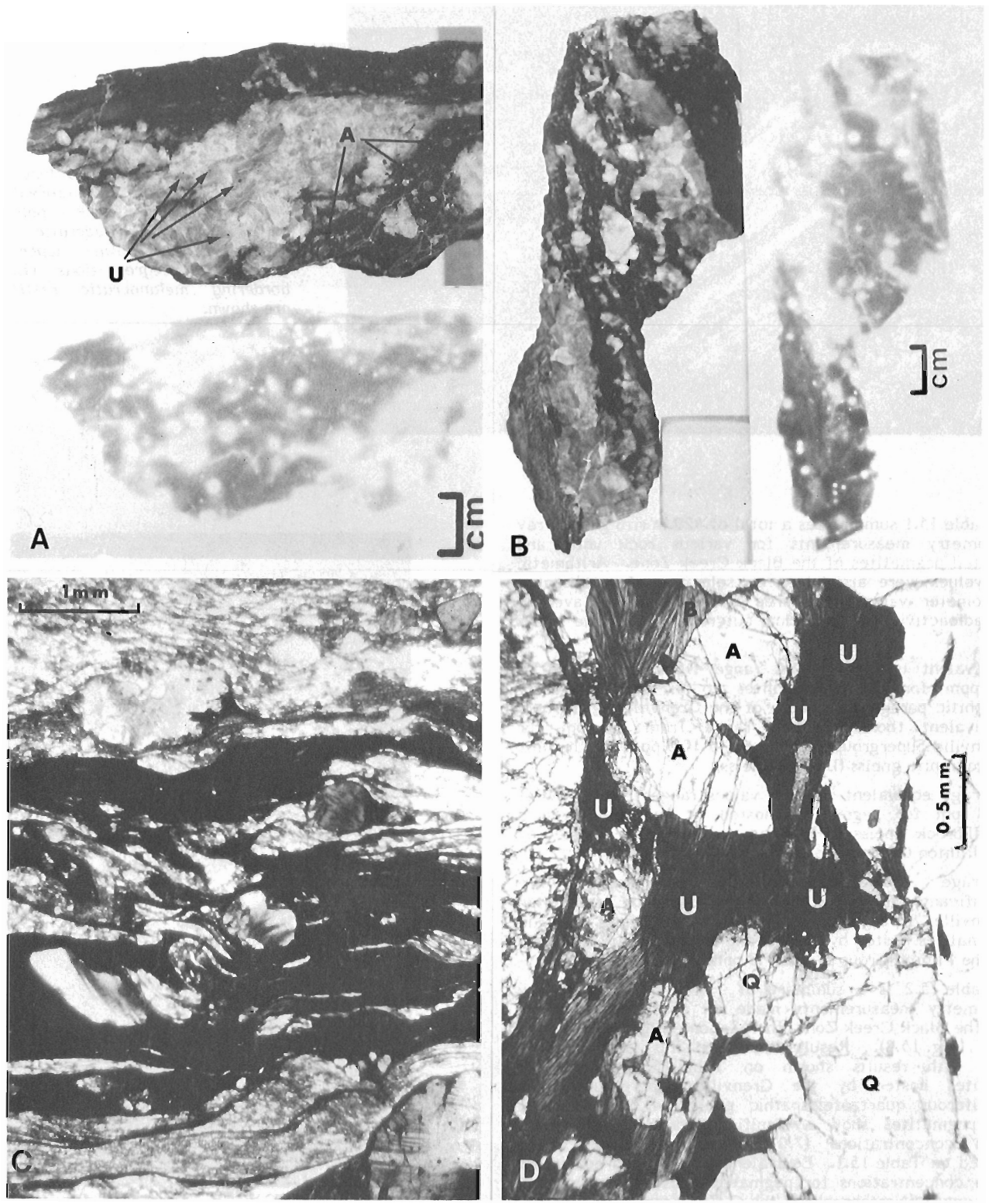

A, B. *Mylonitized, augen-textured, biotite-apatite-uraninite rich zone associated with a massive white pegmatite. (U – uraninite, A – apatite). In situ gamma spectrometric analysis, eU = 4200 ppm; eTh = 370 ppm.*

C. *Photomicrograph of portion of 1A showing development of mortar and augen textures (X – Nicols).*

D. *Photomicrograph showing biotite-apatite-uraninite association (B – biotite, A – apatite, U – uraninite, Q – quartz). In situ gamma spectrometric analysis, eU = 2400 ppm; eTh = 800 ppm.*

Plate 15.1. *Hand specimens, autoradiographs, and photomicrographs of mylonitized rocks from the Black Creek Zone.*

Plate 15.2

Contact relationships in Black Creek Zone.

A. Stromatic migmatite structure at the contact between quartzofeldspathic biotite-garnet gneiss (P – paleosome) and massive leucocratic white pegmatite (not shown – upper right). Leucocratic segrega-tions (L) with bordering melanocratic restite (M) are shown.

Table 15.1 summarizes a total of 429 in situ gamma ray spectrometry measurements for various rock units and associated pegmatites of the Black Creek Zone. Arithmetic mean values were arrived at by selection of total count scintillometer values considered to represent the average total radioactivity for individual outcrops. This table shows that:

1. Equivalent uranium values range from an average of 1.5 ppm for the amphibolites to 4.7 ppm for rusty graphitic paragneisses, both of the Grenville Supergroup. Equivalent thorium values range from 2.9 ppm for Grenville Supergroup carbonates to 10.9 ppm for the pink leucogranite gneiss (Lavant Gneiss).
2. Average equivalent thorium values range from a low of 11.8 ppm for pegmatites hosted by the grey granite Northbrook Gneiss to 39.3 ppm for pegmatites hosted by the Flinton Group metasediments.
3. Average equivalent uranium concentrations are significantly higher in pegmatites hosted by pre-Flinton Grenville Supergroup gneisses (29 to 41 ppm) than in pegmatites hosted by the Lavant or Northbrook gneisses, or the Flinton Group (3.1 to 7.8 ppm).

Table 15.2 is a summary of 127 in situ gamma ray spectrometry measurements made on two detailed zones within the Black Creek Zone, the 68-Zone (Fig. 15.7) and the G-Zone (Fig. 15.8). Results shown on this table compare closely with results shown on Table 15.1 except for pegmatites hosted by the Grenville Supergroup's grey magnetiferous quartzofeldspathic gneiss of the 68-Zone. These pegmatites show a significant drop in equivalent thorium concentrations (7.0 ppm) compared to values presented on Table 15.1. Equivalent uranium and equivalent thorium concentrations for pegmatites hosted by the grey granite gneiss (Northbrook) of the G-Zone are slightly higher than for pegmatite hosted by this same rock in the Black Creek Zone as a whole (17.9 ppm vs. 11.8 ppm for eTh and 12.8 ppm vs. 7.8 ppm for eU).

Thus in summary, pegmatites average about 30 ppm equivalent uranium regionally when they are hosted by pre-Flinton Grenville Supergroup rocks. They average

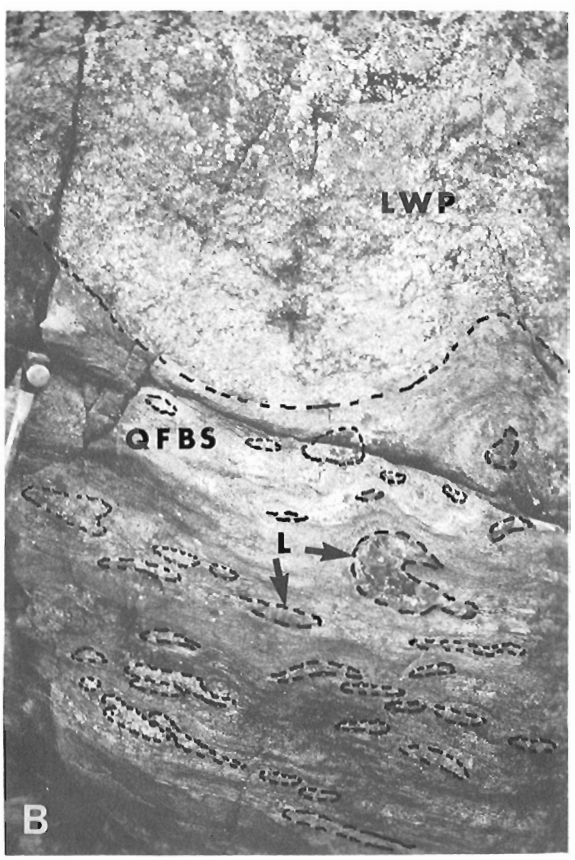

B. Contact between massive leucocratic white pegmatite (LWP) and quartzofeldspathic biotite schist (QFBS) in which there has been development of leucocratic segregations (L) similar to the massive pegmatite.

Table 15.1. Compilation of in situ gamma ray spectrometric measurements*, Black Creek area, Palmerston Township, Ontario

	Rock type (**)	K% Arithmetic Mean	eU ppm Arithmetic Mean	eTh ppm Arithmetic Mean	eU/eTh Arithmetic Mean	Maximum Measured Concentration eU ppm	Maximum Measured Concentration eTh ppm
	Pink leucogranite gneiss (117) (ALG, Fig. 15.3)	3.4	2.8	10.9	0.26		
	Pegmatite (11)	4.7	3.1	35.8	0.13	30	231
	Flinton Group metasediments (16)	2.3	1.9	8.2	0.24		
	Pegmatite (18)	5.4	6.5	39.3	0.33	71	285
	Grey granite gneiss (48) (NG, Fig. 15.3)	1.9	3.2	8.4	0.40		
	Pegmatite (9)	4.4	7.8	11.8	0.70	1079	140
Grenville Supergroup (pre-Flinton)	Calcitic and dolomitic carbonate (44)	0.6	3.0	2.9	1.17		
	Pegmatite (19)	5.3	28.6	21.4	1.63	2002	552
	Rusty quartzofeldspathic biotite schist (graphitic-pyritiferous) (38)	2.8	4.7	9.6	0.51		
	Pegmatite (16)	5.0	31.2	38.2	0.99	284	1167
	Grey quartzofeldspathic biotite gneiss (magnetiferous) (28)	2.2	3.4	7.7	0.58		
	Pegmatite (19)	4.1	36.0	24.9	2.24	5211	2209
	Amphibolite and amphibole-rich gneisses (35)	1.1	1.5	3.1	0.56		
	Pegmatite (11)	3.5	41.4	24.3	2.11	444	87

* Arranged according to increasing uranium content in pegmatites
** Number of measurements considered for arithmetic mean excluding maximum measured concentrations

Table 15.2. Compilation of in situ gamma ray spectrometric measurements, 68-Zone and G-Zone, Black Creek area, Palmerston Township

	Rock type (*) 68-Zone	K% Arithmetic Mean	eU ppm Arithmetic Mean	eTh ppm Arithmetic Mean	eU/eTh Arithmetic Mean	Maximum Measured Concentration eU ppm	Maximum Measured Concentration eTh ppm
Grenville Supergroup (pre-Flinton)	1. Grey quartzofeldspathic biotite gneiss (magnetiferous) (10)	1.6	3.0	5.1	0.67		
	2. Amphibolite (7)	0.8	0.8	1.8	0.46		
	3. Rusty quartzofeldspathic biotite schist (graphitic-pyritiferous) (11)	2.4	4.7	7.3	0.66		
	4. Calcitic and dolomitic carbonate (7)	0.3	2.0	1.6	1.40		
	5. Grey granite gneiss (12) (NG, Fig. 15.3)	1.7	2.3	7.8	0.32		
	Pegmatite (hosted predominantly by 1) (17)	3.2	36.8	7.0	5.46	742	147
	Pegmatite (hosted predominantly by 3 and 4) (19)	4.8	27.6	28.1	1.09	198	1194
	G-Zone						
	Pegmatite (hosted by grey granite gneiss) (13)	4.1	12.8	17.9	0.76	49	166
	Pegmatite (hosted by quartzo-feldspathic biotite schist) (31)	4.4	28.9	27.1	1.45	6953	2594

* Number of measurements considered for arithmetic mean excluding maximum measured concentrations

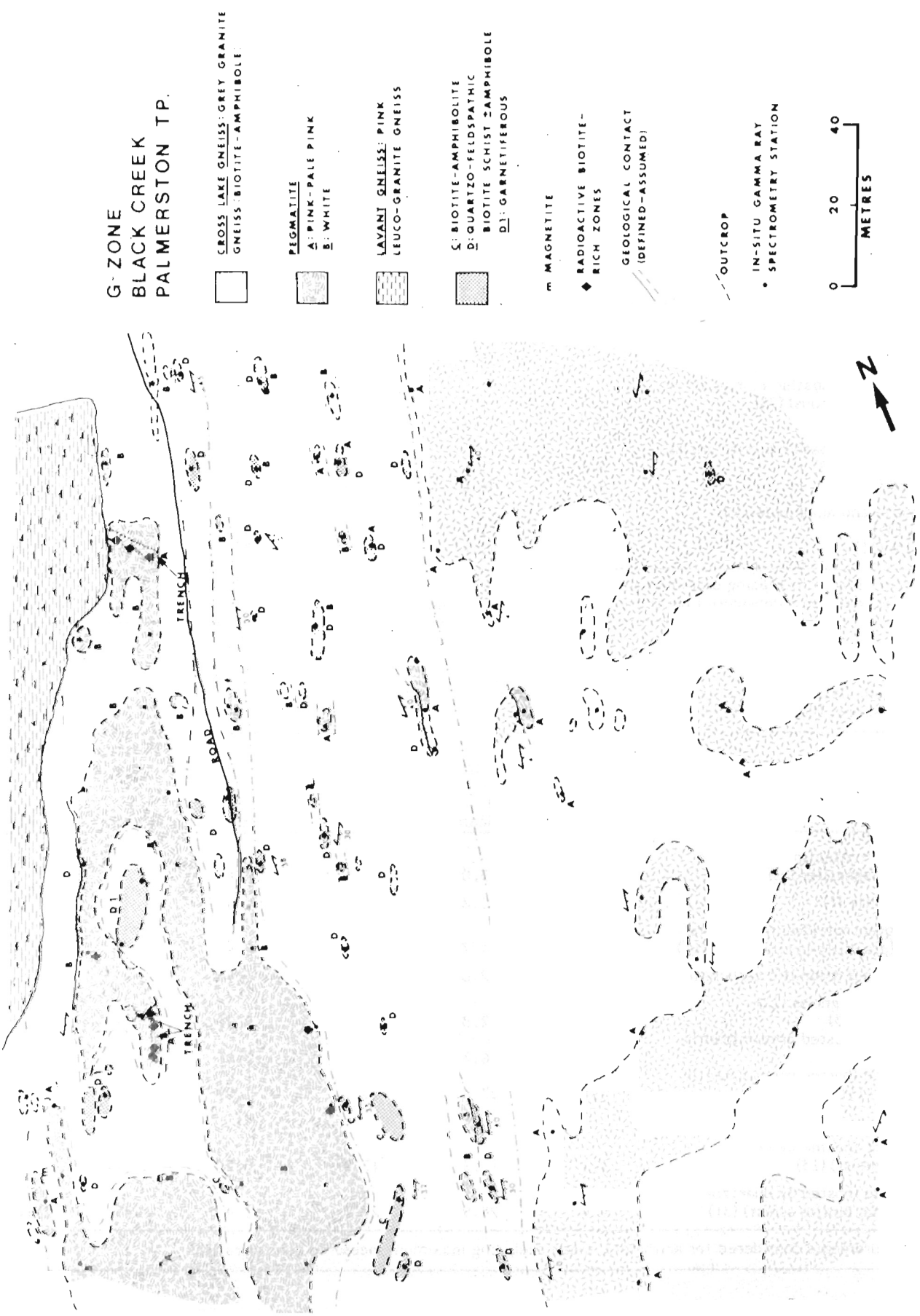

Figure 15.8. Geology, G-Zone, Black Creek, Palmerston Township.

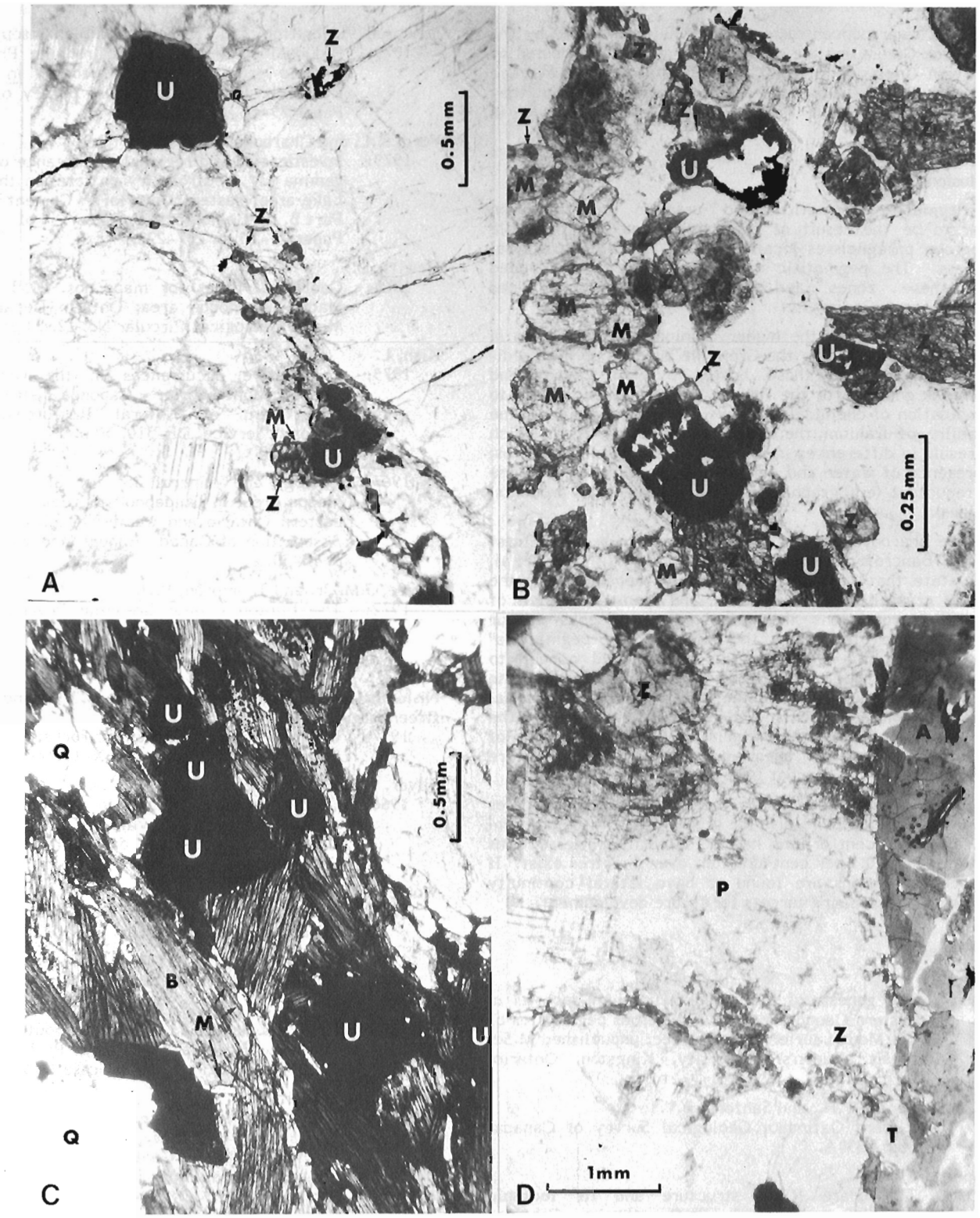

A. *U – uraninite, Z – zircon, M – monazite, T – altered thorium-rich phase, possibly thorite or uranothorite. In situ gamma spectrometric analysis, eU = 510 ppm; eTh = 200 ppm.*

B. *U – uraninite, Z – zircon, M – monazite, T – altered thorium-rich phase, possibly thorite or uranothorite. In situ gamma spectrometric analysis, eU = 810 ppm; eTh = 632 ppm.*

C. *U – uraninite, B – biotite, M – muscovite, Q – quartz. In situ gamma spectrometric analysis, eU = 7000 ppm; eTh = 2600 ppm.*

D. *Z – zircon, T – altered thorium-rich phase, possibly thorite or uranothorite, P – plagioclase, A – allanite (altered to mixture of chlorite, thorite, ilmenite and bastnaesite). In situ gamma spectrometric analysis, eU = 190 ppm; eTh = 117 ppm.*

Plate 15.3. *Photomicrographs showing variety of mineralogical and textural features in Black Creek Zone.*

somewhat lower concentrations when they are hosted by the Northbrook Gneiss and are substantially lower when hosted by the Lavant Gneiss or Flinton Group. The pegmatites average about 30 ppm equivalent thorium regionally; however they can show considerable local variation as indicated in Table 15.2.

Conclusions

Pegmatite formation and uranium mineralization appear to be the result of anatexis of selected Grenville Supergroup paragneisses localized along zones of structural weakness. The pegmatitic material thus derived intruded along these zones and into adjacent rock types (i.e. Northbrook Gneiss).

The reasons for the higher uranium concentrations in the pegmatites hosted by the Grenville Supergroup metasediments compared to those hosted by the Lavant and Northbrook gneisses, or the Flinton Group may be related to a combination of chemical and physical factors including, the availability of uranium, the bulk chemistry of the rocks which may result in differences in minimum melting temperatures, the presence of water and carbon dioxide, and the presence of a reductant (e.g. graphite and/or its breakdown products, sulphides).

The Sharbot Lake pegmatites appear to be in contrast with the Bancroft style of mineralization. Nishimori et al. (1977) state that Bancroft mineralization appears to be the result of crystallization of granitic and syenitic magmas of batholithic proportions that exsolved an aqueous vapour phase. On the other hand, the "metamorphic pegmatites" (Kish, 1975) of the Mont Laurier area would appear to resemble the Sharbot Lake pegmatites. At Mont Laurier, the pegmatites are thought to be the result of localized partial melting of metasediments (Allen, 1971). However, the localization of pegmatitic material in relation to zones of structural weakness or shearing seems to be a feature characteristic to the Sharbot Lake area.

The well defined linear distribution of pegmatites within the Sharbot Lake district greatly facilitates uranium exploration. Recent drilling has indicated that intersections of greater than 0.1 per cent uranium over 3 metres exist. If these concentrations are found to have lateral continuity they would be promising targets for future development.

References

Allen, J.M.
1971: The genesis of Precambrian uranium deposits in eastern Canada and the uraniferous pegmatites of the Mont Laurier area, Quebec; unpublished M.Sc. thesis, Queen's University, Kingston, Ontario, 83 p.

Baer, A.J., Poole, W.H., and Sanford, B.V.
1971: Rivière Gatineau; Geological Survey of Canada, Map 1334A.

Chappell, J.F.
1978: The Clare River structure and its tectonic setting; unpublished Ph.D. thesis, Carleton University, Ottawa, Ontario, 184 p.

Davidson, A., Britton, J.M., Bell, K., and Blenkinsop, J.
1979: Regional synthesis of the Grenville Province of Ontario and western Quebec; in Current Research, Part B, Geological Survey of Canada, Paper 79-1B, p. 153-172.

Ford, K.L. and Charbonneau, B.W.
1979: Investigation and regional significance of airborne gamma ray spectrometry patterns in the Sharbot Lake area, eastern Ontario; in Current Research, Part B, Geological Survey of Canada, Paper 79-1B, p. 207-222.

Hewitt, D.F.
1964: Geological notes for maps nos. 2053 and 2054, Madoc-Gananoque area; Ontario Department of Mines, Geological Circular No. 12, 33 p.

Kish, L.
1975: Radioactive occurrences in the Grenville of Quebec, Mont Laurier – Cabonga district; Quebec Department of Natural Resources, Mineral Deposits Service, DP-310, 30 p.

Lumbers, S.B.
1967: Geology and mineral deposits of the Bancroft-Madoc area; in Guidebook to geology in parts of eastern Ontario and western Quebec; Geological Association of Canada Annual Meeting, Kingston, p. 13-30.

Moore, J.M. Jr. and Thompson, P.H.
1972: The Flinton Group; Grenville Province, eastern Ontario, Canada; Proceedings of the 24th International Geological Congress, Montreal, Sect. 1, p. 221-229.

Nishimori, R.K., Ragland, P.C., Rogers, J.J.W., and Greenberg, J.K.
1977: Uranium deposits in granitic rocks; United States Department of Energy, GJBX-13(77).

Silver, L.T. and Lumbers, S.B.
1966: Geochronological studies in the Bancroft-Madoc area of the Grenville Province, Ontario; Geological Society of America, Special Publications 87, p. 156.

Wolfe, J.M.
1978: Geology of the Kaladar area, Southern Ontario; Ontario Geological Survey, OFR 5252, 146 p.

1979: Geology of the Long Lake area, Frontenac County; Ontario Geological Survey, OFR 5271, 174 p.

1980: Sharbot Lake area, District of Southern Ontario; Ontario Geological Survey, Preliminary Map P. 2373, Geological Series, Scale 1:15840.

Wynne-Edwards, H.R.
1972: The Grenville Province; in Variations in Tectonic Styles in Canada, ed. R.A. Price and R.J.W. Douglas; Geological Association of Canada, Special Paper 11, p. 264-334.

16.

INFLUENCE OF A METAMORPHOSED GABBRO IN THE CONTROL OF URANIUM-BEARING PEGMATITE DYKES, MADAWASKA MINES, BANCROFT, ONTARIO

Richard L. Bedell[1]
University of Toronto

Bedell, R.L., Influence of a metamorphosed gabbro in the control of uranium-bearing pegmatite dykes, Madawaska Mines, Bancroft, Ontario; in Uranium in Granites, ed. Y.T. Maurice; Geological Survey of Canada, Paper 81-23, p. 139-143, 1982.

Abstract

Of the numerous uranium deposits in the Grenville Province of Ontario, that of Madawaska Mines Limited is the only one currently in production. In the Spring of 1980, a two-year study was undertaken to examine the structure in the vicinity of Madawaska Mines as a controlling factor for the uranium-bearing pegmatitic granites and syenites that constitute the orebodies.

These relatively undeformed rocks are confined to the deformed anorthositic Faraday metagabbro complex. This paper examines firstly the strain distribution within the Faraday metagabbro complex in order to predict paths of least resistance along which the younger pegmatites were emplaced. Secondly, certain geochemical properties of the metagabbro host rock that may have had an influence on the formation of the ore deposits are described.

Résumé

Parmi les nombreux dépôts d'uranium dans la province de Grenville en Ontario, celui de Madawaska Mines Limited est le seul qui soit en exploitation actuellement. Au printemps de 1980, on a entrepris une étude de deux ans pour examiner l'influence de la structure dans le voisinage de Madawaska Mines, sur le contrôle des granites et syénites pegmatitiques uranifères qui constituent les gisements.

Ces roches relativement non déformées sont confinées au complexe déformé anorthositique connu sous le nom de metagabbro de Faraday. Ce document étudie d'abord la distribution des tensions à l'intérieur du métagabbro de Faraday en vue de prédire les trajets de moindre résistance le long desquels les pegmatites plus récentes ont été mises en place. Ensuite, on décrit certaines propriétés géochimiques du métagabbro, qui peuvent avoir eu une influence sur la formation des gisements.

Introduction

The Madawaska Mine originally started production in 1957 as the Faraday Mine which closed in 1964. It did not resume production until 1976 when it was bought by Madawaska Mines Limited. The ore minerals are predominantly uraninite and uranothorite, and the ore bodies average from 0.07-0.1 per cent U_3O_8. The mill has a 1400 tonnes per day capacity and from 1976 to 1979 produced 778 853 kg U_3O_8. After refining at Port Hope, Ontario, the uranium is shipped to Italy for use as a fuel in electricity generation.

Geology

A major feature of the regional geology (Fig. 16.1) is the Algonquin Batholith, a broad zone of gneisses that separates older supracrustal rocks (2.5-1.8 Ga) to the north and west from younger supracrustal rocks (1.5-1.25 Ga) to the south and east (Schwerdtner and Lumbers, 1980). The mine area is located in the southeastern region within the younger supracrustal domain which consists of a large variety of metasediments including coarse clastics, greywackes, shales, limestones, and dolostones. Volcanic activity occurred simultaneously with sedimentation. These supracrustals were later intruded by plutonic rocks, some with alkalic affinity including syenites, alkalic granites, and gabbroic rocks. The mine area lies within the southern portion of the alkalic belt approximately 5 km southwest of Bancroft (Fig. 16.2). The pegmatite orebodies are hosted by the Faraday metagabbro complex the most undeformed portions of which indicate that it was originally an anorthositic gabbro with alkalic pyroxene.

The mine area is bounded by two major fault zones. The McArthur's Mills fault zone extends approximately northeast parallel to Highway 28. A second fault zone trends east-northeast parallel to Monk Road, just north of the Faraday metagabbro complex (Fig. 16.2). This was most recently mapped by S. Masson (personal communication, 1981) who has named it the Derry Lake fault zone.

The southeastern border of the Faraday metagabbro complex is shown in Figure 16.3. The ore-bearing pegmatites are confined within this complex which intrudes the dominantly ENE-trending metasediments consisting locally of marble and minor metasandstones. These also occur as xenoliths within the metagabbro. Near the contact with the complex, a zone of mylonitized marble and an adjacent unit of disharmonically folded metasandstone testify to the severity of the deformation undergone by the metasediments when intrusion of the anorthositic gabbro took place.

Fine grained gabbroic sills also intrude the metasediments giving rise to diopside-rich skarn assemblages in contact with the marble.

Faulting occurs along lithological contacts and the strain increases as one approaches the McArthur's Mill fault. This increase in strain translates into a more pronounced foliation and greater abundance of slickensided surfaces. Furthermore, the regional ENE fabric becomes gradually concordant on approaching the NE-trending fault zone. Within the fault itself, strain intensity is quite variable.

[1] Department of Geology, Toronto, Ontario M5S 1A1

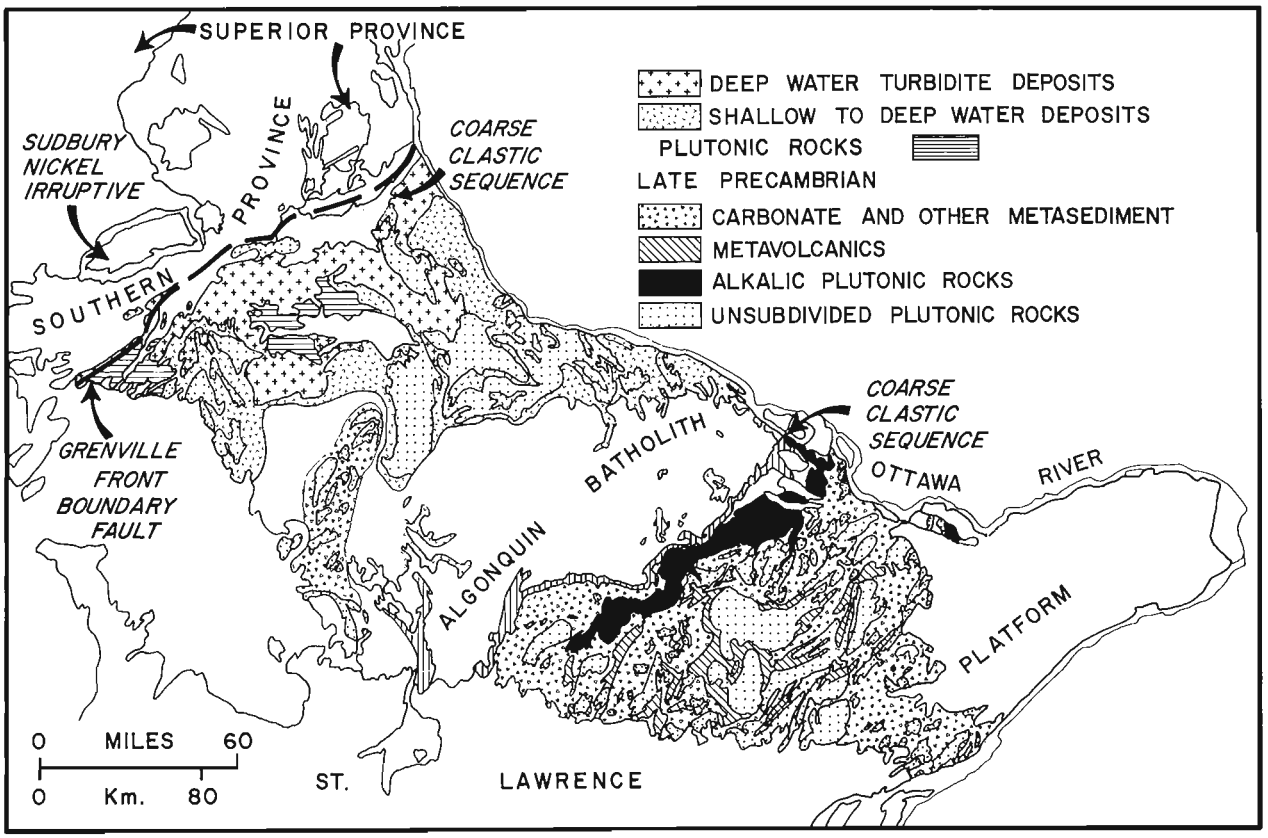

Figure 16.1. Generalized map of the Grenville Province in Ontario after Schwerdtner and Lumbers (1980).

Uranium Mineralization

There are two schools of thought as to the source of the uranium. Bright (1980), using field and petrographical data, suggested that the late tectonic pegmatites which locally host uranium mineralization were initially derived at depth by partial melting of the Anstruther Lake Group basal arenites during Grenville metamorphism. Along the flanks of basement gneiss domes, where metamorphism was high, those pegmatites which were stratigraphically emplaced within the Hermon Group, metasomatically derived uranium from this lithology.

S.B. Lumbers (personal communication, 1981), using field, petrographical, chemical, and isotopic data, suggested that the source of uranium is related to the alkalic belt and regional fenitization. Because of the alkalic affinity there must have been at least some mantle component involved. The Madawaska property lies near the southern edge of this alkalic belt.

The ore is confined to pegmatitic bodies and their immediate vicinity. The pegmatites are gradational into granite and syenite, but in this paper, they are collectively referred to as pegmatites.

The basic pegmatite mineralogy is microcline, albite, peristerite, alkalic pyroxene, and amphibole with sporadic occurrences of biotite, magnetite, and quartz. Accessories are apatite, titanite, tourmaline, and sulphides, including chalcopyrite, pyrite, pyrrhotite, marcasite, and molybdenite. Calcite and anhydrite occur as well-segregated masses both within and outside the pegmatites. The anhydrite has been interpreted as being of magmatic origin (Little, 1969).

The ore minerals are essentially uraninite and uranothorite. Other primary radioactive species are thorite, kainosite, tritomite-(Y), allanite, and zircon. The ore has a U:Th ratio of approximately 2:1. Backscattered electron imaging studies (Rimsaite, 1980) have found additional phases of fluorite, tin oxide, galena, and Fe-Si-U-Ca alteration compounds associated with the ore.

Areas of ore-grade pegmatites contain deep red hematite staining, have undergone at least two periods of alteration, and may show quenching against mafic country rock (R. Alexander, personal communication, 1980). The quench effect creates a sharp contact containing high grades of U-ore and is most pronounced where the fine grained, relatively anhydrous dykes intrude the most mafic gabbro.

Influence of the Structure on the Uranium Mineralization

A regional lineation is present throughout all the rocks and extends into the Algonquin Batholith. In all of these rocks the level of strain and the attitude of the lineation are similar. This was interpreted as being possibly due to diapirism of the batholith during the Grenville Orogeny (Schwerdtner and Lumbers, 1980). The lineation dies out to the south and east side of the McArthur's Mills fault zone (S.B. Lumbers, personal communication, 1981). It occurs as a down dip lineation within the ENE-trending metasediments and as stretched mafic minerals within the metagabbro complex.

The lineation in the mine area strikes dominantly 140°E ± 10° with an average plunge of 40° ranging from 20-70°. Pegmatites locally assume a plunge parallel to this

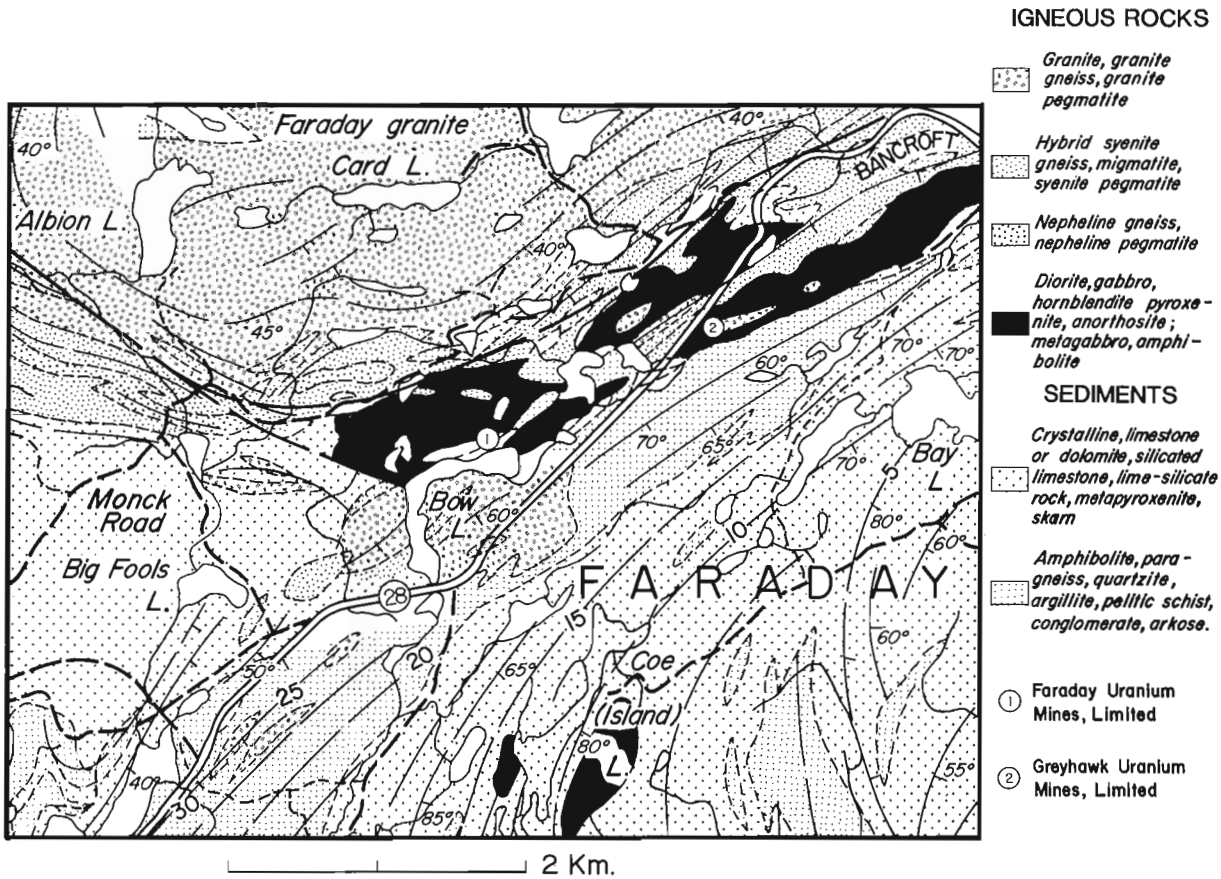

Figure 16.2. *An enlarged portion of Map no. 1957b, Haliburton-Bancroft Area, Ontario Department of Mines (Hewitt and Satterly, 1957).*

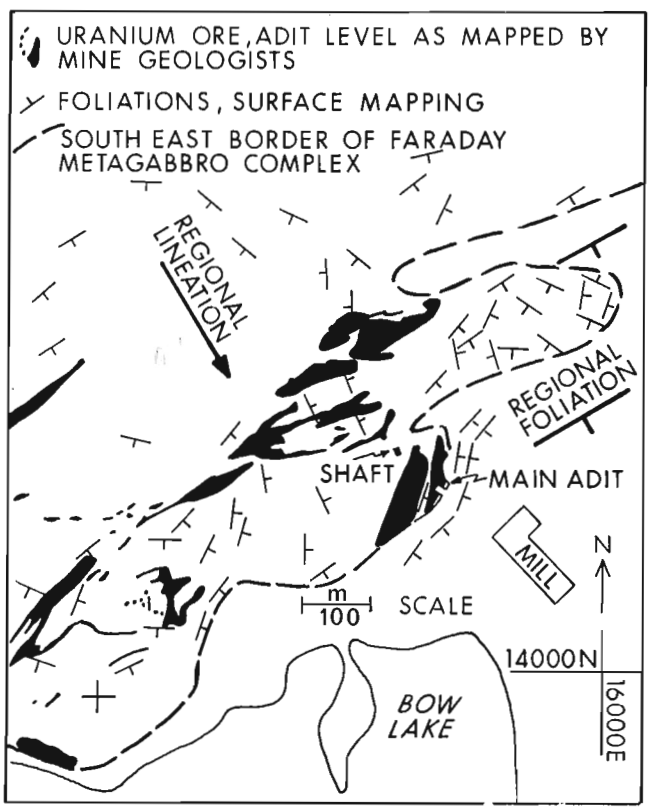

Figure 16.3. *Southeast border region of the Faraday metagabbro complex after Bedell and Schwerdtner (1980).*

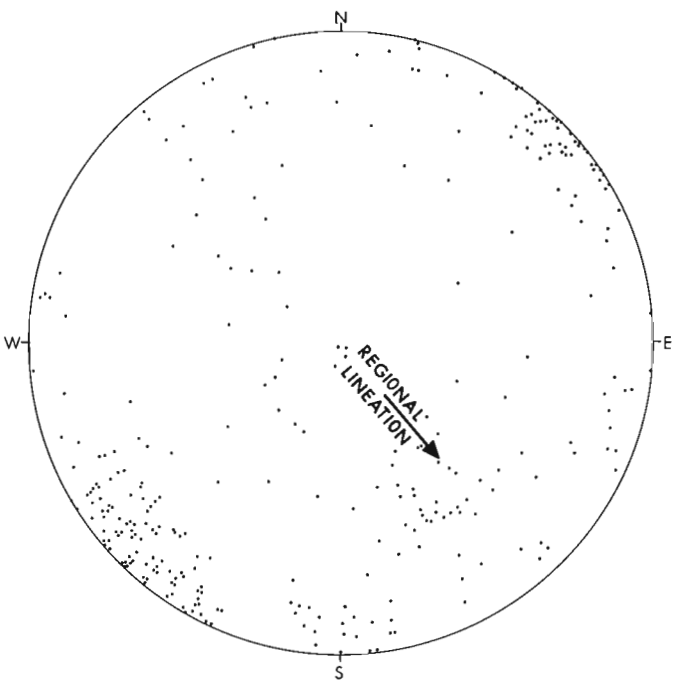

Figure 16.4. *Pi diagram showing poles to joints throughout the Faraday metagabbro complex.*

regional lineation. Most folds delineated within the metagabbro maintain axial planar relationships to the lineation, and the prominent set of joints within the metagabbro is parallel to the strike of the lineation with a second set perpendicular to it (Fig. 16.4).

Foliation within the metagabbro complex is also defined by strained mafic minerals. The boundary of the complex shows well developed foliation (Fig. 16.3), but this weakens towards the centre where lineation is the more dominant strain feature. Foliation is also well developed parallel to the pegmatites. When these hot volatile bodies intruded, they often produced a local foliation that may not represent the original fabric of the metagabbro complex. In interpreting these features, it is important to distinguish the original strain fabric of the complex from the later fabric imposed by pegmatite emplacement. The foliation measurements shown on Figure 16.3 are all from surface mapping. The metagabbro is a topographic high and therefore the fabric observed is above the adit level pegmatites.

The textures and proportions of minerals within the metagabbro complex are variable and may be correlated with strain. The least strained and metamorphosed portions of the complex are made up of an anorthositic gabbro. The feldspar can be as calcic as labradorite and the pyroxene is alkalic. With increase in strain there is an increase in the reaction pyroxene-amphibole, labradorite becomes increasingly sodic, up to oligoclase, and there is a general increase in mafics, e.g. amphibole and biotite. For a more detailed description of the deformation mechanisms, see Bedell and Schwerdtner (1981). The increase in mafics is similar to that found by Schwerdtner and Lumbers (1980) in the Algonquin Batholith. They also correlated strain with the bulk density of the rock.

The arcuate southeast border of the complex (Fig. 16.3) contains parallel arcuate foliation trajectories and coincident pegmatites. This relationship holds for all levels of the mine. It is suggested that this region of high strain, created during intrusion of the metagabbro, became a preferred zone for pegmatite emplacement at a late stage during Grenville metamorphism.

Pegmatites towards the centre of the complex are not easily correlated with the structure of the gabbro complex. However, there appears to be a general parallelism between the pegmatites and the regional foliation. Future work will include testing the hypothesis that the regional ENE fabric imposed an overall strain on the gabbro when it was intruded. The central array of pegmatites may be related to that gross strain pattern.

Geochemical Influence of the Metagabbro Complex on the Uranium Mineralization

The metagabbro complex may be an important ore-controlling factor not only from a structural, but also from a geochemical view point. High grade mineralization, containing uraninite, occurs at the contact with the most mafic country rock or around mafic xenoliths incorporated within the pegmatites. It is suggested that the sulphide-bearing metagabbro reduced the oxygen-rich pegmatite magma causing the precipitation of tetravalent uranium.

Figure 16.5. *Pegmatite dyke, approximately 6 cm across, cutting a hornblende gneiss (lower unit) and a quartz-feldspar gneiss (upper unit). Taken from near post 7, Lookout Trail, Algonquin Provincial Park.*

According to Kimberley (1978), redox reactions are probably the dominant precipitation mechanism for uranium at high temperatures in the same way as they are at low temperatures. However, the scarcity of data concerning high temperature uranium geochemistry introduces some uncertainty regarding the effect of other factors such as pH or cooling.

Another property of the metagabbro may render this rock type particularly suitable to host the uraniferous pegmatites at Madawaska Mines. Its high melting point may have had the effect of more efficiently containing the pegmatite magma than, for instance, a quartzofeldspathic sedimentary or igneous rock which would have a melting point closer to that of the pegmatite melt resulting in a higher plasticity of the host and a greater degree of mixing. This point is illustrated in Figure 16.5, taken in the vicinity of post 7 on the Lookout Trail in Algonquin Provincial Park. The pegmatite dyke intersects an amphibolite and a quartzofeldspathic metasediment. Within the amphibolite, the dyke is well contained but as it progresses into the quartzofeldspathic metasediment it tapers as its constituents mix with the host as a result of lower melting point.

Conclusions

Some time prior to the Grenville Orogeny an alkalic anorthositic gabbro intruded a regional ENE trending fabric. The gabbro body was then subjected to regional metamorphism (Grenville Orogeny) of upper amphibolite grade. During late Grenville metamorphism, pegmatites preferentially intruded the dilatant metagabbro complex along preexisting structures. The sulphide-bearing metagabbro may have acted as a geochemical trap reducing and precipitating the uranium along the contacts with the intruding pegmatites. High melting temperatures of the metagabbro favoured containment of the uranium-bearing pegmatites and minimized dispersion of the mobile elements.

Acknowledgments

I thank my assistants Patrick Ramsay and Steve Hall for help in the field and laboratory, Professor W.M. Schwerdtner of the University of Toronto for initiating and supervising the project, V. Vertolli, S.B. Lumbers and R.I. Gait of the Royal Ontario Museum for assistance in the field and accessibility to their informative collection of rocks and minerals. I also thank S. Masson of Laurentian University and R. Alexander, L. Richardson, and O. Zavesiczky of Madawaska Mines for sharing their knowledge of local geology. I am most grateful for the assistance, financial and otherwise, of the Ontario Geological Survey.

References

Bedell, R.L. and Schwerdtner, W.M.
1980: Structural controls of U-ore bodies in the Madawaska Mines area, Bancroft, Ontario; Ontario Geological Survey, Geoscience Research Abstracts.

1981: Structural controls of U-ore bodies in the Madawaska Mines area, Bancroft, Ontario; Ontario Geological Survey Miscellaneous Paper 98, p. 13-17.

Bright, E.G.
1980: Uranium mineralization associated with mafic to alkalic volcanism within the Late Precambrian Grenville Supergroup, Bancroft area, Ontario; Ontario Geological Survey, Geoscience Research Abstracts.

Hewitt, D.F. and Satterly, J.
1957: Haliburton-Bancroft area; Ontario Department of Mines, Map no. 1957b.

Kimberley, M.M.
1978: High temperature uranium geochemistry; short course in uranium deposits: their mineralogy and origin; ed. M.M. Kimberley; Mineralogical Association of Canada, v. 3, p. 101-103.

Little, H.W.
1969: Anhydrite-pegmatite uranium ore at Bancroft, Ontario; Economic Geology, v. 64, p. 691-693.

Rimsaite, J.Y.H.
1980: Mineralogy of radioactive occurrences in the Grenville Structural Province, Bancroft Area, Ontario: a progress report; in Current Research, Part A, Geological Survey of Canada, Paper 80-1A, p. 253-264.

Schwerdtner, W.M. and Lumbers, S.B.
1980: Major diapiric structures in the Superior and Grenville provinces of the Canadian Shield; in The Continental Crust and its Mineral Deposits, ed. D. Strangway; Geological Association of Canada Special Paper 20, p. 149-180.

17.

URANIUM MINERALIZATION AND LITHOGEOCHEMISTRY OF THE SURPRISE LAKE BATHOLITH, ATLIN, BRITISH COLUMBIA

S.B. Ballantyne[1] and A.L. Littlejohn[1]
Geological Survey of Canada

Ballantyne, S.B. and Littlejohn, A.L., Uranium mineralization and lithogeochemistry of the Surprise Lake Batholith, Atlin, British Columbia; in Uranium in Granites, ed. Y.T. Maurice; Geological Survey of Canada, Paper 81-23, p. 145-155, 1982.

Abstract

The upper Cretaceous quartz monzonitic Surprise Lake Batholith, near Atlin in northwestern British Columbia, exhibits many chemical and petrological peculiarities of 'specialized' granitoid intrusions. Surface rock and diamond drill core samples were examined to ascertain petrographical, mineralogical and lithogeochemical features which might explain its abnormally high radioelement and lithophile element concentrations. The results are developed into a model describing the metallogeny of uranium and base metal mineralization observed within the intrusion.

This granitoid is characterized by high SiO_2 (>76 per cent) and low Al_2O_3 (<12.5 per cent) contents. Similarly to Tischendorf's 'specialized' granites, it shows depletion of TiO_2, FeO, Fe_2O_3, MgO, CaO and elevated K_2O concentrations compared to normal granites. Geochemical enrichment of U, Th, F, Sn, Rb, Li, Y, Nb, Zn, Pb, Ag and depletion of Sr, Ba, Zr, Cu and Mn compared to Turekian and Wedepohl's average low-calcium granite also indicates specialization.

Orthomagmatic uranium-bearing thorite is a ubiquitous though not plentiful accessory mineral, occurring as inclusions in biotite or in quartz. It is thought to be the major primary radioactive mineral responsible for the high average uranium (14.6 ppm) and thorium (45.6 ppm) concentrations found in surface rock samples.

Autometasomatic beta-uranophane mineralization occurs in a zone of argillic alteration. This redistributed uranium results in concentrations of up to 150 ppm U and explains a strong linear increase in the U/Th ratio with increasing uranium concentrations. Analyses of thorites from different parts of the intrusion suggest that uranium leached from this mineral was probably the main source of uranium for the beta-uranophane.

Postmagmatic processes are demonstrated by the presence of authigenic kasolite and metazeunerite in some near surface fractures within the quartz monzonite. Other postmagmatic processes are shown by the sphalerite-magnetite veins at the apex of the intrusion and base metal enrichments within the drill core. The base metal mineralization appears to postdate the lithophile enrichment.

Résumé

Le batholite monzonitique-quartzifère de Surprise Lake, datant de la fin Crétacé, près de Atlin dans le nord-ouest de la Colombie Britannique, présente plusieurs particularités chimiques et pétrologiques des intrusions granitoïdes 'spécialisées'. On a examiné des roches de surface et des échantillons de carottes obtenues par forage au diamant, afin de vérifier les propriétés pétrographiques, minéralogiques et lithogéochimiques qui pourraient expliquer les concentrations anormalement élevées des radioéléments et d'éléments lithophiles de cette intrusion. On a utilisé les résultats pour mettre au point un modèle décrivant la métallogénie de l'uranium et la minéralisation en métaux de base observée à l'intérieur de l'intrusion.

Ce granitoïde est caractérisée par une teneur élevée en SiO_2 (>76 per cent) et une faible teneur en Al_2O_3 (<12.5 per cent). Comme dans le cas des granites 'spécialisés' de Tischendorf, il présente également un appauvrissement en TiO_2, FeO, Fe_2O_3, MgO et CaO, et des concentrations élevées de K_2O par comparaison avec les granites normaux. L'enrichissement géochimique en U, Th, F, Sn, Rb, Li, Y, Nb, Zn, Pb, Ag et l'appauvrissement en Sr, Ba, Zr, Cu et Mn, par comparaison avec le granite de Turekian et Wedepohl à faible teneur moyenne en calcium, indiquent aussi cette spécialisation.

La thorite orthomagmatique uranifère est omniprésente, bien qu'elle ne soit pas un minéral accessoire abondant; on la retrouve sous forme d'inclusions dans la biotite ou dans le quartz. On pense que les concentrations moyennes élevées d'uranium (14.6 ppm) et de thorium (45.6 ppm) qu'on trouve dans des échantillons de surface sont dues principalement à ce minéral primaire radioactif.

La minéralisation autométasomatique en béta-uranophane se rencontre dans une zone d'altération argillique. Ce minéral est responsable pour des concentrations d'uranium allant jusqu'à 150 ppm et explique une forte augmentation linéaire du rapport U/Th avec une augmentation des concentrations d'uranium. Les analyses de thorites provenant de différentes parties de l'intrusion permettent de croire que de l'uranium lessivé de ce minéral a été la source principale de l'uranium du béta-uranophane.

[1] 601 Booth Street, Ottawa, Ontario K1A 0E8

Les transformations post-magmatiques sont démontrées par la présence de kasolite authigène et de métazeunérite dans des fractures situées près de la surface à l'intérieur de la monzonite-quartzifère. D'autres transformations post-magmatiques sont révélées par des filons de sphalérite-magnétite au sommet de l'intrusion et par des enrichissements en métaux de base à l'intérieur des carrotes de forage. La minéralisation en métaux de base semble s'être produite après l'enrichissement en éléments lithophiles.

Introduction

The Surprise Lake Batholith covers an area of approximately 30 x 54 km^2 and is located east of Atlin, British Columbia (Fig. 17.1, 17.2). It is a leucocratic, hypidiomorphic, medium grained, inequigranular quartz monzonite dated at 73.5 ± 2.5 Ma (N.C. Carter, personal communication, 1979). The occurrence of uranium in the area was first noted by Aitken (1959) and further geochemical studies by Ballantyne et al. (1978) confirmed the uranium potential of the batholith. Regional stream sediment and water survey results collected during the National Geochemical Reconnaissance – Uranium Reconnaissance Program (Geological Survey of Canada, 1978) showed that 93 samples from streams draining the Surprise Lake Batholith contained anomalous uranium concentrations. Stream waters were reported to have an arithmetic mean of 1.05 ppb over a range of 0.02-5.6 ppb uranium; stream sediments yielded an arithmetic mean of 56.6 ppm over a range of 2.4-399.0 ppm uranium.

In this paper, diamond drill core and surface rock samples are examined petrographically and lithogeochemically in an attempt to formulate a genetic model to explain the various types of uranium concentrations within the intrusion.

Geology

The Surprise Lake quartz monzonite exhibits a variety of textures with contacts that are both gradual and abrupt (Aitken, 1959). In core samples from three diamond drill holes located near Trout Lake (Fig. 17.2, 17.3) fine grained equigranular varieties occur in the upper portions of DDH78-1 and DDH78-2 and coarse grained varieties occur in DDH78-3. Inequigranular varieties with small phenocrysts of alkali feldspar often constitute the more typical medium grained textural type. The rock consists of perthitic alkali feldspar, rounded smoky quartz often in graphic intergrowth with the perthite, plagioclase laths and minor biotite. Interstitial fluorite and muscovite overgrowths on biotite represent the last stage of crystallization. Miarolitic cavities are found in places. Common accessory minerals in unaltered quartz monzonite are ilmenite, zircon, monazite and uranium-bearing thorite. Arsenopyrite is rare. These minerals are usually found as subidiomorphic inclusions in or near the biotite and not all occur in every sample.

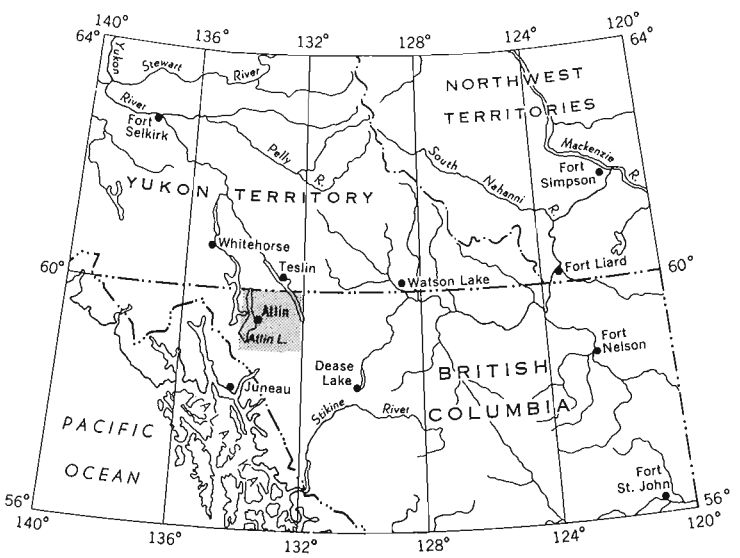

Figure 17.1. *Location of study area.*

Hydrothermal alteration of the quartz monzonite is pervasive and is associated with fracturing and jointing within the intrusion. Two alteration assemblages have been recognized – propylitic and argillic. The propylitic assemblage (montmorillonite, chlorite, sericite, quartz, stilbite) is dominant in DDH78-3 which was drilled in a deeper level of the intrusion than DDH78-1 and DDH78-2 (Fig. 17.3). Fracturing and alteration are less intense in these rocks compared to others examined for this report. The argillic assemblage (kaolinite, sericite, montmorillonite, nontronite, manganese oxides, quartz) is dominant in DDH78-1 and DDH78-2. In these rocks, montmorillonite rather than chlorite is the alteration product of biotite and also of plagioclase. Nontronite, quartz and manganese oxides form in fractures; sericite and kaolinite replace alkali feldspar.

Mineralization

In addition to uranium, Aitken (1959) reports tungsten mineralization within the batholith. At the Adanac deposit, molybdenite mineralization is found in the 22 km^2 partially zoned Mount Leonard boss (Fig. 17.2), a quartz monzonite satellite of the main batholith west of Surprise Lake (White et al., 1976).

On Weir Mountain (Fig. 17.2, 17.3), which can be considered to lie near the apex of the batholith, a system of fractures and vein-like bodies occurs within sheared and silicified quartz monzonite. Fluorite and sphalerite-magnetite mineralization are confined to the veins; kasolite, metazeunerite and wulfenite occur in fractured rocks. In the purple fluorite-bearing veins, fluorite forms aggregates within an altered matrix of quartz, perthite, plagioclase and chlorite. Niobium-bearing ilmenite and cassiterite are minor vein constituents. The sphalerite-magnetite veins contain variable amounts of these minerals and dark green Mn-bearing biotite or chlorite in an altered matrix of quartz, perthite and plagioclase.

In the Trout Lake drill cores, magnetite, sphalerite, galena, pyrite and chalcopyrite are also found in fractures; intense sphalerite mineralization occurs in highly altered or silicified quartz monzonite. Sphalerite, sometimes rimmed by magnetite, has replaced argillized feldspars and quartz. In DDH78-1 and DDH78-2 beta-uranophane occurs as bright yellow prismatic crystals up to 1 mm in length on fracture planes, interstitially to quartz grains and feldspar, in small miarolitic cavities, and within argillized feldspars. Thin coatings of this mineral also occur on quartz, feldspars and on fracture walls. It is found sporadically to depths of 60 m in both relatively fresh and intensely altered rock (Fig. 17.4). Samples from DDH78-3 do not contain beta-uranophane.

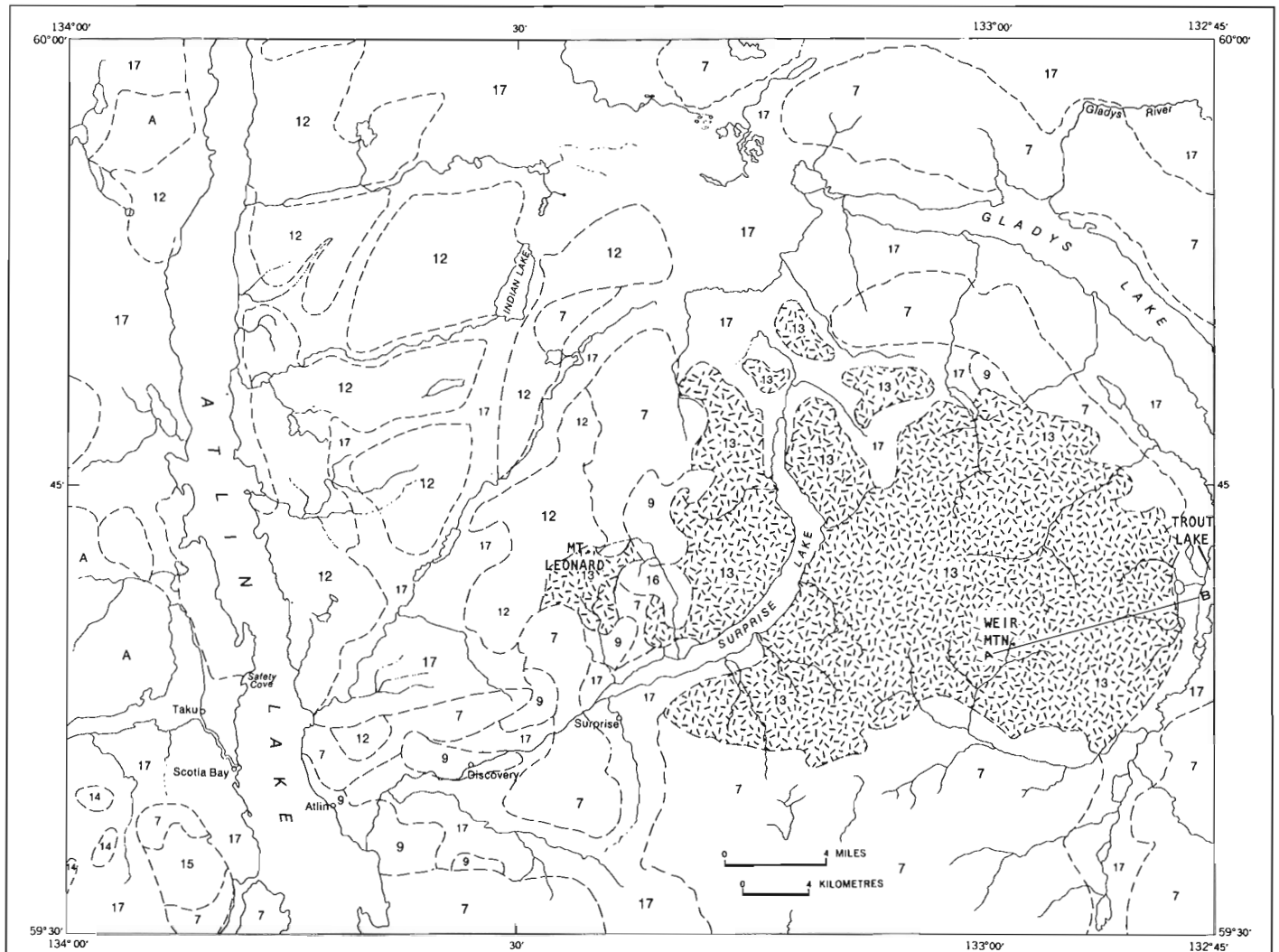

LEGEND

CENOZOIC

QUATERNARY
PLEISTOCENE AND RECENT
17 — *Glacial drift, alluvium.*

TERTIARY AND QUATERNARY
16 — *Olivine basalt and scoria.*

TERTIARY (?)
15 — *Quartz monzonite; granophyre; gabbro and diorite.*

CRETACEOUS OR TERTIARY
SLOKO GROUP
14 — *Andesite, basalt; rhyolite, conglomerate, sandstone.*

CRETACEOUS
13 — *Alaskite, quartz monzonite*

JURASSIC *(May be in part older and younger)*
COAST INTRUSIONS
12 — *Undifferentiated granitic rocks.*

PALEOZOIC

PENNSYLVANIAN AND PERMIAN
ATLIN INTRUSIONS
9 — *Peridotite; meta-diorite and meta-gabbro; serpentinite*

CACHE CREEK GROUP
7 — *Chert, argillite, chert-pebble conglomerate; greenstone and volcanic greywacke; limestone and limestone breccia*

A — *Undifferentiated, mainly volcanic rocks of uncertain, possibly several ages, perhaps Triassic.*

Figure 17.2. *General geology, Surprise Lake Batholith (Unit 13), British Columbia, after Aitken (1959).*

Lithogeochemistry

Major and minor element results in Table 17.1 characterize the Surprise Lake Batholith as a 'specialized' granitoid according to Tischendorf's (1977) classification. Compared to Tischendorf's 'normal' granites this batholith exhibits higher contents of SiO_2 and K_2O and lower contents of Al_2O_3, TiO_2, Fe_2O_3, MgO and CaO. Examination of the selected trace element data contained in Table 17.2 shows it to be enriched in U, Th, Li, Rb, Y, Nb, Sn, Zn, Pb, Ag, F and depleted in Sr, Zr, Ba, Cu and Mn compared to the low-calcium granites of Turekian and Wedepohl (1961).

Figure 17.5 shows the distribution and variation of U and Th contents of the drill core samples. A strong linear increase in the U/Th ratio with increasing U concentrations is evident (Fig. 17.5a). The U/Th ratio appears to be independent of Th concentration (Fig. 17.5b). These relationships indicate that uranium has been redistributed within the batholith while thorium has remained relatively fixed. A plot of U against Th (Fig. 17.5c) does not clearly indicate these relationships. These figures also indicate that the satellite Mount Leonard boss has similar radioelement concentrations and distribution as the Surprise Lake Batholith.

Figure 17.4 profiles the U and Th concentrations of Trout Lake drill core samples, the U/Th ratio, and the location of mineralization at various depths. The arithmetic means for uranium and thorium for all the cores sampled in each drill hole are also illustrated. Profiles for drill holes DDH78-1 and DDH78-2 (Fig. 17.4a, b) demonstrate that the increase in U/Th ratio with increasing uranium concentration (up to 150 ppm) results from the accumulation of beta-uranophane in the zone of argillic alteration. The relatively constant U/Th ratio profile for DDH78-3 (Fig. 17.4c) indicates that uranium has not been redistributed in the zone of propylitic alteration which occurs at a deeper level of the intrusion.

Discussion

Four major classes of uranium occurrences related to magmatic evolution have been recognized by Mathews (1978). These are: (1) orthomagmatic, (2) pegmatitic, (3) hydrothermal and (4) metasomatic. During the orthomagmatic stage of crystallization, syngenetic disseminated uranium minerals form at the same time as the major rock-forming minerals. During ascent of a magma, a water-rich fluid charged with lithophile elements (including uranium) is formed. If the magma is tapped at this stage of its evolution then pegmatitic and hydrothermal uranium deposits may form. If the magma remains untapped, then the late stage aqueous phase may permeate the crystallized pluton and cause metasomatic alterations and enrichment of uranium rather than pegmatites or hydrothermal veins. A genetic model for uranium mineralization in the Surprise Lake Batholith is schematically illustrated in Figure 17.3.

Abundant contacts between quartz monzonites of differing texture suggests that the batholith may have evolved in part by foundering of roof blocks that consisted of solidified quartz monzonite (Aitken, 1959). Pegmatites and aplites are lacking and miarolitic cavities are present, suggesting that final solidification was roughly synchronous with saturation of the magma. Thus, much of the uranium was not fractionated into a separate aqueous phase but remained initially in the orthomagmatic phase.

Abundant interstitial fluorite, deuteric overgrowths of muscovite on biotite, and pervasive argillic alteration in the upper levels of the pluton indicate reactions between late-stage aqueous magmatic fluids and the previously crystallized

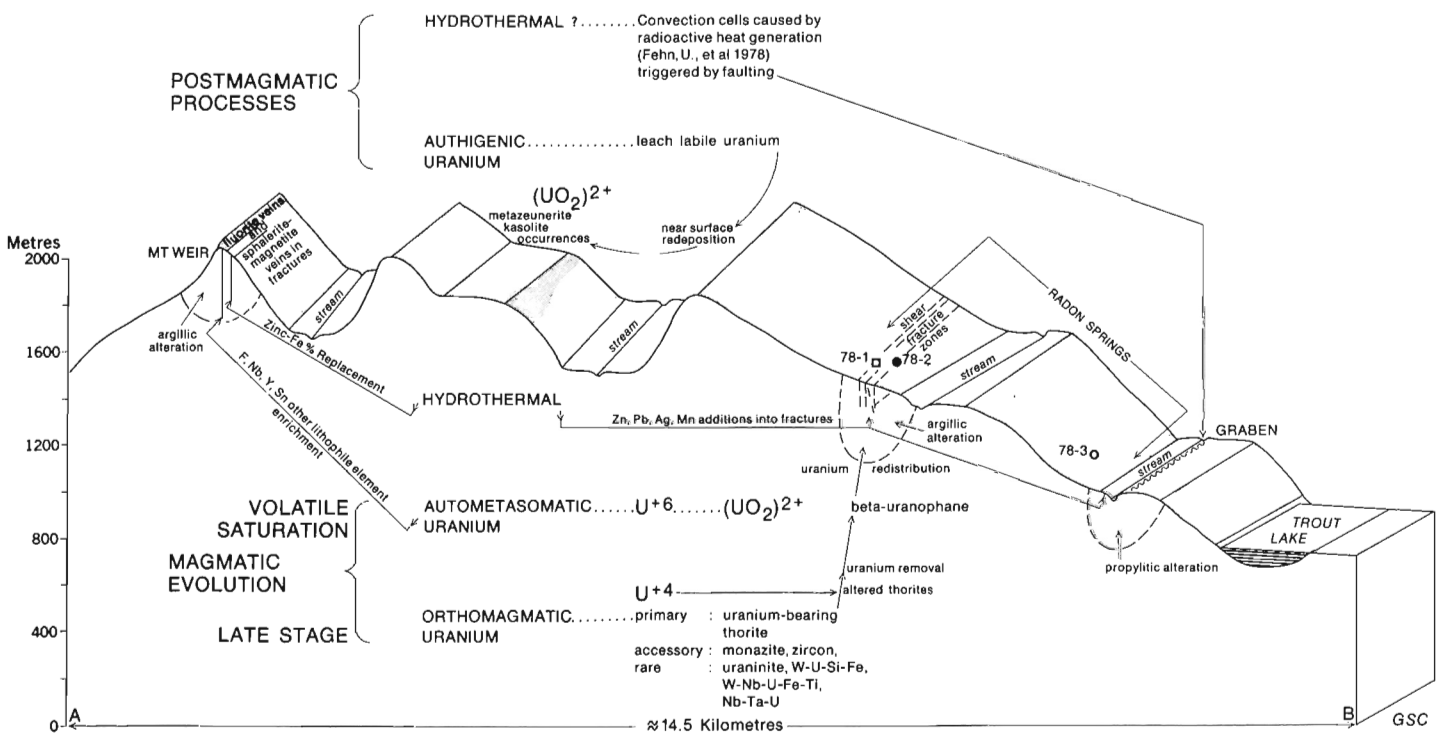

Figure 17.3. *Schematic genetic model of mineralization within the Surprise Lake Batholith along cross-section AB (Weir Mtn.-Trout Lake), Figure 17.2. 78-1 to 78-3 are locations of diamond drill holes (DDH).*

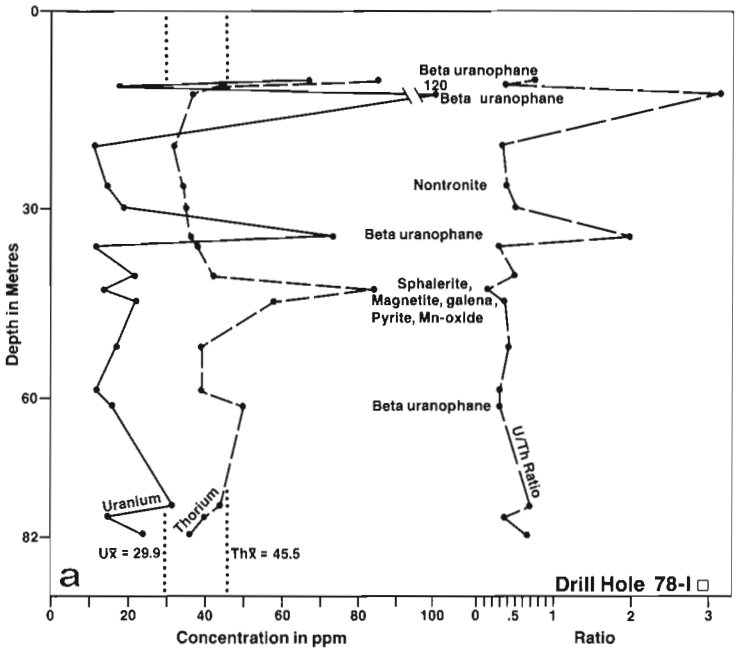

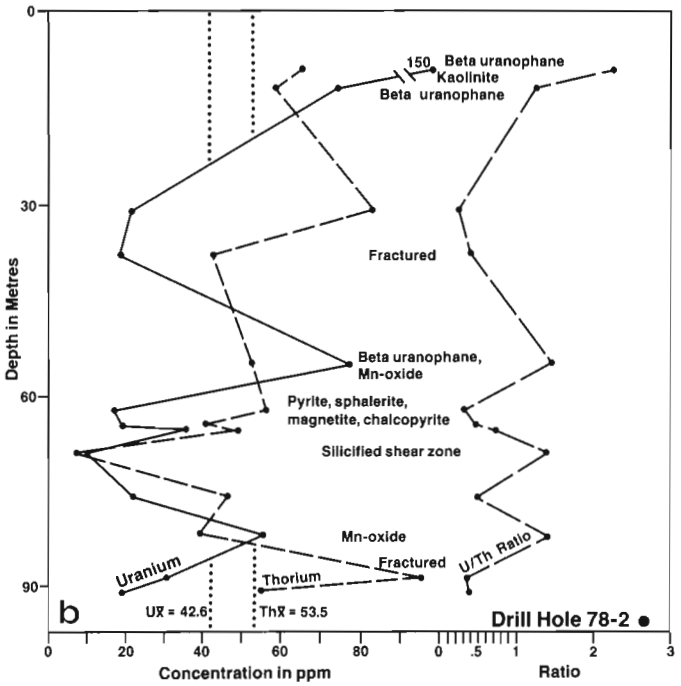

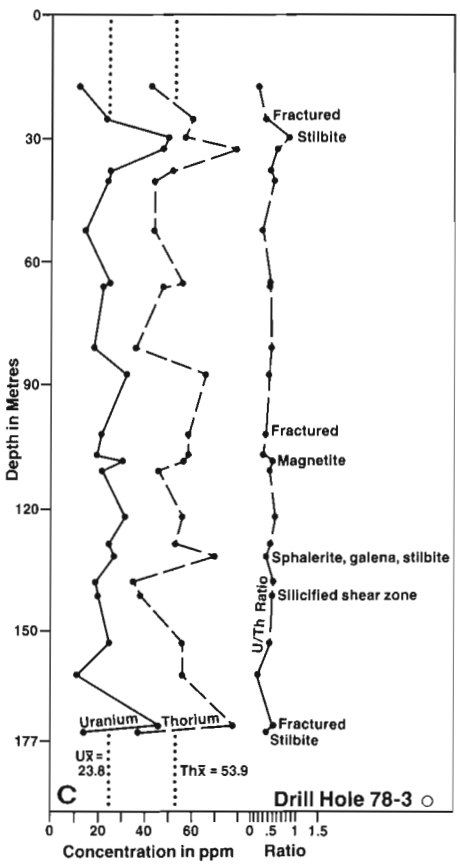

a. Vertical profile drill hole 78-1, argillic alteration,

b. Vertical profile drill hole 78-2, argillic alteration,

c. Vertical profile drill hole 78-3, propylitic alteration.

Figure 17.4. *U and Th concentrations, U/Th ratios and observed mineralization for drill core samples, Trout Lake area, Surprise Lake Batholith.*

Table 17.1. Average* major and minor element composition** of the Surprise Lake Batholith and some specialized, or low-calcium, or tin-bearing granites of the world

Region or Source	Surprise Lake Batholith, Atlin, British Columbia, Canada	Fresh granite, Lost River Mine, Seward Peninsula, Alaska U.S.A.	Specialized or stannigene granites (Group I)	Normal granites (Group III)	Average biotite alkali granite	Biotite granite, Younger Granite Province, Northern Nigeria	Weighted mean of tin-bearing granites of the world (without Bolivia)
Author	this paper	Salinsbury (1964)	Tischendorf (1977)	Tischendorf (1977)	Nockolds (1954)	MacLeod, et al. (1971)	Stemprok and Skvor (1974)
Number of Analyses	54	3	(67 averages) 962 samples	(7 averages) 2327 samples	12	12	
SiO_2	76.68	75.73	73.38 ± 1.39	70.84 ± 1.41	75.01	75.49	73.02
TiO_2	0.09	0.02	0.16 ± 0.10	0.34 ± 0.08	0.17	0.12	0.21
Al_2O_3	12.30	13.63	13.97 ± 1.07	14.33 ± 0.23	13.16	12.62	13.90
Fe_2O_3	0.60	0.24	0.80 ± 0.47	1.31 ± 0.29	0.94	0.62	0.74
FeO	0.52	0.56	1.10 ± 0.47	1.78 ± 0.38	0.88	1.02	1.34
Total iron	-	-	-	-	-	-	-
MnO	0.01	0.11	0.045 ± 0.040	0.064 ± 0.03	0.07	0.02	0.05
MgO	0.09	0.19	0.47 ± 0.56	0.81 ± 0.23	0.24	0.16	0.52
CaO	0.58	0.63	0.75 ± 0.41	1.89 ± 0.40	0.56	0.54	1.24
Na_2O	2.97	3.47	3.20 ± 0.61	3.44 ± 0.32	3.48	4.18	3.28
K_2O	4.68	4.70	4.69 ± 0.68	4.34 ± 0.52	5.16	4.63	4.57
P_2O_5	0.03	0.00	-	-	0.11	0.03	0.15
H_2O	0.80	0.89	-	-	0.37	0.47	0.90
CO_2	0.10	0.07	-	-	-	-	-
Li_2O	-	-	0.059	0.008	-	-	-
F	0.39	0.55	0.318 ± 0.15	0.085	-	0.20	-
Cl	0.024	-	-	-	-	-	-

* Surprise Lake Batholith, median values; other data, arithmetic mean. Concentrations in per cent.
** Analytical methods (Surprise Lake Batholith) : F by fusion and specific-ion electrode, Cl by colorimetric method, other analyses by X-ray fluorescence.

Table 17.2. Average* selected trace element composition** of the Surprise Lake Batholith, low-calcium granites, and the stanniferous Younger Granites, Nigeria

Region or Source	n	U	Th	Li	Rb	Sr	Y	Zr	Nb	Sn	Ba	Ta	Zn	Cu	Pb	Ag	Mn	As	Mo	W	F	Cl
A	17	18	39	82	450	60	98	140	37	5	280	<5	145	9	30	0.33	90	1.2	2	1	3927	302
B	13	22	53	86	490	40	146	130	56	46	60	<5	211	9	40	0.40	75	8.0	2	1	4000	206
C	24	25	56	88	460	50	113	150	39	8	120	<5	52	4	22	0.23	105	1.1	2	1	3750	189
D	-	4.7	20	40	170	100	41	175	21	3	840	4.2	39	10	19	0.037	390	1.5	1.3	2.2	850	200
E	73	-	46	84	651	7	157	177	136	22	68	-	166	16	24	-	170	-	-	-	4330	-

A – Drill core samples (DDH78-1) Surprise Lake Batholith: argillic alteration.
B – Drill core samples (DDH78-2) Surprise Lake Batholith: argillic alteration.
C – Drill core samples (DDH78-3) Surprise Lake Batholith: propylitic alteration.
D – Low-Ca granites: Turekian and Wedepohl (1961).
E – Means of Trace Elements in stanniferous granites, from the Younger Granites, northern Nigeria, Olade (1980).

* A, B and C, median values; D and E, arithmetic mean
** Analytical methods (A, B and C): Zn, Cu, Pb, Ag, Mn, Mo, As, Li by atomic absorption spectrophotometry following a total decomposition using HF, HNO_3, $HClO_4$ acid mixture; Nb, Ta, Y, Sn, Rb, Sr, Zr by X-ray fluorescence; U and Th by neutron activation analysis; W, by colorimetric method; F by fusion and specific-ion electrode; Cl by colorimetric method.

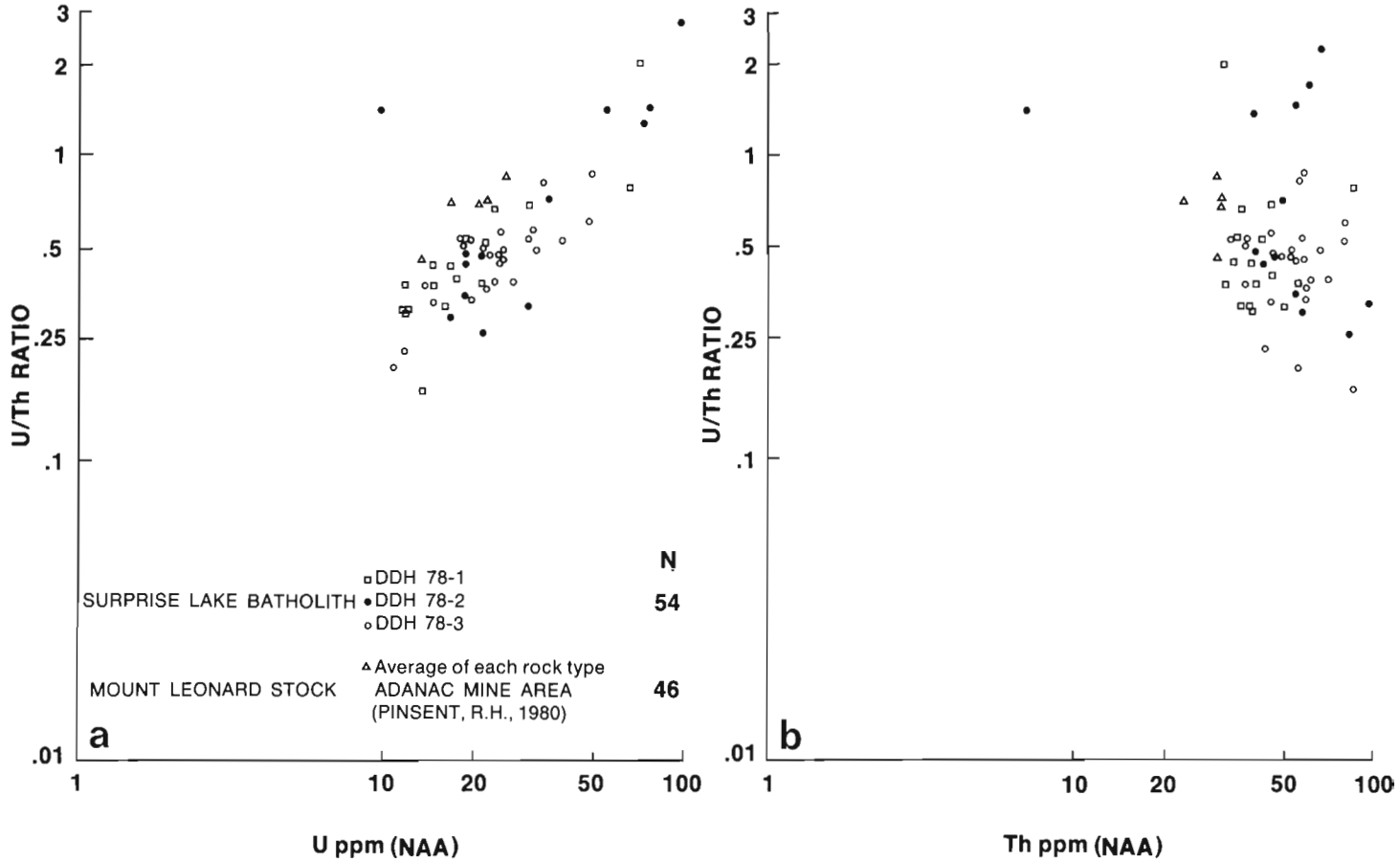

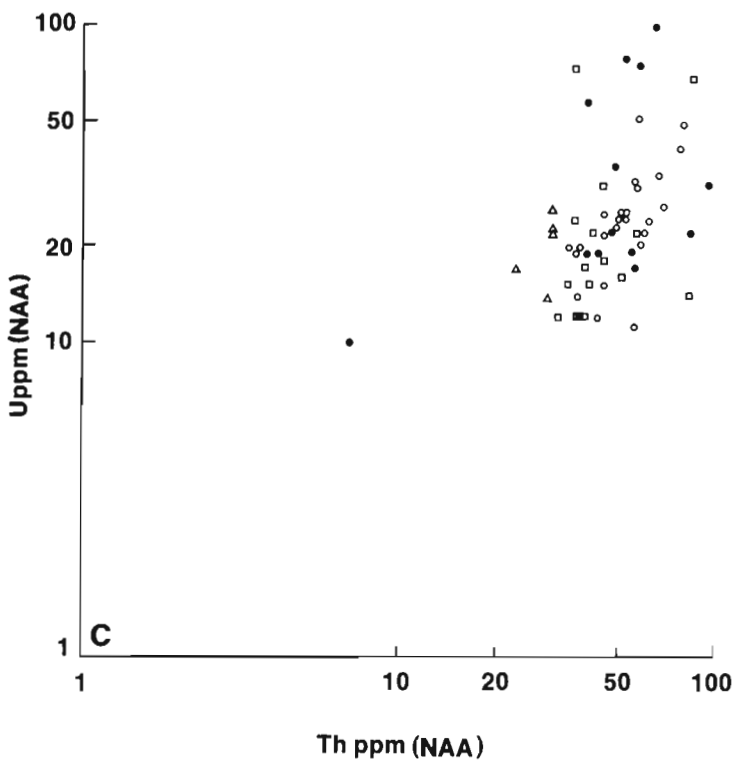

a. U ppm versus U/Th ratio,

b. Th ppm versus U/Th ratio,

c. U ppm versus Th ppm.

Figure 17.5. *U and Th relationships in drill core samples from the Surprise Lake Batholith (n=54) and its satellite, the Mount Leonard boss (n=46). U and Th determined by neutron activation analysis.*

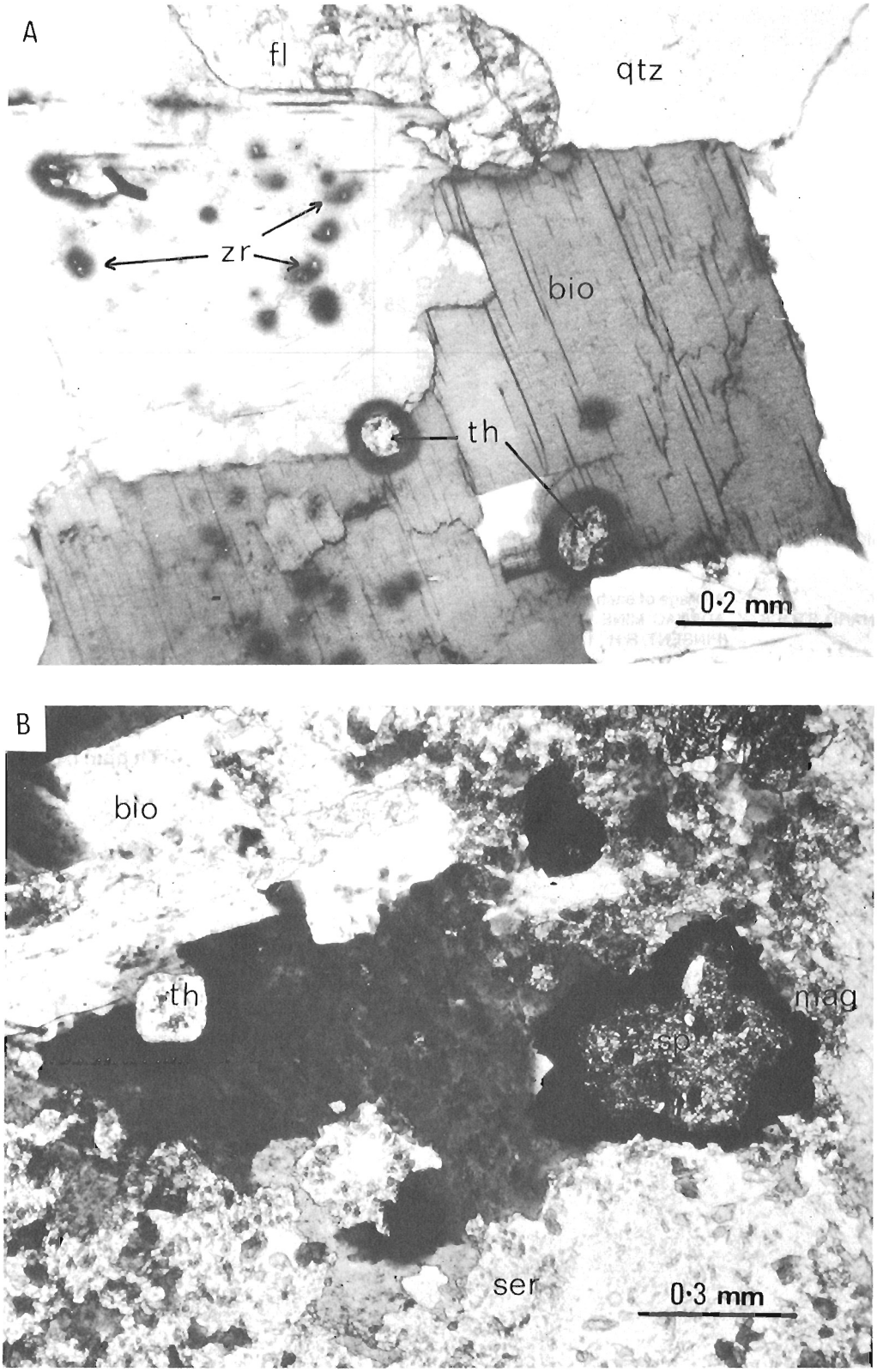

A. Surprise Lake Batholith quartz monzonite, B. Sphalerite-magnetite veins, Weir Mtn. Minerals shown are thorite (th), biotite (bio), zircon (zr), quartz (qtz), fluorite (fl), sericite (ser), sphalerite (sp) and magnetite (mag.)

Figure 17.6. *Photomicrographs of orthomagmatic thorite.*

quartz monzonite. At the apex of the intrusion (Weir Mountain), where these fluids would be concentrated, they penetrated along fractures and partially replaced the quartz monzonite forming fluorite veins. The lithophile nature of these fluids is confirmed by the presence of small amounts of cassiterite and niobium-bearing ilmenite in these veins, and by the fluorite itself which is yttrium-bearing. Such a fluid would oxidize tetravalent orthomagmatic uranium and remove it as hexavalent uranium during autometasomatism. Thorium would remain in the orthomagmatic phase.

Orthomagmatic uranium-bearing thorite is a ubiquitous, though not plentiful accessory mineral, occurring as inclusions in biotite or in quartz (Fig. 17.6A). This mineral is also found as an accessory in the fluorite and sphalerite-magnetite veins. It has the same habit as in the quartz monzonite but is included in chlorite, biotite, fluorite, sphalerite, and in a clay mineral matrix (Fig. 17.6B). It is probably the major radioactive mineral responsible for the high uranium and thorium contents of the Surprise Lake Batholith as shown by forty-six surface rock samples collected from the Trout Lake area. These contained an average of 14.6 ppm uranium and 45.6 ppm thorium. Other very rare orthomagmatic accessory uranium minerals are uraninite and unidentified altered phases containing W-U-Si-Fe, W-Nb-U-Fe-Ti and Nb-Ta-U assemblages. Zircon and monazite are also present but contain only traces of uranium.

Table 17.3. Electron microprobe analyses of thorites illustrated in Figure 17.7 (oxide wt. %)

	A	B	C
SiO_2	22.9	16.0	10.5
P_2O_5	-	0.7	2.8
CaO	-	2.6	0.3
Y_2O_3	0.8	0.8	4.0
ThO_2	52.8	52.0	52.9
UO_2	23.4	14.8	5.0
H_2O*	0.1	13.1	24.5

* Calculated by the difference between the sum of the oxides and 100%. Other light elements (e.g. F, C) may be present.

Autometasomatic uranium mineralization occurs in the form of beta-uranophane in the argillized quartz monzonite in DDH78-1 and DDH78-2. This redistributed uranium accounts for the high uranium levels (up to 150 ppm) observed in the drill core samples and explains the strong increase in U/Th ratio with increasing U concentration (Fig. 17.4, 17.5).

Evidence for leaching of orthomagmatic uranium minerals by autometasomatic fluids was confirmed by the analysis of thorites. With rare exceptions all the thorites have been altered by hydration to some degree. Progressive hydration of thorite is illustrated in Figure 17.7 and Table 17.3. As alteration increases, the appearance of the grains changes from a well formed cubic uranothorite (Fig. 17.7A) to a mottled grain of low relief surrounded by cracks along which the attacking solution has passed and deposited late forming minerals such as fluorite, pyrite and sericite (Fig. 17.7B, C). There is a significant decrease in UO_2 and SiO_2 as H_2O increases, while ThO_2 remains constant.

Analysis of thorites (Table 17.4) from the different zones of alteration and levels of the intrusion show that uranium loss from thorites is probably the major source for autometasomatic beta-uranophane mineralization. If unaltered uranothorite represents the composition of the primary orthomagmatic mineral, then the altered thorites in the different zones are depleted in uranium relative to the unaltered grain, while thorium remains constant. Thorites from unmineralized core (DDH78-3) contain on average 3.5 times the uranium concentration found in thorites from mineralized beta-uranophane-bearing core (DDH78-1, 2) and veins.

Table 17.4. Means and ranges of thorite analyses, Surprise Lake Batholith (wt %)

	Unaltered uranothorite DDH78-2	Beta-uranophane-free core DDH78-3	Beta-uranophane-bearing core DDH78-1, 78-2	Fluorite veins Mt. Weir	Sphalerite-magnetite veins Mt. Weir
n	1	9	5	2	4
Si	10.7	7.0 (4.8-8.3)	5.0 (3.8-6.2)	4.3 (4.2-4.3)	6.7 (4.2-10.4)
P	-	0.5 (0.2-0.9)	1.5 (0.9-2.3)	2.6 (1.1-4.1)	0.3 (0.0-0.8)
Ca	-	1.2 (0.3-1.8)	0.2 (0.0-0.3)	0.3 (0.1-0.4)	- -
Fe	-	0.3 (0.0-0.8)	0.3 (0.0-0.7)	0.5 (0.0-0.9)	4.2 (2.9-6.2)
Zn	-	- -	- -	- -	1.8 (0.7-3.4)
Y	0.6	1.4 (0.4-3.6)	3.6 (0.3-6.9)	9.9 (8.7-11.1)	2.9 (0.2-6.6)
Pb	-	- -	- -	- -	1.1 (0.0-3.0)
Th	46.4	46.7 (42.3-52.4)	49.7 (38.7-58.7)	42.2 (34.5-49.8)	47.8 (34.4-56.3)
U	20.6	12.6 (0.4-23.8)	3.6 (0.2-6.3)	3.0 (0.7-5.3)	2.6 (0.9-3.4)

Analytical methods: Energy dispersive spectrometry using an electron microprobe. The data were corrected for background, peak overlap and matrix effects. The precision of the analysis is ±4% of the amount present for concentrations >5.0 wt %. For <5.0 wt % the error is somewhat greater and increases with decreasing concentration.

n = number of thorite grains analyzed.

- = not detected.

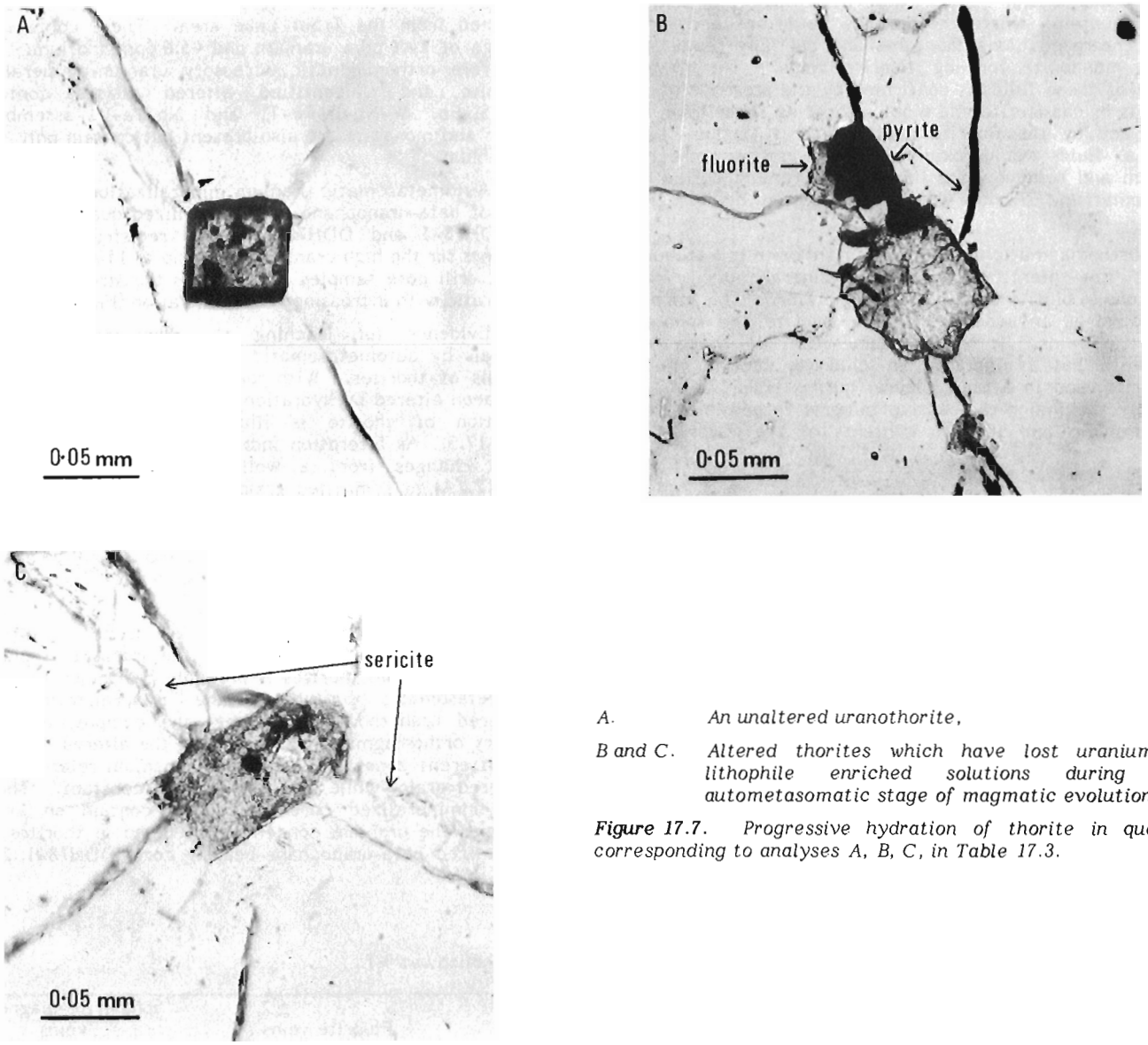

A. *An unaltered uranothorite,*

B and C. *Altered thorites which have lost uranium to lithophile enriched solutions during the autometasomatic stage of magmatic evolution.*

Figure 17.7. *Progressive hydration of thorite in quartz, corresponding to analyses A, B, C, in Table 17.3.*

Postmagmatic processes may remove labile uranium and concentrate it within or outside the pluton. The broad pattern of anomalous concentrations of uranium is stream water and sediments associated with the Surprise Lake Batholith indicates the presence of a leachable uranium component. At the surface of the intrusion, authigenic kasolite and metazeunerite occur as coatings on fracture walls within the quartz monzonite. Wulfenite is found associated with the kasolite. This demonstrates that concentration of labile uranium into secondary enrichments occurs in the surficial environment.

Other postmagmatic processes are shown by the presence of sphalerite-magnetite veins on Weir Mountain and base metal enrichments within the drill core (Fig. 17.3, 17.4). Textural evidence suggests that the sphalerite-magnetite veins postdate the fluorite vein emplacement. Thorites from both types of veins and mineralized (beta-uranophane-bearing) core are enriched in yttrium compared to unmineralized core (Table 17.4). This is a result of lithophile enrichment during autometasomatism. However, only thorites found in the replacement sphalerite-magnetite veins are enriched in zinc, lead and iron (Table 17.4) suggesting that the base metal mineralization postdates the lithophile enrichment.

According to Fehn et al. (1978), postmagmatic processes within granites of abnormally high radioelement contents may include the development of convection cells driven by the radiogenic heat generated within the granite. They used as their model the Conway Granite of New Hampshire which has been described as a low – grade uranium – thorium resource (Adams et al., 1962). The similarity between the two plutons (Conway and Surprise Lake) is striking when the size, uranium/thorium concentrations and permeability (abundance of fractures and joints) are compared. Fehn et al. (1978) concluded that postmagmatic hydrothermal uranium deposits may form within an area of

strong upwelling or strong downwelling of fluids within a convection cell. The unusually high radon content of springs (Fig. 17.3) issuing at deep joints may reflect buried post-magmatic hydrothermal uranium deposits formed in this manner.

Acknowledgments

The authors gratefully acknowledge the co-operation of Union Oil Company of Canada Ltd., Getty Mines Ltd., and Malabar Mines Ltd., who kindly donated the drill core samples for this study. We also thank Mattagami Lake Mines Ltd. and Placer Development Ltd. for their assistance, and Dr. N.C. Carter for the age determination of the Surprise Lake Batholith. We thank A.C. Roberts for the mineral identification by XRD and G.J. Pringle for assistance with the microprobe work.

References

Adams, J.A.S., Kline, M.C., Richardson, K.A., and Rogers, J.J.W.
1962: The Conway Granite of New Hampshire as a major low-grade thorium resource; National Academy of Sciences, Proceedings, v. 48, p. 1898-1905.

Aitken, J.D.
1959: Atlin Map Area, B.C. (104N); Geological Survey of Canada, Memoir 307, 89 p.

Ballantyne, S.B., Boyle, D.R., Goodfellow, W.D., Jonasson, I.R., and Smee, B.W.
1978: Some orientation surveys for uranium mineralization in parts of the Atlin Area, British Columbia; in Current Research, Part A, Geological Survey of Canada, Paper 79-1A, p 467-471.

Fehn, U., Cathles, L.M., and Holland, H.D.
1978: Hydrothermal convection and uranium deposits in abnormally radioactive plutons; Economic Geology, v. 73, p. 1556-1566.

Geological Survey of Canada
1978: Regional stream sediment and water geochemical reconnaissance data, northwestern British Columbia (NTS 104N); Geological Survey of Canada, Open File 517, National Geochemical Reconnaissance, Release NGR 28-1977 (Revised and re-released 1979), 389 p.

MacLeod, W.N., Turner, D.C., and Wright, E.P.
1971: The geology of the Jos Plateau, Volume 1, General Geology; Geological Survey of Nigeria, Bulletin no. 32, 119 p.

Mathews, G.W.
1978: Uranium occurrences in and related to plutonic igneous rocks; in Geologic Characteristics of Environments Favourable for Uranium Deposits, GJBX-67(78), BENDIX Field Engineering Corp., Grand Junction, Colo., p. 121-180.

Nockolds, S.R.
1954: Average chemical compositions of some igneous rocks; Geological Society of America, Bulletin, v. 65, no. 10, p. 1007-1032.

Olade, M.A.
1980: Chemical characteristics of tin-bearing and tin-barren granites, Northern Nigeria; Economic Geology, v. 75, no. 1, p. 71-82.

Pinsent, R.H.
1980: Report on the uranium content and distribution in the Adanac Molybdenum deposit, Atlin Mining Division, 104N, British Columbia; prepared by Placer Development Ltd., submitted to 'The Royal Commission of Inquiry into the Health and Environmental Aspects of Uranium Mining in British Columbia', Feb. 1980, 18 p.

Sainsbury, C.L.
1964: Geology of Lost River Mine area, Alaska; U.S. Geological Survey Bulletin, 1129, 81 p.

Stemprok, M. and Skvor, P.
1974: Composition of tin-bearing granites from the Krusne Hory metallogenic province of Czechoslovakia; Journal of Geological Sciences, Economic Geology, Mineralogy, Prague, v. 16, p. 7-87.

Tischendorf, G.
1977: Geochemical and petrographic characteristics of silicic magmatic rocks associated with rare-earth mineralization; in Metallization Associated with Acid Magmatism, ed., M. Stemprok, L. Burnol, G. Tischendorf; International Geological Correlation Programme, v. 2, p. 41-96.

Turekian, K.K. and Wedepohl, K.H.
1961: Distribution of the elements in some major units of the earth's crust; Geological Society of America, Bulletin v. 72, no. 2, p. 175-191.

White, H.W., Stewart, D.R., and Ganster, M.W.
1976: Adanac (Ruby Creek), porphyry molybdenum deposits of the calc-alkaline suite; in Porphyry Deposits of the Canadian Cordillera, ed. A. Sutherland Brown; Canadian Institute of Mining and Metallurgy, Special volume 15, part D, paper 47, p. 476-483.

18.

IMAGE PROCESSING OF COINCIDENT BINARY PATTERNS FROM GEOLOGICAL AND GEOPHYSICAL MAPS OF MINERALIZED AREAS[1]

Andrea G. Fabbri[2]
Geological Survey of Canada

Fabbri, A.G., Image processing of coincident binary patterns from geological and geophysical maps of mineralized areas; in Uranium in Granites, ed. Y.T. Maurice; Geological Survey of Canada, Paper 81-23, p. 157-165, 1982.

Abstract

Binary images of different map units can be extracted, in registration with each other, from systematically digitized maps of an area. The images are transformed and combined with one another to define regional geological situations which are described by the resulting new sets of coincident patterns.

Binary transformations provide quantitative measures of orientation and distributions of map units, and of interrelations between them. Fast parallel processing, for producing the transformations, can be obtained by compressing the binary data to one bit per pixel, and by using both Boolean and bit shift operators which are available on most computers.

To exemplify the approach, these techniques are used in the study by minicomputer of selected geological information on two areas in the Canadian Shield being assessed for mineral resources. In one area patterns are extracted which are related to uranium occurrences; in the other area a relationship is derived between the orientation pattern of gravity anomaly contours and that of deep seated granitic intrusions.

Résumé

Des images binaires de différentes unités cartographiques peuvent être extraites, alignées les unes par rapport aux autres, à partir de cartes numérisées d'une même zone. On transforme les images et on les combine les unes avec les autres pour définir les situations géologiques régionales qui sont décrites par ces nouveaux groupes de diagrammes coincidents.

Les transformations binaires donnent des mesures quantitatives de l'orientation et de la distribution des unités cartographiques et de leurs interrelations. On peut utiliser le traitement parallèle rapide, pour produire les transformations, en comprimant les données binaires à un bit par pixel et en utilisant les opérateurs de Boole et de décalage de bit qui sont accessibles sur la plupart des ordinateurs.

Pour illustrer l'approche, ces techniques sont utilisées dans l'étude par mini-ordinateur de renseignements géologiques choisis dans deux régions du Bouclier Canadien, en voie d'être évaluées pour leurs ressources minérales. Dans une région, on a extrait des diagrammes réliés aux occurrences d'uranium; dans l'autre région, on a déduit une relation entre l'orientation des contours d'anomalies gravimétriques et celui d'intrusions granitiques profondes.

Introduction

One of the objectives of image processing is the extraction of features from digital images. These are computer processable arrays of numbers in point-to-point correspondence with very small areas, pixels, in the original picture material. Image processing, in general, does not deal with hierarchically structured data, as is done in computer graphics. The reason is mostly one of computational convenience, but it is also because much pictorial data is currently available as raster formatted images, e.g., remotely sensed information, and this facilitates data integration.

Integrating geoscience data from different sources, offers the opportunity to use the computer for broadening the work of the economic geologist in the construction of maps which, in a quantitative form, represent the probability, associated with particular geological areas, of the occurrence of mineral deposits. Geometrical probability concepts have been developed for this purpose by Agterberg and Fabbri (1978) in the analysis of black and white images. In such binary images, each pixel indicates the presence of a given rock by the value binary 1, and its absence by a binary 0. Each rock type can be considered as a set of 1-valued pixels.

If a number of maps of ancillary data are also available, beside a geological map (e.g. mineral occurrence distribution maps, geophysical and geochemical contour maps, or remotely sensed pictures) it becomes feasible to develop statistical models for mineral resources estimation and to process images of maps as sets of pixels. The theory of sets can then be applied and processing is made easier. In general, such models are based on the relationships between known mineral occurrences and the characteristics of their neighbourhoods in terms of the ancillary information.

Geometrical probability theory and applications have been developed in several fields indirectly related to geology, such as mathematical morphology (Matheron, 1975), geometrical probability and stereology (Serra, 1978) or

---

[1] This paper was originally published in the Proceedings of the 7th Conference of Canadian Man-Computer Communication Society, 10-12 June, 1981, Waterloo, Ontario, p. 323-333.

[2] Guest Worker with the National Research Council of Canada; 601 Booth Street, Ottawa, Ontario K1A 0E8

mathematical geology (Switzer, 1976). Some of the applications have been performed on 'image analyzers': special purpose instruments in which a microprocessor, a television camera, and a microscope, or some other projecting devices, are interfaced (Hougardy, 1975). Image analyzers are real time instruments which can become very powerful and complex systems if interfaced with large computers or if provided with sophisticated special purpose hardware, as the T.A.S. (Texture Analyzing System) described by Nawrath and Serra (1979). Other applications are performed on even more powerful 'pipeline processors' like the Cytocumputer, used by Gillies (1978) for real time pattern recognition. The cost of dedicated hardware, however, limits its availability, particularly in nonroutine research work for which general purpose computers may be more accessible.

The approach pursued in this paper, is the analysis of relatively large images (1024 pixels x 1024 pixels) by a small general purpose computer. The images are digitized from geological maps and, in one example, from ancillary data related to uranium resources. The analysis has been, and can be, performed by one person, a geologist, who uses an interactive Fortran program package, GIAPP, developed by Fabbri (1980) for the analysis of geological data in picture form. In particular, GIAPP computes transformations of binary images which are in the compressed form of one bit per pixel.

Digitization of Boundaries of Geological Maps

On geological maps the boundaries, observed and inferred, between 'outcrops' of different map units (either lithological or age units) are represented by continuous and broken lines. In general, each boundary completely surrounds areas ('outcrops') in which an observed map unit is classified stratigraphically or lithologically, and is identified in a legend in which the different colours and the map units are associated. Frequently, graphical patterns and scattered symbols can overlap or even substitute the colours when the latter are too expensive to reproduce. The colours on geological maps appear uniform to the human eye, but, unfortunately, are not so to automatic scanning devices (for example, uniform looking colours may consist of patterns of differently coloured dots). The maps also contain much additional information such as symbols for fractures, folds, mineral occurrences and various kinds of topographical features including geographical names. For these reasons, they may require redrafting (scribing) or recolouring in order to be efficiently scanned by automatic devices. It is also required that several maps of different types, but covering the same area on the ground, are digitized so as to be in registration with each other.

Digitization by a 34 cm x 34 cm graphic tablet is here preferred as a practically simpler and faster means of producing raster binary images of map contours. Additional processing provides the automatic identification of all individual areas, and the interactive classification of the areas into map units. The extraction of binary images corresponding to each unit becomes a simple procedure. Before digitizing, a number of corresponding rectangular subareas, smaller than the tablet size, are marked on all the maps of a set. Each subarea is placed on the tablet, and the digitization is performed by tracing all boundaries within the subarea with the stylus. Reference points and vectors obtained from the tablet are stored on magnetic tape for each subarea. These are later transformed into a raster image of boundaries by simply computing, for a given resolution, which squares in a superimposed regular grid, are crossed by the vectors. These squares become black pixels with value binary 1, as shown in Figure 18.1a. In cases of digitizing errors or of poor resolution, interactive editing is done while displaying magnified subareas of binary images on a graphic screen. A line thinning algorithm is used to reduce the width of boundaries to a single pixel, as shown in Figure 18.1b. Several smaller images are then mapped into a larger one, like the image shown in Figure 18.1c, for geological map. The image represents a 760 pixels x 1004 pixels mosaic of four subimages of 380 pixels x 502 pixels.

If the boundary lines are now described by connected chains of black pixels, it becomes a simple procedure to identify by unique numbers all areas enclosed within the boundaries (component labeling). The next processing step consists of displaying magnified subareas of the binary image of boundaries, and of interactively pointing once at the inside of each area to record a new map unit label and its image co-ordinates. When this process is completed, a correspondence is established between the labels for the individual areas (components) and the new map unit labels (phases). This correspondence is used for computing either a phase-labeled image (in which all pixels belonging to a same map unit are assigned its label), or a different binary image for each map unit.

The desired information is captured from the geological map and the spatial correspondence with the original map is retained.

Quantification and identification of features from maps can also be achieved while remaining within the line graphics domain as, for example, was done by Bouille (1976). However, while some kinds of measurements, such as computing boundary lengths, are easier with graphic data than with raster data, it is not so easy to compute either logical operations between images or shrinking and expanding transformations on images. As described in the next section, operations and transformations, are intuitive and relatively simple with a raster data base.

In the remainder of this paper, descriptions are provided of what such computations can do in the field of regional resource assessment where, as a general case, it may not be known in advance which kinds of processing of the digitized data will be most useful.

Logical Operations and Transformations of Binary Compressed Images

If binary images are compressed to one bit per pixel, besides the obvious convenience in the reduction of storage space and in input/output time, logical operations between images and binary neighbourhood transformations can be computed at relatively fast rates by combining Boolean and bit shift operators which exist on all general purpose computers. This is done in order to exploit the limited degree of parallellism permitted by the word length of the computer.

By these techniques, useful results are obtained in the analysis of binary images extracted from a boundary image, shown in Figure 18.1c, which represents the 1:250 000 bedrock geology map of the Whiskey Jack Lake-Kasmere Lake area, in northwestern Manitoba where, during the past eight years, there has been exploration for uranium.

Binary neighbourhood transformations are 'erosions' and 'dilatations' by structuring elements or templates. As described by Fabbri (1980), the latter can be imagined as

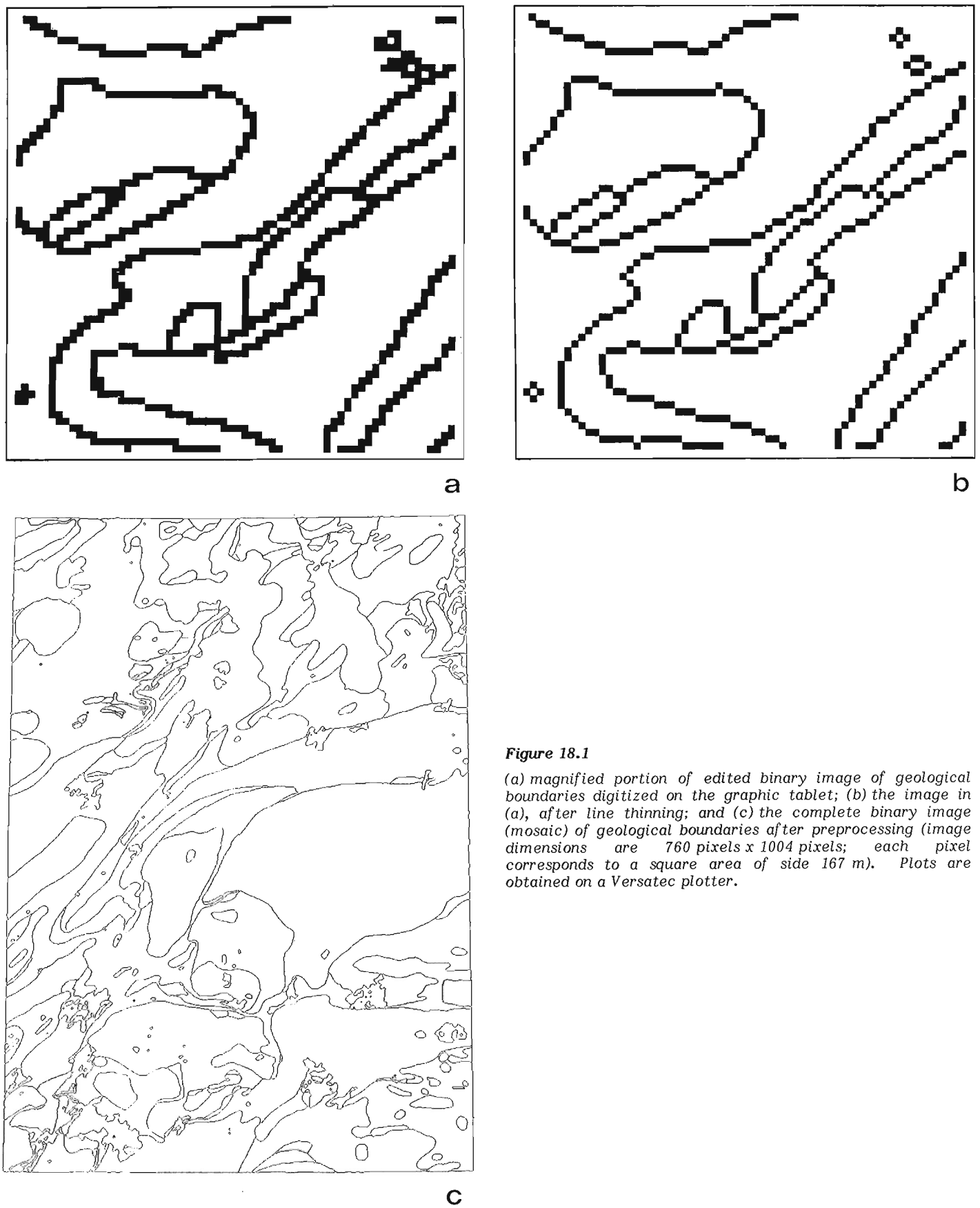

Figure 18.1

(a) magnified portion of edited binary image of geological boundaries digitized on the graphic tablet; (b) the image in (a), after line thinning; and (c) the complete binary image (mosaic) of geological boundaries after preprocessing (image dimensions are 760 pixels x 1004 pixels; each pixel corresponds to a square area of side 167 m). Plots are obtained on a Versatec plotter.

small binary images which are swept across each pixel of an image in order to transform its 1 or 0 values into 0 or 1 according to the degree of coincidence between the pixels in its neighbourhood and the corresponding pixels in the template. Figure 18.2 shows examples of logical operations and binary transformations for two images of the study area: the image of a map unit extracted from the image in Figure 18.1c, and the image of 10 km square cells centred around the locations of the 12 uranium occurrences known in the study area. By appropriate transformations, a variety of geometrical properties can be measured (often in terms of proportions of black to white pixels in the image before and after the transformations) which are immediately recomputed into geometrical probabilities.

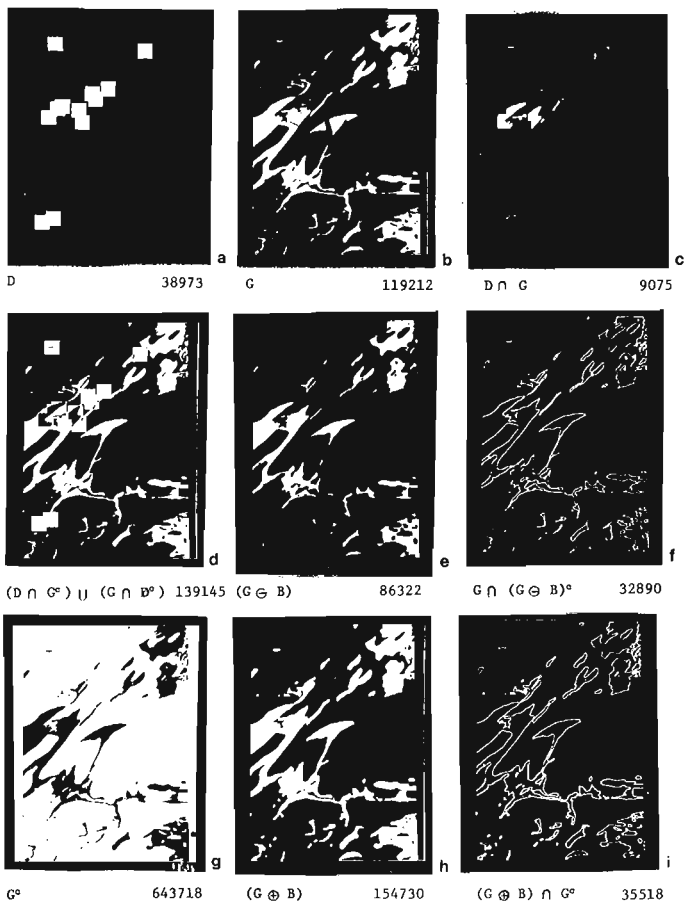

Figure 18.2. *Transformations of binary images. The numbers of black pixels in the images (here displayed in white on a Tektronix 611 storage display unit) are shown below the right corners of the plots. Below the left corners the expressions for the transformations are shown. (a) image D of 61 pixels x 61 pixels neighbourhoods (10 km x 10 km squares) of 12 uranium occurrences; (b) the image G of Aphebian pelitic metasediments; (c) the intersection (overlap or coincidence) between D and G; (d) the image produced by the .EXOR. or exlusive .OR.'ing logical operation (the union of two non-overlapping subsets) between D and G, which shows one image in the context of the other; (e) image G eroded by a 5 pixels x 5 pixels black template; (f) image of the pixels eroded from G; (g) the image of the complement or negation of G; (h) image G dilatated by a 5 pixels x 5 pixels black template; and (i) image of the black pixels 'added' to the image G during dilatation.*

Extraction of Patterns of Areas Related to Uranium Occurrences

If binary images are transformed and combined to obtain derived patterns as coincidencies of desirable characteristics, then the approach can represent a new geological tool in the study of regional resources. An application of this concept in the study area of northwestern Manitoba, is summarized in Figure 18.3. A synthesis of the economic geology of the area was provided by Weber et al. (1975). The application is described in more detail elsewhere by Fabbri and Kasvand (1981). In the study, four ancillary maps have been digitized: aeromagnetic anomaly contours, gravity anomaly contours, airborne gamma ray spectrometric contours of the ratio of equivalent uranium to equivalent thorium elemental concentrations, and the location of twelve 10 km square areas centred around each of the uranium occurrences known to exist in the area. By digitizing the geological and geophysical maps, images are extracted for several map units which are then related to each other according to the following model: (1) the gradational contact between Aphebian (Proterozoic) pelitic metasediments and Aphebian conglomeratic and psammitic metasediments, is a likely trap for uranium deposition; (2) aeromagnetic and gravity lows correspond to areas of thickest sedimentary piles; and (3) high values for the ratio of equivalent uranium/equivalent thorium, are related to the occurrence of granitic and pegmatitic intrusive rocks in which uranium concentration was locally observed. The coincidence of these factors should portray 'environments' related to uranium mineralization within favourable structural and lithological settings.

A representation of this situation is modelled in Figure 18.3, where images are computed by combining one transformation by a structuring element, and several logical operations. Expressions for the operations and transformations can be written using the following symbols: B for a 5x5 black pixels structuring element set, $\oplus$ for dilatation of a set, $\cap$ for intersection, and $\cup$ for union of two sets. If mnemonics are used for indicating the binary images, we can write: G1 and G2 for the images of the two Aphebian metasedimentary units, AL for aeromagnetic anomaly lows, GL for gravity anomaly lows, and UT for the equivalent uranium/equivalent thorium ratios. Then the 850 m wide transitional-contact-zone binary image, set CT, between map units G1 and G2 can be written:

$$CT = (G1 \oplus B) \cap (G2 \oplus B).$$

The extracted pattern, shown in Figure 18.3d, can be written as:

$$EP = (AL \cap GL \cap CT) \cup (AL \cap UT \cap CT).$$

It is of interest to observe that, while CT represents 1.9 per cent of the total image area, EP represents .5 per cent. This can be expressed as a .005 probability that a random pixel sweeping throughout the image set EP, hits a black pixel. This probability can be appreciated by eye in Figure 18.3d, and it can be easily related to the context of other binary images. Representations of this kind are useful in the analysis of geological and ancillary data on resources.

This is a simple example of a technique for describing one particular uranium related 'environment' by forcing geophysical anomaly contours into a discrete number of intervals. In general, it is the task of the specialist to design different models for deriving contour intervals for particular purposes. A specialist is also aware of the uncertainties

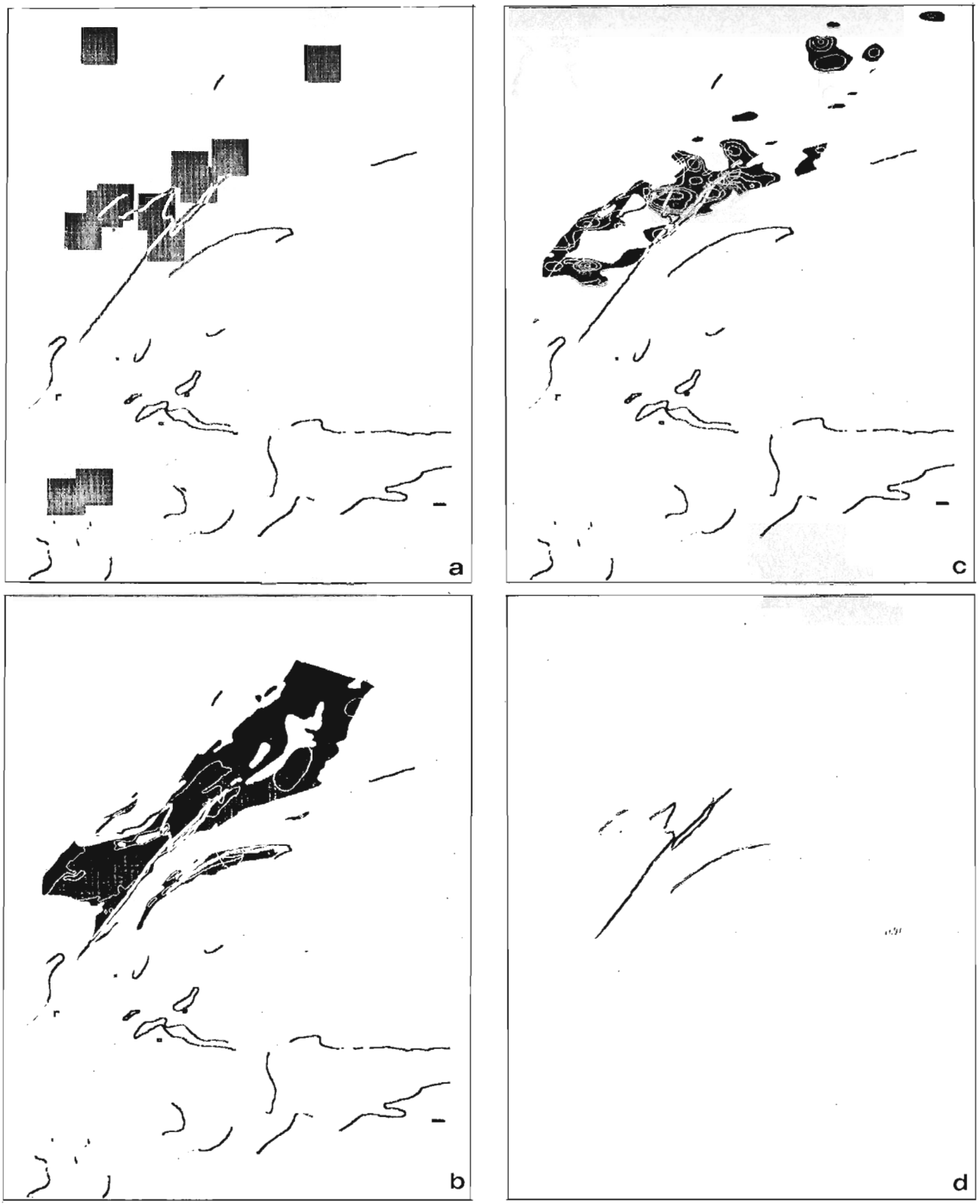

Figure 18.3. *Extraction of pattern of coincidencies. (a) intersection of the two dilatated binary images of Aphebian (Proterozoic) pelitic metasediments, and Aphebian conglomeratic and psammitic metasediments. The image shows the set CT, of the 850 m wide zones of contact between the two geological map units. The set CT is exclusive OR'ed with the image D, of 61 x 61 black pixels squares centred around 12 uranium occurrence pixels. (b) intersection of the images of aeromagnetic anomaly lows, AL (less than 2100 gammas) and of gravity lows, GL (less than -70 milligals) exclusive OR'ed with CT. (c) intersection of the image AL with the image of equivalent uranium/equivalent thorium ratio highs, UT (grater than .2), exclusive OR'ed with CT. (d) partitioning of CT into likely sites for new discoveries: i.e. the extracted pattern EP. Additional explanation is in the text.*

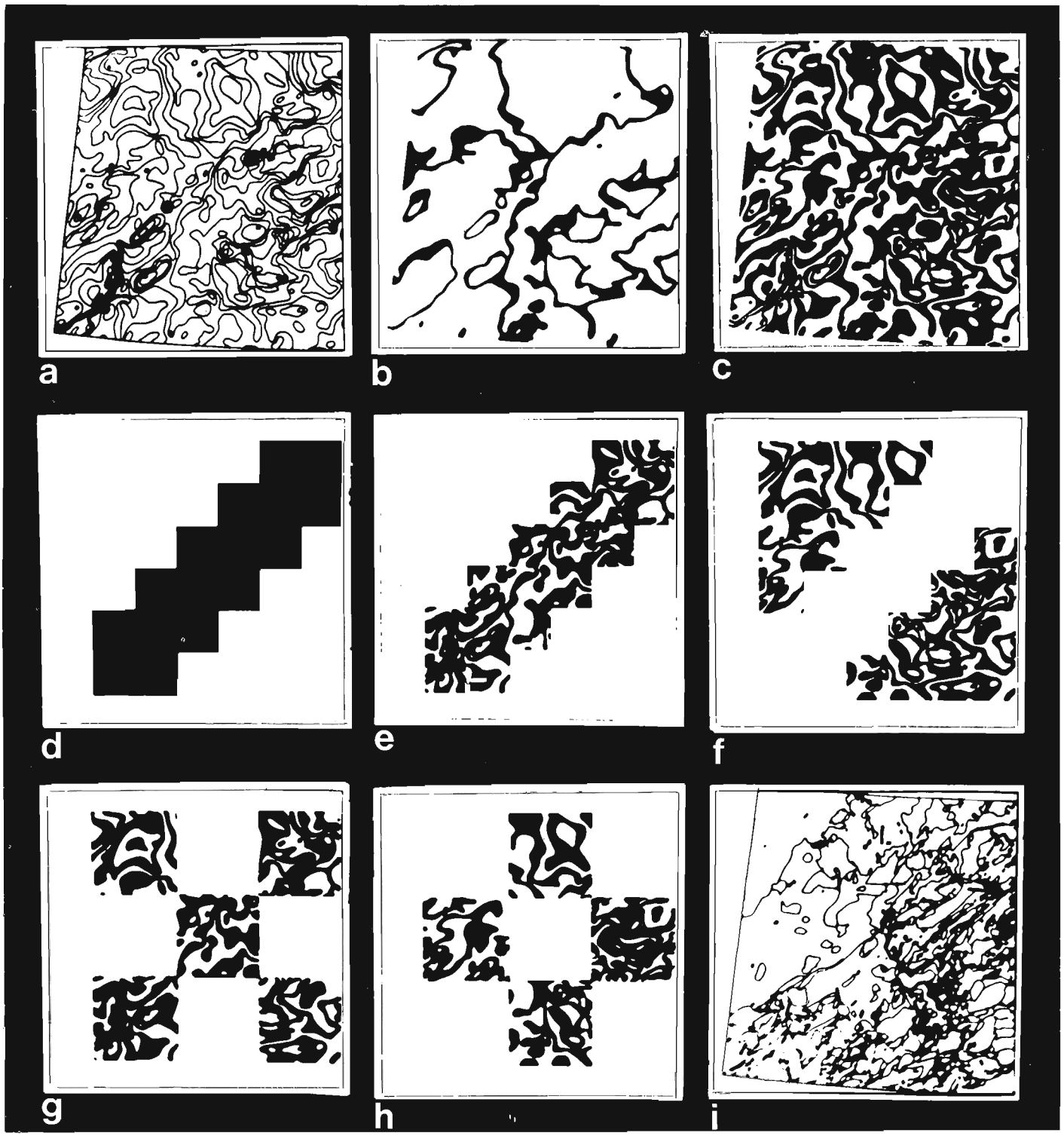

Figure 18.4. *Processing for orientation patterns. (a) binary image of thinned gravity contours (of dimension 915 pixels x 915 pixels; each pixel corresponds to a square area of side 500 m); (b) extraction of image of gravity anomaly interval -60/-65 milligals; (c) extraction of 'zebra map', the union of images for every other interval extracted from (a); (d) a binary image mask, for partitioning (c); (e) intersection between (c) and (d) to produce image of subarea B; (f) subareas A (upper left) and C (lower right) extracted from (c) by two masks complementary to (d) within a 768 pixels x 768 pixels square; (g) 256 pixels x 256 pixels subareas 1,3,5,7, and 9 extracted from (c); (h) 256 pixels x 256 pixels subareas 2,4,6, and 8 extracted from (c); and (i) binary image of thinned geological boundaries digitized in registration with (a).*

associated with the data used for resources analysis: i.e., with the geological boundaries and the geophysical contours, or the unavoidable bias in a classification model based on the prior knowledge of one individual.

Measurements of Orientation Patterns of Gravity Anomaly Contours

This second application is part of a preliminary geomathematical analysis made by Agterberg et al. (1981), in the southern District of Keewatin, Northwest Territories. The preferred orientation of the Bouguer anomalies in the area was investigated using digitized data similar to what has been described earlier. Figure 18.4a shows a binary image of the contours for 5 milligal intervals constructed for gravity measurements at intervals of about 12 km. The contours have been digitized from 1:500 000 Bouguer anomaly gravity maps, where the anomaly reflects the specific gravity of rocks at deep levels below the surface. The preferrred orientation of the gravity contours analyzed is likely to represent the dominant structural trends of the rocks, in the upper part of the Earth's crust, which may not be directly mappable on a geological map.

Clearly many contours in Figue 18.4a, have a prominent northeast trend, whereas other contours have a weaker orientation perpendicular to this direction. A simple way to study the orientation of the contours in a given area is to compute a rose diagram. This is obtained by approximating the contours by successive straight line segments that are sufficiently short, and by constructing the histogram of the combined lengths of all line-segments pointing in directions bounded by class limits (e.g. 10 degrees apart). RODIA (for ROse DIAgram) is an algorithm written by Agterberg (1979) which was used for constructing a smoothed histogram of the contact between black and white pixels in a binary image.

Several experiments have been performed on the image (of size 915 pixels x 915 pixels) of all gravity anomaly contours shown in Figure 18.4a. Each pixel corresponds to a square area of side 500 m. First, the image of contours was changed into another image, the 'zebra map' shown in Figure 18.4c, by extracting the binary images of every other interval and computing their union. One interval is shown in Figure 18.4b, between values of -60 and -65 milligals. Next a square subarea of 768 pixels x 768 pixels was outlined on the zebra map, so that it is at least 5 pixels removed from the edges of the zebra map in the east-west and north-south directions. The square was divided into subareas according to two different methods. A first set of three subareas B, A, and C, shown in Figures 18.4e and 18.4f, respectively, was obtained by intersecting the zebra map with binary images (masks) like the one shown in Figure 18.4d. Area A in Figure 18.4f is roughtly tri-angular in shape and covers the northwestern part of the region; area B, in Figure 18.4e, is a southwest oriented strip across the centre; and area C, in Figure 18.4f, covers the southeastern part of the region. A second set of sub-areas was obtained simply by dividing the 768 pixels x 768 pixels binary image of the zebra map, into 9 equal area images of 256 pixels x 256 pixels. These areas have been numbered from 1 to 9, from top to bottom and from left to right: they are shown as mosaics of plots in Figures 18.4g and 18.4h.

Table 18.1. Geometrical covariance array for computing the rose diagram plot shown in Figure 18.6 for subarea 3 of Figure 18.4g. Co-ordinate values and signs indicate image shifts in pixels for west (-), east (+) and south (-) directions. Numbers of coincident black pixels are shown.

	-5	-4	-3	-2	-1	0	1	2	3	4	5
0	22667.	24107.	25740.	27483.	29273.	31078.	29227.	27390.	25599.	23919.	22433.
-1	23332.	24784.	26381.	27961.	29223.	29279.	28012.	26331.	24636.	23051.	21706.
-2	23750.	25074.	26368.	27418.	27813.	27489.	26431.	25049.	23533.	22160.	21031.
-3	23798.	24812.	25690.	26173.	26195.	25756.	24852.	23684.	22467.	21348.	20429.
-4	23445.	24142.	24592.	24746.	24597.	24152.	23373.	22447.	21503.	20665.	19926.
-5	22836.	23208.	23402.	23384.	23180.	22741.	22100.	21423.	20758.	20097.	19493.
	-5	-4	-3	-2	-1	0	1	2	3	4	5

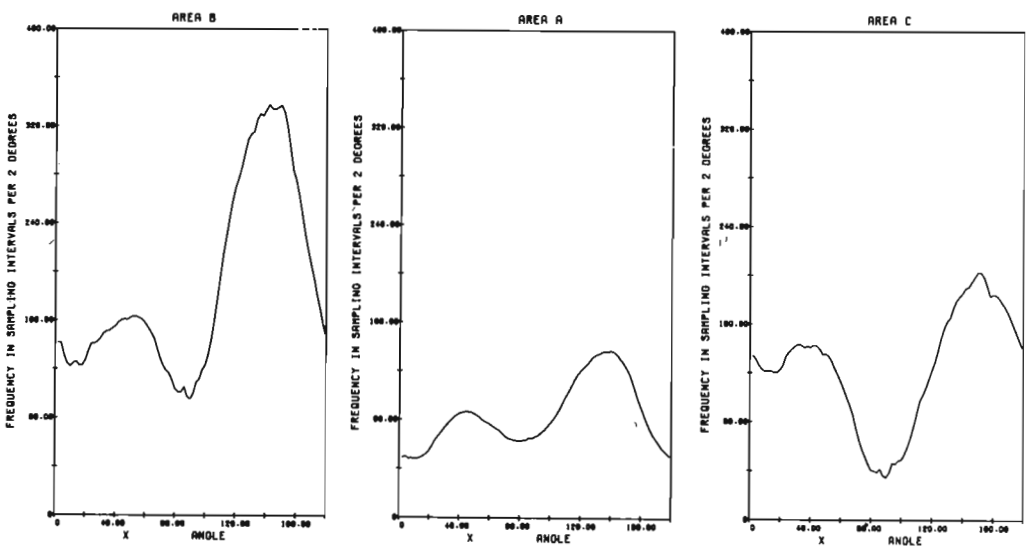

Figure 18.5

The rose diagrams computed for subareas A, B, and C of Figures 18.4e and 18.4f.

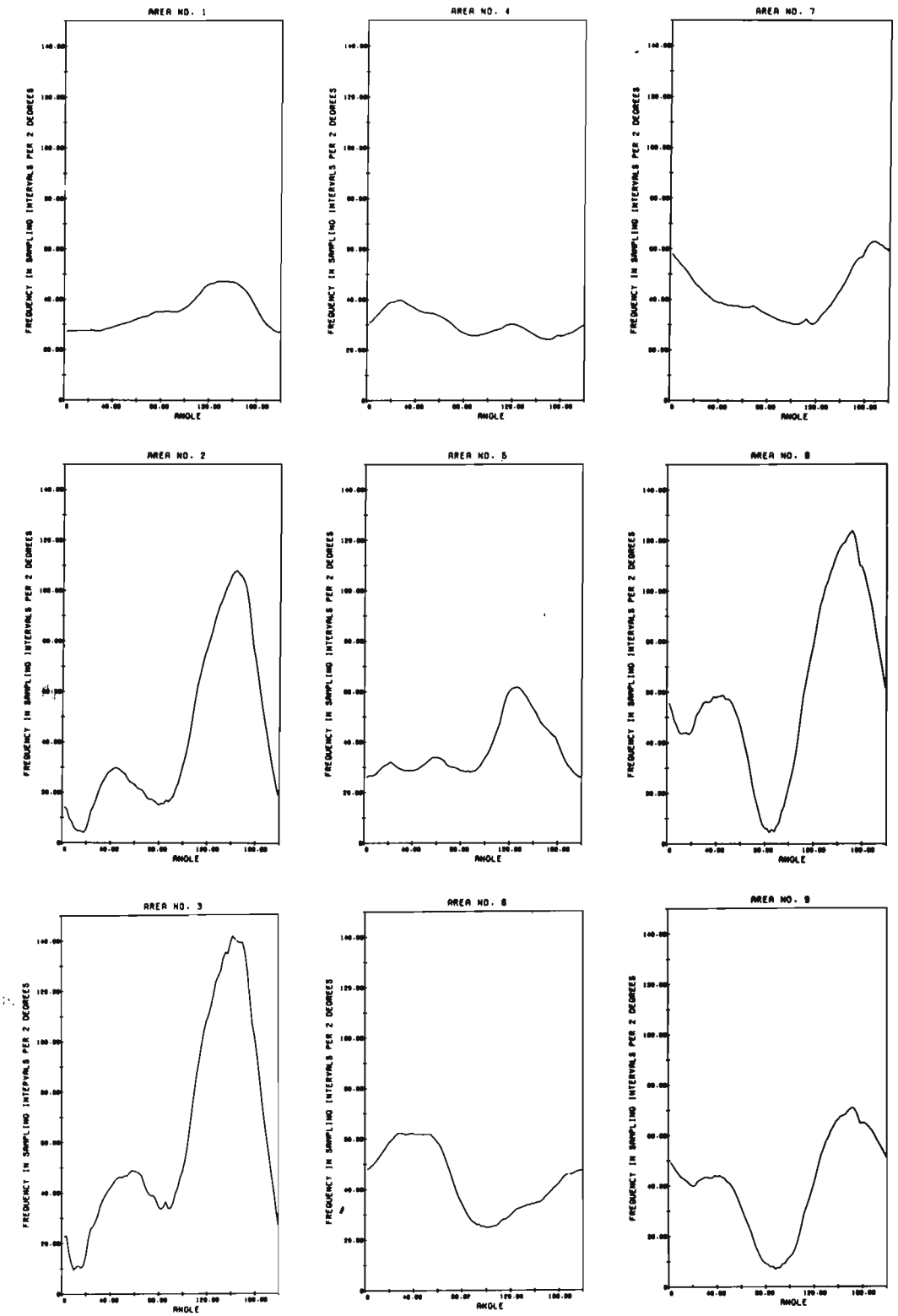

Figure 18.6. *The rose diagrams computed for subareas 1 to 9 of Figures 18.4g and 18.4h.*

Each of the 12 binary images was shifted across the image of the zebra map, for distances of 0 to 5 pixels in eastern, southern, and western directions. The geometrical covariance, i.e. the number of coinciding black pixels in the two images was measured for each shift using GIAPP. The result was a set of 61 covariance values which were used as the input to RODIA. Such an input for subarea 3 of Figure 18.4g, is shown in Table 18.1. From this array a rose diagram is computed. The results should be evaluated by comparing histograms for different subareas with one another.

In Figure 18.5, the histograms are shown for subareas A, B, and C. In each histogram, the frequencies are plotted vertically, and the corresponding directions are plotted for clockwise rotation in the horizontal direction starting from 0 degrees for the west-to-east direction, and ending with 180 degrees for the east-to-west direction. These patterns of histograms show that there are two main preferred orientations in areas A, B, and C, with the northeast orientation better developed than the northwest orientation in all three subareas. The strongly preferred orientation in area B (Fig. 18.4e) is reflected in the pronounced northeast trend of the surface rocks as shown on the geological boundary map of the area in Figure 18.4i.

In Figure 18.6, the histograms are shown for subareas 1 to 9 of Figures 18.4g and 18.4h, in their respective locations. Most of these patterns of orientations confirm the results obtained for areas A, B, and C; however, locally one or both of the preferred orientations may be less well developed than in other parts of the study region. The northwest orientation, well developed in areas 4 and 6 of Figure 18.4h, is possibly related to younger, high level granite masses, in area 6, and to abundant high level granite plutons in area 4. According to K.E. Eade (Geological Survey of Canada, personal communication) the northwest orientation represents a younger trend in the crust associated with granitic plutons. Such a trend, not well expressed in the orientation of the geological boundaries, is of interest for the interpretation of the economic geology of the region.

Concluding Remarks

In this paper, two experiments on large binary images have been described for the extraction of patterns of coincidencies and of orientations of features from regional geological and geophysical maps in areas in northern Canada, which are being assessed for uranium resources.

The approach consists of using Fortran programming on a general purpose small computer (a Modcomp II with 64 K words of 16 bits read/write memory), digitizing boundaries from maps in registration, and of computing special transformations of binary compressed images extracted from the digitized boundaries. The philosophy of the technique is to enable one single geologist to control applications to mineral resources.

An additional advantage of the approach, is that statistical concepts of geometrical probabilities are observable as sets of binary images. This facilitates both interpretation and communication.

Acknowledgments

The author is grateful for the enthusiastic assistance provided by the Electrical Engineering Division of the National Research Council of Canada, and in particular for the collaboration of Dr. Tonis Kasvand, of the Computer Graphics Section. The Geological Survey of Canada has actively supported this research.

References

Agterberg, F.P.
1979: Algorithm to estimate the frequency values of rose diagrams for boundaries of map features; Computers and Geosciences, v. 5, p. 215-230.

Agterberg, F.P. and Fabbri, A.G.
1978: Spatial correlation of stratigraphic units quantified from geological maps; Computers and Geosciences, v. 4, p. 285-294.

Agterberg, F.P., Chung, C.F., Divi, S.R., Eade, K.E., and Fabbri, A.G.
1981: Preliminary geomathematical analysis of geological, mineral occurrence, and geophysical data, southern District of Keewatin, Northwest Territories; Geological Survey of Canada, Open File 718.

Bouille, F.
1976: Graph theory and digitization of geological maps; International Association of Mathematical Geology, Journal, v. 8, p. 375-393.

Fabbri, A.G.
1980: GIAPP: geological image analysis program package for estimating geometrical probabilities; Computers and Geosciences, v. 6, p. 153-161.

Fabbri, A.G. and Kasvand, T.
1981: Applications at the interface between pattern recognition and geology; Sciences de la Terre, Série 'Informatique Géologique', n. 15, p. 87-111.

Gillies, A.W.
1978: An image processing computer which learns by example; in Image Understanding Systems and Industrial Applications ed. R. Nevatia; Proceedings of the Society of Photo-Optical Instrumentation Engineers, SPPIE, Aug. 30-31, 1978, San Diego, California, v. 155, p. 120-126.

Hougardy, H.P.
1975: Automatic image analysing instruments today; Proceedings of the 4th International Congress for Stereology, Gaithersburg, Maryland, NBS Special Publication 431, p. 141-148.

Matheron, G.
1975: Random sets and intergral geometry; John Wiley & Sons, New York, 261 .

Nawrath, R. and Serra, J.
1979: Quantitative image analysis: theory and instrumentation; Microscopica Acta, v. 82, p. 101-111.

Serra, J.
1978: One, two, three,... infinity; in Geometrical Probability and Biological Structure: Buffon's 200th Anniversary; ed. R.L. Miles and J. Serra; New York, Springer-Verlag, p. 137-152.

Switzer, P.
1976: Applications of random process models to the description of spatial distributions of qualitative geologic variables: in Random Processes in Geology, ed. D.F. Merriam; New York, Springer-Verlag, p. 124-134.

Weber, W., Schledewitz, D.C.P., Lamb, C.F., and Thomas, K.A.
1975: Geology of the Kasmere Lake – Whiskey Jack Lake (North Half) Area (Kasmere project); Manitoba Department of Mines, Resources and Environmental Management, Mineral Resources Division, Geological Services Branch, Publication 74-2, 163 p.

19.

SOME RELATIONSHIPS BETWEEN GRANITIC PLUTONS AND THE DISTRIBUTION OF URANIUM DEPOSITS

V. Ruzicka[1]
Geological Survey of Canada

Ruzicka, V., Some relationships between granitic plutons and the distribution of uranium deposits; in Uranium in Granites, ed. Y.T. Maurice; Geological Survey of Canada, Paper 81-23, p. 167-168, 1982.

Abstract

A major portion of the known global uranium resources occurs in deposits spatially related to granitic rocks.

Uranium deposits in the Lower Proterozoic quartz-pebble conglomerates, such as those in the Elliot Lake and Witwatersrand mining districts, occur at the margins of Archean complexes containing abundant granitic rocks. It is postulated that these deposits formed from detritus derived from uranium-bearing granites. Uranium deposits related to major Proterozoic unconformities, such as those in the Athabasca Basin or Pine Creek Geosyncline, occur in areas containing granitic rocks exhibiting above normal uranium contents. The magmatic/anatectic deposits, such as those in the Rössing or Bancroft areas, are hosted by granite or syenite pegmatites. The intragranitic and peribatholithic veins of the Hercynian Orogen in Europe are spatially and perhaps also genetically related to plutons containing certain (usually binary) phases of granitic rocks. Elsewhere, e.g. in the Beaverlodge area, the uranium-bearing veins occur in metamorphic rocks adjacent to extensive granitic terranes.

A conceptual model simulating formation of epigenetic uranium deposits in sandstones, postulates removal of uranium from granitic rocks and its deposition in these semiconsolidated sedimentary rocks along redox fronts. Deposits of miscellaneous types, such as uraniferous calcretes and modern uranium-bearing placers, commonly occur in terranes containing abundant granitic rocks, as do some volcanogenic deposits.

Conceptual genetic models, simulating formation of the above mentioned types of uranium deposits, commonly postulate granitic rocks as primordial sources of uranium. The primary concentration of uranium in these rocks may be plausibly explained using either of the recently proposed theories: (a) the uranium-bearing granites originated from subducted parts of the lithosphere; (b) the 'hot' granites have been derived from thermal or chemical plumes rich in uranium and other elements incompatible with the surroundings.

Studies on Canadian uranium deposits and uranium metallogenic subprovinces, using a complex lithological, structural, mineralogical and chemical approach, support the hypothesis of chemical plumes for interpretation of the distribution of the uraniferous metallotects.

Résumé

Une partie importante des ressources d'uranium connues se trouve dans des gisements reliés dans l'espace aux roches granitiques.

Des gisements d'uranium dans les conglomérats de galets de quartz du début du Protérozoïque, comme ceux des régions minières de Elliot Lake et de Witwatersrand, se rencontrent à la limite de complexes archéens contenant une abondance de roches granitiques. On suppose que ces gisements se sont formés à partir de matériel détritique dérivant de granites uranifères. Les gisements d'uranium reliés aux principales discordances du Protérozoïque, comme ceux du bassin de l'Athabasca ou de la région du géosynclinal de Pine Creek, se trouvent dans des régions contenant des roches granitiques présentant une teneur en uranium plus élevée que la normale. Les gisements magmatiques et anatectiques, comme ceux des régions de Rössing ou de Bancroft, se logent dans des pegmatites granitiques ou syénitiques. Les filons intragranitiques ou péribatholitiques de l'orogénèse hercynienne, en Europe, sont reliés dans l'espace et peut-être aussi génétiquement à des intrusifs contenant certaines phases (généralement binaires) de roches granitiques. Ailleurs, par exemple dans la région de Beaverlodge, les filons uranifères se rencontrent dans des roches métamorphiques adjacentes à de vastes terrains granitiques.

Un modèle conceptuel simulant la formation de gisements d'uranium épigénétiques dans les grès suppose que l'uranium a été enlevé des roches granitiques et déposé dans des roches sédimentaires semi-consolidées le long de fronts d'oxydo-réduction. Des gisements de types divers, comme les sols calcareux uranifères, certains gisements volcanogéniques et les placers uranifères modernes, se rencontrent couramment dans des terrains contenant d'abondantes roches granitiques.

[1]601 Booth St., Ottawa, Ontario K1A 0E8

Des modèles conceptuels génétiques simulant la formation des gisements d'uranium des types ci-haut mentionnés supposent en principe que les roches granitiques sont la source primordiale de l'uranium. La concentration primaire de l'uranium dans ces roches peut être vraisemblablement expliquée par l'une des théories proposées récemment: a) les granites uranifères proviennent de parties effondrées de la lithosphère; b) les granites "chauds" sont dérivés de panaches thermiques ou chimiques riches en uranium et autres éléments incompatibles avec les roches environnantes.

Des études sur les gisements canadiens d'uranium et les régions uranifères, utilisant une approche complexe lithologique, structurale, minéralogique et chimique, soutiennent l'hypothèse des panaches chimiques pour l'interprétation de la distribution des gisements d'uranium.

20. # SIGNATURES OF METALLIFEROUS GRANITES IN THE BRITISH ISLES

J. Plant[1], G.C. Brown[2] and P.R. Simpson[1]

Plant, J., Brown, G.C., and Simpson, P.R., Signatures of metalliferous granites in the British Isles; in Uranium in Granites, ed. Y.T. Maurice; Geological Survey of Canada, Paper 81-23, p. 169-170, 1982.

Abstract

Suites of metalliferous and nonmetalliferous Caledonian and Hercynian granites (sensu lato) of northern Scotland and southwest England were examined in relation to tectonic setting, new 1:250 000 scale geophysical and geochemical maps prepared by the Institute of Geological Sciences, whole-rock trace element data, and recently published isotopic data.

Criteria for the recognition of metalliferous intrusions include a posttectonic setting at a high structural level, a low pressure thermal aureole and isotopic compositions indicative of a predominantly 'juvenile' source. Many of these intrusions have large negative Bouguer gravity anomalies and broad, large amplitude magnetic anomalies and are therefore readily distinguished on regional geophysical maps. They are identified on regional geochemical maps by their contrast with the country rocks, but the trace element associations vary; high Mo-Cu-Ba-Pb-Sr values occur over porphyry-type intrusions such as those of Kilmelford and high Sn-Be-Li-U-K-Rb-Th-F over more alkaline intrusions such as Cairngorm. Granites of the latter association are also characterized by low K/Rb, Sr/Y and high Rb/Sr, U/Th, Cs/K and K/Ba ratios, and by REE patterns that are light REE enriched with marked negative Eu anomalies. The most incompatible LIL elements (U, Th, Rb) are enriched independent of other LIL elements such as Ba and negatively correlated with HFS elements such as Zr; levels of the HFS elements Sn and Ta are relatively high and levels of Zr, Hf, and Ti low.

In the Scottish Caledonides, it is suggested that metalliferous intrusions rose rapidly along deep fractures following their uplift and collision of the Scottish and English/Welsh plates. The magmas supplied heat, metals and elements such as fluorine for complexing, but metalliferous mineralization is associated with intrusions only where rising magma interacted with epizonal water during or after emplacement. Petrographical, isotopic and geochemical changes attributed to water/rock interaction during hydrothermal mineralization are discussed.

Mineralization in the Scottish Caledonides is limited by prior metamorphism of the country rocks and subaerial setting of volcanic centres over some of the plutons, resulting in a lack of water and especially of brines, for extraction of metals from the magma. Metalliferous mineralization is most commonly associated with granitic intrusions emplaced into low grade metamorphic rocks or those which are cut by major fault systems. The possibility of finding economic mineralization associated with granites is also limited by the present level of erosion. In the southern province of the Caledonides and southwest England, metamorphism is greenschist facies which makes late granites such as Shap, Skiddaw, Weardale and the Cornubian Batholith more favourable for mineralization.

Metallogenic models in terms of plate tectonics are aided when the geochemistry of posttectonic granites is the basis of comparison, since metalliferous mineralization resulting from hydrothermal circulation mostly reflects near surface geochemical interaction between magmas and epizonal waters. Geochemical and geophysical maps should be used with metallogenic maps for such investigations.

It is suggested that the classification of granites and associated metalliferous mineralization into S and I type is misleading when applied to posttectonic granites such as the late discordant intrusions of northern Scotland.

Résumé

Des suites de granites (au sens large) métallifères et non métallifères calédoniens et hercyniens du nord de l'Écosse et du sud-ouest de l'Angleterre ont été examinées en relation avec leur environnement tectonique, de nouvelles cartes géophysiques et géochimiques à l'échelle de 1:250 000 préparées par l'Institute of Geological Sciences et des données sur les éléments traces et isotopiques publiées récemment.

Les critères qui permettent de reconnaître les intrusions métallifères comprennent une mise en place post-tectonique à un niveau structural élevé, une auréole thermique de basse pression et des compositions isotopiques indiquant une source 'juvénile' prédominante. Beaucoup de ces intrusions comportent d'importantes anomalies gravimétriques négatives de Bouguer et des anomalies magnétiques de grande amplitude et sont, par conséquent, faciles à distinguer sur des cartes géophysiques régionales. Elles sont identifiées sur des cartes géochimiques régionales par leur contraste avec les roches encaissantes, mais les associations d'éléments traces varient; des concentrations élevées de Mo, Cu, Ba, Pb, Sr se rencontrent aux endroits des intrusions de type porphyrique comme celles de Kilmelford et des concentrations élevées de Sn, Be, Li, U, K, Rb, Th et

[1] Institute of Geological Sciences, London, England
[2] Department of Earth Sciences, Open University, Milton Keynes, England

F aux endroits d'intrusions plus alcalines comme celle de Cairngorm. Les granites de cette dernière association sont aussi caractérisés par de faibles rapports K/Rb, Sr/Y et des rapports élevés Rb/Sr, U/Th, Cs/K et K/Ba, et par des configurations de terres rares montrant un enrichissement en terres rares légères avec des anomalies négatives d'europium marquées. Les éléments LIL les plus incompatibles (U, Th, Rb) sont enrichis indépendamment des autres éléments LIL comme le Ba et reliés négativement avec des éléments HFS comme le Zr; les concentrations en éléments HFS, Sn et Ta, sont relativement élevés et les concentrations en Zr, Hf et Ti sont basses.

Dans les Calédonides d'Ecosse, on croit que les intrusions métallifères ont pénétré rapidement le long de fractures profondes, suite à leur formation et à l'entrée en collision des plaques écossaise et anglaise. Les magmas ont fourni de la chaleur, des métaux et des éléments comme le fluor pour la formation de complexes, mais la minéralisation métallifère est reliée à des intrusions seulement aux endroits où le magma montant a réagi avec les eaux épizonales pendant ou après la mise en place. Les changements pétrographiques, isotopiques et géochimiques attribués à l'interaction eau/roche durant la période de minéralisation hydrothermale furent étudiés.

La minéralisation des Calédonides d'Ecosse est limitée par le métamorphisme antérieur des roches encaissantes et la formation subaérienne de centres volcaniques au-dessus de certains plutons, ce qui a produit un manque d'eau, et surtout de saumures, nécessaires à l'extraction des métaux du magma. La minéralisation métallifère est le plus souvent reliée aux intrusions granitiques mises en place dans les roches faiblement métamorphisées ou celles qui sont coupées par des systèmes de failles importantes. La possibilité de rencontrer une minéralisation économique associée avec les granites est aussi limitée par le niveau d'érosion actuel. Dans les régions sud des Calédonides et au sud-ouest de l'Angleterre, le métamorphisme est à faciès de schiste vert ce qui rend les granites tardifs comme ceux de Shap, de Skiddaw, de Weardale et du batholite cornubien plus favorables à la minéralisation.

Les modèles métallogéniques en termes de tectonique des plaques, sont plus valables lorsque la géochimie des granites post-tectoniques sert de base de comparaison, étant donné que la minéralisation métallifère résultant de la circulation hydrothermale réflète principalement l'interaction géochimique près de la surface entre les magmas et les eaux épizonales. Les cartes géochimiques et géophysiques devraient être utilisées avec les cartes métallogéniques pour de telles recherches.

On suggère que la classification des granites et de la minéralisation métallifère connexe en type S et type I peut porter à confusion lorsqu'elle est appliquée aux granites post-tectoniques comme les intrusions discordantes tardives du nord de l'Ecosse.

21.

GEOCHEMISTRY AND GEOLOGY OF SOME URANIFEROUS GRANITES IN LABRADOR

J.A. Kerswill[1] and J.W. McConnell[2]

Kerswill, J.A. and McConnell, J.W., Geochemistry and geology of some uraniferous granites in Labrador; in Uranium in Granites, ed. Y.T. Maurice; Geological Survey of Canada, Paper 81-23, p. 171-172, 1982.

Abstract

Uranium mineralization was discovered in the Lake Melville and Notakwanon River areas of Labrador during detailed geochemical, geophysical and geological follow-up of regional Uranium Reconnaissance Program lake sediment and lake water uranium anomalies.

In the Lake Melville area, located in the Grenville Province (NTS 13 G/14), anomalous radioactivity occurs in relatively undeformed granitoid rocks (leucogranites) that appear to intrude older felsic and mafic gneisses. The leucogranite body corresponds closely with the core area of the geochemical anomaly. The geochemical surveys provided significant information relevant to the geology in addition to what had been previously indicated by earlier reconnaissance mapping. This earlier mapping grouped together rocks of the study area as granite gneiss gradational into paragneiss but included heterogeneous banded or veined gneisses and more homogeneous granitoid gneisses.

The radioactivity is related to disseminated uraninite occurring with molybdenite, pyrite and fluorite and intimately associated with segregations of mafic minerals that are generally conformable with the regional foliation. The mafic segregations occur in two forms: 1) as garnetiferous biotite-rich bands and schlieren often associated with increased quartz concentrations (pods, veinlets) in a sodic phase of the leucogranite, and 2) as a biotite-rich hybrid gneissic rock developed at the contact between a more potassic phase of the leucogranite and the mafic gneisses. Zones of greatest radioactivity in which uranium contents might be expected to average about 1000 ppm (estimated radiometrically) are distributed only locally and are quite restricted in extent (usually less than a few square metres). More extensive areas of bedrock containing significantly less but still enhanced uranium content, in the range of 30 to 60 ppm, occur over a much broader zone (50 m by 600 m) that includes the apparently isolated patches of greatest radioactivity.

The genesis of the uranium mineralization on the Lake Melville area anomaly can be linked directly to the genesis of the granitoid rocks. However, the nature of the source material for the granitic rocks as well as the relative importance of magmatic versus metamorphic (ultrametamorphic, anatectic) processes are at present undefined.

Follow-up work on the regional lake sediment anomaly in the Notakwanon River area, Churchill Province (NTS 13 M/9,16), found it to be composed of two distinct smaller anomalies both of which are underlain by Aphebian leucogranite. The rest of the surveyed area is underlain by younger Elsonian anorthosites and related rocks of the Nain igneous complex. As in the Lake Melville area, the anomalies closely reflect important lithological variations that were not apparent during reconnaissance mapping.

Radioactivity of up to twenty times background, probably in the range of 80 to 100 ppm uranium, occurs quite commonly in isolated areas of limited size (less than a few square metres) throughout the older leucogranite which outcrops over an area of about 15 km^2. The radioactivity is associated with mafic minerals, principally biotite, along either the well developed foliation or within apparent shear zones. In one area of about 1.5 km^2 containing numerous patches of such relatively low radioactivity, several highly radioactive pitchblende and kasolite-bearing veins were found along fractures and shear zones that both parallel and crosscut the foliation. Uranium contents fall sharply from several per cent in samples containing pitchblende to an average of 6 ppm in samples of leucogranite more than a metre from the veins but still within the area of mineralization. Generally no visible alteration is associated with the veins which are of unknown continuity and extent. A tentative genetic model for the uranium mineralization proposes that uranium originally present in the older granites was later remobilized and concentrated within fractures, perhaps during intrusion of the Elsonian magmas.

[1] Geological Survey of Canada, 601 Booth Street, Ottawa, Ontario K1A 0E8
[2] Mineral Development Division, Department of Mines and Energy, P.O. Box 4750, St. John's, Newfoundland A1C 5T7

Résumé

Des minéralisations d'uranium ont été découvertes dans les régions du lac Melville et de la rivière Notakwanon au Labrador suite à des études géochimiques, géophysiques et géologiques détaillées d'anomalies en uranium détectées dans les sédiments et les eaux de lacs au cour du programme de recherche pour l'uranium.

Dans la région du lac Melville, dans la province de Grenville (NTS 13 G/14), une radioactivité anormale se trouve dans les roches granitoïdes relativement peu déformées (leucogranites) qui semblent avoir fait intrusion dans les gneiss felsiques et mafiques plus anciens. Le leucogranite correspond à peu près à la partie centrale de l'anomalie géochimique. Les levés géochimques ont permis d'obtenir des renseignements utiles relatifs à la géologie qui s'ajoutent à ceux obtenus préalablement lors de la cartographie de reconnaissance. Cette cartographie antérieure regroupait les roches de la région étudiée en gneiss granitiques se changant progressivement en paragneiss, mais ceux-ci incluaient des gneiss hérérogènes rubanés ou veinés et des gneiss granitoïdes plus homogènes.

La radioactivité est reliée à de l'uraninite disséminée, se trouvant avec de la molybdénite, de la pyrite et de la fluorine et associée intimement à des ségrégations de minéraux mafiques qui sont généralement conformes à la foliation régionale. Les ségrégations mafiques se rencontrent sous deux formes: 1) des bandes riches en biotite contenant du grenat et des schlieren souvent associés à des concentrations accrues de quartz (lentilles, veinules) dans une phase sodique du leucogranite, et 2) une roche gneissique hybride riche en biotite qui s'est formée au contact entre une phase plus potassique du leucogranite et les gneiss mafiques. Les zones de plus grande radioactivité dans lesquelles on peut s'attendre à trouver de l'uranium avec une teneur moyenne d'environ 1000 ppm (estimée radiométriquement) ne sont distribuées que localement et sont bien limitées en étendue (habituellement moins de quelques mètres carrés). Des zones plus vastes, contenant des teneur encore élevées en uranium mais inférieures aux prédédentes, de l'ordre de 30 à 60 ppm, se trouvent dans une région beaucoup plus étendue (50 mètres sur 600 mètres) qui renferme les taches isolées de plus grande radioactivité.

La genèse de la minéralisation d'uranium dans l'anomalie de la région du lac Melville peut être reliée directement à la genèse des roches granitoïdes. Toutefois, la nature des matériaux qui furent à l'origine des roches granitiques tout autant que l'importance relative des processus magmatiques et métamorphiques (ultramétamorphiques, anatectiques) sont actuellement indéfinies.

Le travail complémentaire sur l'anomalie régionale des sédiments lacustres dans la région de la rivière Notakwanon dans la province de Churchill (NTS 13 M/9, 16), a permi de découvrir qu'elle était composée de deux anomalies plus petites, distinctes, reposant toutes les deux sur du leucogranite aphébien. Le reste de la région étudiée repose sur des anorthosites elsoniennes plus jeunes et des roches reliées du complexe igné de Nain. Comme dans la région du lac Melville, les anomalies reflètent de très près des variations lithologiques importantes qui n'étaient pas apparentes pendant la cartographie de reconnaissance.

Une radioactivité atteignant vingt fois les valeurs de fond, probablement de l'ordre de 80 à 100 ppm d'uranium, se rencontre assez fréquemment dans des régions isolées de dimentions limitées (moins de quelques mètres carrés) dans l'ancien leucogranite qui affleure sur une superficie d'environ 15 km^2. La radioactivité est associée aux minéraux mafiques, principalement la biotite, le long de la foliation bien développée ou de zones de cisaillement apparentes. Dans une zone d'environ 1,5 km^2 contenant de nombreuses taches de cette radioactivité relativement faible, on a trouvé plusieurs veines fortement radioactives porteuses de pitchblende ou de kasolite le long de fractures ou de zones de cisaillement soit parallèles à ou recoupant la foliation. La teneur en uranium tombe brusquement de quelque pour-cent dans des échantillons contenant de la pitchblende jusqu'à une moyenne de 6 ppm dans des échantillons de leucogranite à plus d'un mètre des veines, mais encore dans la zone de minéralisation. Généralement aucune altération visible n'est associée aux veines qui sont d'une étendue et d'une continuité inconnue. Un modèle génétique à l'essai propose que de l'uranium présent à l'origine dans les granites plus anciens fut ensuite remobilisé et concentré dans des fractures, peut être pendant l'intrusion des magmas de l'Elsonien.

AUTHOR INDEX

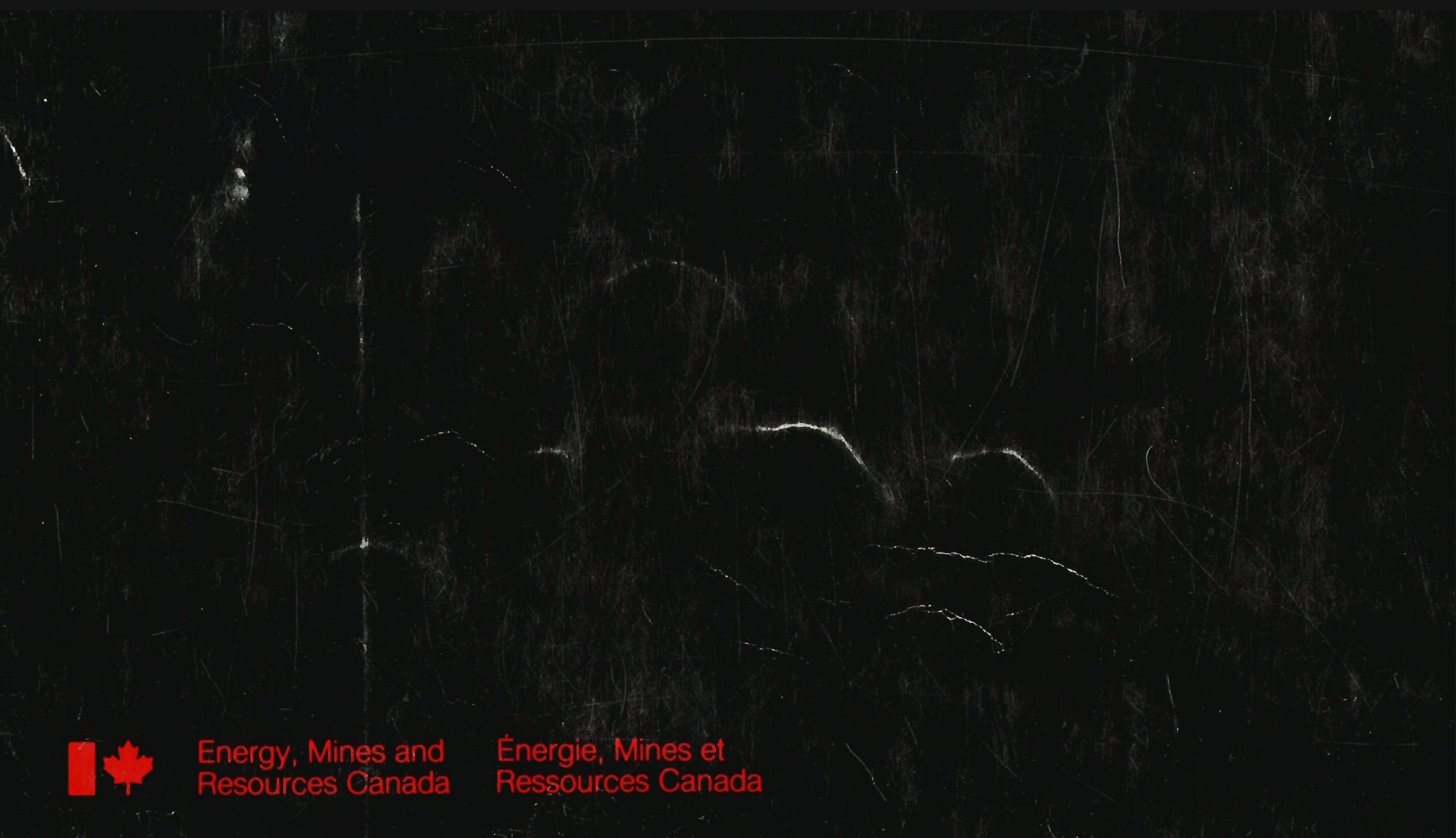

Energy, Mines and Resources Canada
Énergie, Mines et Ressources Canada